BIOGEOCHEMICAL PROCESSES IN ANTARCTIC AQUATIC ENVIRONMENTS: LINKAGES AND LIMITATIONS

by

Trista Juliana Vick-Majors

A thesis submitted in partial fulfillment
of the requirements for the degree

of

Doctor of Philosophy

in

Ecology and Environmental Sciences

MONTANA STATE UNIVERSITY
Bozeman, Montana

January 2016

ACKNOWLEDGEMENTS

I would like to thank my advisor Dr. John Priscu, for giving me the opportunity to be involved in so many amazing projects, for opening the door to the Antarctic (I didn't even know it had one), and for giving me the freedom and support to explore my ideas. I am especially grateful to my committee members, John Dore, Eric Boyd, Anne Camper, and Dan Miller for their support and guidance. Special thanks to John Dore for seeing me through both of my graduate degrees, and Eric Boyd for always having an open door.

The work in this dissertation would not have been possible without collaborations with many excellent scientists on the McMurdo LTER, the WISSARD Project, and beyond. Amanda Achberger and Alex Michaud – "we're still in this!" Thank you for your camaraderie and talking science with me. My research and fieldwork would not have been possible without Brent Christner and Mark Skidmore, and I am grateful for their support. Special thanks to Susan Kelly, for being a wonderful friend and advocate, and giving me the opportunity to share my science with the public. Pamela Santibáñez, thank you for your constant support and sharing your wonderful mind with me.

My friends and family have seen me though a long road to get here, and I am grateful to all of them. Thank you, Pa, for teaching me to love nature, and Mom, for teaching me to love learning. To my wonderful husband, Shelby – you are my rock. I can't thank you enough. And to Aunt Jayme, for being there when we needed you.

My research was funded by the National Science Foundation Office of Polar Programs (grants to John C. Priscu), grants from the Montana Institute on Ecosystems, and an American Association of University Women Fellowship.

TABLE OF CONTENTS

TABLE OF CONTENTS – CONTINUED

TABLE OF CONTENTS – CONTINUED

TABLE OF CONTENTS – CONTINUED

LIST OF TABLES

Table Page

LIST OF TABLES - CONTINUED

Table Page

LIST OF FIGURES

Figure Page

LIST OF FIGURES-CONTINUED

Figure Page

ABSTRACT

The research presented in this dissertation focused on microbially-mediated biogeochemical processes and microbial ecology in Antarctic lakes and seawater. The major objective of my research was to examine the impact of environmentally imposed energetic constraints on nutrient cycling in mirobially-dominated systems. I used three ice-covered aquatic environments as natural laboratories for my investigations. The permanently ice-covered lakes of the McMurdo Dry Valleys (MCM) are located in Victoria Land, East Antarctica. The MCM have been studied intensively as part of the McMurdo Long Term Ecological Research Project since 1993. My work built on the extensive MCM dataset via high-throughput DNA sequencing to examine microbial communities from all three domains of life during the transition to winter, and by quantifying rates of dark inorganic carbon-fixation. This worked showed the importance of flexible metabolisms in the microbial ecosystems of the MCM lakes. The ocean beneath the McMurdo Ice Shelf (MIS) is the gateway between the Ross Sea and the dark ocean of the Ross Ice Shelf cavity. The area supports a biological carbon pump that is important in ocean biogeochemistry. Ice shelves around Antarctica are under threat of collapse, but little is known about the ecosystems beneath them. My work used a combination of biogeochemical measurements and assessment of microbial community structure to characterize the ecosystem beneath the MIS and its connections to the open ocean. The data showed the importance of nutrients advected from open water to the MIS cavity and projected an organic carbon deficit farther from the ice shelf edge. Subglacial Lake Whillans lies 800 m beneath the surface of the West Antarctic Ice Sheet near the end of a hydrological continuum that terminates in the ocean beneath the Ross Ice Shelf. Primarily through the use of biogeochemical rate measurements and determinations of organic matter quantity and quality, this work established the presence of an active microbial ecosystem in the subglacial lake, and estimated the annual subglacial flux of carbon and nutrients to the ocean under the ice shelf. Together, these projects show the importance of microbial activity in regional biogeochemical processes and of metabolic flexibility under energy-limited conditions.

CHAPTER 1

INTRODUCTION

Structure of the Dissertation

Chapter 1 is an introduction to Antarctic aquatic environments, which establishes the background for and significance of my dissertation, *Biogeochemical Processes in Antarctic Aquatic Environments: Linkages and Limitations*. It provides descriptions of my research sites, and the overarching hypotheses addressed by my research. The remainder of my dissertation is comprised of six manuscripts. I used approaches ranging from the examination of microbial community structure, to geochemical characterization and the measurement of microbially-mediated transformations of carbon to examine biogeochemical processes in Antarctic aquatic environments and the linkages between and among organisms, processes, and systems. Chapters 2 and 3 focus on the permanently ice-covered lakes of the McMurdo Dry Valleys area of Antarctica. Chapter 2, published in the ISME Journal (Vick-Majors *et al.*, 2014), describes changes in microbial community structure and uses network analysis to identify key potential metabolisms (those with many linkages to other organisms) during the transition to Antarctic winter (the Polar Night). Chapter 3, in review at Microbial Ecology, reports rates of dark inorganic carbon fixation in, and constructs organic carbon budgets for, two of the McMurdo Dry Valley lakes, highlighting the importance of chemolithoautotrophy as a source of organic carbon to these lakes. The next chapter begins a focus on subglacial aquatic environments and provides a methodological umbrella for the

remaining chapters. Chapter 4, published in Antarctic Science (Priscu *et al.*, 2013), describes the methods and equipment used to ensure microbiologically clean access to pristine subglacial aquatic environments, which is important methodological background for the rest of the dissertation. Chapter 5, in press in Limnology and Oceanography, provides a rare look beneath the McMurdo Ice Shelf at microbial (bacterial and archaeal) community structure and biogeochemical processes in the sea under 80 m of ice. Chapter 6, published in Nature (Christner *et al.*, 2014), describes a microbial ecosystem under the West Antarctic Ice Sheet (Subglacial Lake Whillans) in terms of activity, diversity, and geochemistry. Chapter 7, in preparation for Nature, builds on Chapter 6 to determine the sources and sinks for organic matter in Subglacial Lake Whillans and estimate the subglacial fertilization of the Southern Ocean beneath the Ross Ice Shelf. The final chapter (Chapter 8) summarizes my conclusions, and proposes future directions for research.

Microbial Ecology in Antarctic Aquatic Environments

Biological fluxes of the major elements (C, H, N, O, P, S) are largely driven by the activities of microorganisms (Falkowski *et al.*, 2008). Of the estimated 4 - 6 x 10^{30} bacterial and archaeal cells on earth (Whitman *et al.*, 1998), the greatest proportions are found in oceanic and terrestrial subsurface environments (3.0 x 10^{30} and 2.5 x 10^{30} cells, respectively; (Whitman *et al.*, 1998)) and in subglacial environments (4.0 x 10^{29} cells; (Priscu *et al.*, 2008)). These subsurface and sub-ice environments are aphotic, and are either completely removed from inputs of photosynthetically-derived organic carbon, are

separated from such carbon on timescales of thousands to millions of years (Lever *et al.*, 2015), or receive very low fluxes (e.g. (Røy *et al.*, 2012)). Low fluxes of energy and poor quality organic matter combine with other factors, such as nutrient limitation (of anabolism), that may be physiologically dissimilar to but difficult to disentangle from energy limitation (of catabolism) (Lever *et al.*, 2015), to make most of the Earth's biosphere appear energy limited (Morita, 1997; LaRowe and Amend, 2015). Much of the microbial biosphere and the activities associated with it are under sampled, either because of difficult to access locations (e.g. deep oceans, subglacial lakes) or high biodiversity, which is difficult to catalogue and understand (e.g. soils). As a consequence of under sampling, we have a limited understanding of how microorganisms in low energy environments interact and survive, and of their integration into global fluxes of carbon and nutrients (Rousk and Bengtson, 2014). Much of what is known about low energy environments comes from studies of deep subsurface and deep sea sediments, but Antarctic studies of aquatic environments also provide insight into microbial communities and microbially mediated biogeochemical processes under energy limitation.

Surface aquatic environments in the Antarctic are subject to the bimodal light/dark cycle typical of high latitudes, providing an intermediate between the permanently dark subsurface and the usual diel light/dark cycles of moderate latitudes. Subglacial aquatic environments, on the other hand, are found under tens (mountain glaciers) to thousands (the Antarctic ice sheet) of meters of ice, leaving them permanently dark. A major consequence of lack of light is the loss of contemporaneous photosynthetic

primary production at the base of the food chain. Photosynthesis is the primary source of energy in the sunlit biosphere, fixing an estimated 60 Gt of carbon in the oceans per year (Behrenfeld *et al.*, 2005). With the exception of deep sea hydrothermal vents, where strong chemical gradients support high rates of microbial activity e.g. (Orcutt *et al.*, 2011), systems removed from local photosynthetic inputs often exhibit low metabolic rates (Røy *et al.*, 2012). Antarctic aquatic environments, which are often dominated by microorganisms (see, for example Priscu *et al.*, 1999; Cavicchioli, 2015, comprise relatively isolated and pristine environments in which to study microbial ecosystems that are either seasonally or permanently deprived of photosynthetic inputs.

In spite of its reputation as a frozen mass of ice, the Antarctic provides numerous habitats for aquatic microbial life. The Southern Ocean, which surrounds the continent, contains diverse microbial communities in its waters and sea ice, with key roles in global biogeochemical processes (Cavicchioli, 2015). The Antarctic continent itself hosts lakes and ponds located in small, ice-free coastal areas of the continent such as the Vestfold Hills and the McMurdo Dry Valleys (~0.5% of the total land area; (Convey *et al.*, 2014)). The microbially dominated lakes and ponds cover a range of nutrient conditions, fall on a salinity spectrum from fresh water to hyper saline, and range from oxygen over saturation to anoxia, and from seasonal to permanent ice covers (Spigel and Priscu, 1998), providing a range of natural conditions under which to study microbial processes. Subglacial lakes and wetlands, which were unknown until the late 20th century (Oswald and Robin, 1973), are an almost completely unexplored microbial habitat (Priscu *et al.*, 2008). With 379 subglacial lakes discovered to date all over the Antarctic continent

(Wright and Siegert, 2012), the diversity of subglacial geochemical conditions and microbial communities is likely to rival that of the surface lakes. Figure 1 shows a schematic view of the aquatic environments examined in my dissertation.

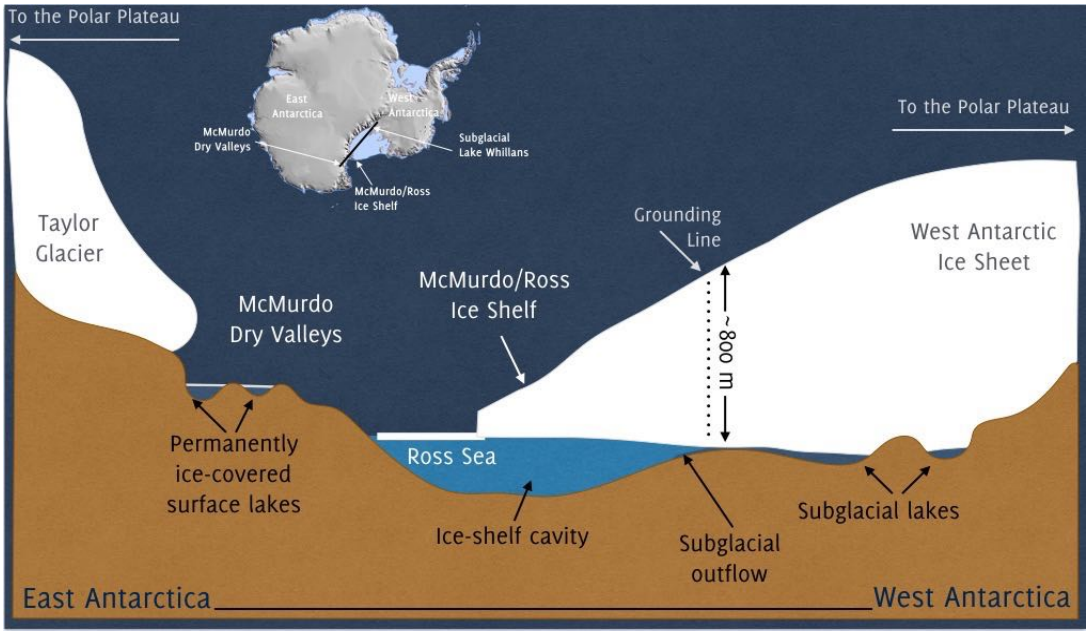

Figure 1. Schematic view of the aquatic environments discussed in this dissertation. The black line across the map of Antarctica shows where the cross-section was drawn from (~700 km). The Taylor Glacier represents the terminus of the East Antarctic Ice Sheet, which ends in the Transantarctic Mountains, leaving the McMurdo Dry Valleys free of ice cover except for it's permanently ice-covered lakes (Chapters 2 and 3). The Dry Valleys terminate in the McMurdo Sound area of the Ross Sea, which is shown here partially covered with seasonal sea ice. The subglacial lakes (Chapters 6 and 7) shown beneath the Whillans Ice Stream portion of the West Antarctic Ice Sheet periodically drain into the ocean, indicated by subglacial outflow in the drawing. The grounding line indicates where the West Antarctic Ice Sheet leaves the continental land mass and begins to flow over the ocean, forming the Ross Ice Shelf. The Ross Ice Shelf joins the McMurdo Ice Shelf closer to the McMurdo Sound region and the two share an ice-shelf cavity (Chapter 5). The drawing is not to scale. The map of Antarctica (modified from OpenStreetMap) is used under the Creative Commons Attribution-ShareAlike 2.0 License.

McMurdo Dry Valley Lakes

The perennially ice-covered lakes of the McMurdo Dry Valleys lie in East Antarctica in the coldest, driest desert on earth. The lakes are physicochemically stable environments and contain microbially dominated ecosystems (Priscu *et al.*, 1999; Spigel and Priscu, 1998; Takacs and Priscu, 1998; Vick and Priscu, 2012). As the sole year-round source of liquid water, such lakes provide the only continuous habitat for aquatic life in the ice-free regions of the Antarctic continent. Permanent ice-covers on the lakes severely attenuate the penetration of solar irradiance to <1% of incident light (Lizotte and Priscu, 1992) and prohibit wind driven turbulence, propagating an environment continuously stratified with regard to solar energy and nutrients.

The Taylor Valley is located in the McMurdo Dry Valleys, and contains four lakes, three of which are discussed in this dissertation. Lake Fryxell is located at the eastern end of Taylor Valley, near McMurdo Sound, while Lake Bonney is located at the western end of the valley, adjacent to the Taylor Glacier, the easternmost extent of the East Antarctic Ice Sheet. Lake Fryxell is an ~18 m deep, closed basin lake characterized by relatively nutrient-rich waters with an anoxic, brackish hypolimnion. The lake is in direct contact with the adjacent Canada Glacier. Lake Bonney is ~40 m deep, and its closed basin is divided into East Lobe and West Lobe Bonney. The deep waters of the two lobes are separated by a sill at ~13 m depth, while their surface waters exchange across the sill. The deep waters of West Lobe Bonney are anoxic, and the lake is influenced by subglacial outflow from Blood Falls beneath the Taylor Glacier (Mikucki *et al.*, 2007); East Lobe Bonney has a suboxic hypolimnion and salinity ~10 times

seawater. The closed nature and disparate geochemistries of the Taylor Valley lakes make them important “natural laboratories” for the study of microbial responses to changing availability of energy sources and nutrients.

Life Under Ice Shelves

Ice shelves form where grounded ice sheets leave the land and float over the ocean; the waters beneath ice shelves are referred to as “marine cavities”. Seventy-five percent of Antarctica’s coastline is surrounded by ice shelves, covering 1.5×10^6 km^2 of ocean (Rignot *et al.*, 2013). West Antarctic ice shelves are thinning dramatically(Wouters *et al.*, 2015), and together with intrusions of warm Circumpolar Deep Water beneath East Antarctic ice shelves such as the Totten Glacier (Greenbaum *et al.*, 2015)make ice-shelf melt the single largest source of ablation in Antarctica (Rignot *et al.*, 2013). Not only do these coastal ice shelves buttress the Antarctic Ice Sheet, which contains 58 m sea level equivalent worth of ice (Rignot *et al.*, 2013), but seawater that flows beneath larger ice sheets (such as the Ronne) is modified to form Antarctic Bottom Water, which is key to cooling and ventilating oceans worldwide (Nicholls *et al.*, 1991). The loss of Antarctic ice shelves is predicted to modify ocean circulation (Bougamont *et al.*, 2007). The Southern Ocean is also an important sink for CO_2. Changing atmospheric patterns are predicted to impact the functioning of the sink, but the magnitude and consequences of projected changes are not well known (Achterberg, 2014). Even less well known are the potential impacts of climate change on sub-ice shelf ecosystems, or how changing those ecosystems might impact the Southern Ocean carbon pump. Following the breakup of the Larsen A and B ice shelves, researchers found evidence for increased biological CO_2

pumping (Bertolin and Schloss, 2009), and although the opening of preciously ice covered waters should increase CO_2 pumping via new photosynthetic activity, it is difficult to interpret post-ice-shelf-breakup responses without baseline data. Baseline studies of sub-ice shelf ecosystems are almost entirely lacking due to the difficultly of accessing the ocean beneath thick ice; those data that do exist describe communities ranging from surprisingly diverse (Post *et al.*, 2014) to scavenger-dominated (Lipps *et al.*, 1979). The shift in nutrient concentrations from relatively nutrient rich water flowing into the Ross Ice Shelf cavity (Chapter 5) to the oligotrophic outflow from the cavity to McMurdo Sound (Hodson *et al.*, 1981; J C Priscu *et al.*, 1990) indicates significant biogeochemical modification of sub-ice shelf waters during residence time in the cavity. Understanding sub-ice shelf biogeochemical processes is important for predicting Southern Ocean responses to climate change, and provides new insight into microbial responses to the loss of locally produced photosynthetic carbon closer to the interior of the marine cavity.

Subglacial Aquatic Environments

In spite of being covered by 27 million km^3 of ice up to ~3.5 km thick (Fretwell *et al.*, 2013), the Antarctic continent hosts significant biological diversity (Chown *et al.*, 2015). Perhaps the most important physical driver of habitability in Antarctic terrestrial environments is the availability of liquid water. Liquid water can be found on and near the surface of glaciers in the Antarctic, forming supraglacial habitats (Stibal *et al.*, 2012) such as cryoconite holes that are hot spots of microbial activity (Foreman *et al.*, 2007). Beneath the ice sheet, liquid water can form wherever temperatures reach the pressure

melting point, either due to geothermal heat flux (Fisher *et al.*, 2015) or volcanic activity(Gaidos *et al.*, 2009), although the latter has only been hypothesized in West Antarctica (Blankenship *et al.*, 1993). The resulting subglacial lakes, streams, water saturated sediments, and wetlands are thought to contain ~10^6 km^3 of water (J C Priscu *et al.*, 2008) and serve as habitats for microbial life (J C Priscu, Adams, *et al.*, 1999; Christner *et al.*, 2006; Lanoil *et al.*, 2009). Subglacial microbial life has been found in debris-rich basal ice, sediments, and water beneath temperate, Arctic, and Antarctic valley glaciers (Sharp *et al.*, 1999; Skidmore *et al.*, 2000; Mikucki *et al.*, 2007). Biotic and abiotic weathering processes liberate nutrients and energy sources for microorganisms beneath glaciers (Montross *et al.*, 2013), while overriden organic carbon or subglacially produced hydrogen (Telling *et al.*, 2015) may fuel methanogenesis(Boyd *et al.*, 2010; Wadham *et al.*, 2012) and provide carbon and energy for methanotrophs (Dieser *et al.*, 2014), Michaud et al., in prep). Chemolithotrophic metabolisms may be supported by iron and sulfur (Boyd *et al.*, 2014; Purcell *et al.*, 2014; Mikucki *et al.*, 2009)or nitrogen (Boyd *et al.*, 2011) (see also Chapter 6). Heterotrophic metabolism has received comparatively less attention than chemolithotrophic metabolism in subglacial environments, although the ultimate source of ammonium to support nitrification (Chapter 6) must be the remineralization of organic matter. Heterotrophic microorganisms may use recalcitrant or semi-labile relict organic matter present under glaciers as an energy source (Bardgett *et al.*, 2007). Organic matter produced by chemoautotrophy can also support heterotrophic growth, however its production and

remineralization may be uncoupled, especially under conditions of energy limitation where cells are less likely to leak organic matter (Carlson *et al.*, 2007).

Subglacial Lake Whillans (SLW) is the only Antarctic subglacial lake to have been directly sampled to date (Tulaczyk *et al.*, 2014). The lake lies 800 m beneath the surface of the Whillans Ice Stream (WIS) in West Antarctica. It is one of the "active" subglacial lakes along Antarctica's Siple Coast, so named for the active hydrology that connects lakes in the region to each other and to the Ross Sea downstream (Fricker *et al.*, 2007). The net fluxes of carbon and nutrients mediated by microorganisms in SLW, and other subglacial lakes, are important to quantify as a means of understanding subglacial contributions to downstream environments. The study of microorganisms in subglacial lakes adds to our understanding of microbial physiology, and of the potential for microbial life on icy worlds in our solar system and beyond (Mikucki *et al.*, 2015).

Significance of My Research

My dissertation focuses on the microbial ecology of, and microbially mediated biogeochemical processes in, ice-covered Antarctic aquatic environments. The combination of liquid water and thick, permanent ice covers creates oases in the Antarctic desert(J C Priscu *et al.*, 1998). The unique characteristics of ice-covered, liquid water habitats such as truncated ecosystems devoid of metazoans and/or photosynthetic primary producers, permanent darkness, and isolation from exchange with atmosphere make these desert oases excellent places to study microbial processes and interactions. I applied microbiological techniques to samples from two McMurdo Dry Valley lakes (Fryxell and

West Lobe Bonney) to provide the first in-depth, simultaneous description of microbial community structure from all three domains of life (Bacteria, Archaea, Eukarya) in these lakes and to examine microbial community shifts and interactions during the transition to the Polar Night. To better understand the potential importance of chemoautotrophic inorganic carbon fixation in the Dry Valley lakes, I studied rates of inorganic carbon fixation in Lake Fryxell and East Lobe Lake Bonney, and found that chemoautotrophy can help balance the organic carbon deficit imposed by the lack of photosynthetic activity during the winter. While the bimodal light/dark cycle associated with high latitudes has a direct impact on the McMurdo Dry Valley lakes, the waters beneath the McMurdo Ice Shelf and those in Subglacial Lake Whillans beneath the West Antarctic Ice Sheet, are permanently dark. I used microbiological and geochemical techniques to describe biogeochemical conditions under the McMurdo Ice Shelf, the first study of its kind. The baseline characterization of the sub-McMurdo Ice Shelf environment is especially important as Antarctic ice shelves are increasingly threatened with collapse (Rignot *et al.*, 2013). My work on Subglacial Lake Whillans provided the first measurements of microbial activity, abundance and carbon and nutrients in an Antarctic subglacial lake and showed the potential for West Antarctic subglacial aquatic environments to impact Southern Ocean biogeochemical processes downstream. Together, the studies encompassed by my dissertation provide new insights into microbial diversity and activity in Antarctic aquatic systems and begin to address biogeochemical linkages with habitats beyond my study sites.

Hypotheses and Objectives

The overarching question behind my dissertation is, “how does the ensemble of environmentally imposed energetic constraints impact nutrient cycling in microbially dominated systems?” The energetic constraints examined here include quality of organic matter and shifts in organic matter sources as a consequence of seasonal change or location. I discuss the implications for nutrient cycling directly (e.g. as rates of carbon transformations in Subglacial Lake Whillans) and indirectly (e.g. via shifts in microbial community structure and identification of key metabolisms in the McMurdo Dry Valley lakes).

Hypothesis 1: The transition from summer to winter, characterized by the loss of summer sunlight, will be associated with shifts in microbial community structure and key potential metabolisms in Antarctic surface lakes.

Associated objectives:

1. Characterize the bacterial, archaeal, and eukaryotic microbial communities present in Lake Fryxell and the West Lobe of Lake Bonney before and after the start of the seasonal sunset.
2. Determine whether microbial communities are different between summer and autumn.
3. Determine co-occurance patterns of microorganisms.
4. Identify important groups and putative functions within the communities.
5. Determine whether dark fixation of inorganic carbon (chemoautotrophy) can meet the estimated annual carbon deficit.

Hypothesis 2: Waters beneath the McMurdo Ice Shelf contain carbon, nutrients and energy sources advected from open water, which can support microbial communities beneath the ice.

Associated objectives:

1. Compare measured current flow to published data on currents in the area to determine whether water at our sample site was likely advected from McMurdo Sound.
2. Determine the concentrations of nutrients and the quality and quantity of organic matter at the sample site.
3. Determine the abundance and diversity of prokaryotic microorgansims.
4. Determine whether phytoplankton are present under the ice and whether they contain chlorophyll.

Hypothesis 3: Subglacial Lake Whillans is a nutrient-poor environment that hosts metabolically active microorgansims.

Associated objectives:

1. Develop, test, and implement procedures for microbiologically clean access to the subglacial environment.
2. Determine whether microbial cells are present and quantify microbial cells in Subglacial Lake Whillans.
3. Determine whether microbial cells in Subglacial Lake Whillans are active.
4. Determine rates of heterotrophic and autotrophic activity.
5. Measure concentrations of inorganic nutrients and organic matter.

Hypothesis 4: Subglacial Lake Whillans is an important source of organic matter and nutrients to coastal environments downstream.

Associated objectives:

1. Determine rates of dark CO_2 incorporation (chemoautotrophic production of organic carbon).
2. Determine the heterotrophic demand for organic carbon (incorporation + respiration of carbon).
3. Estimate the annual contributions of chemoautotrophy, ice-melt, inflow from upstream, diffusion from sediment porewater, and inflow of groundwater to the Subglacial Lake Whillans organic carbon pool.
4. Using the sources and sinks above, calculate the accumulation time of the measured organic matter pool in SLW and compare to known hydrology.
5. Using the data derived above along with published data on water discharge, estimate the annual flux of organic matter and nutrients from the Siple Coast to the Southern Ocean.

References

Achterberg EP. (2014). Grand challenges in marine biogeochemistry. *Frontiers in Marine Science* **1**:50.

Bardgett RD, Richter A, Bol R, Garnett MH, Bäumler R, Xu X, *et al.* (2007). Heterotrophic microbial communities use ancient carbon following glacial retreat. *Biology Letters* **3**:487–490.

Behrenfeld MJ, Boss E, Siegel DA, Shea DM. (2005). Carbon-based ocean productivity and phytoplankton physiology from space. *Global Biogeochem Cycles* **19**:n/a–n/a.

Bertolin ML, Schloss IR. (2009). Phytoplankton production after the collapse of the Larsen A Ice Shelf, Antarctica. *Polar Biology* **32**:1435–1446.

Blankenship DD, Bell RE, Hodge SM, Brozena JM, BEHRENDT JC, Finn CA. (1993). Active Volcanism Beneath the West Antarctic Ice-Sheet and Implications for Ice-Sheet Stability. *Nature* **361**:526–529.

Bougamont M, Hunke EC, Tulaczyk S. (2007). Sensitivity of ocean circulation and sea-ice conditions to loss of West Antarctic ice shelves and ice sheet. *Journal of Glaciology* **53**:490–498.

Boyd ES, Hamilton TL, Havig JR, Skidmore ML, Shock EL. (2014). Chemolithotrophic primary production in a subglacial ecosystem. *Applied and Environmental Microbiology* **80**:6146–6153.

Boyd ES, Lange RK, Mitchell AC, Havig JR, Hamilton TL, Lafrenière MJ, *et al.* (2011). Diversity, abundance, and potential activity of nitrifying and nitrate-reducing microbial assemblages in a subglacial ecosystem. *Applied and Environmental Microbiology* **77**:4778–4787.

Boyd ES, Skidmore M, Mitchell AC, Bakermans C, Peters JW. (2010). Methanogenesis in subglacial sediments. *Environmental Microbiology Reports* **2**:685–692.

Carlson CA, del Giorgio PA, Herndl GJ. (2007). Microbes and the dissipation of energy and respiration: from cells to ecosystems. *Oceanog* **20**:89–100.

Cavicchioli R. (2015). Microbial ecology of Antarctic aquatic systems. *Nat Rev Micro* **13**:691–706.

Chown SL, Clarke A, Fraser CI, Cary SC, Moon KL, McGeoch MA. (2015). The changing form of Antarctic biodiversity. *Nature* **522**:431–438.

Christner BC, Priscu JC, Achberger AM, Barbante C, Carter SP, Christianson K, *et al.* (2014). A microbial ecosystem beneath the West Antarctic ice sheet. *Nature* **512**:310–313.

Christner BC, Royston-Bishop G, Foreman CM, Arnold BR, Tranter M, Welch KA, *et al.* (2006). Limnological conditions in Subglacial Lake Vostok, Antarctica. *Limnol Oceangr* **51**:2485–2501.

Convey P, Chown SL, Clarke A, Barnes DKA, Bokhorst S, Cummings V, *et al.* (2014). The spatial structure of Antarctic biodiversity. *Ecological Monographs* **84**:203–244.

Dieser M, Sletten R, Hagedorn B, Christner BC, Junge K, Choquette K, *et al.* (2014). Molecular and biogeochemical evidence for methane cycling beneath the western margin of the Greenland Ice Sheet. *ISME J* **8**:2305–2316.

Falkowski PG, Fenchel T, DeLong EF. (2008). The microbial engines that drive Earth's biogeochemical cycles. *Science* **320**:1034–1039.

Fisher AT, Mankoff KD, Tulaczyk SM, Tyler SW, Foley N, WISSARD Science Team. (2015). High geothermal heat flux measured below the West Antarctic Ice Sheet. *Science Advances* **1**:e1500093–e1500093.

Foreman CM, Sattler B, Mikucki JA, Porazinska DL, Priscu JC. (2007). Metabolic activity and diversity of cryoconites in the Taylor Valley, Antarctica. *J Geophys Res* **112**:G04S32–11.

Fretwell P, Pritchard HD, Vaughan DG, Bamber JL, Barrand NE, Bell R, *et al.* (2013). Bedmap2: improved ice bed, surface and thickness datasets for Antarctica. *The Cryosphere* **7**:375–393.

Fricker HA, Scambos T, Bindschadler R, Padman L. (2007). An active subglacial water system in West Antarctica mapped from space. *Science* **315**:1544–1548.

Gaidos E, Marteinsson V, Thorsteinsson T, Jóhannesson T, Rúnarsson ÁR, Stefánsson A, *et al.* (2009). An oligarchic microbial assemblage in the anoxic bottom waters of a volcanic subglacial lake. *ISME J* **3**:486–497.

Greenbaum JS, Blankenship DD, Young DA, Richter TG, Roberts JL, Aitken ARA, *et al.* (2015). Ocean access to a cavity beneath Totten Glacier in East Antarctica. *Nature Geosci* **8**:294–298.

Hodson RE, Azam F, Carlucci AF, Fuhrman JA, Karl DM, Holm-Hansen O. (1981). Microbial Uptake of Dissolved Organic-Matter in Mcmurdo-Sound, Antarctica. *Mar Biol* **61**:89–94.

Lanoil B, Skidmore M, Priscu JC, Han S, Foo W, Vogel SW, *et al.* (2009). Bacteria beneath the West Antarctic Ice Sheet. *Environmental Microbiology* **11**:609–615.

LaRowe DE, Amend JP. (2015). Catabolic rates, population sizes and doubling/replacement times of microorganisms in natural settings. **315**:167–203.

Lever MA, Rogers KL, Lloyd KG, Overmann J, Schink B, Thauer RK, *et al.* (2015). Life under extreme energy limitation: a synthesis of laboratory- and field-based investigations Giudici-Orticoni, M-T (ed). *FEMS Microbiology Reviews* **39**:688–728.

Lipps JH, Ronan TE, DeLaca TE. (1979). Life Below the Ross Ice Shelf, Antarctica. *Science* **203**:447–449.

Lizotte MP, Priscu JC. (1992). Spectral irradiance and bio-optical properties in perennially ice-covered lakes of the dry valleys (McMurdo Sound, Antarctica). American Geophysical Union: Washington, D. C.

Mikucki JA, Lee PA, Ghosh D, Purcell AM, Mitchell AC, Mankoff KD, *et al.* (2015). Subglacial Lake Whillans microbial biogeochemistry: a synthesis of current knowledge. *Philosophical Transactions of the Royal Society A* **374**:20140290.

Mikucki JA, Priscu JC, Mikucki JA. (2007). Bacterial Diversity Associated with Blood Falls, a Subglacial Outflow from the Taylor Glacier, Antarctica. *Applied and Environmental Microbiology* **73**:4029–4039.

Mikucki JA, Schrag DP, Mikucki JA, Priscu JC, Pearson A, Johnston DT, *et al.* (2009). A Contemporary Microbially Maintained Subglacial Ferrous 'Ocean'. *Science* **324**:397–400.

Montross SN, Skidmore M, Tranter M, Kivimaki AL, Parkes RJ. (2013). A microbial driver of chemical weathering in glaciated systems. *Geol* **41**:215–218.

Morita RY. (1997). Bacteria in oligotrophic environments: starvation-survival lifestyle. Chapman & Hall: New York.

Nicholls KW, Makinson K, Robinson AV. (1991). Ocean circulation beneath the Ronne ice shelf. *Nature* **354**:221–223.

Orcutt BN, Sylvan JB, Knab NJ, Edwards KJ. (2011). Microbial Ecology of the Dark Ocean above, at, and below the Seafloor. *Microbiology and Molecular Biology Reviews* **75**:361–422.

Oswald G, Robin GQ. (1973). Lakes beneath the Antarctic ice sheet. *Nature* **245**:251–254.

Post AL, Galton-Fenzi BK, Riddle MJ, Herraiz-Borreguero L, O'Brien PE, Hemer MA, *et al.* (2014). Modern sedimentation, circulation and life beneath the Amery Ice Shelf, East Antarctica. *Continental Shelf Research* **74**:77–87.

Priscu JC, Achberger AM, Cahoon JE, Christner BC, Edwards RL, Jones WL, *et al.* (2013). A microbiologically clean strategy for access to the Whillans Ice Stream subglacial environment. *Ant Sci* **25**:637–647.

Priscu JC, Adams EE, Fritsen CH. (1998). Perennial Antarctic lake ice: an oasis for life in a polar desert. **280**:2095–2098.

Priscu JC, Adams EE, Lyons WB, Voytek MA, Mogk DW, Brown RL, *et al.* (1999). Geomicrobiology of subglacial ice above Lake Vostok, Antarctica. *Science* **286**:2141–2144.

Priscu JC, Downes MT, Priscu LR, Palmisano AC, Sullivan CW. (1990). Dynamics of Ammonium Oxidizer Activity and Nitrous-Oxide (N2o) Within and Beneath Antarctic Sea Ice. *Mar Ecol Prog Ser* **62**:37–46.

Priscu JC, Tulaczyk S, Studinger M, Kennictt MC II, Christner BC, Foreman CM. (2008). Antarctic Subglacial Water: Origin, Evolution, and Ecology. In:*Polar Lakes and Rivers*, Vincent, WF & Laybourn-Parry, J (eds), Polar Lakes and Rivers, pp. 119–135.

Priscu JC, Wolf CF, Takacs CD. (1999). Carbon transformations in a perennially ice-covered Antarctic lake. *BioScience* **49**:997.

Purcell AM, Mikucki JA, Achberger AM, Alekhina IA, Barbante C, Christner BC, *et al.* (2014). Microbial sulfur transformations in sediments from Subglacial Lake Whillans. *Front Microbio* **5**:594.

Rignot E, Jacobs S, Mouginot J, Scheuchl B. (2013). Ice-shelf melting around Antarctica. *Science* **341**:266–270.

Rousk J, Bengtson P. (2014). Microbial regulation of global biogeochemical cycles. *Front Microbio* **5**:103.

Røy H, Kallmeyer J, Adhikari RR, Pockalny R, Jørgensen BB, D'Hondt S. (2012). Aerobic microbial respiration in 86-million-year-old deep-sea red clay. *Science* **336**:922–925.

Sharp M, Parkes J, Cragg B, Fairchild IJ, Lamb H. (1999). Widespread bacterial populations at glacier beds and their relationship to rock weathering and carbon cycling. *Geol* **27**:107.

Skidmore ML, Foght JM, Sharp MJ. (2000). Microbial life beneath a high Arctic glacier. *Applied and Environmental Microbiology* **66**:3214–3220.

Spigel RH, Priscu JC. (1998). Physical Limnology of the Mcmurdo Dry Valleys Lakes. American Geophysical Union: Washington, D. C.

Stibal M, Šabacká M, Žárský J. (2012). Biological processes on glacier and ice sheet surfaces. *Nature Geosci* **5**:771–774.

Takacs C, Priscu J. (1998). Bacterioplankton Dynamics in the McMurdo Dry Valley Lakes, Antarctica: Production and Biomass Loss over Four Seasons. *Microbial Ecology* **36**:239–250.

Telling J, Boyd ES, Bone N, Jones EL, Tranter M, MacFarlane JW, *et al.* (2015). Rock comminution as a source of hydrogen for subglacial ecosystems. *Nature Geosci* **8**:851–855.

Tulaczyk S, Mikucki JA, Siegfried MR, Priscu JC, Barcheck CG, Beem LH, *et al.* (2014). WISSARD at Subglacial Lake Whillans, West Antarctica: scientific operations and initial observations. *Annals of Glaciology* **55**:51–58.

Vick TJ, Priscu JC. (2012). Bacterioplankton productivity in lakes of the Taylor Valley, Antarctica, during the polar night transition. *Aquat Microb Ecol* **68**:77–90.

Vick-Majors TJ, Priscu JC, Amaral-Zettler LA. (2014). Modular community structure suggests metabolic plasticity during the transition to polar night in ice-covered Antarctic lakes. *ISME J* **8**:778–789.

Wadham JL, Arndt S, Tulaczyk S, Stibal M, Tranter M, Telling J, *et al.* (2012). Potential methane reservoirs beneath Antarctica. *Nature* **488**:633–637.

Whitman WB, Whitman WB, Coleman DC, Coleman DC, Wiebe WJ, Wiebe WJ. (1998). Prokaryotes: The unseen majority. *Proceedings of the National Academy of Sciences* **95**:6578–6583.

Wouters B, Martin-Español A, Helm V, Flament T, van Wessem JM, Ligtenberg SRM, *et al.* (2015). Dynamic thinning of glaciers on the Southern Antarctic Peninsula. *Science* **348**:899–903.

Wright A, Siegert M. (2012). A fourth inventory of Antarctic subglacial lakes. *Ant Sci* **24**:659–664.

CHAPTER TWO

MODULAR COMMUNITY STRUCTURE SUGGESTS METABOLIC PLASTICITY DURING THE TRANSITION TO POLAR NIGHT IN ICE-COVERED ANTARCTIC LAKES

Contribution of Authors and Co-Authors

Manuscript in Chapter 2

Author: Trista J. Vick-Majors

Contributions: Analyzed and interpreted data, carried out statistical analyses, generated figures and tables, and wrote the manuscript.

Co-Author: John C. Priscu

Contributions: Provided funding, oversight, samples, conceived the study, and aided in manuscript preparation.

Co-Author: Linda A. Amaral-Zettler

Contributions: Oversaw DNA sequencing and sequence data preparation, provided diversity statistics, provided funding, conceived the study, and aided in manuscript preparation.

Manuscript Information Page

Trista J. Vick-Majors, John C. Priscu, Linda Amaral-Zettler
The ISME Journal
Status of Manuscript:
____ Prepared for submission to a peer-reviewed journal
____ Officially submitted to a peer-review journal
____ Accepted by a peer-reviewed journal
_X_ Published in a peer-reviewed journal

Nature Publishing Group
In Volume 8, 778-789, 2014

The ISME Journal (2014) 8, 778–789

www.nature.com/ismej

ORIGINAL ARTICLE

Modular community structure suggests metabolic plasticity during the transition to polar night in ice-covered Antarctic lakes

Trista J Vick-Majors[1], John C Priscu[1] and Linda A Amaral-Zettler[2,3]
[1]*Montana State University, Department of Land Resources and Environmental Sciences, Bozeman, MT, USA;* [2]*The Josephine Bay Paul Center for Comparative Molecular Biology and Evolution, Marine Biological Laboratory, Woods Hole, MA, USA and* [3]*Department of Geological Sciences, Brown University, Providence, RI, USA*

High-latitude environments, such as the Antarctic McMurdo Dry Valley lakes, are subject to seasonally segregated light–dark cycles, which have important consequences for microbial diversity and function on an annual basis. Owing largely to the logistical difficulties of sampling polar environments during the darkness of winter, little is known about planktonic microbial community responses to the cessation of photosynthetic primary production during the austral sunset, which lingers from approximately February to April. Here, we hypothesized that changes in bacterial, archaeal and eukaryotic community structure, particularly shifts in favor of chemolithotrophs and mixotrophs, would manifest during the transition to polar night. Our work represents the first concurrent molecular characterization, using 454 pyrosequencing of hypervariable regions of the small-subunit ribosomal RNA gene, of bacterial, archaeal and eukaryotic communities in permanently ice-covered lakes Fryxell and Bonney, before and during the polar night transition. We found vertically stratified populations that varied at the community and/or operational taxonomic unit-level between lakes and seasons. Network analysis based on operational taxonomic unit level interactions revealed nonrandomly structured microbial communities organized into modules (groups of taxa) containing key metabolic potential capacities, including photoheterotrophy, mixotrophy and chemolithotrophy, which are likely to be differentially favored during the transition to polar night.
The ISME Journal (2014) **8,** 778–789; doi:10.1038/ismej.2013.190; published online 24 October 2013
Subject Category: Microbial population and community ecology
Keywords: ice-covered lake; McMurdo Dry Valleys; microbial diversity; MIRADA-LTERS; network analysis; polar night

Introduction

Microbial diversity and function in aquatic ecosystems are tightly coupled to the physical and geochemical environment (Judd *et al.*, 2006; Galand *et al.*, 2008; Bielewicz *et al.*, 2011). The importance of seasonal succession is increasingly being recognized within the context of geochemically distinct environments (Crump *et al.*, 2003; Andersson *et al.*, 2010; Ghiglione and Murray, 2012; Grzymski *et al.*, 2012). Polar environments are subject to strong seasonal light gradients, where 24-hour daylight drives continual photoautotrophic primary production during the summer, often coinciding with high rates of heterotrophic bacterioplankton production (Takacs and Priscu, 1998; Morán *et al.*, 2001; Alonso-Sáez *et al.*, 2008). Winter sampling is logistically difficult in the polar regions, and thus studies examining microbial dynamics during the darkness of winter and the spring and autumn transition periods are few. Recent studies have shown higher bacterial community richness (Ghiglione and Murray, 2012) and the increased importance of chemolithotrophic Archaea in the Southern Ocean during winter (Grzymski *et al.*, 2012; Williams *et al.*, 2012), whereas others have shown that trophic plasticity is a key survival strategy for protists during the summer–winter transition in Antarctic lakes (Bielewicz *et al.*, 2011).

The perennially ice-covered lakes of the McMurdo (MCM) Dry Valleys, which lie in East Antarctica in the coldest, driest desert on earth, comprise physicochemically stable environments containing microbially dominated ecosystems (Spigel and Priscu, 1998; Takacs and Priscu, 1998;

Correspondence: LA Amaral-Zettler, The Josephine Bay Paul Center, Marine Biological Laboratory, 7 MBL Street Woods Hole, Woods Hole, MA 02543, USA.
E-mail: amaral@mbl.edu
Received 15 May 2013; revised 23 August 2013; accepted 20 September 2013; published online 24 October 2013

Priscu *et al.*, 1999; Vick and Priscu, 2012). As the sole year-round source of liquid water, such lakes provide the only continuous habitat for aquatic life in the ice-free regions of the Antarctic continent. Permanent ice covers on the lakes severely attenuate the penetration of solar irradiance to between 1% and 2% of incident light (Lizotte and Priscu, 1994) and prohibit wind-driven turbulence, propagating an environment continuously stratified with regard to solar energy and nutrients. A few studies have examined the molecular diversity of bacterial, archaeal (Karr *et al.*, 2005; Glatz *et al.*, 2006; Karr *et al.*, 2006) or protistan (Bielewicz *et al.*, 2011; Kong *et al.*, 2012a) communities in MCM lakes and found that communities are distinctly stratified by depth. The physicochemical stability of these environments makes them excellent locations to examine the impact of seasonal light–dark cycles on microbial community dynamics.

Most studies of the MCM lakes have been confined to summer, when phytoplankton primary production and glacial melt water streams supply >50% of the organic matter supporting heterotrophic growth (Takacs *et al.*, 2001), but a few have examined the activities of bacterioplankton (Takacs and Priscu, 1998; Vick and Priscu, 2012), phytoplankton (Lizotte *et al.*, 1996), flagellates (Thurman *et al.*, 2012) and the diversity of protists (Bielewicz *et al.*, 2011) during the transition periods flanking summer and winter. Mixotrophy, via the combined use of photosynthesis and phagotrophy, is a key adaptive strategy for phytoplankton in MCM lakes that likely allows populations to persist throughout the winter (McKnight *et al.*, 2000; Laybourn-Parry, 2002; Bielewicz *et al.*, 2011; Thurman *et al.*, 2012), whereas metabolic plasticity, such as the ability to switch carbon substrates, is important for heterotrophic bacterioplankton to remain active during winter when phytoplankton-produced organic carbon is in short supply (Vick and Priscu, 2012). Clearly, trophic and metabolic versatilities are vital to the survival of given populations in these lakes and are important to the maintenance of overall ecosystem function.

In addition to physicochemical controls on microbial community structure, recent studies have also shown that microbial co-occurrence patterns can help define ecologically meaningful interactions between species and across domains (Horner-Devine *et al.*, 2007; Fuhrman and Steele, 2008; Steele *et al.*, 2011) and that co-occurring species are often organized into groups, or modules, of functional significance (Chaffron *et al.*, 2010; Barberán *et al.*, 2012). In light of the physicochemical stability of the MCM lakes, we sought to determine the importance of both community succession and operational taxonomic unit (OTU)-level co-occurrence patterns to overall community structure during the summer – autumn transition period (November–March). We used pyrosequencing of the V6 (bacterial and archaeal) and V9 (eukaryotic) hypervariable regions of the small-subunit ribosomal RNA gene on samples from two geochemically distinct MCM lakes, Lake Fryxell (FRX) and the West Lobe of Lake Bonney (WLB), during the austral summer (November) and autumn (March) to analyze microbial community composition, and implemented molecular ecological network analysis to examine inter- and intra-domain co-occurrence patterns.

We provide the first evidence for seasonal shifts in bacterial, archaeal and eukaryotic communities in these Antarctic lakes. Our data also suggest the importance of metabolically plastic taxa in maintaining overall ecosystem function and document the proliferation of several archaeal lineages, which may be important primary producers during the darkness of winter. In combination with studies from the polar oceans (Grzymski *et al.*, 2012; Ghiglione and Murray, 2012; Williams *et al.*, 2012), our results reveal that shifts in community diversity may be characteristic of polar ecosystems during winter and have particular importance in fueling continued biogeochemical cycling in the absence of photosynthetic primary production.

Methods

Sample collection

Duplicate samples for DNA extraction were collected from FRX (depth ~18 m) and WLB (depth ~38 m) during the Austral summer and autumn at depths of 6 m (bacterial and primary production maximum) and 9 m (chemocline; chlorophyll-*a* maximum) in FRX (2 November 2007 and 25 March 2008) and 13 m (chemocline; bacterial production, chlorophyll-*a,* primary production maximum) and 18 m (hypersaline, bottom of trophogenic zone) in WLB (30 November 2007 and 12 March 2008). Corresponding environmental data were collected by the MCM Long-Term Ecological Research program ~1 week before and 1 week after samples for DNA collection and interpolated to the DNA sample collection date (11 November and 5 December 2007, and 20 and 28 March for FRX; 25 November and 15 December 2007, and 7 and 14 March for WLB). In WLB, environmental data were collected at 17 and 20 or 25 m and interpolated to 18 m. Complete environmental data and methods are available on the MCM Long-Term Ecological Research website (http://www.mcmlter.org/) and are published elsewhere (Vick and Priscu, 2012), and the minimum information about a marker gene sequence-compliant (Yilmaz *et al.*, 2011) environmental data are summarized in supplementary information. Representative vertical profiles of temperature, conductivity and oxygen from each lake are shown in Supplementary Figure S1, and environmental data in Supplementary Table S1. Temperature and conductivity were measured with a SBE 25 Sealogger CTD according to Spigel and Priscu (1998), and dissolved oxygen was measured

using the azide modification of the mini-Winkler titration. All water samples were collected through a borehole in the ice cover using a Niskin bottle. Samples for DNA extraction were filtered onto 0.2-μM Sterivex filters (Millipore, Billerica, MA, USA) and stored with 2.0 ml of Puregene lysis buffer at −20 °C until further processing. DNA was extracted as described previously (Amaral-Zettler *et al.*, 2009), and water filtration and DNA extraction protocols can be found at http://amarallab.mbl.edu.

Sequencing
We amplified V6 hypervariable regions using primers targeting positions (according to the *E. coli* numbering scheme) 947–1046 (Bacteria) and positions 958–1048 (Archaea) of the 16S ribosomal RNA gene. For Eukarya, amplification of the V9 hypervariable region followed established protocols (Amaral-Zettler *et al.*, 2009). We multiplex-sequenced the resulting amplicons using bar-coded primers (Huber *et al.*, 2007; Amaral-Zettler *et al.*, 2009) on a 454 Genome Sequencer FLX (Roche, Switzerland) using the manufacturer's recommended protocol. The number of reads obtained on a single sample ranged from 1724 to 23 334 (Archaea), 2997 to 15 552 (Bacteria) and 2602 to 12 504 (Eukarya) (Supplementary Table S2).

Sequence processing
Sequences were trimmed, and low-quality reads were removed according to Huse *et al.*, 2007. Sequences were clustered into OTUs using ESPRIT, SLP and mothur to precluster (2%) sequences using single linkage and construct final clusters based on pairwise alignment and average linkage (Huse *et al.*, 2010). Three-percent cluster widths were used for bacterial and archaeal analyses and 6% for eukaryotic analyses. This clustering method is equally effective as 'denoising' data via methods such as Pyronoise to minimize OTU inflation (Quince *et al.*, 2011). All of our sequence data are minimum information about a marker gene sequence-compliant (Yilmaz *et al.*, 2011) and have been deposited in the National Center for Biotechnology Information normal and Sequence Read Archives under the accession number SRP028879.

Taxonomy assignment
Taxonomic classification was assigned using the Global Alignment for Sequence Taxonomy (GAST) method (Huse *et al.*, 2008). Briefly, hypervariable tag reference sets (V6 or V9) were created from a ribosomal RNA reference database based on the SILVA database (Pruesse *et al.*, 2007), with taxonomy assigned by the RDP Classifier (Wang *et al.*, 2007). We then aligned the tag sequences against the top 100 reference sequences using MUSCLE and considered the best GAST match. Smaller GAST distances equate to better matches. We assigned a tag to a given genus if two-thirds or more of the full-length reference ribosomal RNA sequences containing the exact hypervariable region shared the same genus. If there was no agreement, we moved up the tree one level to family and so on until a consensus was reached.

Diversity calculations
Parametric alpha diversity estimates for Bacteria and Archaea were calculated using CatchAll version 3.2 (Bunge *et al.*, 2012), and eukaryotic nonparametric (Chao2) richness estimates (Chao, 1987) were calculated with the program SPADE (Chao and Shen, 2010). All calculations were performed on pooled sequences from duplicate samples for bacteria and archaea and separate replicated samples for eukaryotes. We performed these calculations using full data sets, as well as normalized data sets in which the number of sequences per sample was made equal through random resampling.

Network analysis
To determine associations between microbial populations and between microbial populations and the environment, we calculated Spearman correlations between environmental data, relative abundances of bacterial and archaeal OTUs and presence–absence of eukaryotic OTUs. Significant correlations ($P<0.01$; $r\geqslant0.8$) were extracted and the resulting matrix of correlation coefficients was loaded into the program Cytoscape (Shannon *et al.*, 2003) for visualization. In total, we included 899 variables in our correlation analysis: 186 eukaryotic, 637 bacterial and 69 archaeal OTUs, as well as 7 environmental variables.

Statistics
Statistics were carried out in R (R Development Core Team, 2008). Beta diversity was examined and plotted using the function nmds (non-metric multidimensional scaling) in the R library labdsv (Roberts, 2010). The importance of environmental factors in partitioning of beta diversity was tested using permutational analysis of variance (Anderson, 2001) with the adonis function, and *C*-scores were calculated using the oecosimu function with nestedchecker (Stone and Roberts, 1990) and quasiswap (Miklós and Podani 2004) in the R library vegan (Oksanen *et al.*, 2010). Network statistics, including modularity calculations, were carried out using Cytoscape (Shannon *et al.*, 2003; Supplementary Information).

Results and discussion

Seasonal variation in microbial communities
Species richness (alpha diversity) was relatively low across all samples and all three domains, but it

followed trends observed in other environments with bacterial richness surpassing archaeal and eukaryotic richness by an order of magnitude (Huber *et al*., 2007, McCliment *et al*., 2012). Alpha diversity was generally higher in autumn samples for bacterial and eukaryotic communities in FRX, whereas the opposite was true in WLB (except for 18 m bacterial communities). Archaeal diversity was lower than bacterial and eukaryotic diversity (Figure 1), with coverage (observed/expected diversity) ranging from 53 to 90%. Eukaryotic coverage was highest, ranging from 87 to 98%, whereas bacterial coverage was comparatively low (15 to 50%; Supplementary Table S2).

Actinobacteria and Bacteroidetes dominated the bacterial communities of both lakes. This is consistent with reports from other freshwater systems (Newton *et al*., 2011). The Proteobacteria was the next most abundant phylum in both lakes, with the class Betaproteobacteria dominating FRX and Gammaproteobacteria dominating WLB, a difference that may be explained by the influence of Blood Falls, a Gammaproteobacteria-dominated subglacial feature that flows into the western terminus of WLB (Mikucki and Priscu, 2007). Marine Group I Crenarchaeota dominated the archaeal communities, similar to the upper and intermediate waters of Arctic meromictic Lake A (Comeau *et al*., 2012), followed by Thermoplasmatales-related Euryarchaeotes and Methanomicrobia. Eukaryotic community composition varied between lakes and depths, with Cryptomonadales and Ciliophora OTUs being the most frequently encountered in FRX, whereas WLB contained OTUs most frequently affiliated with Cryptomonadales, Stramenopiles and Dinoflagellata (Figure 2).

Bacterial and eukaryotic communities both grouped by lake (permutational analysis of variance; $P=0.0010$ for Bacteria, $P=0.0020$ for Eukarya) and depth ($P=0.0010$ for Bacteria and Eukarya). Season (summer vs autumn) was not significant alone, but when included in a model that first accounted for the interaction between lake and depth it explained a significant portion of the variation in the bacterial and eukaryotic communities ($P=0.013$ and $P=0.042$, respectively). These results indicate that within lake and depth, bacterial and eukaryotic communities were significantly different between seasons (Figure 3). Archaeal communities did not clearly partition by lake, depth or season, but a model accounting for lake and season indicated that depth was the most important factor explaining the variation between communities ($P=0.042$; Figure 3). The effects of lake and season were marginally significant for the Archaea ($P=0.14$ and 0.12, respectively). These results are similar to the seasonal and depth partitioning observed in Arctic meromictic Lake A, where bacterial and eukaryotic phyla varied as a function of both depth and time, and archaeal phylum-level seasonal changes were minor, but depth partitioning was strong (Charvet *et al*., 2012a, Comeau *et al*., 2012).

Seasonal changes in community composition were apparent at the OTU level as the percentage of OTUs that went from being rare (<0.1% of community) or absent in summer samples to being abundant (>0.1% of community; Crump *et al*., 2012) in autumn samples. The changes in composition, shown in Figure 4 as points falling along the *y* axes, were especially pronounced for the Archaea, describing 28% and 23% of the 6 m and 9 m FRX communities, respectively, and 14% and 10% of the 13 m and 18 m WLB communities, respectively. OTU-level changes in community composition were comparatively small for the Bacteria (0.8 to 5.5% of the communities) and Eukarya (1.7 to 3.0% of OTUs). The use of a higher cutoff (1.0%) for the rare to abundant transition did not change the pattern, although it decreased the percentages (Archaea = 4 to 12%, Bacteria = 0.2 to 1.0%, Eukarya = 0 to 2.0%).

Although they were not the dominant members of the communities overall, Stramenopiles (mostly chrysophytes) dominated the eukaryotic OTUs that became abundant during autumn. Charvet *et al*. (2012b) suggested that the generally small size of chrysophyte cells, relative to other phytoplankton, may account for their dominance in oligotrophic

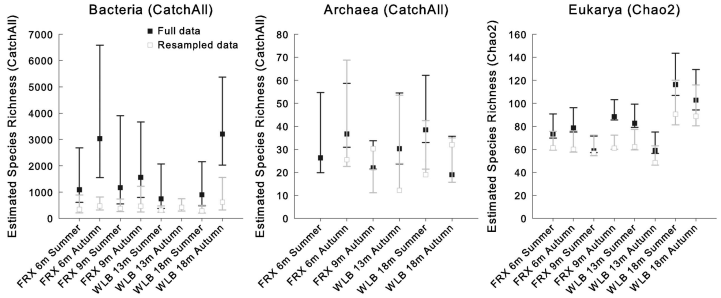

Figure 1 Alpha diversity estimates with Bonferroni-corrected confidence bounds calculated with CatchAll for Bacteria and Archaea and as the Chao2 index for Eukarya. Archaeal diversity estimates could not be calculated for the FRX 9 m and WLB 13 m summer samples owing to insufficient numbers of reads.

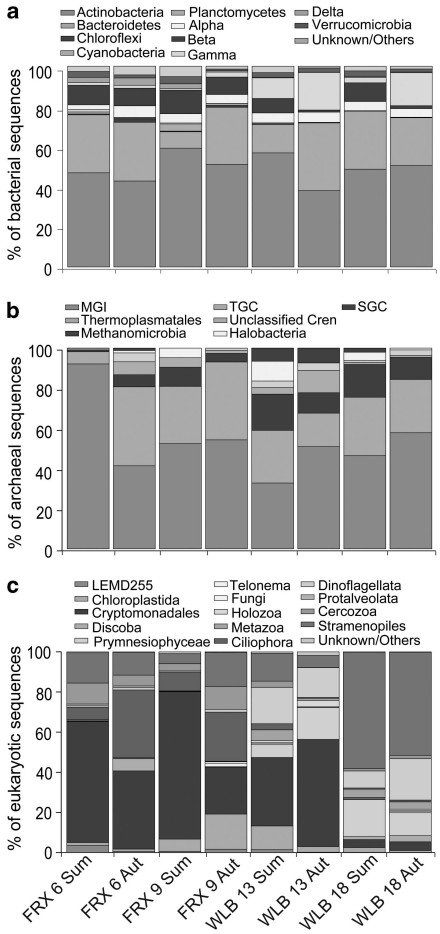

Figure 2 Phylum-level diversity of bacterial (**a**), archaeal (**b**) and eukaryotic (**c**) communities in Lakes FRX and WLB during summer (Sum) and autumn (Aut). Bacterial and archaeal OTUs were determined at 97% sequence similarity, and eukaryotic OTUs were determined at 94% sequence similarity. Alpha, Beta, Gamma and Delta refer to the subclasses of Proteobacteria. MGI refers to Marine Group I Crenarchaeota, TGC refers to Terrestrial Group Crenarchaeota and SGC refers to Soil Group Crenarchaeota.

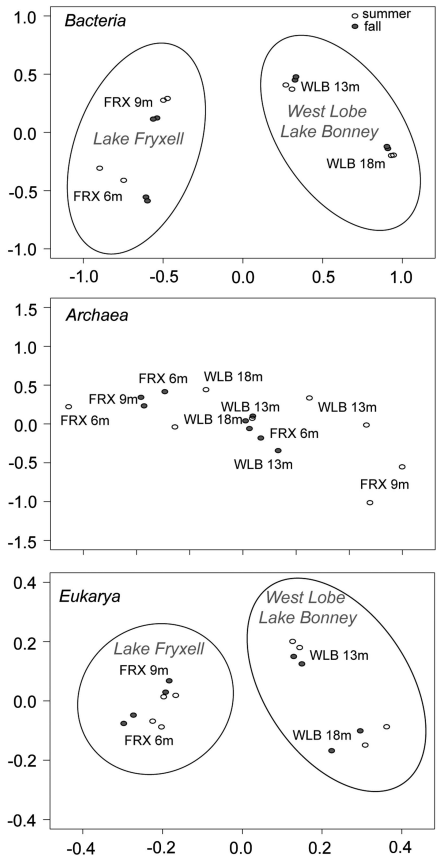

Figure 3 Non-metric multidimensional scaling of bacterial and archaeal (relative abundance; Bray-Curtis dissimilarity; stress = 2.49 and 4.97, respectively) and eukaryotic (presence-absence; Sørensen's similarity; stress = 4.68) communities.

Arctic lakes; decreasing phosphorous concentrations in autumn samples (Vick and Priscu, 2012) may have favored the proliferation of chrysophytes in FRX and WLB. Lizotte *et al.* (1996) found that chrysophyte communities in the Lake Bonney photic zone were dominated by the mixotrophic genera *Ochromonas*, which may persist through the seasonal sunset by switching to phagotrophy. The Alphaproteobacteria dominated the autumn proliferation of bacterial OTUs. This contrast with the Actinobacteria- or Bacteroidetes-dominated total communities (summer and autumn together; Figure 2) indicates that the most numerically abundant phyla in the lakes are also capable of persisting through changing environmental conditions, whereas less abundant phyla may opportunistically increase under changing conditions.

Sixty-eight percent of the archaeal OTUs that increased in density during autumn belonged to the Euryarchaeota; half of those grouped with marine or aquatic lineages, whereas the other half grouped with methanogenic clades. The non-methanogenic Euryarchaeota that became abundant during autumn were all members of the Marine Group II, which are known to form seasonal blooms in the surface waters of the North Sea (Pernthaler *et al.*, 2002). One Marine Group II OTU (Archaea_03_5) increased from 3.0% and 0% to 27.3% and 16.5% of the archaeal sequences in the surface and 9 m waters, respectively, of FRX. Thirty-two percent of the autumn archaeal OTUs belonged to the Crenarchaeota, which were dominated by terrestrial and soil groups (42.9%), followed by the Marine Group I Crenarchaeota (28.6%). The increase in euryarchaeal

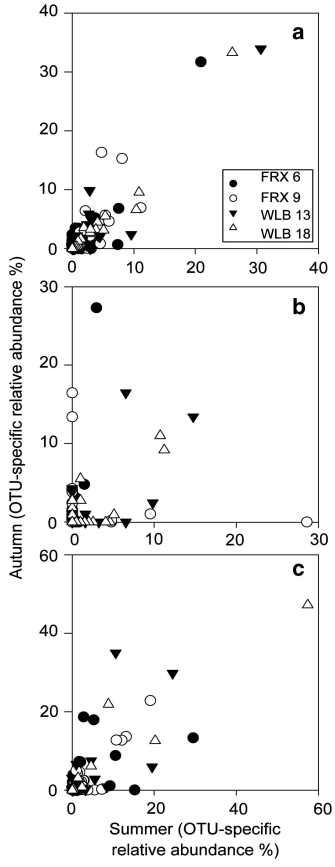

Figure 4 Relative abundances (%) of bacterial (**a**), archaeal (**b**) and eukaryotic (**c**) OTUs during summer and autumn. Bacterial and archaeal OTUs were calculated at 97% sequence similarity, and eukaryotic OTUs were calculated at 94% sequence similarity.

OTUs relative to crenarchaeal OTUs was distinct from the composition of the overall communities, which were dominated by Crenarchaeota rather than Euryarchaeota (Figure 2).

The proliferation of archaeal phylotypes (Grzymski *et al.*, 2012) and proteins associated with chemolithotrophic Archaea (Williams *et al.*, 2012) was reported in Southern Ocean waters during the winter, suggesting that summer communities dominated by photoautotrophy shift to chemolithotrophy during the polar night. Molecular and cultivation studies have revealed the presence of diverse chemolithotrophic microorganisms in FRX and WLB (Priscu *et al.*, 1996, Voytek *et al.*, 1999; Karr *et al.*, 2005; Sattley and Madigan 2006; Kong *et al.*, 2012a), and dark carbon fixation attributed to chemolithotrophs has been measured in these same lakes (Priscu *et al.*, 1996, Vick and Priscu, unpublished data). Kong *et al.* (2012b) showed that Proteobacteria actively produced RubisCO in WLB during February and March, indicating that chemolithotrophic bacteria were active during the summer–autumn transition. Currently, there are no data regarding the activities of chemolithotrophic archaea in the photic zones of the MCM lakes, but the proliferation of archaeal sequences during autumn suggests that they may be important.

Part of the autumn archaeal 'bloom' was also owing to the appearance of Terrestrial and Soil Group Crenarchaeota, indicating that allochthonous inputs may affect community structure. Eolian transport is an important dispersal mechanism in the MCM (Šabacká *et al.*, 2012), and the downward migration of lake ice particulate matter (Squyres *et al.*, 1991; Jepsen *et al.*, 2010) may introduce microorganisms (Paerl and Priscu, 1998; Priscu *et al.*, 1998; Gordon *et al.*, 2000) into the water column. Similarly, mid-summer stream-flow is an important source of nutrients, particulate matter (Takacs *et al.*, 2001; Foreman *et al.*, 2004) and perhaps microorganisms (Vincent and Howard-Williams, 1986) to the lakes. Alternatively, the sequences may group with terrestrial lineages, but actually represent native aquatic organisms. Whether these putatively terrestrial sequences are transient, inactive or represent part of the active microbial assemblage is unknown.

Putatively methanogenic lineages (Methanomicrobia and Methanobacteria) accounted for 27% of the autumn proliferation of archaeal OTUs, although the most abundant methanogenic lineages decreased between summer and autumn. All of our samples were taken from oxygenated portions of the water column, but all known Methanomicrobia and Methanobacteria are strict anaerobes. Methanomicrobial sequences in soils surrounding FRX and WLB (Takacs-Vesbach unpublished data) and functional methanogens in the deep waters of FRX (Karr *et al.*, 2006) are possible sources of methanogenic sequences; however, a local BLAST search showed that none of the terrestrial or FRX sequences matched the sequences in our study (data not shown). It is possible that our methanogenic sequences are not functionally methanogens, but their average GAST distances were small (0 to 0.03), indicating >95% accuracy of GAST taxonomic assignments (Huse *et al.*, 2008). Methane production has been documented in oxygenated seawater (Karl *et al.*, 2008, Damm *et al.*, 2010) and an oxygenated oligotrophic lake, where planktonic and phytoplankton-attached Archaea actively transcribed the methyl coenzyme *M reductase A* gene for methanogenesis (Grossart *et al.*, 2011). Damm *et al.* (2010) and Grossart *et al.* (2011) both connected methanogenesis in oxygenated water to phytoplankton activity, and the high concentrations of DMSP in WLB at 13 m (Lee *et al.*, 2004) may provide a substrate pool for methanogenesis through its degradation product methanethiol (Damm *et al.*, 2010). Although the metabolic state of the putatively

methanogenic cells in our study is unknown, their presence combined with the supersaturation of methane starting at 12 m in WLB (Priscu and Dore, unpublished data) suggests the possibility of active methanogenesis.

Co-occurrence patterns and the molecular ecological network

Nonrandom community assembly, denoted by nonrandom co-occurrence patterns, is characteristic of assemblages of organisms across domains of life (Gotelli and McCabe, 2002; Horner-Devine *et al*., 2007). We compared the co-occurrence patterns found in our bacterial, archaeal and eukaryotic sequence data with those of a null distribution, representing random co-occurrence, and used the *C*-score metric (Stone and Roberts 1990) to determine whether our data differed significantly from a randomly assembled community. We observed nonrandom co-occurrence patterns for our whole data set (*C*-score = 1.56, $P = 0.01$) and for the Bacteria and Eukarya (*C*-score = 1.52, $P = 0.01$ and *C*-score = 1.61, $P = 0.01$, respectively), whereas the *C*-score for the Archaea alone was marginally significant (*C*-score = 1.41, $P = 0.19$).

To describe the importance of biotic and abiotic interactions in explaining the nonrandom co-occurrence patterns, we generated a molecular ecological network based on Spearman correlations ($P \leqslant 0.01$, $r \geqslant 0.8$) between relative abundances of Bacterial and Archaeal OTUs, presence–absence of Eukaryotic OTUs and discrete values of environmental parameters. In total, we found 20 793 significant correlations between 872 variables (Supplementary Figure S2). We used modularity to detect community structure in our network (Fortunato, 2010; Supplementary Information), resulting in 27 modules containing groups of interconnected nodes (Figure 5; Supplementary Table S3). Each module was designated by a key (the OTU with the highest assignment value to the module) and numbered for convenience in the discussion (Table 1). The modules most important to the network structure were determined based on betweenness centrality (BC). González *et al.*, 2010 showed that nodes with high BC scores were particularly important in maintaining the connectivity of an ecological network, and compared them with keystone species. Nine of 27 modules in our network had BC scores > 0 (range 0.005–0.19; Table 1).

We examined the modules with significant BC scores and the modules containing the autumn blooming Archaea in detail, and attempted to assign functions based on the putative physiologies of the organisms present (Supplementary Table S5). Bielewicz *et al*., (2011) suggested that trophic or metabolic plasticity allows organisms to be more successful in the MCM lakes, and our module analysis supports the importance of innovative energy capture and metabolic flexibility during the transition to polar night.

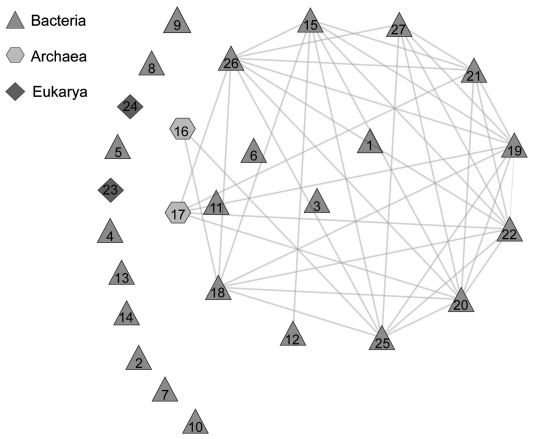

Figure 5 Modules in the molecular ecological network determined by ModuLand. Each module is named according to the node with maximum assignment value to the module.

On the basis of its high BC score (0.19; nearly twice the next highest BC), Module 15 forms the keystone (González *et al*., 2010) of the MCM network. Five OTUs (40% of the module) were related to taxa that can produce proteorhodopsins (Atamna-Ismaeel *et al*., 2008, Oh *et al*., 2011, Huggett and Rappé, 2012), including the module key, Alphaproteobacteria_03_91 (*Pelagibacter*, GAST = 0.049), Bacteroidetes_03_1 (Flavobacteriacea, GAST = 0.0029) and Gammaproteobacteria_03_175 (*Oceanospirillales*, GAST = 0.0026). Proteorhodopsins are light-driven proton pumps found mainly in marine and freshwater Alphaproteobacteria, Gammaproteobacteria, Flavobacteria and some Euryarchaeota, which, along with heterotrophic metabolism, can generate energy for growth ('photoheterotrophy'; Giovannoni *et al*., 2005; Frigaard *et al*., 2006; Atamna-Ismaeel *et al*., 2008; DeLong and Béjà, 2010; Steindler *et al*., 2011) and provide a competitive advantage under conditions of organic carbon or nutrient limitation (Giovannoni *et al*., 2005), such as those found in the MCM lakes. Fluctuations in the quality and quantity of available organic carbon are thought to affect heterotrophic bacterioplankton metabolism in the MCM lakes during autumn (Vick and Priscu, 2012), and although nutrient limitation is perennial in these lakes phytoplankton activity results in a spring/summer drawdown of N and P (Lizotte *et al*., 1996). In addition to putatively photoheterotrophic OTUs, which account for 40% of the module, Module 15 contains two OTUs of the genus *Hydrogenophaga* (GAST = 0.0014 and 0.002), which are typically facultatively autotrophic organisms capable of oxidizing hydrogen or using organic carbon to generate energy (for example, Yoon *et al*., 2008). In total, 53% of the module belongs to groups known to be metabolically flexible, suggesting that oligotrophy

Table 1 Highest-level taxonomy definition for module keys with the average GAST distance for the reported taxonomy and the betweenness centrality score for each module

Module ID	*Module Number*	*Taxonomy*	*Average GAST Distance*	*Module Betweenness Centrality Score*
Acidobacteria_03_11260	1	*Acidobacteriaceae*	0.241	0
Acidobacteria_03_15770	2	*Acidobacteriaceae*	0.258	0
Acidobacteria_03_18	3	*Geothrix*	0.003	0
Acidobacteria_03_1982	4	*Acidobacteriaceae*	0.0165	0
Acidobacteria_03_231	5	*Solibacter*	0.0531	0
Acidobacteria_03_5976	6	*Acidobacteriaceae*	0.254	0
Actinobacteria_03_11036	7	*Acidimicrobiaceae*	0.105	0
Actinobacteria_03_3	8	*Actinobacteria*	0.0026	0
Actinobacteria_03_4	9	*Sporichthyaceae*	0.0016	0
Actinobacteria_03_91	10	*Micrococcus*	0.0031	0
Alphaproteobacteria_03_13239	11	*Rhodospirilliaceae*	0.281	0
Alphaproteobacteria_03_2014	12	*Rickettsiaceae*	0.0482	0
Alphaproteobacteria_03_62	13	*Caulobacteraceae*	0.0052	0
Alphaproteobacteria_03_6621	14	*Sneathiella*	0.0078	0
Alphaproteobacteria_03_91	15	*Pelagibacter*	0.0496	0.19
Archaea_03_117	16	*Methanomicrobiales*	0	0
Archaea_03_17	17	*Thermoplasmatales*	0.0102	0
Bacteroidetes_03_1296	18	*Flexibacter*	0.0188	0.07
Bacteroidetes_03_168	19	*Croceibacter*	0.0236	0.04
Bacteroidetes_03_262	20	*Flavobacterium*	0.0005	0.04
Betaproteobacteria_03_143	21	*Herbaspirillum*	0.0827	0.02
Betaproteobacteria_03_51	22	*Methyloversatilis*	0.0063	0.04
Eukarya_06_1718	23	*Pteridomonas*	0.023	0
Eukarya_06_1772	24	*Chlorogonium*	0.023	0
Gammaproteobacteria_03_4	25	*Pseudomonas*	0.0015	0.1
Planctomycetes_03_726	26	*Planctomyces*	0.0169	0.04
Verrucomicrobia_03_119	27	*Opitutus*	0.0077	0.005

and the strong seasonality associated with the MCM lakes favor the ability to shift between energy resources in response to changing environmental conditions. In addition, Module 15's keystone status indicates that these abilities are integral to the MCM lake ecosystem function.

Module 17 contained five of the nodes representing the autumn proliferation of archaeal phylotypes (Figure 4, Supplementary Table S3; Archaea_03_17), and it provides another example of competitive energy acquisition in MCM lakes. Two of the nodes belong to the Marine Group I Crenarchaeota and may signify an autumn shift in favor of chemolithotrophic metabolisms similar to that found in the Southern Ocean (Grzymski *et al.*, 2012; Williams *et al.*, 2012). Nodes representing the Marine Group II of the Euryarchaeota also group with Module 17. Currently, there are no cultured representatives of Marine Group II, and thus little is known about their range of metabolic capabilities. However, a complete genome representing the Marine Group II Euryarchaeota was recovered from a Puget Sound metagenome (Iverson *et al.*, 2012), revealing a photoheterotrophic, proteorhodopsin-containing organism. A PCR-based study of Archaea from the North Pacific Subtropical Gyre concluded that approximately 10% of Euryarchaeota contained proteorhodopsin genes (Frigaard *et al.*, 2006). If the putative functions assigned to the Archaea in Module 17 are correct, the module provides further evidence for the importance of metabolic flexibility and suggests that chemolithotrophy may be important in fueling ecosystem production during the polar night.

Protistan organisms often rely on mixotrophic lifestyles to cope with the oligotrophic conditions and seasonal light–dark cycles in MCM lakes (Laybourn-Parry 2002; Bielewicz *et al.*, 2011; Thurman *et al.*, 2012). Phototrophic nanoflagellates in WLB increased their grazing rates on fluorescently labeled bacterial prey throughout the month of March (Thurman *et al.*, 2012), supporting the suggestion of Bielewicz *et al.* (2011) that cryptophyte populations use phagotrophy as an adaptive strategy during the summer – winter transition. Similarly, our results showed that Chrysophyceae, which are generally dominated by the mixotrophic genus *Ochromonas* in these lakes (Lizotte *et al.*, 1996), likely increased in abundance during the autumn. Module 22 (BC = 0.04, Supplementary Table S3, Betaproteobacteria_03_51) contained 35% of the eukaryotic OTUs that became abundant during autumn, including all of the Chrysophyceae, the heterotrophic nanoflagellate *Cryothecomonas* and a ciliate.

Module 26 (BC = 0.04) contained Actinobacteria (22% of the module), including members of the genus *Microthrix* (Actinobacteria_03_174; GAST = 0.0095). *Microthrix* and other Actinobacteria generate carbon and energy storage compounds (triacylglcerols), store polyphosphates and possess high-affinity Pst *P*-uptake systems, all of which may

help the organisms compete under conditions of unbalanced growth and *P*-limiting conditions (McIlroy *et al.* 2013), such as those found in Lake Bonney (Dore and Priscu, 2001). In addition, *Planktophila* (Actinobacteria_03_32; GAST = 0.0028) are important polysaccharide degraders with the ability to mineralize *N*-acetylglucosamine, a breakdown product of bacterial cell walls, which may assist in winter survival, and contain actinorhodopsin (Garcia *et al.*, 2013), suggesting a role for photoheterotrophy in Module 26.

Module 21 (BC = 0.02; Key = Betaproteobacteria_03_143) contained mostly heterotrophic bacteria and a few Archaea, and a majority of the OTUs in the module increased between the summer and autumn sampling points, especially in the shallower waters of the lakes. Typically, phytoplankton production is thought to draw down nutrient concentrations during the summer, leading to increased nutrient depletion in the already oligotrophic waters of the FRX and WLB photic zones. Members of the Actinobacteria have been shown to proliferate under low-nutrient conditions (reviewed in Newton *et al.*, 2010). The module also contains putative nitrogen-fixing bacteria, which may have increased in response to decreasing nutrient concentrations (Alphaproteobacteria_03_431, Alphaproteobacteria_03_15, Alphaproteobacteria_03_808 and Betaproteobacteria_03_143, the module key).

Taken together, these modules provide evidence for the importance of metabolic and trophic plasticity and nutrient scavenging in the MCM lakes. Other significant modules are discussed in Supplementary Information and provide further examples of the adaptation to oligotrophic or changing environments, along with insights into organic matter processing and eukaryote – prokaryote interactions in lakes FRX and WLB.

Conclusions

Our study comprises the first high-throughput sequencing evaluation of the diversity of Bacteria, Archaea and Eukarya in permanently ice-covered lakes of the Antarctic MCM Dry Valleys. We found that these light- and nutrient-limited systems exhibit low diversity overall, but that the autumn decrease in solar radiation coincides with increases or shifts in microbial diversity across all three domains of life. The statistically significant partitioning of bacterial and eukaryotic communities by season within lake and depth suggests, in agreement with past studies, that these communities are strongly controlled by the vertically stratified water columns of lakes FRX and Bonney, but that they also respond to the change in season. The low archaeal diversity was offset by an autumn 'bloom' of archaeal OTUs, which likely stemmed from a combination of allochthonous inputs and proliferation of organisms adapted to the winter darkness. Similarly, we found OTUs whose closest relatives are adapted to low-nutrient environments, photoheterotrophic and mixotrophic lifestyles, to be particularly important in the modular community structure in these lakes. We suggest future studies focusing on functional gene analysis, metagenomics or transcription to examine the relationships revealed by our molecular ecological network analysis.

Conflict of Interest

The authors declare no conflict of interest.

Acknowledgements

We would like to thank the MCM Microbial Observatory, Sukkyun Han, Chao Tang, Amy Chiuchiolo and Marie Šabacká for assistance with sample collection, the 2007–2008 McMurdo Long-Term Ecological Research limnology team for assistance with environmental data collection and Elizabeth McCliment for assistance with sequencing. Funding was provided by NSF DEB-0717390 to Linda A Amaral-Zettler (MIRADA-LTERS) and OPP-1115254, OPP-0838953, OPP-1027284 and OPP- 0839075 to John C Priscu. The Montana Space Grant Consortium provided additional funding for Trista Vick-Majors.

References

Alonso-Sáez L, Sánchez O, Gasol JM, Balagué V, Pedrós-Alio C. (2008). Winter-to-summer changes in the composition and single-cell activity of near-surface Arctic prokaryotes. *Environ Microbiol* **10**: 2444–2454.

Amaral-Zettler LA, McCliment EA, Ducklow HW, Huse SM. (2009). A method for studying protistan diversity using massively parallel sequencing of V9 hypervariable regions of small-subunit ribosomal RNA genes. *PLoS One* **4**: e6372.

Anderson MJ. (2001). A new method for non-parametric multivariate analysis of variance. *Austral Ecology* **26**: 32–46.

Andersson AF, Riemann L, Bertilsson S. (2010). Pyrosequencing reveals contrasting seasonal dynamics of taxa within Baltic Sea bacterioplankton communities. *ISME J* **4**: 171–181.

Atamna-Ismaeel N, Sabehi G, Sharon I, Witzel K-P, Labrenz M, Jürgens K *et al.* (2008). Widespread distribution of proteorhodopsins in freshwater and brackish ecosystems. *ISME J* **2**: 656–662.

Barberán A, Bates ST, Casamayor EO, Fierer N. (2012). Using network analysis to explore co-occurrence patterns in soil microbial communities. *ISME J* **6**: 343–351.

Bielewicz S, Bell E, Kong W, Friedberg I, Priscu John C, Morgan-Kiss RM. (2011). Protist diversity in a permanently ice-covered Antarctic lake during the polar night transition. *ISME J* **5**: 1559–1564.

Bunge J, Woodard L, Böhning D, Foster J, Connolly S, Allen H. (2012). Estimating population diversity with CatchAll. *Bioinformatics* **28**: 1045–1047.

Chaffron S, Rehrauer H, Jakob Pernthaler, von Mering C. (2010). A global network of coexisting microbes from

environmental and whole-genome sequence data. *Genome Res* **20**: 947–959.
Chao A. (1987). Estimating the population size for capture-recapture data with unequal catchability. *Biometrics* **43**: 783–791.
Chao A, Shen TJ. (2010). Program SPADE (Species Prediction And Diversity Estimation). Available at http://chao.stat.nthu.edu.tw/.
Charvet S, Vincent W, Comeau A, Lovejoy C. (2012a). Pyrosequencing analysis of the protist communities in a High Arctic meromictic lake: DNA preservation and change. *Front Microbiol* **3**: 422.
Charvet S, Vincent WF, Lovejoy C. (2012b). Chrysophytes and other protists in High Arctic lakes: molecular gene surveys, pigment signatures and microscopy. *Polar Biol* **35**: 733–748.
Comeau A, Harding T, Galand P, Vincent WF, Lovejoy C. (2012). Vertical distribution of microbial communities in a perennially stratified Arctic lake with saline, anoxic bottom waters. *Sci Rep* **2**: 604.
Crump BC, Kling GW, Bahr M, Hobbie JE. (2003). Bacterioplankton community shifts in an Arctic lake correlate with seasonal changes in organic matter source. *Appl Environl Microbiol* **69**: 2253–2268.
Crump BC, Amaral-Zettler L, Kling G. (2012). Microbial diversity in arctic freshwaters is structured by inoculation of microbes from soils. *ISME J* **6**: 1629–1639.
Damm E, Helmke E, Thoms S, Schauer U, Nöthig E, Bakker K *et al.* (2010). Methane production in aerobic oligotrophic surface water in the central Arctic Ocean. *Biogeosciences* **7**: 1099–1108.
DeLong EF, Béjà O. (2010). The light-driven proton pump proteorhodopsin enhances bacterial survival during tough times. *PLoS Biol* **8**: e1000359.
Dore J, Priscu J. (2001). Phytoplankton phosphorus deficiency and alkaline phosphatase activity in the McMurdo Dry Valley Lakes, Antarctica. *Limnol Oceanogr* **46**: 1331–1346.
Foreman CM, Wolf CF, Priscu J C. (2004). Impact of episodic warming events on the physical, chemical, and biological relationships of Lakes in the McMurdo Dry Valleys, Antarctica. *Aq Geochem* **10**: 239–368.
Fortunato S. (2010). Community detection in graphs. *Phys Rep* **486**: 75–174.
Frigaard N-U, Martinez A, Mincer TJ, DeLong Edward F. (2006). Proteorhodopsin lateral gene transfer between marine planktonic Bacteria and Archaea. *Nature* **439**: 847–850.
Fuhrman J, Steele J. (2008). Community structure of marine bacterioplankton: patterns, networks, and relationships to function. *Aquatic Microbial Ecology* **53**: 69–81.
Glatz R, Lepp P, Ward B, Francis C. (2006). Planktonic microbial community composition across steep physical/chemical gradients in permanently ice-covered Lake Bonney, Antarctica. *Geobiology* **4**: 53–67.
Galand PE, Lovejoy C, Pouliot J, Garneau M, Vincent WF. (2008). Microbial community diversity and heterotrophic production in a coastal Arctic ecosystem: a stamukhi lake and its source waters. *Limnol Oceangr* **53**: 813–823.
Garcia SL, McMahon KD, Martinez-Garcia M, Srvastava A, Sczyrba A, Stepanauskas R *et al.* (2013). Metabolic potential of a single cell belonging to one of the most abundant lineages in freshwater bacterioplankton. *ISME J* **7**: 137–147.
Ghiglione JF, Murray A.E. (2012). Pronounced summer to winter differences and higher wintertime richness in coastal Antarctic marine bacterioplankton. *Environ Microbiol* **14**: 617–629.
Giovannoni SJ, Bibbs L, Cho J, Stapels M, Desiderio R, Vergin K *et al.* (2005). Proteorhodopsin in the ubiquitous marine bacterium SAR11. *Nature* **438**: 82–85.
González M, Dalsgaard A, Olesen JB. (2010). Centrality measures and the importance of generalist species in pollination networks. *Ecol Complex* **7**: 36–43.
Gordon DA, Priscu J, Giovannoni S. (2000). Origin and phylogeny of microbes living in permanent Antarctic lake ice. *Microb Ecol* **39**: 197–202.
Gotelli NJ, McCabe DJ. (2002). Species co-occurrence: a meta-analysis of J. M. Diamond's assembly rules model. *Ecology* **83**: 2091–2096.
Grossart HP, Frindte K, Dziallas C, Eckert W, Tang KW. (2011). Microbial methane production in oxygenated water column of an oligotrophic lake. *Proc Natl Acad Sci USA* **108**: 19657–19661.
Grzymski JJ, Riesenfeld CS, Williams TJ, Dussaq AM, Ducklow H, Erickson M *et al.* (2012). A metagenomic assessment of winter and summer bacterioplankton from Antarctica Peninsula coastal surface waters. *ISME J* **2**: 1–15.
Horner-Devine MC, Silver JM, Leibold MA, Bohannan BJM, Colwell RK, Fuhrman JA *et al.* (2007). A comparison of taxon co-occurrence patterns for macro- and microorganisms. *Ecology* **88**: 1345–1353.
Huber JA, Mark Welch DB, Morrison HG, Huse SM, Neal PR, Butterfield DA *et al.* (2007). Microbial population structures in the deep marine biosphere. *Science* **318**: 97–100.
Huggett M, Rappé M. (2012). Genome sequence of strain HIMB30, a novel member of the marine Gammaproteobacteria. *J Bacteriol* **194**: 723–733.
Huse SM, Huber JA, Morrison HG, Sogin ML, Welch DM. (2007). Accuracy and quality of massively parallel DNA pyrosequencing. *Genome Biol* **8**: R143.
Huse SM, Dethlefsen L, Huber JA, Mark Welch D, Relman DA, Sogin ML. (2008). Exploring microbial diversity and taxonomy using SSU rRNA hypervariable tag sequencing. *PLoS Genet* **4**: e1000255.
Huse SM, Welch DM, Morrison HG, Sogin ML. (2010). Ironing out the wrinkles in the rare biosphere through improved OTU clustering. *Environ Microbiol* **12**: 1889–1898.
Iverson V, Morris RM, Frazar CD, Berthiaume CT, Morales RL, Armbrust EV. (2012). Untangling genomes from metagenomes: revealing an uncultured class of marine Euryarchaeota. *Science* **335**: 587–590.
Jepsen S, Adams E, Priscu JC. (2010). Sediment melt-migration dynamics in perennial Antarctic lake ice. *Arctic Antarctic Alpine Res* **42**: 57–66.
Judd KE, Crump Byron C, Kling George W. (2006). Variation in dissolved organic matter controls bacterial production and community composition. *Ecology* **87**: 2068–2079.
Karl DM, Beversdorf L, Björkman KM, Church MJ, Martinez A, Delong EF. (2008). Aerobic production of methane in the sea. *Nat Geoscience* **7**: 473–478.
Karr EA, Ng JM, Belchik SM, Sattley WM, Madigan MT, Achenbach LA. (2006). Biodiversity of methanogenic and other Archaea in the permanently frozen Lake Fryxell, Antarctica. *Appl Environ Microbiol* **72**: 1663–1666.
Karr EA, Sattley WM, Madigan MT, Achenbach LA. (2005). Diversity and distribution of sulfate-reducing

bacteria in permanently frozen Lake Fryxell, McMurdo Dry Valleys, Antarctica. *Appl Environ Microbiol* **71**: 6353–6359.

Kong W, Dolhi JM, Chiuchiolo A, John Priscu, Morgan-Kiss RM. (2012a). Evidence of form II RubisCO (cbbM) in a perennially ice-covered Antarctic lake. *FEMS Microbiol Ecol* **82**: 491–500.

Kong W, Ream DC, Priscu JC, Morgan-Kiss RM. (2012b). Diversity and expression of RubisCO genes in a perennially ice-covered Antarctic lake during the polar night transition. *Appl Environ Microbiol* **78**: 4358–4366.

Laybourn-Parry J. (2002). Survival mechanisms in Antarctic lakes. *Philos Trans R Soc London Ser B Biol Sci* **357**: 863–869.

Lee PA, Priscu JC, Ditullio GR, Riseman SF, Tursich N, DeMora SJ. (2004). Elevated levels of dimethylated-sulfur compounds in Lake Bonney, a poorly ventilated Antarctic lake. *Limnol Oceanogr* **49**: 1044–1055.

Lizotte MP, Priscu JC. (1994). Natural fluorescence and quantum yields in vertically stationary phytoplankton from perennially ice-covered lakes. *Limnol Oceanogr* **39**: 1399–1410.

Lizotte MP, Sharp TR, Priscu JC. (1996). Phytoplankton dynamics in the stratified water column of Lake Bonney, Antarctica: biomass and productivity during the winter-spring transition. *Polar Biol* **16**: 155–162.

McCliment EA, Nelson CE, Carlson CA, Alldredge AL, Witting J, Amaral-Zettler LA. (2012). An all-taxon microbial inventory of the Moorea coral reef ecosystem. *ISME J* **6**: 309–319.

McIlroy SJ, Kristiansen R, Albertsen M, Karst SM, Rossetti S, Nielsen JL *et al.* (2013). Metabolic model for the filamentous '*Candidatus* Microthrix pavicella' based on genomic and Metagenomic analyses. *ISME J* **7**: 1161–1172.

McKnight DM, Howes BL, Taylor CD, Goehringer DD. (2000). Phytoplankton dynamics in a stably stratified Antarctic lake during winter darkness. *J Phycology* **36**: 852–861.

Miklós I, Podani J. (2004). Randomization of presence–absence matrices: comments and new algorithms. *Ecology* **85**: 86–92.

Mikucki JA, Priscu JC. (2007). Bacterial diversity associated with Blood Falls, a subglacial outflow from the Taylor Glacier, Antarctica. *Appl Environ Microbiol* **73**: 4029–4039.

Morán X, Gasol J, Pedrós-Alió C, Estrada M. (2001). Dissolved and particulate primary production and bacterial production in offshore Antarctic waters during austral summer: coupled or uncoupled? *Mar Ecol Prog Ser* **222**: 25–39.

Newton RJ, Jones SE, Eiler A, McMahon KD, Bertilsson S. (2011). A guide to the natural history of freshwater lake bacteria. *Microbiol Mol Biol Rev* **75**: 14–49.

Oh HM, Kang I, Lee K, Jang Y, Lim S, Cho J. (2011). Complete genome sequence of strain IMCC9063, belonging to SAR11 subgroup 3, isolated from the Arctic Ocean. *J Bacteriol* **193**: 3379–3380.

Oksanen J, Guillaume Blanchet F, Kindt R, Legendre P, O'Hara RB, Simpson GL *et al.* (2010). vegan: Community ecology package. R Package version 1.17-3.

Paerl HW, Priscu JC. (1998). Microbial phototrophic, heterotrophic, and diazotrophic activities associated with aggregates in the permanent ice cover of Lake Bonney, Antarctica. *Microb Ecol* **36**: 221–230.

Pernthaler A, Preston CM, Pernthaler J, DeLong EF, Amann R. (2002). Comparison of fluorescently labeled oligonucleotide and polynucleotide probes for the detection of pelagic marine bacteria and archaea. *Appl Environ Microbiol* **68**: 661–667.

Priscu JC, Downes MT, McKay CP. (1996). Extreme supersaturation of nitrous oxide in a poorly ventilated Antarctic lake. *Limnol Oceanogr* **41**: 1544–1551.

Priscu JC, Fritsen CH, Adams EE, Giovannoni SJ, Paerl HW, McKay CP *et al.* (1998). Perennial Antarctic lake ice: an oasis for life in a polar desert. *Science* **280**: 2095–2098.

Priscu JC, Wolf CF, Takacs CD, Fritsen CH, Laybourn-Parry J, Roberts EC *et al.* (1999). Carbon transformations in a perennially ice-covered Antarctic lake. *Bioscience* **49**: 997–1008.

Pruesse E, Quast C, Knittel K, Fuchs BM, Ludwig W, Peplies J *et al.* (2007). SILVA: a comprehensive online resource for quality checked and aligned ribosomal RNA sequence data compatible with ARB. *Nucleic Acids Res* **35**: 7188–7196.

Quince C, Lanzen A, Davenport RJ, Turnbaugh PJ. (2011). Removing noise from pyrosequenced amplicons. *BMC Bioinformatics* **12**: 38.

R Development Core Team (2008). *R: a language and environment for statistical computing. Vienna, Austria. www.R-project.org.*

Roberts D. (2010). labdsv: ordination and multivariate analysis for ecology package. R Package version 1.4-1.

Šabacká M, Priscu JC, Basagic HJ, Fountain AG, Wall DH, Virginia RA *et al.* (2012). Aeolian flux of biotic and abiotic material in Taylor Valley, Antarctica. *Geomorphology* **155-156**: 102–111.

Sattley WM, Madigan MT. (2006). Isolation, characterization, and ecology of cold-active, chemolithotrophic, sulfur-oxidizing bacteria from perennially ice-covered Lake Fryxell, Antarctica. *Appl Environ Microbiol* **72**: 5562–5568.

Shannon P, Markiel A, Ozier O, Baliga NS, Wang JT, Ramage D *et al.* (2003). Cytoscape: a software environment for integrated models of biomolecular interaction networks. *Genome Res* **13**: 2498–2504.

Spigel RH, Priscu JC. (1998). Physical limnology of the McMurdo Dry Valley lakes. In: Priscu JC (ed.) *Ecosystem Dynamics in a Polar Desert: the McMurdo Dry Valleys, Antarctica. Antarctic Research Series* Vol. 72. American Geophysical Union: Washington D.C., pp 153–187.

Squyres S, Andersen D, Nedell S, Wharton R. (1991). Lake Hoare, Antarctica: sedimentation through a thick perennial ice cover. *Sedimentology* **38**: 363–379.

Steele JA, Countway PD, Xia L, Vigil PD, Beman JM, Kim DY *et al.* (2011). Marine bacterial, archaeal and protistan association networks reveal ecological linkages. *ISME J* **5**: 1414–1425.

Steindler L, Schwalbach MS, Smith DP, Chan F, Giovannoni SJ. (2011). Energy starved *Candidatus* Pelagibacter ubique substitutes light-mediated ATP production for endogenous carbon respiration. *PLoS One* **6**: e19725.

Stone L, Roberts A. (1990). The checkerboard score and species distributions. *Oecologia* **85**: 74–79.

Takacs CD, Priscu JC. (1998). Bacterioplankton dynamics in the McMurdo Dry Valley lakes, Antarctica: production and biomass loss over four seasons. *Microb. Ecol* **36**: 239–250.

Takacs CD, Priscu JC, McKnight DM. (2001). Bacterial dissolved organic carbon demand in McMurdo Dry Valley Lakes, Antarctica. *Limnol Oceanogr* **46**: 1189–1194.

Thurman J, Parry J, Hill PJ, Priscu John C, Vick TJ, Chiuchiolo A *et al.* (2012). Microbial dynamics and flagellate grazing during transition to winter in Lakes Hoare and Bonney, Antarctica. *FEMS Microbiol Ecol* **82**: 449–458.

Vick TJ, Priscu JC. (2012). Bacterioplankton productivity in lakes of the Taylor Valley, Antarctica during the polar night transition. *Aquat Microb Ecol* **68**: 77–90.

Vincent W, Howard-Williams C. (1986). Antarctic stream ecosystems: physiological ecology of a blue-green algal epilithon. *Freshwater Biol* **16**: 219–233.

Voytek MA, Priscu JC, Ward BB. (1999). The distribution and relative abundance of ammonia-oxidizing bacteria in lakes of the McMurdo Dry Valley, Antarctica. *Hydrobiologia* **401**: 113–130.

Wang Q, Garrity GM, Tiedje JM, Cole JR. (2007). Naive Bayesian classifier for rapid assignment of rRNA sequences into the new bacterial taxonomy. *Appl Environ Microbiol* **73**: 5261–5267.

Williams TJ, Long E, Evans F, Demaere MZ, Lauro FM, Raftery MJ *et al.* (2012). A metaproteomic assessment of winter and summer bacterioplankton from Antarctic Peninsula coastal surface waters. *ISME J* **2**: 1–18.

Yilmaz P, Kottmann R, Field D, Knight R, Cole JR *et al.* (2011). Minimum information about a marker gene sequence (MIMARKS) and minimum information about any (x) sequence (MixS) specifications. *Nat Biotechnol* **29**: 415–420.

Yoon KS, Tsukada N, Sakai Y, Ishii M, Igarashi Y, Nishihara H. (2008). Isolation and characterization of a new facultatively autotrophic hydrogen-oxidizing Betaproteobacterium, *Hydrogenophaga* sp. AH-24. *FEMS Microbiol Lett* **278**: 94–100.

Supplementary Information accompanies this paper on The ISME Journal website (http://www.nature.com/ismej)

Supplemental Methods:

To determine whether our MEN comprised a non-random network, we compared the entire network, and the entire network minus the Archaea, to 100 randomly generated networks (Erdos-Renyi model; Erdös & Rényi 1959) of similar size using the Random Network tool in Cytoscape. The observed clustering coefficient and mean shortest path length (0.88 and 3.53, respectively) for the entire network including Archaea, were greater than the clustering coefficient and mean shortest path length for the random networks ($0.06 \pm 4.0 \times 10^{-4}$ and $1.97 \pm 4.8 \times 10^{-4}$, respectively) indicating that our MEN was more organized than would be expected of a random network of similar size. Removal of the Archaea from the network increased the clustering coefficient to 0.89 and decreased the mean shortest path length to 3.39. Our clustering coefficients and mean shortest path lengths (with and without Archaea) were also greater than that observed for a three-domain association network from the open ocean (Steele *et al.* 2011). Similar to the results found by Steele *et al*. (2011), our network also exhibited the small world pattern (Watts & Strogatz 1998), which is characterized by few, highly connected nodes and expected of a non-random ecological network. Given the significant C-score for the complete dataset and the minor variation in path length and clustering coefficient between the total network and network minus Archaea, we chose to continue our analysis with the entire dataset, including the Archaea.

Module identification algorithms and/or the corresponding modularity metric (*Q* or *M*) have been used to identify important groups of nodes in pollinator networks (M = 0.52; Olesen *et al*. 2007), soil microbial communities (Q = 0.77; Barberán *et al*. 2012), the yeast interactome (Q and M not calculated; Kovács *et al*. 2010), and farm food webs (M = 0.70 to 0.88; Macfadyen *et al*. 2011). We calculated modularity for our complete network, using the ClusterMaker plugin (Morris *et al*. 2011) for Cytoscape, based on four different modularity methods: Markov Cluster

Algorithm (MCL; Enright *et al*. 2002), GLay (Su *et al*. 2010), Connected Components Cluster (CCC; Morris *et al*. 2011), and Spectral Clustering of Protein Sequences (SCPS; Nepusz *et al*. 2010). These methods cover each of the classes of modularity algorithms discussed by Fortunato (2010). All four methods revealed modularity scores > 0.8, indicating that the FRX and WLB microbial communities have a modular structure (where a module is a group of connected nodes; Table 1), allowing us to use modules to simplify our MEN. To visualize the modules in our MEN, we used the ModuLand plugin (Szalay-Beko *et al*. 2012) for Cytoscape. The ModuLand calculation resulted in 27 modules ranging in size from 100 nodes with 705 connections to 2 nodes with a single connection (Table S3 and Figure S2). ModuLand used the name of the node (OTU) with the maximum assignment value to each module as the module key. We subsequently assigned each module a number and both designations are used in the text (Table 2, Figure 5, Table S4).

The ClusterMaker plugin does not generate diagrams of modules, or provide information about the nodes contained in each module. In order to describe the modules, we used the ModuLand (Szalay-Beko *et al*. 2012) package in Cytoscape. ModuLand does not determine module structure based on modularity scores, and therefore does not calculate modularity scores; rather, it is based on a 3-D calculation of the community network where “hills” in the 3-D landscape (nodes with greater influence over the network structure) correspond to network modules. Details of the modularity calculations are provided by Kovács *et al*. (2010).

Supplemental Discussion of Significant Modules:

Module 22 contained nodes apparently related to the cycling of C1 compounds, including the most abundant putatively methanogenic OTUs (Archaea_03_102 and Archaea_03_50) in the total dataset, three bacterial OTUs related to candidate division OD1 and one related to candidate division OP9, which have been putatively connected to methane cycling (Orphan *et al.* 2001, Perua *et al.* 2012), five putatively methylotrophic lineages and one member of the Syntrophaceae, which are known to form syntrophic partnerships with hydrogenotrophic methanogens. Putative methanogens were most abundant at the deep chlorophyll maxima of both lakes (DCM; FRX 9 m and WLB 13 m) and decreased between summer and autumn (9.5% to 4.3% [FRX] and 18.0% to 10.2% [WLB]). Karl *et al.* (2008) suggested that aerobic methane production may be a side-effect of phosphorus limitation in surface seawater, while Grossart *et al.* (2011), and Damm *et al.* (2010) suggested a connection between by-products of photoautotrophy and methane production. High levels of particulate dimethylsulfoniopropionate (DMSP) at the WLB DCM (32 nmol L^{-1}; Lee *et al.* 2004) may serve as a substrate or precursor to methanogenesis, via its degradation product, methanethiol (Kiene 1996; Damm *et al.* 2010).

Module 25 (BC = 0.1), which contained the highest abundance of putative methanogens after Module 22, also contained methylotrophic lineages that may be able to use dimethylsulfide (DMS) as a carbon source. Unlike DMSP, DMS concentrations are nearly below detection at the WLB DCM (Lee *et al.* 2004), perhaps because of quick utilization by methylotrophs. Members of the genus *Loktanella*, which are present in Module 25, have been shown to cleave DMSP to DMS and acrylate and genes for DMSP-degrading enzymes are widespread in other Alphaproteobacteria (see review by Moran *et al.* 2012). Modules 22 and 25 may have important roles in linking carbon and sulfur biogeochemistry in the MCM lakes.

Module 19 (BC=0.04; key = Bacteroidetes_03_168, a member of the *Crocibacter*) is comprised primarily of heterotrophic bacteria, mainly of the Bacteroidetes and the Alpha and Gamma clades of the Proteobacteria in association with a few heterotrophic and phototrophic eukaryotic OTUs. Members of the *Flavobacteria* have been implicated in East Antarctic Southern Ocean processing of algal organic matter, which, once broken down, is then utilized by Alpha- and Gammaproteobacteria (Williams *et al.* 2012). Within the module, the nodes Gammaproteobacteria_03_1630 (*Legionella*), Verrucomicrobia_03_57 (*Chthoniobacter*), and Eukarya_06_2105 (*Cyclonexis*) formed a three-way positive interaction with no direct connection to any other members of the module. This three-way interaction is an example of a potential close association between a primary producer (*Cyclonexis*) and two heterotrophic bacterial OTUs. Cultivated members of the *Chthoniobacter* are known to grow on plant-related saccharides (Sangwan *et al.* 2004), and may break down organic matter excreted by *Cyclonexis*. *Legionalla pneumophila* has been found living in close association with cyanobacteria, apparently utilizing photosynthetic exudates as carbon and energy sources (Tison *et al.* 1980), but other studies with *Legionella* have shown that it does not effectively utilize large organic molecules (Chien *et al.* 2004). We suggest that this three-way interaction is bound by an initial breakdown of *Cyclonexis*-related organic matter by *Chthoniobacter*, followed by utilization of smaller molecules by *Legionella*.

Module 20 (BC = 0.04; Key = Bacteroidetes_03_262) was characterized by tightly connected groups of eukaryotic and bacterial OTUs, 52% of which showed positive interactions between heterotrophic bacterial OTUs and phototrophic OTUs. The heterotrophic guilds were highly diverse, with OTUs from 8 phyla (Table S4), and differentiating their putative functions was not possible. Three phototrophic OTUs were represented in the module (Eukarya_06_1327

[*Micractinium*; GAST = 0.03], Eukarya_06_1388 [*Goniochloris*; GAST = 0.13], and Euk_9221 [*Nannochloropsis;GAST* = 0.06]). *Micractinium* (a chlorophyte) primarily interacted with members of the Bacteroidetes, followed by the Plantomycetes and Verrucomicrobia, while the Eustigmatophytes, *Nannochloropsis* and *Goniochloris* primarily interacted with Alphaproteobacteria, suggesting either preferential feeding on exudates from different phytoplankton, or similar responses to environmental conditions.

Module 27 (BC = 0.005; Key = Verrucomicrobia_03_119) contained only five OTUs, two Bacteroidetes, one Actinobacteria, one Verrucomicrobia, and one eukaryote related to the frequent metazoan symbionts and parasites, the Apostomatia. Except for Bacteroidetes_03_457 (*Algoriphagus*) all of the bacterial OTUs are likely to be at least facultatively anaerobic and capable of fermentation. It is possible that Module 27 reflects a connection to the FRX and WLB metazoan communities, of which little is known. Sequence data from the MIRADA project suggested the presence of a few Maxillopoda and Brachiopoda.

Module 18, (BC = 0.07) contained mostly heterotrophic bacteria, and was dominated by OTUs thought be capable of flexibility in substrate utilization (the module key is *Flexibacter*, GAST = 0.0188), including many members of the Flavobacteria, which are known to degrade large carbon compounds, making smaller molecules available as substrate for other heterotrophs (Williams *et al* 2012).

References

Barberán A, Bates ST, Casamayor EO, Fierer N. (2012). Using network analysis to explore co-occurrence patterns in soil microbial communities. The ISME Journal 6:343–51.

Chien M, Morozova I, Shi S, Sheng H, Chen J, Gomez S, *et al.* (2004). The genomic sequence of the accidental pathogen *Legionella pneumophila*. Science 305:1966-1968.

Damm E, Helmke E, Thoms S, Schauer U, Nöthig E, Bakker K, Kiene RP. (2010). Methane production in aerobic oligotrophic surface water in the central Arctic Ocean. Biogeosciences 7:1099-1108.

Enright AJ, Van Dongen S, Ouzounis CA. (2002). An efficient algorithm for large-scale detection of protein families. Nucleic Acids Research 30:1575–1584.

Erdös P, Rényi A. (1959). On random graphs. I. Publicationes Mathematicae (Debrecen) 6:290–297.

Fortunato S. (2010). Community detection in graphs. Physics Reports 486:75–174.

Grossart HP, Frindte K, Dziallas C, Eckert W, Tang KW. (2011). Microbial methane production in oxygenated water column of an oligotrophic lake. Proceedings of the National Academy of Sciences 108:19675-19661.

Karl DM, Beversdorf L, Björkman KM, Church MJ, Martinez A, Delong EF. (2008). Aerobic production of methane in the sea. Nature Geoscience 7:473-478.

Kiene R. (1996). Production of methanethiol from dimethylsulfoniopropionate in marine surface waters. Marine Chemistry 54:69-83.

Kovács IA, Palotai R, Szalay MS, Csermely P. (2010). Community landscapes: an integrative approach to determine overlapping network module hierarchy, identify key nodes and predict network dynamics. PloS ONE 5(9):e12528.

Lee PA, Priscu, JC, Ditullio GR, Riseman SF, Tursich N, DeMora SJ. (2004). Elevated levels of dimethylated-sulfur compounds in Lake Bonney, a poorly ventilated Antarctic lake. Limnology and Oceanography 49:1044-1055.

Moran MA, Reisch CR, Kiene RP, Whitmans WB. (2012). Genomic insights into bacterial DMSP transformations. Annual Review of Marine Science 4:523-542.

Morris JH, Apeltsin L, Newman AM, Baumbach J, Wittkop T, Su G, *et al*. (2011). ClusterMaker: a multi-algorithm clustering plugin for Cytoscape. BMC Bioinformatics 12:436.

Nepusz T, Sasidharan R, Paccanaro A. (2010). SCPS: a fast implementation of a spectral method for detecting protein families on a genome-wide scale. BMC Bioinformatics 11:120. http://www.biomedcentral.com/1471-2105/11/120.

Olesen JM, Bascompte J, Dupont YL, Jordano P. (2007). The modularity of pollination networks. Proceedings of the National Academy of Sciences of the United States of America 104:19891–19896.

Orphan VJ, Hinrichs K-U, Ussler III W, Paull CK, Taylor LT, Sylva SP, Hayes JM, Delong EF. (2001). Comparative analysis of methane-oxidizing Archaea and sulfate-reducing Bacteria in anoxic marine sediments. Applied and Environmental Microbiology 67:1922-1934.

Perua S, Eiler A, Bertilsson S, Nykänen H, Tirola M, Jone R. (2012). Distinct and diverse anaerobic bacterial communities in boreal lakes dominated by candidate division OD1. The ISME Journal 6:1640-1652.

Sangwan P, Chen X, Hugenholtz P, Janssen PH. (2004). *Chthoniobacter flavus* gen. nov., sp. nov., the first pure-culture representative of subdivision two, *Spartobacteria classis* nov., of the phylum *Verrucomicrobia*. Applied and Environmental Microbiology 70:5875-5881.

Steele JA, Countway PD, Xia L, Vigil PD, Beman JM, Kim DY, *et al*. (2011). Marine bacterial, archaeal and protistan association networks reveal ecological linkages. ISME Journal 5:1414–1425.

Su G, Kuchinsky A, Morris JH, States DJ, Meng F. (2010). GLay: community structure analysis of biological networks. Bioinformatics (Oxford, England) 26:3135–7.

Szalay-Beko M, Palotai R, Szappanos B, Kovács I a, Papp B, Csermely Péter. (2012). ModuLand plug-in for Cytoscape: determination of hierarchical layers of overlapping network modules and community centrality. Bioinformatics 28:2202–2204.

Tison DL, Pope DH, Cherry WB, Fliermans CB. (1980). Growth of *Legionella pneumophila* in association with blue-green algae. Applied and Environmental Microbiology 39:456-459.

Watts DJ, Strogatz SH. (1998). Collective dynamics of "small-world" networks. Nature 393:440–2.

Williams TJ, Wilkins D, Long E, Evans F, DeMaere MZ, Raftery MJ, Cavicchioli R. (2012). The role of planktonic *Flavobacteria* in processing algal organic matter in coastal East Antarctica revealed using metagenomics and metaproteomics. Environmental Microbiology 15:1302-1317.

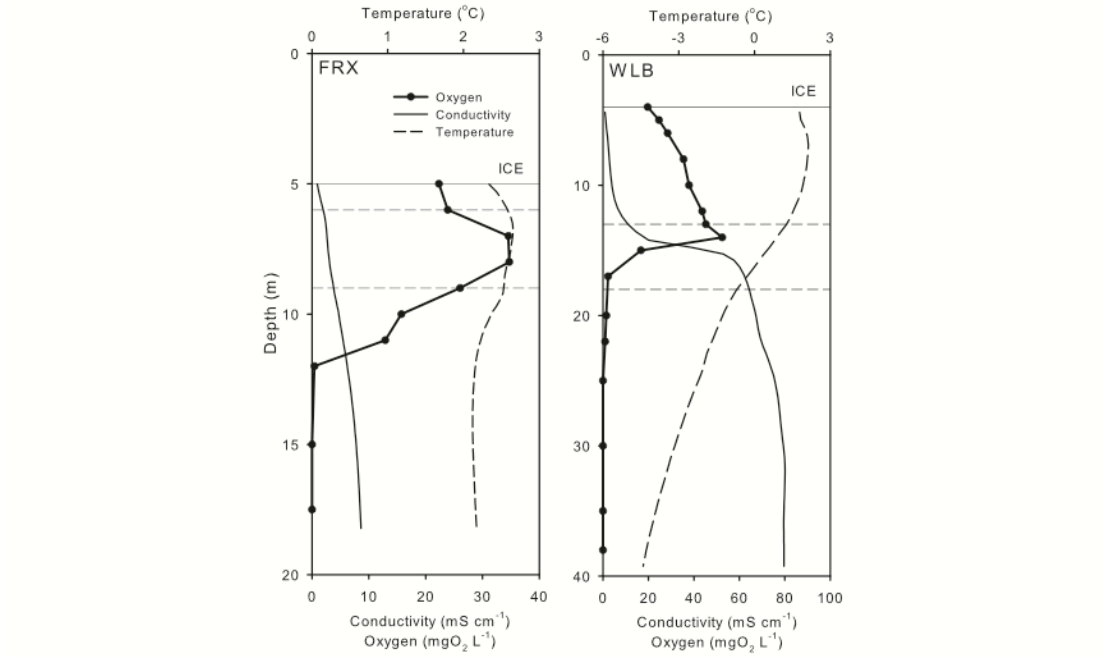

Figure S1. Profiles of oxygen, temperature and conductivity from Lake Fryxell (FRX) and the West Lobe of Lake Bonney (WLB) taken during March 2008. The solid and dashed horizontal lines represent the thickness of the ice-cover and the depths at which samples for molecular analysis were taken, respectively.

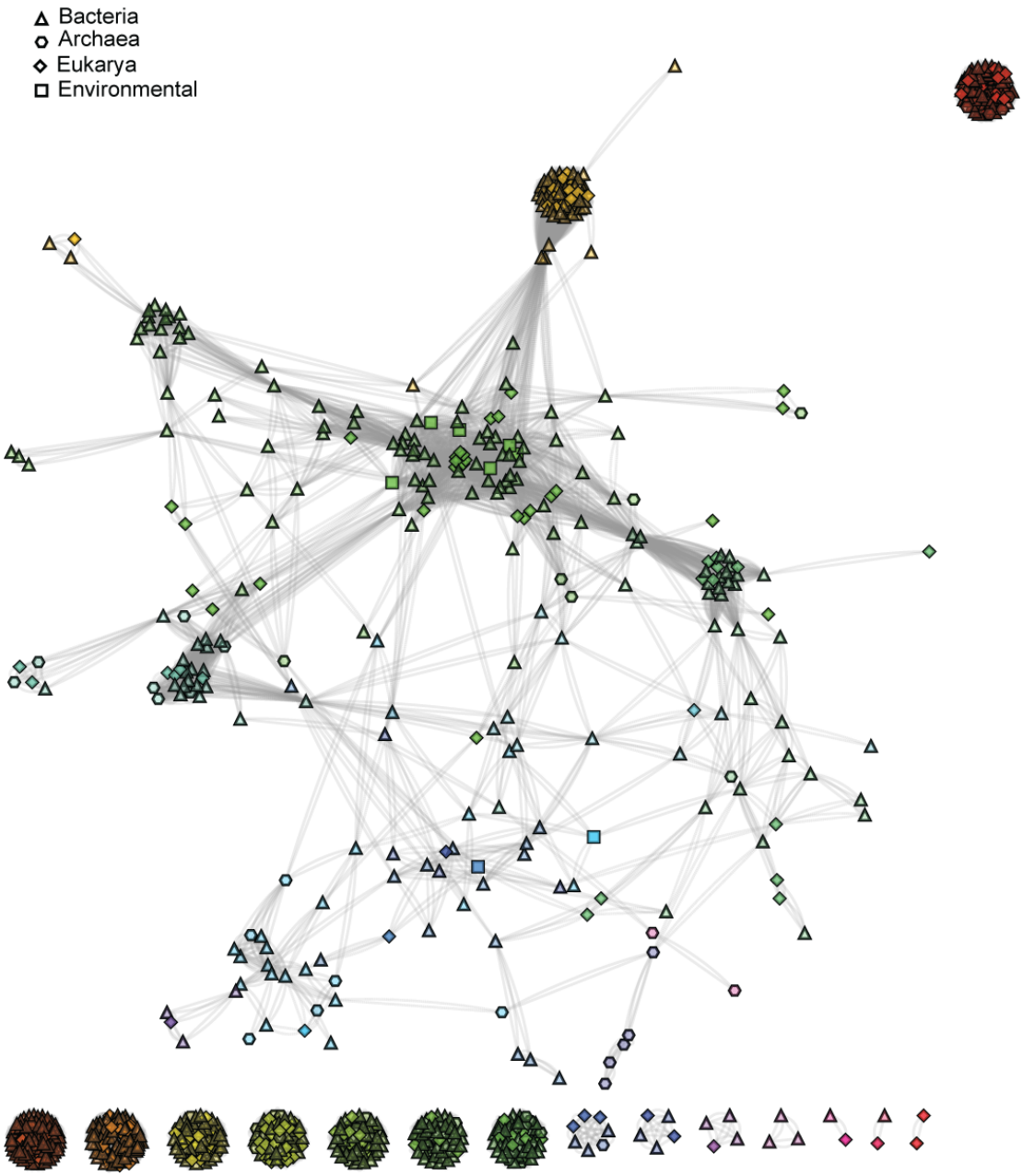

Figure S2. Complete molecular ecological network (MEN), based on significant ($P \leq 0.01$) Spearman correlations on ranks between bacterial, archaeal, and eukaryotic OTUs and environmental variables. Nodes correspond to individual OTUs or environmental parameters and colors correspond to modules. "Environmental" refers to physicochemical data used in the network analysis.

Table S1. Environmental Data

Sample ID	*Collection Date* UTC	*Depth* Meters	*Lake Name*	*Latitude* Decimal Degree	*Longitude* Decimal Degree	*Ammonium* µmol L^{-1}	*Pressure* db	*Chlorophyll* µg L^{-1}
MCM_1	11/22/07	6	Lake Fryxell	-77.61031	85.53597	0.3	5.27	3.3
MCM_2	11/22/07	9	Lake Fryxell	-77.61031	85.53597	0.17	8.2	5.04
MCM_3	11/30/07	13	West Lobe Bonney	-77.72006	84.57732	0.96	12.23	4.03
MCM_4	11/30/07	18	West Lobe Bonney	-77.72006	84.57732	172.9	17.51	0.94
MCM_5	3/17/08	13	West Lobe Bonney	-77.72006	84.57732	0.67	12.3	5.53
MCM_6	3/17/08	18	West Lobe Bonney	-77.72006	84.57732	157.75	17.42	0.77
MCM_7	3/25/08	6	Lake Fryxell	-77.61031	85.53597	0.08	5.28	3.99
MCM_8	3/25/08	9	Lake Fryxell	-77.61031	85.53597	0.32	8.2	10.05

Sample ID	*Conductivity* mS cm^{-1}	*Dissolved Inorganic Nitrogen* µmol L^{-1}	*Dissolved Organic Carbon* µmol L^{-1}	*Dissolved Organic Nitrogen* µmol L^{-1}	*Dissolved Oxygen* µmol L^{-1}	*Nitrate* µmol L^{-1}	*Nitrite* µmol L^{-1}	*Bacterial Cells* x10^{6} ml^{-1}
MCM_1	1.36	0.57	237.48	21.38515266	802.67	0.15	0.11	1.13
MCM_2	3.3	0.34	472.22	33.31	914.54	0.08	0.09	0.84
MCM_3	12.54	13.26	370	6.62	1591.72	11.21	1.09	0.05
MCM_4	65.13	189.12	1033.33	53.84	58.55	13.2	3.02	0.07
MCM_5	10.01	9.94	320	2.99	1562.62	9.53	0.45	0.09
MCM_6	64.08	174.08	758.1	56.41	68.72	14.68	2.32	0.04
MCM_7	1.83	0.31	170	11.58	807.32	0.1	0.14	1.42
MCM_8	2.04	0.58	514.29	36.4	764.52	0.09	0.17	1.25

Sample ID	*Particulate Carbon* µg L^{-1}	*Particulate Nitrogen* µmol L^{-1}	*pH* Log H+	*Phosphate* µmol L^{-1}	*Salinity* PSU	*Silicate* µmol L^{-1}	*Temperature* °C	*Water Column Depth* Meters
MCM_1	370.16	3.78	8.02	0.13	1.26	200	1.42	18.64
MCM_2	437.44	4.32	7.73	0.28	3.12	220	2.17	18.64
MCM_3	339.4	2.01	7.05	0.05	13.55	200	1.03	41.45
MCM_4	241.8	1.78	5.87	0.27	90.02	220	-0.72	41.45
MCM_5	517.94	1.72	7.62	0.04	10.61	200	1.25	41.45
MCM_6	212.5	1.57	5.97	0.19	88.08	220	-0.65	41.45
MCM_7	533.62	3.29	8.18	0.06	1.82	200	1.31	18.64
MCM_8	1014.5	5.34	7.73	0.15	1.96	220	1.83	18.64

Table S2. OTU and Diversity Data

Dataset	*Number of Reads*[*]	*Number of OTUs*	*Coverage*	*Number of Reads*[*]	*Number of OTUs*	*Coverage*	*Number of Reads*[*]	*Number of OTUs*	*Coverage*
	Bacteria			Archaea			Eukarya		
FRX6N	24662	363	0.33	25554	16	0.61	8299	69	0.94
FRX6N R		170	0.50					59	0.96
FRX6M	15466	464	0.15	8678	26	0.71	13393	74	0.94
FRX6M R		185	0.39		17	0.53		57	0.95
FRX9N	18252	363	0.31	9645			7336	57	0.97
FRX9N R		191	0.50					54	0.95
FRX9M	12046	298	0.19	15036	19	0.86	2074	85	0.96
FRX9M R		154	0.33		11	0.90		60	0.98
WLB13N	15545	229	0.31	14232			13929	78	0.94
WLB13N R		155	0.50					59	0.95
WLB13M	8632	161	0.38	3904	20	0.66	10572	56	0.95
WLB13M R		161	0.38		20	0.66		46	0.95
WLB18N	14587	270	0.30	20894	27	0.70	13173	102	0.88
WLB18N R		129	0.45		19	0.75		77	0.85
WLB18M R	18644	539	0.17	4183	14	0.74	9425	90	0.88
WLB18M		166	0.27		14	0.74		77	0.87

R = Resampled dataset

[*]Replicates pooled

Coverage = observed number of OTUs/expected number of OTUs

Table S3. Module Assignments and Taxonomy. * = Module Key

Node	*Module ID*	*Taxonomy*
Acidobacteria_03_11260*	1	Bacteria;Acidobacteria;Acidobacteria;Acidobacteriales;Acidobacteriaceae
Acidobacteria_03_118	1	Bacteria;Acidobacteria;Acidobacteria;Acidobacteriales;Acidobacteriaceae
Acidobacteria_03_185	1	Bacteria;Acidobacteria;Acidobacteria;Acidobacteriales;Acidobacteriaceae
Actinobacteria_03_137	1	Bacteria;Actinobacteria;Actinobacteria;Actinomycetales;Sporichthyaceae;Planktophila
Actinobacteria_03_189	1	Bacteria;Actinobacteria;Actinobacteria;Acidimicrobiales;Acidimicrobiaceae
Actinobacteria_03_229	1	Bacteria;Actinobacteria;Actinobacteria;Acidimicrobiales;Acidimicrobiaceae
Actinobacteria_03_9523	1	Bacteria;Actinobacteria;Actinobacteria;Acidimicrobiales;Acidimicrobiaceae
Bacteroidetes_03_622	1	Bacteria;Bacteroidetes;Sphingobacteria;Sphingobacteriales;Rhodothermaceae
Bacteroidetes_03_1309	1	Bacteria;Bacteroidetes;Sphingobacteria;Sphingobacteriales
Bacteroidetes_03_3254	1	Bacteria;Bacteroidetes;Sphingobacteria;Sphingobacteriales
Bacteroidetes_03_28519	1	Bacteria;Bacteroidetes;Sphingobacteria;Sphingobacteriales;Chitinophagaceae;Sediminibacterium
Cyanobacteria_03_5701	1	Bacteria;Cyanobacteria;Cyanobacteria;SubsectionIII;Unassigned;Leptolyngbya
OD1_03_14	1	Bacteria;OD1
OD1_03_2939	1	Bacteria;OD1
OP11_03_4956	1	Bacteria;OP11
Planctomycetes_03_7	1	Bacteria;Planctomycetes;Planctomycetacia;Planctomycetales;Planctomycetaceae
Planctomycetes_03_10155	1	Bacteria;Planctomycetes;Planctomycetacia;Planctomycetales;Planctomycetaceae
Planctomycetes_03_16886	1	Bacteria;Planctomycetes;Planctomycetacia;Planctomycetales;Planctomycetaceae
Alphaproteobacteria_03_443	1	Bacteria;Proteobacteria;Alphaproteobacteria;Sphingomonadales;Sphingomonadaceae;Sphingopyxis
Alphaproteobacteria_03_444	1	Bacteria;Proteobacteria;Alphaproteobacteria;Rhodospirillales;Rhodospirillaceae
Alphaproteobacteria_03_1848	1	Bacteria;Proteobacteria;Alphaproteobacteria;Rhodospirillales;Rhodospirillaceae
Alphaproteobacteria_03_3051	1	Bacteria;Proteobacteria;Alphaproteobacteria;Caulobacterales;Caulobacteraceae
Alphaproteobacteria_03_4780	1	Bacteria;Proteobacteria;Alphaproteobacteria;Rhodospirillales;Acetobacteraceae;Roseomonas
Betaproteobacteria_03_6	1	Bacteria;Proteobacteria;Betaproteobacteria;Burkholderiales;Comamonadaceae
Betaproteobacteria_03_1313	1	Bacteria;Proteobacteria;Betaproteobacteria
Betaproteobacteria_03_9200	1	Bacteria;Proteobacteria;Betaproteobacteria;Burkholderiales;Comamonadaceae;Acidovorax
Betaproteobacteria_03_10877	1	Bacteria;Proteobacteria;Betaproteobacteria;Burkholderiales;Comamonadaceae;Rhodoferax
Gammaproteobacteria_03_98	1	Bacteria;Proteobacteria;Gammaproteobacteria;Pseudomonadales;Pseudomonadaceae;Pseudomonas
Gammaproteobacteria_03_1234	1	Bacteria;Proteobacteria;Gammaproteobacteria;Xanthomonadales;Sinobacteraceae
Gammaproteobacteria_03_1291	1	Bacteria;Proteobacteria;Gammaproteobacteria;Legionellales;Coxiellaceae
Gammaproteobacteria_03_2262	1	Bacteria;Proteobacteria;Gammaproteobacteria
Gammaproteobacteria_03_2980	1	Bacteria;Proteobacteria;Gammaproteobacteria;Enterobacteriales;Enterobacteriaceae;Brenneria;rubrifaciens
Gammaproteobacteria_03_22057	1	Bacteria;Proteobacteria;Gammaproteobacteria;Alteromonadales;Alteromonadaceae;Marinimicrobium

Deltaproteobacteria_03_1311	1	Bacteria;Proteobacteria;Deltaproteobacteria;Bdellovibrionales;Bacteriovoraceae;Peredibacter
Deltaproteobacteria_03_2323	1	Bacteria;Proteobacteria;Deltaproteobacteria;Myxococcales
BacteriaNA_03_936	1	Bacteria
Archaea_03_376	1	Archaea;Euryarchaeota;Thermoplasmata;Thermoplasmatales;Terrestrial_Miscellaneous_Group
Archaea_03_392	1	Archaea;Crenarchaeota;Miscellaneous_Crenarchaeotic_Group
Archaea_03_4088	1	Archaea;Crenarchaeota;Marine_Group_I
Archaea_03_6978	1	Archaea;Crenarchaeota;Marine_Group_I
Euk_1179	1	Eukaryota;SAR;Rhizaria;Cercozoa;Thecofilosea;uncultured
Euk_14612	1	Eukaryota;SAR;Alveolata;Ciliophora;Intramacronucleata;Conthreep;Prostomatea;Cryptocaryon
Euk_22746	1	Eukaryota;Cryptophyceae;Cryptomonadales
Euk_29005	1	Eukaryota;Opisthokonta;Fungi;LKM15
Eukarya_06_1006	1	Eukaryota;SAR;Stramenopiles;Chrysophyceae;LG21-05
Eukarya_06_1607	1	Eukaryota;Opisthokonta;Holozoa;Corallochytrium
Eukarya_06_1710	1	Eukaryota;SAR;Stramenopiles
Eukarya_06_1847	1	Eukaryota;SAR;Alveolata
Eukarya_06_312	1	Eukaryota;SAR;Stramenopiles;Chrysophyceae;Ochromonadales;Paraphysomonas
Eukarya_06_329	1	Eukaryota;SAR;Stramenopiles;Chrysophyceae;Ochromonadales;Paraphysomonas
Eukarya_06_6423	1	Eukaryota;SAR;Stramenopiles;Synurales;Mallomonas
Acidobacteria_03_15770*	2	Bacteria;Acidobacteria;Acidobacteria;Acidobacteriales;Acidobacteriaceae
Actinobacteria_03_445	2	Bacteria;Actinobacteria;Actinobacteria;Acidimicrobiales
Actinobacteria_03_447	2	Bacteria;Actinobacteria;Actinobacteria;Acidimicrobiales
Actinobacteria_03_2306	2	Bacteria;Actinobacteria;Actinobacteria;Actinomycetales;Micrococcaceae;Nesterenkonia
Actinobacteria_03_10904	2	Bacteria;Actinobacteria;Actinobacteria;Actinomycetales;Sporichthyaceae
Bacteroidetes_03_30	2	Bacteria;Bacteroidetes;Sphingobacteria;Sphingobacteriales;Cyclobacteriaceae;Algoriphagus
Bacteroidetes_03_299	2	Bacteria;Bacteroidetes;Sphingobacteria;Sphingobacteriales;Chitinophagaceae
Bacteroidetes_03_1362	2	Bacteria;Bacteroidetes;Sphingobacteria;Sphingobacteriales;Sphingobacteriaceae;Sphingobacteriaceae;Pedobacter
Bacteroidetes_03_8459	2	Bacteria;Bacteroidetes;Sphingobacteria;Sphingobacteriales;Chitinophagaceae
Bacteroidetes_03_8909	2	Bacteria;Bacteroidetes;Sphingobacteria;Sphingobacteriales
Chlamydiae_03_124	2	Bacteria;Chlamydiae;Chlamydiae;Chlamydiales;Simkaniaceae;Rhabdochlamydia
Chlamydiae_03_379	2	Bacteria;Chlamydiae;Chlamydiae;Chlamydiales
Cyanobacteria_03_5311	2	Bacteria;Cyanobacteria;Cyanobacteria
Deferribacteres_03_6450	2	Bacteria;Deferribacteres;Deferribacteres;Deferribacterales;Unassigned;Caldithrix
Firmicutes_03_5597	2	Bacteria;Firmicutes;Clostridia;Clostridiales;Ruminococcaceae
OD1_03_5	2	Bacteria;OD1
OD1_03_326	2	Bacteria;OD1
OD1_03_921	2	Bacteria;OD1
OP3_03_32	2	Bacteria;OP3
OP3_03_470	2	Bacteria;OP3
OP11_03_2821	2	Bacteria;OP11
ProteobacteriaNA_03_5	2	Bacteria;Proteobacteria
Alphaproteobacteria_03_246	2	Bacteria;Proteobacteria;Alphaproteobacteria;Rhizobiales;Bradyrhizobiaceae;Bradyrhizobium

Alphaproteobacteria_03_417	2	Bacteria;Proteobacteria;Alphaproteobacteria;Rhodobacterales;Rhodobacteraceae
Alphaproteobacteria_03_1113	2	Bacteria;Proteobacteria;Alphaproteobacteria;Caulobacterales;Caulobacteraceae;Caulobacter
Alphaproteobacteria_03_1267	2	Bacteria;Proteobacteria;Alphaproteobacteria;Sphingomonadales;Sphingomonadaceae;Sandarakinorhabdus
Alphaproteobacteria_03_4192	2	Bacteria;Proteobacteria;Alphaproteobacteria;Rhodospirillales;Acetobacteraceae;Roseomonas
Alphaproteobacteria_03_6461	2	Bacteria;Proteobacteria;Alphaproteobacteria;Rhodospirillales;Rhodospirillaceae
Alphaproteobacteria_03_10317	2	Bacteria;Proteobacteria;Alphaproteobacteria;Rickettsiales;Holosporaceae;Holospora
Alphaproteobacteria_03_24265	2	Bacteria;Proteobacteria;Alphaproteobacteria;Rhodobacterales;Rhodobacteraceae;Pseudoruegeria
Betaproteobacteria_03_116	2	Bacteria;Proteobacteria;Betaproteobacteria
Betaproteobacteria_03_124	2	Bacteria;Proteobacteria;Betaproteobacteria;Burkholderiales;Alcaligenaceae
Betaproteobacteria_03_145	2	Bacteria;Proteobacteria;Betaproteobacteria
Betaproteobacteria_03_171	2	Bacteria;Proteobacteria;Betaproteobacteria;Burkholderiales;Alcaligenaceae
Betaproteobacteria_03_186	2	Bacteria;Proteobacteria;Betaproteobacteria;Burkholderiales;Comamonadaceae
Betaproteobacteria_03_238	2	Bacteria;Proteobacteria;Betaproteobacteria;Burkholderiales;Comamonadaceae
Betaproteobacteria_03_240	2	Bacteria;Proteobacteria;Betaproteobacteria;Burkholderiales;Oxalobacteraceae
Betaproteobacteria_03_381	2	Bacteria;Proteobacteria;Betaproteobacteria;Rhodocyclales;Rhodocyclaceae
Betaproteobacteria_03_1327	2	Bacteria;Proteobacteria;Betaproteobacteria;Burkholderiales;Burkholderiaceae;Polynucleobacter
Betaproteobacteria_03_3704	2	Bacteria;Proteobacteria;Betaproteobacteria;Burkholderiales;Oxalobacteraceae;Duganella
Betaproteobacteria_03_6606	2	Bacteria;Proteobacteria;Betaproteobacteria;Burkholderiales;Oxalobacteraceae
Betaproteobacteria_03_6702	2	Bacteria;Proteobacteria;Betaproteobacteria;Burkholderiales;Oxalobacteraceae
Betaproteobacteria_03_9629	2	Bacteria;Proteobacteria;Betaproteobacteria;Burkholderiales;Oxalobacteraceae;Massilia
Gammaproteobacteria_03_26	2	Bacteria;Proteobacteria;Gammaproteobacteria;Pseudomonadales;Moraxellaceae;Acinetobacter
Gammaproteobacteria_03_463	2	Bacteria;Proteobacteria;Gammaproteobacteria;Legionellales;Coxiellaceae;Coxiella
Gammaproteobacteria_03_2318	2	Bacteria;Proteobacteria;Gammaproteobacteria;Legionellales;Legionellaceae;Legionella
Gammaproteobacteria_03_2982	2	Bacteria;Proteobacteria;Gammaproteobacteria;Legionellales;Coxiellaceae;Aquicella
Gammaproteobacteria_03_3242	2	Bacteria;Proteobacteria;Gammaproteobacteria;Oceanospirillales
Gammaproteobacteria_03_4104	2	Bacteria;Proteobacteria;Gammaproteobacteria;Pasteurellales;Pasteurellaceae
Gammaproteobacteria_03_5304	2	Bacteria;Proteobacteria;Gammaproteobacteria;Legionellales;Coxiellaceae;Aquicella
Deltaproteobacteria_03_49	2	Bacteria;Proteobacteria;Deltaproteobacteria;Myxococcales
Deltaproteobacteria_03_154	2	Bacteria;Proteobacteria;Deltaproteobacteria;Myxococcales
Deltaproteobacteria_03_350	2	Bacteria;Proteobacteria;Deltaproteobacteria;Myxococcales
Deltaproteobacteria_03_707	2	Bacteria;Proteobacteria;Deltaproteobacteria;Myxococcales

Deltaproteobacteria_03_1288	2	Bacteria;Proteobacteria;Deltaproteobacteria;Myxococcales;Phaselicystidaceae;Phaselicystis
Deltaproteobacteria_03_1370	2	Bacteria;Proteobacteria;Deltaproteobacteria;Syntrophobacterales;Syntrophaceae;Desulfobacca
Deltaproteobacteria_03_5217	2	Bacteria;Proteobacteria;Deltaproteobacteria;Myxococcales;Cystobacteraceae;Anaeromyxobacter
Deltaproteobacteria_03_19667	2	Bacteria;Proteobacteria;Deltaproteobacteria;Myxococcales
TG-1_03_243	2	Bacteria;TG-1
TM7_03_78	2	Bacteria;TM7
Verrucomicrobia_03_115	2	Bacteria;Verrucomicrobia;Verrucomicrobiae;Verrucomicrobiales;Verrucomicrobiaceae;Prosthecobacter
Verrucomicrobia_03_146	2	Bacteria;Verrucomicrobia;Spartobacteria
Verrucomicrobia_03_5195	2	Bacteria;Verrucomicrobia;Verrucomicrobiae;Verrucomicrobiales;Verrucomicrobiaceae;Prosthecobacter;vanneervenii
BacteriaNA_03_6189	2	Bacteria
Archaea_03_3	2	Archaea;Euryarchaeota;Methanomicrobia;Methanosarcinales;Methanosarcinaceae;ANME-3
Archaea_03_13	2	Archaea;Euryarchaeota;Thermoplasmata;Thermoplasmatales;Marine_Group_II
Archaea_03_85	2	Archaea;Euryarchaeota;Methanomicrobia;Methanosarcinales;Methanosarcinaceae
Archaea_03_125	2	Archaea;Euryarchaeota;Methanobacteria;Methanobacteriales;Methanobacteriaceae
Archaea_03_137	2	Archaea;Euryarchaeota;Thermoplasmata;Thermoplasmatales;CCA47
Archaea_03_155	2	Archaea;Crenarchaeota;Miscellaneous_Crenarchaeotic_Group
Archaea_03_164	2	Archaea;Euryarchaeota;Thermoplasmata;Thermoplasmatales;CCA47
Archaea_03_262	2	Archaea;Euryarchaeota;Methanomicrobia;Methanomicrobiales;Methanolinea
Archaea_03_333	2	Archaea;Crenarchaeota;Miscellaneous_Crenarchaeotic_Group
Archaea_03_600	2	Archaea;Euryarchaeota;Halobacteria;Halobacteriales;Deep_Sea_Hydrothermal_Vent_Group_6
Archaea_03_1643	2	Archaea;Euryarchaeota;Methanobacteria;Methanobacteriales;Methanobacteriaceae;Methanosphaera
Euk_553	2	Eukaryota;SAR;Rhizaria;Cercozoa;Endomyxa;Novel Clade 10
Euk_597	2	Eukaryota;SAR;Rhizaria;Cercozoa;Thecofilosea;WHOI-LI1-14
Euk_6684	2	Eukaryota;Excavata;Discoba;Jakobida;Andalucia
Euk_21291	2	Eukaryota;SAR;Stramenopiles;Bicosoecida;P34.6
Eukarya_06_217	2	Eukaryota;SAR;Alveolata;Ciliophora;Intramacronucleata;Litostomatea;Mesodiniidae
Eukarya_06_282	2	Eukaryota;Excavata;Discoba;Jakobida;Andalucia
Eukarya_06_3268	2	Eukaryota;Opisthokonta;Fungi;Fungi;Basal fungi;Basal fungi;Chytridiomycota
Eukarya_06_5199	2	Eukaryota;Opisthokonta;Fungi;Fungi;Basal fungi;Basal fungi;Chytridiomycota
Eukarya_06_6667	2	Eukaryota;Archaeplastida;Chloroplastida;Chlorophyta;Chlorophyceae;Chlamydomonas
Euk_43	2	Eukaryota;Incertae Sedis;Telonema
Eukarya_06_20	2	Eukaryota;SAR;Stramenopiles;Chrysophyceae;Ochromonadales;Paraphysomonas
Eukarya_06_470	2	Eukaryota;SAR;Stramenopiles;Dictyochophyceae;Pedinellales;Pedinella
Acidobacteria_03_18*	3	Bacteria;Acidobacteria;Holophagae;Holophagales;Holophagaceae;Geothrix
Acidobacteria_03_6056	3	Bacteria;Acidobacteria;Acidobacteria;Acidobacteriales;Acidobacteriaceae
Actinobacteria_03_8	3	Bacteria;Actinobacteria;Actinobacteria;Actinomycetales;Sporichthyaceae
Actinobacteria_03_304	3	Bacteria;Actinobacteria;Actinobacteria;Actinomycetales;Microbacteriaceae;Microbacterium
Actinobacteria_03_3291	3	Bacteria;Actinobacteria;Actinobacteria;Actinomycetales;Actinomycetaceae;Actinomyces
Bacteroidetes_03_96	3	Bacteria;Bacteroidetes;Flavobacteria;Flavobacteriales;Flavobacteriaceae;Salegentibacter
Bacteroidetes_03_150	3	Bacteria;Bacteroidetes;Sphingobacteria;Sphingobacteriales;Flammeovirgaceae

Bacteroidetes_03_171	3	Bacteria;Bacteroidetes;Sphingobacteria;Sphingobacteriales;Chitinophagaceae
Bacteroidetes_03_332	3	Bacteria;Bacteroidetes;Flavobacteria;Flavobacteriales;Flavobacteriaceae
Bacteroidetes_03_803	3	Bacteria;Bacteroidetes;Sphingobacteria;Sphingobacteriales;Flammeovirgaceae;Amoebophilus
Bacteroidetes_03_929	3	Bacteria;Bacteroidetes;Sphingobacteria;Sphingobacteriales;Chitinophagaceae
Bacteroidetes_03_2759	3	Bacteria;Bacteroidetes;Sphingobacteria;Sphingobacteriales;Cyclobacteriaceae;Algoriphagus
Bacteroidetes_03_3255	3	Bacteria;Bacteroidetes;Sphingobacteria;Sphingobacteriales;Saprospiraceae;Haliscomenobacter
Chloroflexi_03_13604	3	Bacteria;Chloroflexi;Dehalococcoidetes;Unassigned;Unassigned;Dehalogenimonas
Fibrobacteres_03_1037	3	Bacteria;Fibrobacteres;Fibrobacteria
Firmicutes_03_5903	3	Bacteria;Firmicutes;Clostridia;Clostridiales;Ruminococcaceae;Acetivibrio
Firmicutes_03_13458	3	Bacteria;Firmicutes;Bacilli;Bacillales
Firmicutes_03_15022	3	Bacteria;Firmicutes;Bacilli;Lactobacillales;Lactobacillaceae;Lactobacillus;durianis
Nitrospirae_03_1	3	Bacteria;Nitrospirae;Nitrospira;Nitrospirales;Nitrospiraceae;Nitrospira
Nitrospirae_03_39	3	Bacteria;Nitrospirae;Nitrospira;Nitrospirales
OD1_03_220	3	Bacteria;OD1
Alphaproteobacteria_03_13	3	Bacteria;Proteobacteria;Alphaproteobacteria;Rickettsiales;SAR11;Pelagibacter
Alphaproteobacteria_03_21	3	Bacteria;Proteobacteria;Alphaproteobacteria;Rickettsiales;SAR11;Pelagibacter
Alphaproteobacteria_03_107	3	Bacteria;Proteobacteria;Alphaproteobacteria;Rhizobiales;Bradyrhizobiaceae;Bradyrhizobium
Alphaproteobacteria_03_1027	3	Bacteria;Proteobacteria;Alphaproteobacteria;Rickettsiales;Rickettsiaceae;Rickettsia
Alphaproteobacteria_03_4657	3	Bacteria;Proteobacteria;Alphaproteobacteria;Rhodospirillales;Acetobacteraceae;Acidocella
Betaproteobacteria_03_7	3	Bacteria;Proteobacteria;Betaproteobacteria;Burkholderiales;Comamonadaceae;Rhodoferax
Betaproteobacteria_03_1243	3	Bacteria;Proteobacteria;Betaproteobacteria;Burkholderiales;Burkholderiaceae;Burkholderia
Gammaproteobacteria_03_3	3	Bacteria;Proteobacteria;Gammaproteobacteria;Pseudomonadales;Moraxellaceae;Acinetobacter
Gammaproteobacteria_03_156	3	Bacteria;Proteobacteria;Gammaproteobacteria
Gammaproteobacteria_03_335	3	Bacteria;Proteobacteria;Gammaproteobacteria;Legionellales;Legionellaceae;Legionella
Gammaproteobacteria_03_955	3	Bacteria;Proteobacteria;Gammaproteobacteria;Chromatiales;Chromatiaceae
Gammaproteobacteria_03_8491	3	Bacteria;Proteobacteria;Gammaproteobacteria;Legionellales;Coxiellaceae;Aquicella
Deltaproteobacteria_03_1	3	Bacteria;Proteobacteria;Deltaproteobacteria;SAR324
Deltaproteobacteria_03_120	3	Bacteria;Proteobacteria;Deltaproteobacteria;Desulfuromonadales;Geobacteraceae;Geobacter
Deltaproteobacteria_03_250	3	Bacteria;Proteobacteria;Deltaproteobacteria;Bdellovibrionales;Bacteriovoraceae;Peredibacter
Deltaproteobacteria_03_1205	3	Bacteria;Proteobacteria;Deltaproteobacteria;Myxococcales
Deltaproteobacteria_03_2738	3	Bacteria;Proteobacteria;Deltaproteobacteria;Myxococcales;Haliangiaceae;Haliangium
Deltaproteobacteria_03_27423	3	Bacteria;Proteobacteria;Deltaproteobacteria;Myxococcales
Epsilonproteobacteria_03_1223	3	Bacteria;Proteobacteria;Epsilonproteobacteria;Campylobacterales;Campylobacteraceae;Arcobacter
Epsilonproteobacteria_03_3577	3	Bacteria;Proteobacteria;Epsilonproteobacteria;Campylobacterales;Helicobacteraceae;Wolinella
Archaea_03_51	3	Archaea;Euryarchaeota;Thermoplasmata;Thermoplasmatales;Marine_Group_II
Archaea_03_3746	3	Archaea;Crenarchaeota;Marine_Group_I

Eukarya_06_5182	3	Eukaryota;SAR;Alveolata;Dinoflagellata
Eukarya_06_6352	3	Eukaryota;SAR;Stramenopiles;Labyrinthulomycetes;Thraustochytriaceae;E170
Eukarya_06_6504	3	Eukaryota;SAR;Alveolata;Dinoflagellata;Dinophyceae;Peridiniphycidae;Thoracosphaeraceae
Eukarya_06_620	3	Eukaryota;SAR;Alveolata;Ciliophora;Intramacronucleata;Conthreep;Oligohymenophorea;Peritrichia
Acidobacteria_03_1982*	4	Bacteria;Acidobacteria;Acidobacteria;Acidobacteriales;Acidobacteriaceae
Acidobacteria_03_3587	4	Bacteria;Acidobacteria;Acidobacteria;Acidobacteriales;Acidobacteriaceae
Actinobacteria_03_563	4	Bacteria;Actinobacteria;Actinobacteria;Actinomycetales;Sporichthyaceae;Sporichthya
Bacteroidetes_03_6	4	Bacteria;Bacteroidetes;Flavobacteria;Flavobacteriales;Flavobacteriaceae
Bacteroidetes_03_48	4	Bacteria;Bacteroidetes;Flavobacteria;Flavobacteriales;Flavobacteriaceae
Bacteroidetes_03_383	4	Bacteria;Bacteroidetes;Sphingobacteria;Sphingobacteriales
Bacteroidetes_03_852	4	Bacteria;Bacteroidetes;Sphingobacteria;Sphingobacteriales
Bacteroidetes_03_919	4	Bacteria;Bacteroidetes;Sphingobacteria;Sphingobacteriales;Chitinophagaceae
Bacteroidetes_03_1324	4	Bacteria;Bacteroidetes;Sphingobacteria;Sphingobacteriales
Bacteroidetes_03_12987	4	Bacteria;Bacteroidetes;Flavobacteria;Flavobacteriales;Flavobacteriaceae;Flavobacterium
Bacteroidetes_03_16532	4	Bacteria;Bacteroidetes;Flavobacteria;Flavobacteriales;Flavobacteriaceae;Flavobacterium
Chlamydiae_03_987	4	Bacteria;Chlamydiae;Chlamydiae;Chlamydiales;Parachlamydiaceae
Chloroflexi_03_567	4	Bacteria;Chloroflexi;Dehalococcoidetes;Unassigned;Unassigned;Dehalogenimonas
Chloroflexi_03_2908	4	Bacteria;Chloroflexi
Nitrospirae_03_31	4	Bacteria;Nitrospirae;Nitrospira;Nitrospirales
OD1_03_20	4	Bacteria;OD1
OD1_03_76	4	Bacteria;OD1
OD1_03_116	4	Bacteria;OD1
OD1_03_568	4	Bacteria;OD1
OD1_03_672	4	Bacteria;OD1
OD1_03_1868	4	Bacteria;OD1
OD1_03_2242	4	Bacteria;OD1
OD1_03_6826	4	Bacteria;OD1
OD1_03_7417	4	Bacteria;OD1
OP3_03_267	4	Bacteria;OP3
Alphaproteobacteria_03_470	4	Bacteria;Proteobacteria;Alphaproteobacteria;Rickettsiales;Unassigned;Captivus
Alphaproteobacteria_03_1358	4	Bacteria;Proteobacteria;Alphaproteobacteria;Sphingomonadales;Sphingomonadaceae;Sandarakinorhabdus
Alphaproteobacteria_03_1748	4	Bacteria;Proteobacteria;Alphaproteobacteria;Rickettsiales;Rickettsiaceae
Alphaproteobacteria_03_4617	4	Bacteria;Proteobacteria;Alphaproteobacteria;Rhodospirillales;Acetobacteraceae;Rhodopila
Alphaproteobacteria_03_13580	4	Bacteria;Proteobacteria;Alphaproteobacteria;Rhodospirillales;Rhodospirillaceae;Defluviicoccus
Alphaproteobacteria_03_23303	4	Bacteria;Proteobacteria;Alphaproteobacteria;Rickettsiales;Unassigned;Captivus
Betaproteobacteria_03_21	4	Bacteria;Proteobacteria;Betaproteobacteria;Burkholderiales;Comamonadaceae;Pelomonas
Betaproteobacteria_03_1378	4	Bacteria;Proteobacteria;Betaproteobacteria;Burkholderiales
Gammaproteobacteria_03_1258	4	Bacteria;Proteobacteria;Gammaproteobacteria;Legionellales;Legionellaceae
Gammaproteobacteria_03_1913	4	Bacteria;Proteobacteria;Gammaproteobacteria;Xanthomonadales;Xanthomonadaceae;Rhodanobacter

Gammaproteobacteria_03_3943	4	Bacteria;Proteobacteria;Gammaproteobacteria
Deltaproteobacteria_03_469	4	Bacteria;Proteobacteria;Deltaproteobacteria;Myxococcales
Deltaproteobacteria_03_2875	4	Bacteria;Proteobacteria;Deltaproteobacteria;Myxococcales
Deltaproteobacteria_03_8715	4	Bacteria;Proteobacteria;Deltaproteobacteria;Myxococcales
Deltaproteobacteria_03_9151	4	Bacteria;Proteobacteria;Deltaproteobacteria;Myxococcales
Deltaproteobacteria_03_11056	4	Bacteria;Proteobacteria;Deltaproteobacteria;Myxococcales
Deltaproteobacteria_03_19518	4	Bacteria;Proteobacteria;Deltaproteobacteria;Myxococcales
Spirochaetes_03_1471	4	Bacteria;Spirochaetes;Spirochaetes;Spirochaetales
TG-1_03_4	4	Bacteria;TG-1
Verrucomicrobia_03_2716	4	Bacteria;Verrucomicrobia;Opitutae;Puniceicoccales;Puniceicoccaceae;Coraliomargarita
Archaea_03_61	4	Archaea;Euryarchaeota;Thermoplasmata;Thermoplasmatales;Marine_Group_II
Archaea_03_356	4	Archaea;Crenarchaeota;terrestrial_group
Archaea_03_2461	4	Archaea;Crenarchaeota;Marine_Group_I
Archaea_03_4523	4	Archaea;Crenarchaeota;South_African_Gold_Mine_Group_1
Euk_6780	4	Unknown
Euk_9317	4	Eukaryota;SAR;Rhizaria;Cercozoa;Thecofilosea;Cryomonadida;Protaspidae;Cryothecomonas
Euk_16319	4	Eukaryota;SAR;Rhizaria;Cercozoa;Thecofilosea;Cryomonadida;Protaspidae;Cryothecomonas
Euk_19952	4	Eukaryota;SAR;Rhizaria;Cercozoa;Thecofilosea;Cryomonadida;Protaspidae;Cryothecomonas
Euk_27629	4	Eukaryota;SAR;Rhizaria;Cercozoa;Thecofilosea;Cryomonadida;Protaspidae;Cryothecomonas
Eukarya_06_178	4	Eukaryota;SAR;Alveolata;Ciliophora;Intramacronucleata;Conthreep;Oligohymenophorea;Scuticociliatia
Eukarya_06_3142	4	Eukaryota;SAR;Stramenopiles;MH-XII
Eukarya_06_415	4	Eukaryota;Excavata;Discoba;Discicristata;Euglenozoa;Kinetoplastea;Metakinetoplastina;Eubodonida
Eukarya_06_7196	4	Eukaryota;SAR;Alveolata;Ciliophora;Intramacronucleata;Litostomatea;Trichostomatia;Polyplastron
Eukarya_06_125	4	Eukaryota;Archaeplastida;Chloroplastida;Chlorophyta;Chlorophyceae;Chlamydomonas
Eukarya_06_963	4	Eukaryota;Opisthokonta;Fungi;Fungi;Basal fungi;Basal fungi;Chytridiomycota
Acidobacteria_03_231*	5	Bacteria;Acidobacteria;Acidobacteria;Acidobacteriales;Acidobacteriaceae;Solibacter
Acidobacteria_03_343	5	Bacteria;Acidobacteria;Acidobacteria;Acidobacteriales;Acidobacteriaceae
Acidobacteria_03_668	5	Bacteria;Acidobacteria;Acidobacteria;Acidobacteriales;Acidobacteriaceae
Actinobacteria_03_135	5	Bacteria;Actinobacteria;Actinobacteria;Actinomycetales;Cellulomonadaceae;Actinotalea
Actinobacteria_03_467	5	Bacteria;Actinobacteria;Actinobacteria;Actinomycetales;Kineosporiaceae
Actinobacteria_03_977	5	Bacteria;Actinobacteria;Actinobacteria;Nitriliruptorales;Nitriliruptoraceae;Nitriliruptor
Actinobacteria_03_1344	5	Bacteria;Actinobacteria;Actinobacteria;Acidimicrobiales;Acidimicrobiaceae;Ferrithrix
Actinobacteria_03_6586	5	Bacteria;Actinobacteria;Actinobacteria;Actinomycetales;Microbacteriaceae;Aquiluna
Actinobacteria_03_9488	5	Bacteria;Actinobacteria;Actinobacteria;Actinomycetales;Microbacteriaceae;Frigoribacterium
Bacteroidetes_03_51	5	Bacteria;Bacteroidetes;Flavobacteria;Flavobacteriales;Flavobacteriaceae;Cloacibacterium
Bacteroidetes_03_1967	5	Bacteria;Bacteroidetes;Flavobacteria;Flavobacteriales;Flavobacteriaceae
Bacteroidetes_03_3400	5	Bacteria;Bacteroidetes;Sphingobacteria;Sphingobacteriales;Cytophagaceae
Bacteroidetes_03_5762	5	Bacteria;Bacteroidetes;Sphingobacteria;Sphingobacteriales;Chitinophagaceae;Sediminibacterium

Bacteroidetes_03_18149	5	Bacteria;Bacteroidetes;Flavobacteria;Flavobacteriales;Flavobacteriaceae;Croceibacter
Bacteroidetes_03_23763	5	Bacteria;Bacteroidetes;Flavobacteria;Flavobacteriales;Flavobacteriaceae;Croceibacter
Chlamydiae_03_233	5	Bacteria;Chlamydiae;Chlamydiae;Chlamydiales;Simkaniaceae;Rhabdochlamydia
Chlamydiae_03_835	5	Bacteria;Chlamydiae;Chlamydiae;Chlamydiales;Parachlamydiaceae;Neochlamydia
Chlorobi_03_267	5	Bacteria;Chlorobi;Chlorobia;Chlorobiales
Cyanobacteria_03_183	5	Bacteria;Cyanobacteria;Cyanobacteria;SubsectionI;Unassigned;Gleocapsa
Cyanobacteria_03_356	5	Bacteria;Cyanobacteria
Firmicutes_03_578	5	Bacteria;Firmicutes;Clostridia;Halanaerobiales;Halanaerobiaceae;Halocella
Firmicutes_03_2494	5	Bacteria;Firmicutes;Clostridia;Clostridiales;Ruminococcaceae;Acetivibrio
Firmicutes_03_8830	5	Bacteria;Firmicutes;Bacilli;Bacillales;Bacillaceae;Virgibacillus;carmonensis
OD1_03_124	5	Bacteria;OD1
OD1_03_230	5	Bacteria;OD1
OD1_03_1937	5	Bacteria;OD1
OD1_03_2137	5	Bacteria;OD1
OD1_03_7235	5	Bacteria;OD1
Planctomycetes_03_128	5	Bacteria;Planctomycetes;Phycisphaerae
Alphaproteobacteria_03_9	5	Bacteria;Proteobacteria;Alphaproteobacteria;Rhodobacterales;Rhodobacteraceae
Alphaproteobacteria_03_730	5	Bacteria;Proteobacteria;Alphaproteobacteria;Rickettsiales
Alphaproteobacteria_03_1644	5	Bacteria;Proteobacteria;Alphaproteobacteria;Rhodobacterales;Rhodobacteraceae;Pseudorhodobacter
Alphaproteobacteria_03_1774	5	Bacteria;Proteobacteria;Alphaproteobacteria;Sphingomonadales;Sphingomonadaceae;Sphingopyxis
Alphaproteobacteria_03_2091	5	Bacteria;Proteobacteria;Alphaproteobacteria;Rhizobiales;Hyphomicrobiaceae;Pedomicrobium
Betaproteobacteria_03_98	5	Bacteria;Proteobacteria;Betaproteobacteria;Nitrosomonadales;Gallionellaceae
Betaproteobacteria_03_123	5	Bacteria;Proteobacteria;Betaproteobacteria;Nitrosomonadales;Nitrosomonadaceae
Betaproteobacteria_03_396	5	Bacteria;Proteobacteria;Betaproteobacteria;Hydrogenophilales;Hydrogenophilaceae;Thiobacillus
Gammaproteobacteria_03_8	5	Bacteria;Proteobacteria;Gammaproteobacteria;Alteromonadales;Pseudoalteromonadaceae;Pseudoalteromonas
Gammaproteobacteria_03_10	5	Bacteria;Proteobacteria;Gammaproteobacteria
Gammaproteobacteria_03_42	5	Bacteria;Proteobacteria;Gammaproteobacteria;Methylococcales;Methylococcaceae
Gammaproteobacteria_03_89	5	Bacteria;Proteobacteria;Gammaproteobacteria;Oceanospirillales;Oceanospirillaceae
Gammaproteobacteria_03_741	5	Bacteria;Proteobacteria;Gammaproteobacteria;Legionellales;Coxiellaceae;Aquicella
Gammaproteobacteria_03_1550	5	Bacteria;Proteobacteria;Gammaproteobacteria;Legionellales;Coxiellaceae;Aquicella
Gammaproteobacteria_03_3948	5	Bacteria;Proteobacteria;Gammaproteobacteria;Oceanospirillales;Halomonadaceae;Halomonas
Gammaproteobacteria_03_4328	5	Bacteria;Proteobacteria;Gammaproteobacteria;Legionellales;Coxiellaceae;Aquicella
Gammaproteobacteria_03_7239	5	Bacteria;Proteobacteria;Gammaproteobacteria;Pasteurellales;Pasteurellaceae;Pasteurella;langaaensis
Gammaproteobacteria_03_23866	5	Bacteria;Proteobacteria;Gammaproteobacteria;Salinisphaerales;Salinisphaeraceae;Salinisphaera
Deltaproteobacteria_03_94	5	Bacteria;Proteobacteria;Deltaproteobacteria;Myxococcales;Polyangiaceae;Sorangium
Deltaproteobacteria_03_410	5	Bacteria;Proteobacteria;Deltaproteobacteria;Desulfobacterales;Desulfobulbaceae;Desulfobulbus

Deltaproteobacteria_03_1115	5	Bacteria;Proteobacteria;Deltaproteobacteria;Syntrophobacterales;Syntrophaceae;Syntrophus
Deltaproteobacteria_03_20121	5	Bacteria;Proteobacteria;Deltaproteobacteria;Myxococcales
Deltaproteobacteria_03_21828	5	Bacteria;Proteobacteria;Deltaproteobacteria;Desulfobacterales;Desulfobulbaceae;Desulfocapsa
TM6_03_361	5	Bacteria;TM6
Verrucomicrobia_03_31	5	Bacteria;Verrucomicrobia;Opitutae;Opitutales;Opitutaceae;Opitutus
Verrucomicrobia_03_3477	5	Bacteria;Verrucomicrobia;Verrucomicrobiae;Verrucomicrobiales;Verrucomicrobiaceae;Verrucomicrobium
BacteriaNA_03_909	5	Bacteria
BacteriaNA_03_2028	5	Bacteria
Archaea_03_329	5	Archaea;Euryarchaeota;Methanomicrobia;Methanosarcinales;Methanosarcinaceae;Methanosarcina
Archaea_03_570	5	Archaea;Euryarchaeota;Halobacteria;Halobacteriales;Deep_Sea_Euryarcheotic_Group
Euk_1861	5	Eukaryota;Centrohelida
Euk_1899	5	Eukaryota;Archaeplastida;Chloroplastida;Chlorophyta;Mamiellophyceae;Monomastix
Euk_7927	5	Eukaryota;Excavata;Discoba;Discicristata;Euglenozoa;Kinetoplastea;Prokinetoplastina;Ichthyobodo
Euk_7957	5	Eukaryota;RT5iin25
Euk_14491	5	Eukaryota;SAR;Rhizaria;Cercozoa
Euk_18143	5	Eukaryota;Opisthokonta;Fungi;Fungi;Basal fungi;Basal fungi;Blastocladiomycota
Euk_25112	5	Eukaryota;Excavata;Discoba;Discicristata;Euglenozoa;Kinetoplastea;Metakinetoplastina;Parabodonida
Eukarya_06_1197	5	Eukaryota;SAR;Stramenopiles;Chrysophyceae;Ochromonadales;Paraphysomonas
Eukarya_06_1239	5	Eukaryota;Opisthokonta;Fungi;Basidiomycota;Pucciniomycotina;Microbotryomycetes
Eukarya_06_15	5	Eukaryota;Archaeplastida;Chloroplastida;Charophyta;Phragmoplastophyta;Streptophyta;Embryophyta;Tracheophyta
Eukarya_06_1735	5	Eukaryota;SAR;Stramenopiles;Chrysophyceae
Eukarya_06_2139	5	Eukaryota;SAR;Alveolata;Ciliophora;Intramacronucleata;Conthreep;Nassophorea;Obertrumia
Eukarya_06_2422	5	Eukaryota;SAR;Alveolata;Ciliophora;Intramacronucleata;Litostomatea;Haptoria;Didinium
Eukarya_06_2518	5	Eukaryota;Excavata;Discoba;Discicristata;Euglenozoa;Kinetoplastea;Metakinetoplastina;Neobodonida
Eukarya_06_3727	5	Eukaryota;SAR;Alveolata;Ciliophora;Intramacronucleata;Conthreep;Oligohymenophorea;Peniculia
Eukarya_06_43	5	Eukaryota;SAR;Alveolata;Ciliophora;Intramacronucleata;Conthreep;Oligohymenophorea;Scuticociliatia
Eukarya_06_4827	5	Eukaryota;SAR;Alveolata;Dinoflagellata;Dinophyceae;Peridiniphycidae;Thoracosphaeraceae
Eukarya_06_490	5	Eukaryota;SAR;Alveolata;Ciliophora;Intramacronucleata;Conthreep;Oligohymenophorea;Peritrichia
Eukarya_06_5165	5	Eukaryota;Opisthokonta;Fungi;Basidiomycota;Pucciniomycotina;Agaricostilbomycetes;Sterigmatomyces
Eukarya_06_516	5	Eukaryota;SAR;Alveolata;Ciliophora;Intramacronucleata;Conthreep;Prostomatea;Cryptocaryon
Acidobacteria_03_5976*	6	Bacteria;Acidobacteria;Acidobacteria;Acidobacteriales;Acidobacteriaceae
Actinobacteria_03_9	6	Bacteria;Actinobacteria;Actinobacteria;Actinomycetales;Mycobacteriaceae;Mycobacterium
Actinobacteria_03_2432	6	Bacteria;Actinobacteria;Actinobacteria;Nitriliruptorales;Nitriliruptoraceae;Nitriliruptor
Actinobacteria_03_7884	6	Bacteria;Actinobacteria;Actinobacteria;Actinomycetales
Actinobacteria_03_9272	6	Bacteria;Actinobacteria;Actinobacteria;Actinomycetales;Microbacteriaceae
Bacteroidetes_03_113	6	Bacteria;Bacteroidetes;Flavobacteria;Flavobacteriales;Flavobacteriaceae
Bacteroidetes_03_1293	6	Bacteria;Bacteroidetes;Sphingobacteria;Sphingobacteriales;Saprospiraceae;Lewinella
Bacteroidetes_03_3460	6	Bacteria;Bacteroidetes;Flavobacteria;Flavobacteriales;Flavobacteriaceae

Bacteroidetes_03_17033	6	Bacteria;Bacteroidetes;Flavobacteria;Flavobacteriales
Bacteroidetes_03_27636	6	Bacteria;Bacteroidetes;Sphingobacteria;Sphingobacteriales;Cyclobacteriaceae;Algoriphagus
Chlamydiae_03_376	6	Bacteria;Chlamydiae;Chlamydiae;Chlamydiales;Simkaniaceae;Fritschea
Cyanobacteria_03_61	6	Bacteria;Cyanobacteria;Cyanobacteria;SubsectionIII;Unassigned;Leptolyngbya
Firmicutes_03_435	6	Bacteria;Firmicutes;Bacilli;Bacillales;Staphylococcaceae;Staphylococcus
Firmicutes_03_5073	6	Bacteria;Firmicutes;Clostridia;Clostridiales;Lachnospiraceae
Lentisphaerae_03_1145	6	Bacteria;Lentisphaerae;Lentisphaeria
Lentisphaerae_03_1342	6	Bacteria;Lentisphaerae;Lentisphaeria
Lentisphaerae_03_2153	6	Bacteria;Lentisphaerae;Lentisphaeria
OD1_03_8148	6	Bacteria;OD1
OP3_03_247	6	Bacteria;OP3
Planctomycetes_03_1776	6	Bacteria;Planctomycetes;Planctomycetacia;Planctomycetales;Planctomycetaceae;Rhodopirellula
Alphaproteobacteria_03_82	6	Bacteria;Proteobacteria;Alphaproteobacteria;Rhodobacterales;Rhodobacteraceae
Alphaproteobacteria_03_367	6	Bacteria;Proteobacteria;Alphaproteobacteria;Rhodobacterales;Rhodobacteraceae;Roseovarius
Alphaproteobacteria_03_1553	6	Bacteria;Proteobacteria;Alphaproteobacteria;Rhodobacterales;Rhodobacteraceae
Alphaproteobacteria_03_1654	6	Bacteria;Proteobacteria;Alphaproteobacteria;Rhodobacterales;Rhodobacteraceae
Alphaproteobacteria_03_2853	6	Bacteria;Proteobacteria;Alphaproteobacteria;Rickettsiales
Alphaproteobacteria_03_27270	6	Bacteria;Proteobacteria;Alphaproteobacteria;Rhizobiales;Hyphomicrobiaceae;Pedomicrobium
Gammaproteobacteria_03_2458	6	Bacteria;Proteobacteria;Gammaproteobacteria;Thiotrichales;Thiotrichaceae
Gammaproteobacteria_03_3190	6	Bacteria;Proteobacteria;Gammaproteobacteria;Legionellales;Legionellaceae
Gammaproteobacteria_03_16256	6	Bacteria;Proteobacteria;Gammaproteobacteria;Legionellales;Legionellaceae;Legionella
Deltaproteobacteria_03_5050	6	Bacteria;Proteobacteria;Deltaproteobacteria
TM6_03_1232	6	Bacteria;TM6
Verrucomicrobia_03_228	6	Bacteria;Verrucomicrobia;Verrucomicrobiae;Verrucomicrobiales;Verrucomicrobiaceae;Luteolibacter
Archaea_03_18	6	Archaea;Euryarchaeota;Thermoplasmata;Thermoplasmatales;Marine_Group_II
Archaea_03_91	6	Archaea;Euryarchaeota;Thermoplasmata;Thermoplasmatales;Marine_Group_II
Archaea_03_443	6	Archaea;Crenarchaeota;terrestrial_group
Archaea_03_1159	6	Archaea;Euryarchaeota;Thermoplasmata;Thermoplasmatales;Marine_Group_II
Archaea_03_4463	6	Archaea;Euryarchaeota;Halobacteria;Halobacteriales;Deep_Sea_Hydrothermal_Vent_Group_6
Archaea_03_4628	6	Archaea;Euryarchaeota;Halobacteria;Halobacteriales;Halobacteriaceae;Halobaculum
Archaea_03_6006	6	Archaea;Euryarchaeota;Methanomicrobia;Methanomicrobiales;Methanomicrobiaceae;Methanoculleus
Archaea_03_6367	6	Archaea;Crenarchaeota;terrestrial_group
Euk_3921	6	Eukaryota;SAR;Rhizaria;Cercozoa;Thecofilosea;NIF-3A7
Euk_12690	6	Eukaryota;RT5iin25
Euk_16481	6	Eukaryota;SAR;Rhizaria;Cercozoa;Thecofilosea;BOLA322
Euk_21808	6	Eukaryota;SAR;Alveolata;Ciliophora;Intramacronucleata;Conthreep;Prostomatea;Cryptocaryon
Euk_25078	6	Eukaryota;SAR;Rhizaria;Cercozoa;Thecofilosea;Cryomonadida;Protaspidae;Cryothecomonas
Eukarya_06_1220	6	Eukaryota;SAR;Stramenopiles;Chrysophyceae;Ochromonadales;Epipyxis

Eukarya_06_842	6	Eukaryota;Opisthokonta;Fungi;Ascomycota;Saccharomycotina;Saccharomycetes;Saccharomycetales
Actinobacteria_03_11036*	7	Bacteria;Actinobacteria;Actinobacteria;Acidimicrobiales;Acidimicrobiaceae
Bacteroidetes_03_203	7	Bacteria;Bacteroidetes;Sphingobacteria;Sphingobacteriales
Bacteroidetes_03_204	7	Bacteria;Bacteroidetes
Bacteroidetes_03_223	7	Bacteria;Bacteroidetes;Sphingobacteria;Sphingobacteriales;Chitinophagaceae;Ferruginibacter
Bacteroidetes_03_273	7	Bacteria;Bacteroidetes;Flavobacteria;Flavobacteriales;Flavobacteriaceae;Winogradskyella
Bacteroidetes_03_591	7	Bacteria;Bacteroidetes
Bacteroidetes_03_1737	7	Bacteria;Bacteroidetes;Flavobacteria;Flavobacteriales
Bacteroidetes_03_2395	7	Bacteria;Bacteroidetes;Bacteroidia;Bacteroidales;Rikenellaceae
Bacteroidetes_03_2527	7	Bacteria;Bacteroidetes;Flavobacteria;Flavobacteriales;Cryomorphaceae;Cryomorpha
Bacteroidetes_03_2590	7	Bacteria;Bacteroidetes;Sphingobacteria;Sphingobacteriales
Bacteroidetes_03_3273	7	Bacteria;Bacteroidetes;Sphingobacteria;Sphingobacteriales
Bacteroidetes_03_4057	7	Bacteria;Bacteroidetes;Bacteroidia;Bacteroidales;Marinilabiaceae
Bacteroidetes_03_4142	7	Bacteria;Bacteroidetes;Sphingobacteria;Sphingobacteriales
Bacteroidetes_03_6570	7	Bacteria;Bacteroidetes
Bacteroidetes_03_24493	7	Bacteria;Bacteroidetes;Flavobacteria;Flavobacteriales;Cryomorphaceae;Owenweeksia
BRC1_03_1734	7	Bacteria;BRC1
Chlamydiae_03_79	7	Bacteria;Chlamydiae;Chlamydiae;Chlamydiales
Chloroflexi_03_58	7	Bacteria;Chloroflexi;Caldilineae;Caldilineales;Caldilineaceae;Caldilinea
Chloroflexi_03_330	7	Bacteria;Chloroflexi;Caldilineae;Caldilineales;Caldilineaceae;Caldilinea
Chloroflexi_03_6266	7	Bacteria;Chloroflexi;Caldilineae;Caldilineales
Firmicutes_03_3696	7	Bacteria;Firmicutes;Clostridia;Clostridiales;Ruminococcaceae
Firmicutes_03_5065	7	Bacteria;Firmicutes;Bacilli;Bacillales;Paenibacillaceae;Paenibacillus
Firmicutes_03_5402	7	Bacteria;Firmicutes;Clostridia;Clostridiales;Ruminococcaceae;Acetivibrio
Firmicutes_03_6828	7	Bacteria;Firmicutes;Bacilli;Bacillales;Paenibacillaceae;Paenibacillus
Firmicutes_03_12755	7	Bacteria;Firmicutes;Clostridia;Clostridiales;Lachnospiraceae
Firmicutes_03_14822	7	Bacteria;Firmicutes;Clostridia;Clostridiales;Lachnospiraceae;Blautia
Firmicutes_03_17205	7	Bacteria;Firmicutes;Clostridia;Clostridiales;Ruminococcaceae;Acetivibrio
Firmicutes_03_32038	7	Bacteria;Firmicutes;Clostridia;Clostridiales
Lentisphaerae_03_44	7	Bacteria;Lentisphaerae;Lentisphaeria
Lentisphaerae_03_414	7	Bacteria;Lentisphaerae;Lentisphaeria
Lentisphaerae_03_522	7	Bacteria;Lentisphaerae;Lentisphaeria
Lentisphaerae_03_937	7	Bacteria;Lentisphaerae;Lentisphaeria
Lentisphaerae_03_1945	7	Bacteria;Lentisphaerae;Lentisphaeria
OD1_03_324	7	Bacteria;OD1
OD1_03_1098	7	Bacteria;OD1
OD1_03_2225	7	Bacteria;OD1
OP11_03_91	7	Bacteria;OP11
OP11_03_510	7	Bacteria;OP11
Planctomycetes_03_137	7	Bacteria;Planctomycetes;Phycisphaerae
Planctomycetes_03_621	7	Bacteria;Planctomycetes;Phycisphaerae
Planctomycetes_03_2319	7	Bacteria;Planctomycetes;Phycisphaerae

Alphaproteobacteria_03_96	7	Bacteria;Proteobacteria;Alphaproteobacteria;Rhodobacterales;Rhodobacteraceae;Catellibacterium
Alphaproteobacteria_03_119	7	Bacteria;Proteobacteria;Alphaproteobacteria;Rhodospirillales;Rhodospirillaceae
Alphaproteobacteria_03_288	7	Bacteria;Proteobacteria;Alphaproteobacteria;Rhodobacterales;Rhodobacteraceae;Rhodobacter
Alphaproteobacteria_03_343	7	Bacteria;Proteobacteria;Alphaproteobacteria;Rhodospirillales
Alphaproteobacteria_03_346	7	Bacteria;Proteobacteria;Alphaproteobacteria;Rhodobacterales;Rhodobacteraceae
Alphaproteobacteria_03_651	7	Bacteria;Proteobacteria;Alphaproteobacteria;Rhodospirillales;Rhodospirillaceae;Defluviicoccus
Alphaproteobacteria_03_2223	7	Bacteria;Proteobacteria;Alphaproteobacteria;Rhodospirillales;Acetobacteraceae;Roseomonas
Alphaproteobacteria_03_3014	7	Bacteria;Proteobacteria;Alphaproteobacteria;Rhodobacterales;Rhodobacteraceae
Alphaproteobacteria_03_14676	7	Bacteria;Proteobacteria;Alphaproteobacteria;Rhodobacterales;Rhodobacteraceae
Betaproteobacteria_03_17	7	Bacteria;Proteobacteria;Betaproteobacteria;Burkholderiales;Comamonadaceae;Rhodoferax
Betaproteobacteria_03_42	7	Bacteria;Proteobacteria;Betaproteobacteria;Burkholderiales;Comamonadaceae
Betaproteobacteria_03_112	7	Bacteria;Proteobacteria;Betaproteobacteria;Hydrogenophilales;Hydrogenophilaceae
Betaproteobacteria_03_141	7	Bacteria;Proteobacteria;Betaproteobacteria;Hydrogenophilales;Hydrogenophilaceae;Tepidiphilus
Betaproteobacteria_03_762	7	Bacteria;Proteobacteria;Betaproteobacteria;Burkholderiales;Comamonadaceae;Ottowia
Betaproteobacteria_03_2313	7	Bacteria;Proteobacteria;Betaproteobacteria
Gammaproteobacteria_03_93	7	Bacteria;Proteobacteria;Gammaproteobacteria;Pseudomonadales;Moraxellaceae;Acinetobacter
Gammaproteobacteria_03_99	7	Bacteria;Proteobacteria;Gammaproteobacteria;Xanthomonadales;Xanthomonadaceae
Gammaproteobacteria_03_261	7	Bacteria;Proteobacteria;Gammaproteobacteria;Legionellales;Legionellaceae;Legionella
Gammaproteobacteria_03_279	7	Bacteria;Proteobacteria;Gammaproteobacteria;Legionellales;Legionellaceae;Legionella
Gammaproteobacteria_03_419	7	Bacteria;Proteobacteria;Gammaproteobacteria;Legionellales;Legionellaceae
Gammaproteobacteria_03_426	7	Bacteria;Proteobacteria;Gammaproteobacteria;Xanthomonadales;Sinobacteraceae
Gammaproteobacteria_03_1678	7	Bacteria;Proteobacteria;Gammaproteobacteria;Thiotrichales;Piscirickettsiaceae;Methylophaga
Gammaproteobacteria_03_3678	7	Bacteria;Proteobacteria;Gammaproteobacteria;Methylococcales;Methylococcaceae;Methylomonas;fodinarum
Deltaproteobacteria_03_60	7	Bacteria;Proteobacteria;Deltaproteobacteria;Desulfobacterales;Desulfobulbaceae;Desulforhopalus
Deltaproteobacteria_03_296	7	Bacteria;Proteobacteria;Deltaproteobacteria;Desulfobacterales;Desulfobulbaceae;Desulfocapsa
Deltaproteobacteria_03_1489	7	Bacteria;Proteobacteria;Deltaproteobacteria;Desulfobacterales;Desulfobacteraceae;Desulfofaba;hansenii
Deltaproteobacteria_03_2378	7	Bacteria;Proteobacteria;Deltaproteobacteria;Desulfobacterales;Desulfobacteraceae
Deltaproteobacteria_03_2979	7	Bacteria;Proteobacteria;Deltaproteobacteria;Syntrophobacterales;Syntrophaceae;Smithella
Deltaproteobacteria_03_7891	7	Bacteria;Proteobacteria;Deltaproteobacteria;Desulfobacterales;Desulfobulbaceae;Desulfurivibrio
Deltaproteobacteria_03_33077	7	Bacteria;Proteobacteria;Deltaproteobacteria;Syntrophobacterales;Syntrophaceae
Epsilonproteobacteria_03_129	7	Bacteria;Proteobacteria;Epsilonproteobacteria;Campylobacterales;Helicobacteraceae;Sulfurimonas

Spirochaetes_03_147	7	Bacteria;Spirochaetes;Spirochaetes
Spirochaetes_03_349	7	Bacteria;Spirochaetes;Spirochaetes
Tenericutes_03_33	7	Bacteria;Tenericutes;Mollicutes;Acholeplasmatales;Acholeplasmataceae;Acholeplasma
Verrucomicrobia_03_15	7	Bacteria;Verrucomicrobia;Verrucomicrobiae;Verrucomicrobiales;Verrucomicrobiaceae
BacteriaNA_03_1049	7	Bacteria
Archaea_03_1120	7	Archaea;Euryarchaeota;Halobacteria;Halobacteriales;Deep_Sea_Hydrothermal_Vent_Group_6
Euk_71	7	Eukaryota;Incertae Sedis;Telonema
Euk_2590	7	Eukaryota;SAR;Stramenopiles;Bicosoecida;Bicosoecidae;Bicosoeca
Euk_17442	7	Eukaryota;Cryptophyceae;Cryptomonadales
Eukarya_06_1539	7	Eukaryota;Haptophyta;Pavlovophyceae;Diacronema
Eukarya_06_210	7	Eukaryota;SAR;Stramenopiles;Chrysophyceae;Chromulinales;Uroglena
Eukarya_06_4802	7	Eukaryota;Cryptophyceae;Cryptomonadales
Eukarya_06_5629	7	Eukaryota;Archaeplastida;Chloroplastida;Chlorophyta;Chlorophyceae;Chlamydomonas
Actinobacteria_03_3*	8	Bacteria;Actinobacteria;Actinobacteria;Actinomycetales;Propionibacteriaceae;Propionibacterium
Betaproteobacteria_03_30	8	Bacteria;Proteobacteria;Betaproteobacteria;Burkholderiales;Comamonadaceae;Pelomonas
Euk_595	8	Eukaryota;SAR;Rhizaria;Cercozoa
Eukarya_06_4386	8	Eukaryota;SAR;Alveolata;Ciliophora;Intramacronucleata;Spirotrichea;Hypotrichia;uncultured
Firmicutes_03_1933	8	Bacteria;Firmicutes;Bacilli;Bacillales;Bacillaceae;Bacillus
Actinobacteria_03_4*	9	Bacteria;Actinobacteria;Actinobacteria;Actinomycetales;Sporichthyaceae
Alphaproteobacteria_03_8158	9	Bacteria;Proteobacteria;Alphaproteobacteria;Rickettsiales;Rickettsiaceae
Eukarya_06_2698	9	Eukaryota;Opisthokonta;Holozoa;Choanomonada;Craspedida;Amb-18S-720
Betaproteobacteria_03_58	9	Bacteria;Proteobacteria;Betaproteobacteria;Burkholderiales;Comamonadaceae;Aquabacterium
Actinobacteria_03_91*	10	Bacteria;Actinobacteria;Actinobacteria;Actinomycetales;Micrococcaceae;Micrococcus
Bacteroidetes_03_1875	10	Bacteria;Bacteroidetes
Betaproteobacteria_03_503	10	Bacteria;Proteobacteria;Betaproteobacteria;Burkholderiales;Comamonadaceae
Alphaproteobacteria_03_13239*	11	Bacteria;Proteobacteria;Alphaproteobacteria;Rhodospirillales;Rhodospirillaceae
Bacteroidetes_03_400	11	Bacteria;Bacteroidetes;Sphingobacteria;Sphingobacteriales
Bacteroidetes_03_1414	11	Bacteria;Bacteroidetes;Flavobacteria;Flavobacteriales;Cryomorphaceae;Owenweeksia
Bacteroidetes_03_2068	11	Bacteria;Bacteroidetes;Sphingobacteria;Sphingobacteriales;Sphingobacteriaceae;Sphingobacteriaceae;Pedobacter
Bacteroidetes_03_4593	11	Bacteria;Bacteroidetes;Flavobacteria;Flavobacteriales
Bacteroidetes_03_9103	11	Bacteria;Bacteroidetes;Flavobacteria;Flavobacteriales;Flavobacteriaceae;Flavobacterium
Bacteroidetes_03_20155	11	Bacteria;Bacteroidetes;Flavobacteria;Flavobacteriales;Flavobacteriaceae;Croceibacter
Firmicutes_03_11	11	Bacteria;Firmicutes;Bacilli;Lactobacillales;Streptococcaceae;Streptococcus
Firmicutes_03_7835	11	Bacteria;Firmicutes;Bacilli;Bacillales;Paenibacillaceae;Paenibacillus
OD1_03_43	11	Bacteria;OD1
OD1_03_3041	11	Bacteria;OD1
OD1_03_6947	11	Bacteria;OD1
Planctomycetes_03_2812	11	Bacteria;Planctomycetes;Planctomycetacia;Planctomycetales;Planctomycetaceae;Rhodopirellula
Alphaproteobacteria_03_148	11	Bacteria;Proteobacteria;Alphaproteobacteria;Rhodobacterales;Rhodobacteraceae;Marinosulfomonas
Alphaproteobacteria_03_1	11	Bacteria;Proteobacteria;Alphaproteobacteria;Rhodobacterales;Rhodobacteraceae

552		
Deltaproteobacteria_03_90	11	Bacteria;Proteobacteria;Deltaproteobacteria
Deltaproteobacteria_03_10730	11	Bacteria;Proteobacteria;Deltaproteobacteria;Bdellovibrionales;Bdellovibrionaceae;Bdellovibrio;bacteriovorus
Verrucomicrobia_03_25	11	Bacteria;Verrucomicrobia;Opitutae;Puniceicoccales;Puniceicoccaceae;Lentimonas
Verrucomicrobia_03_410	11	Bacteria;Verrucomicrobia;Spartobacteria;Chthoniobacterales;Xiphinematobacteriaceae
Verrucomicrobia_03_725	11	Bacteria;Verrucomicrobia;Opitutae;Opitutales;Opitutaceae;Opitutus
Verrucomicrobia_03_3738	11	Bacteria;Verrucomicrobia;Spartobacteria;Chthoniobacterales;Xiphinematobacteriaceae
Verrucomicrobia_03_7541	11	Bacteria;Verrucomicrobia;Opitutae;Puniceicoccales;Puniceicoccaceae;Coraliomargarita
BacteriaNA_03_4150	11	Bacteria
Archaea_03_87	11	Archaea;Crenarchaeota;Miscellaneous_Crenarchaeotic_Group
Archaea_03_146	11	Archaea;Euryarchaeota;Methanomicrobia;Methanosarcinales;Methanosarcinaceae;Methanosarcina
Archaea_03_309	11	Archaea;Euryarchaeota;Methanomicrobia;Methanomicrobiales;Methanomicrobiaceae;Methanoculleus
Archaea_03_327	11	Archaea;Euryarchaeota;Halobacteria;Halobacteriales;Deep_Sea_Hydrothermal_Vent_Group_6
Archaea_03_369	11	Archaea;Euryarchaeota;Methanomicrobia;Methanosarcinales;GOM_Arc_I
Archaea_03_404	11	Archaea;Euryarchaeota;Methanomicrobia;Methanomicrobiales
Archaea_03_1559	11	Archaea;Euryarchaeota;Methanobacteria;Methanobacteriales;Methanobacteriaceae;Methanobrevibacter
Euk_27	11	Eukaryota;SAR;Alveolata;Dinoflagellata;Dinophyceae;Gymnodiniphycidae;Incertae Sedis;Cochlodinium
Euk_222	11	Eukaryota;SAR;Rhizaria;Cercozoa;Thecofilosea;WHOI-LI1-14
Euk_9498	11	Eukaryota;Excavata;Discoba;Discicristata;Euglenozoa;Euglenida;Heteronematina;Petalomonas
Eukarya_06_1173	11	Eukaryota;SAR;Alveolata;Protalveolata;Syndiniales;Amoebophrya
Eukarya_06_128	11	Unknown
Eukarya_06_133	11	Unknown
Eukarya_06_1448	11	Eukaryota;SAR;Stramenopiles;Peronosporomycetes;Phytophthora
Eukarya_06_1671	11	Eukaryota;Excavata;Discoba;Discicristata;Euglenozoa;Kinetoplastea;Metakinetoplastina;Neobodonida
Eukarya_06_180	11	Eukaryota;SAR;Alveolata;Ciliophora;Intramacronucleata;Spirotrichea;Choreotrichia;uncultured
Eukarya_06_201	11	Eukaryota;SAR;Alveolata;Protalveolata;Syndiniales;Syndiniales Group II
Eukarya_06_30	11	Eukaryota;SAR;Stramenopiles;Chrysophyceae;Chromulinales;JBNA46
Eukarya_06_317	11	Eukaryota;Opisthokonta;Fungi;Basidiomycota;Ustilaginomycotina;Exobasidiomycetes;Malassezia
Eukarya_06_3194	11	Eukaryota;SAR;Rhizaria;Cercozoa;Thecofilosea;Cryomonadida;Protaspidae;Protaspa
Eukarya_06_3357	11	Eukaryota;SAR;Alveolata;Ciliophora;Intramacronucleata;Litostomatea;Haptoria
Eukarya_06_39	11	Eukaryota;SAR;Alveolata;Dinoflagellata;Dinophyceae;Peridiniphycidae;Gonyaulacales;Neoceratium
Eukarya_06_4087	11	Eukaryota;Opisthokonta;Fungi;LKM15
Eukarya_06_5063	11	Eukaryota;Excavata;Discoba;Discicristata;Euglenozoa;Euglenida;Heteronematina;Petalomonas
Eukarya_06_512	11	Eukaryota;SAR;Alveolata;Dinoflagellata;Dinophyceae;Peridiniphycidae;Peridiniales;Protoperidinium
Eukarya_06_5456	11	Eukaryota;SAR;Alveolata;Dinoflagellata;Dinophyceae;Peridiniphycidae;Thoracosphaeraceae
Eukarya_06_7017	11	Eukaryota;Haptophyta;Prymnesiophyceae
Eukarya_06_84	11	Eukaryota;SAR;Alveolata;Protalveolata;Syndiniales;Syndiniales Group I
Eukarya_06_1160	11	Eukaryota;SAR;Stramenopiles;Dictyochophyceae;Pedinellales
Alphaproteobacteria_03_2014*	12	Bacteria;Proteobacteria;Alphaproteobacteria;Rickettsiales;Rickettsiaceae

Planctomycetes_03_353	12	Bacteria;Planctomycetes;Planctomycetacia;Planctomycetales;Planctomycetaceae;Planctomyces
Betaproteobacteria_03_873	12	Bacteria;Proteobacteria;Betaproteobacteria;Rhodocyclales;Rhodocyclaceae
Eukarya_06_338	12	Eukaryota;Opisthokonta;Holozoa;Corallochytrium
Alphaproteobacteria_03_62*	13	Bacteria;Proteobacteria;Alphaproteobacteria;Caulobacterales;Caulobacteraceae;Brevundimonas
Euk_301	13	Eukaryota;SAR;Rhizaria;Cercozoa;Thecofilosea;Cryomonadida;Protaspidae;Protaspa
Alphaproteobacteria_03_6621*	14	Bacteria;Proteobacteria;Alphaproteobacteria;Sneathiellales;Sneathiellaceae;Sneathiella
Chloroflexi_03_474	14	Bacteria;Chloroflexi;Caldilineae;Caldilineales;Caldilineaceae;Caldilinea
Cyanobacteria_03_38	14	Bacteria;Cyanobacteria;Cyanobacteria;SubsectionIII
Eukarya_06_515	14	Eukaryota;SAR;Stramenopiles;Diatomea;Bacillariophytina;Bacillariophyceae;Asterionellopsis
Eukarya_06_723	14	Eukaryota;SAR;Stramenopiles;Diatomea;Bacillariophytina;Bacillariophyceae;Sellaphora
Archaea_03_112	14	Archaea;Euryarchaeota;Halobacteria;Halobacteriales;Halobacteriaceae;Halobaculum
Eukarya_06_804	14	Eukaryota;Amoebozoa;Conosa;Protosporangiida;Protosporangiidae;Protosporangium
Eukarya_06_285	15	Unknown
Betaproteobacteria_03_28	15	Bacteria;Proteobacteria;Betaproteobacteria;Burkholderiales;Comamonadaceae;Hydrogenophaga
Alphaproteobacteria_03_91*	15	Bacteria;Proteobacteria;Alphaproteobacteria;Rickettsiales;SAR11;Pelagibacter
Bacteroidetes_03_1	15	Bacteria;Bacteroidetes;Flavobacteria;Flavobacteriales;Flavobacteriaceae
Gammaproteobacteria_03_175	15	Bacteria;Proteobacteria;Gammaproteobacteria;Oceanospirillales
Alphaproteobacteria_03_975	15	Bacteria;Proteobacteria;Alphaproteobacteria;Sphingomonadales;Sphingomonadaceae;Novosphingobium
Betaproteobacteria_03_56	15	Bacteria;Proteobacteria;Betaproteobacteria;Burkholderiales;Comamonadaceae
Gammaproteobacteria_03_68	15	Bacteria;Proteobacteria;Gammaproteobacteria
Verrucomicrobia_03_356	15	Bacteria;Verrucomicrobia;Opitutae;Opitutales;Opitutaceae;Opitutus
Bacteroidetes_03_89	15	Bacteria;Bacteroidetes;Sphingobacteria;Sphingobacteriales
Betaproteobacteria_03_46	15	Bacteria;Proteobacteria;Betaproteobacteria;Burkholderiales;Comamonadaceae;Hydrogenophaga
Bacteroidetes_03_23	15	Bacteria;Bacteroidetes;Flavobacteria;Flavobacteriales;Flavobacteriaceae
Bacteroidetes_03_416	15	Bacteria;Bacteroidetes;Flavobacteria;Flavobacteriales;Flavobacteriaceae
Betaproteobacteria_03_1	15	Bacteria;Proteobacteria;Betaproteobacteria;Burkholderiales;Burkholderiaceae;Ralstonia
Bacteroidetes_03_4	15	Bacteria;Bacteroidetes;Flavobacteria;Flavobacteriales;Flavobacteriaceae;Flavobacterium
Archaea_03_117*	16	Archaea;Euryarchaeota;Methanomicrobia;Methanomicrobiales
Archaea_03_14	16	Archaea;Euryarchaeota;Thermoplasmata;Thermoplasmatales;Marine_Group_II
Archaea_03_141	17	Archaea;Crenarchaeota;Marine_Group_I
Archaea_03_200	17	Archaea;Euryarchaeota;Methanomicrobia;Methanomicrobiales
Archaea_03_17*	17	Archaea;Euryarchaeota;Thermoplasmata;Thermoplasmatales;Marine_Group_II
Archaea_03_15	17	Archaea;Euryarchaeota;Thermoplasmata;Thermoplasmatales;Marine_Group_II
Archaea_03_8	17	Archaea;Crenarchaeota;Marine_Group_I
Bacteroidetes_03_1296*	18	Bacteria;Bacteroidetes;Sphingobacteria;Sphingobacteriales;Cytophagaceae;Flexibacter
Gammaproteobacteria_03_13	18	Bacteria;Proteobacteria;Gammaproteobacteria
Planctomycetes_03_3822	18	Bacteria;Planctomycetes;Planctomycetacia;Planctomycetales;Planctomycetaceae
Verrucomicrobia_03_300	18	Bacteria;Verrucomicrobia;Spartobacteria;Chthoniobacterales;Xiphinematobacteriaceae
Gammaproteobacteria_03_	18	Bacteria;Proteobacteria;Gammaproteobacteria;Alteromonadales;Pseudoalteromonadaceae;Pseu

11		doalteromonas;ruthenica
Euk_5461	18	Eukaryota;Centrohelida;M1-18D08
Verrucomicrobia_03_94	18	Bacteria;Verrucomicrobia;Verrucomicrobiae;Verrucomicrobiales;Verrucomicrobiaceae
Bacteroidetes_03_121	18	Bacteria;Bacteroidetes;Flavobacteria;Flavobacteriales;Flavobacteriaceae;Tenacibaculum
Bacteroidetes_03_251	18	Bacteria;Bacteroidetes;Flavobacteria;Flavobacteriales;Flavobacteriaceae;Salegentibacter
Bacteroidetes_03_5	18	Bacteria;Bacteroidetes;Flavobacteria;Flavobacteriales;Flavobacteriaceae;Flavobacterium
Bacteroidetes_03_168*	19	Bacteria;Bacteroidetes;Flavobacteria;Flavobacteriales;Flavobacteriaceae;Croceibacter
Bacteroidetes_03_359	19	Bacteria;Bacteroidetes;Sphingobacteria;Sphingobacteriales;Cyclobacteriaceae;Cyclobacterium
Actinobacteria_03_140	19	Bacteria;Actinobacteria;Actinobacteria;Acidimicrobiales
Actinobacteria_03_15	19	Bacteria;Actinobacteria;Actinobacteria;Actinomycetales;Microbacteriaceae;Microbacterium
Bacteroidetes_03_12	19	Bacteria;Bacteroidetes;Flavobacteria;Flavobacteriales;Flavobacteriaceae
Firmicutes_03_7271	19	Bacteria;Firmicutes;Clostridia;Clostridiales;Ruminococcaceae;Acetivibrio
OD1_03_291	19	Bacteria;OD1
Alphaproteobacteria_03_984	19	Bacteria;Proteobacteria;Alphaproteobacteria
Gammaproteobacteria_03_120	19	Bacteria;Proteobacteria;Gammaproteobacteria;Unassigned;Unassigned;Thiohalophilus
Gammaproteobacteria_03_236	19	Bacteria;Proteobacteria;Gammaproteobacteria;Alteromonadales;Alteromonadaceae;Unassigned;Haliea
Gammaproteobacteria_03_397	19	Bacteria;Proteobacteria;Gammaproteobacteria;Alteromonadales;Colwelliaceae;Colwellia;rossensis
Deltaproteobacteria_03_123	19	Bacteria;Proteobacteria;Deltaproteobacteria;Desulfuromonadales;Geobacteraceae;Geopsychrobacter
TM7_03_17	19	Bacteria;TM7
Euk_459	19	Eukaryota;SAR;Stramenopiles;Bicosoecida;Cafeteriidae;Cafeteria
Euk_759	19	Eukaryota;Excavata;Discoba;Discicristata;Euglenozoa;Kinetoplastea;Metakinetoplastina;Parabodonida
Euk_1165	19	Eukaryota;SAR;Stramenopiles;Labyrinthulomycetes;D2P04F01
Euk_4671	19	Eukaryota;RT5iin25
Eukarya_06_1003	19	Eukaryota;Archaeplastida;Chloroplastida;Chlorophyta;Chlorophyceae
Eukarya_06_1331	19	Eukaryota;SAR;Stramenopiles;Bolidomonas
Eukarya_06_150	19	Eukaryota;SAR;Rhizaria;Cercozoa;Thecofilosea;NIF-3A7
Eukarya_06_3486	19	Eukaryota;Opisthokonta;Fungi;Fungi;Basal fungi;Basal fungi;Chytridiomycota
Eukarya_06_3644	19	Unknown
Eukarya_06_407	19	Eukaryota;Excavata;Discoba;Discicristata;Euglenozoa;Kinetoplastea;Metakinetoplastina;Parabodonida
Eukarya_06_496	19	Eukaryota;Excavata;Discoba;Discicristata;Euglenozoa;Kinetoplastea;Metakinetoplastina;Neobodonida
Eukarya_06_828	19	Eukaryota;SAR;Stramenopiles;Chrysophyceae;Chromulinales;Spumella
Actinobacteria_03_169	19	Bacteria;Actinobacteria;Actinobacteria;Actinomycetales;Unassigned;Demequina
Actinobacteria_03_370	19	Bacteria;Actinobacteria;Actinobacteria;Actinomycetales;Microbacteriaceae;Frigoribacterium
Bacteroidetes_03_198	19	Bacteria;Bacteroidetes;Sphingobacteria;Sphingobacteriales;Chitinophagaceae;Gracilimonas
Bacteroidetes_03_275	19	Bacteria;Bacteroidetes;Flavobacteria;Flavobacteriales;Flavobacteriaceae;Croceibacter
Bacteroidetes_03_385	19	Bacteria;Bacteroidetes;Sphingobacteria;Sphingobacteriales;Chitinophagaceae;Balneola
Bacteroidetes_03_397	19	Bacteria;Bacteroidetes;Flavobacteria;Flavobacteriales;Flavobacteriaceae;Ulvibacter
Bacteroidetes_03_824	19	Bacteria;Bacteroidetes;Flavobacteria;Flavobacteriales;Cryomorphaceae;Brumimimicrobium
Bacteroidetes_03_1289	19	Bacteria;Bacteroidetes;Flavobacteria;Flavobacteriales;Flavobacteriaceae;Psychroflexus

Bacteroidetes_03_1516	19	Bacteria;Bacteroidetes;Flavobacteria;Flavobacteriales;Flavobacteriaceae
Bacteroidetes_03_2401	19	Bacteria;Bacteroidetes;Sphingobacteria;Sphingobacteriales;Saprospiraceae;Haliscomenobacter
Bacteroidetes_03_2818	19	Bacteria;Bacteroidetes;Flavobacteria;Flavobacteriales;Cryomorphaceae;Owenweeksia
Alphaproteobacteria_03_36	19	Bacteria;Proteobacteria;Alphaproteobacteria;Rhodobacterales;Rhodobacteraceae
Alphaproteobacteria_03_169	19	Bacteria;Proteobacteria;Alphaproteobacteria;Rhizobiales;Rhodobiaceae;Parvibaculum
Alphaproteobacteria_03_1599	19	Bacteria;Proteobacteria;Alphaproteobacteria;Caulobacterales;Hyphomonadaceae;Maricaulis
Betaproteobacteria_03_53	19	Bacteria;Proteobacteria;Betaproteobacteria
Betaproteobacteria_03_84	19	Bacteria;Proteobacteria;Betaproteobacteria;Rhodocyclales;Rhodocyclaceae;Azospira
Gammaproteobacteria_03_2	19	Bacteria;Proteobacteria;Gammaproteobacteria;Enterobacteriales;Enterobacteriaceae
Gammaproteobacteria_03_7	19	Bacteria;Proteobacteria;Gammaproteobacteria
Gammaproteobacteria_03_141	19	Bacteria;Proteobacteria;Gammaproteobacteria;Oceanospirillales
Gammaproteobacteria_03_197	19	Bacteria;Proteobacteria;Gammaproteobacteria;Alteromonadales;Alteromonadaceae
Gammaproteobacteria_03_217	19	Bacteria;Proteobacteria;Gammaproteobacteria;Thiotrichales;Piscirickettsiaceae;Mariprofundus
Gammaproteobacteria_03_369	19	Bacteria;Proteobacteria;Gammaproteobacteria;Alteromonadales;Alteromonadaceae
Gammaproteobacteria_03_421	19	Bacteria;Proteobacteria;Gammaproteobacteria
Gammaproteobacteria_03_427	19	Bacteria;Proteobacteria;Gammaproteobacteria;Salinisphaerales;Salinisphaeraceae;Salinisphaera
Gammaproteobacteria_03_636	19	Bacteria;Proteobacteria;Gammaproteobacteria;Thiotrichales;Thiotrichaceae;Leucothrix
Gammaproteobacteria_03_692	19	Bacteria;Proteobacteria;Gammaproteobacteria;Alteromonadales;Alteromonadaceae
Gammaproteobacteria_03_894	19	Bacteria;Proteobacteria;Gammaproteobacteria;Thiotrichales;Piscirickettsiaceae;Methylophaga
TM7_03_101	19	Bacteria;TM7
Verrucomicrobia_03_44	19	Bacteria;Verrucomicrobia;Opitutae;Puniceicoccales;Puniceicoccaceae;Lentimonas
Verrucomicrobia_03_349	19	Bacteria;Verrucomicrobia;Opitutae;Puniceicoccales;Puniceicoccaceae;Coraliomargarita
Verrucomicrobia_03_566	19	Bacteria;Verrucomicrobia;Verrucomicrobiae;Verrucomicrobiales;Verrucomicrobiaceae;Roseibacillus
Verrucomicrobia_03_918	19	Bacteria;Verrucomicrobia;Opitutae;Puniceicoccales;Puniceicoccaceae;Coraliomargarita
Actinobacteria_03_36	19	Bacteria;Actinobacteria;Actinobacteria;Acidimicrobiales;Iamiaceae;Iamia
Gammaproteobacteria_03_431	19	Bacteria;Proteobacteria;Gammaproteobacteria;Xanthomonadales;Xanthomonadaceae;Luteibacter
Euk_1490	19	Unknown
Eukarya_06_1125	19	Eukaryota;SAR;Stramenopiles;MAST-12
Betaproteobacteria_03_151	19	Bacteria;Proteobacteria;Betaproteobacteria
Bacteroidetes_03_252	19	Bacteria;Bacteroidetes;Flavobacteria;Flavobacteriales;Flavobacteriaceae;Lutibacter
Verrucomicrobia_03_62	19	Bacteria;Verrucomicrobia;Verrucomicrobiae;Verrucomicrobiales;Verrucomicrobiaceae;Roseibacillus
Verrucomicrobia_03_57	19	Bacteria;Verrucomicrobia;Spartobacteria;Chthoniobacter
Eukarya_06_2105	19	Eukaryota;SAR;Stramenopiles;Chrysophyceae;Chromulinales;Cyclonexis
Gammaproteobacteria_03_1630	19	Bacteria;Proteobacteria;Gammaproteobacteria;Legionellales;Legionellaceae;Legionella
Alphaproteobacteria_03_24	20	Bacteria;Proteobacteria;Alphaproteobacteria;Sphingomonadales;Sphingomonadaceae;Sphingopyxis

Euk_9221	20	Eukaryota;SAR;Stramenopiles;Eustigmatales;Nannochloropsis
Eukarya_06_1327	20	Eukaryota;Archaeplastida;Chloroplastida;Chlorophyta;Trebouxiophyceae;Micractinium
Node	*Module ID*	*Taxonomy*
Eukarya_06_1388	20	Eukaryota;SAR;Stramenopiles;Eustigmatales;Goniochloris
Eukarya_06_2908	20	Eukaryota;SAR;Rhizaria;Cercozoa
Cyanobacteria_03_66	20	Bacteria;Cyanobacteria;Cyanobacteria;SubsectionIV;Unassigned;Nostoc
Planctomycetes_03_4	20	Bacteria;Planctomycetes;Planctomycetacia;Planctomycetales;Planctomycetaceae;Gemmata
Alphaproteobacteria_03_189	20	Bacteria;Proteobacteria;Alphaproteobacteria;Caulobacterales;Caulobacteraceae;Phenylobacterium
Verrucomicrobia_03_572	20	Bacteria;Verrucomicrobia;Verrucomicrobiae;Verrucomicrobiales;Verrucomicrobiaceae;Verrucomicrobium
Eukarya_06_266	20	Eukaryota;SAR;Stramenopiles;Chrysophyceae;Ochromonadales;Paraphysomonas
Bacteroidetes_03_262*	20	Bacteria;Bacteroidetes;Flavobacteria;Flavobacteriales;Flavobacteriaceae;Flavobacterium
Bacteroidetes_03_1099	20	Bacteria;Bacteroidetes;Flavobacteria;Flavobacteriales;Cryomorphaceae;Fluviicola;taffensis
Alphaproteobacteria_03_1226	20	Bacteria;Proteobacteria;Alphaproteobacteria;Rhodospirillales;Acetobacteraceae;Acidocella
Verrucomicrobia_03_209	20	Bacteria;Verrucomicrobia;Verrucomicrobiae;Verrucomicrobiales;Subdivision3
TM6_03_116	20	Bacteria;TM6
Alphaproteobacteria_03_332	20	Bacteria;Proteobacteria;Alphaproteobacteria;Rhodospirillales
Actinobacteria_03_62	20	Bacteria;Actinobacteria;Actinobacteria;Actinomycetales
Planctomycetes_03_1132	20	Bacteria;Planctomycetes;Planctomycetacia;Planctomycetales;Planctomycetaceae;Gemmata
Eukarya_06_550	20	Eukaryota;SAR;Alveolata;Protalveolata;Colpodellida;Colpodella
Actinobacteria_03_7	20	Bacteria;Actinobacteria;Actinobacteria;Actinomycetales;Microbacteriaceae
Eukarya_06_757	20	Eukaryota;SAR;Alveolata;Ciliophora;Intramacronucleata;Conthreep;Prostomatea;Cryptocaryon
Bacteroidetes_03_933	20	Bacteria;Bacteroidetes;Sphingobacteria;Sphingobacteriales;Chitinophagaceae;Ferruginibacter
Alphaproteobacteria_03_34	20	Bacteria;Proteobacteria;Alphaproteobacteria;Sphingomonadales;Erythrobacteraceae
Alphaproteobacteria_03_8747	20	Bacteria;Proteobacteria;Alphaproteobacteria;Rhodospirillales;Rhodospirillaceae;Defluviicoccus
Betaproteobacteria_03_16	20	Bacteria;Proteobacteria;Betaproteobacteria;Burkholderiales;Comamonadaceae
Gammaproteobacteria_03_748	20	Bacteria;Proteobacteria;Gammaproteobacteria;Legionellales;Legionellaceae;Legionella
Euk_2670	20	Eukaryota;SAR;Rhizaria;Cercozoa;Clathrulinidae;Hedriocystis
Bacteroidetes_03_485	20	Bacteria;Bacteroidetes;Sphingobacteria;Sphingobacteriales
Bacteroidetes_03_1569	20	Bacteria;Bacteroidetes;Sphingobacteria;Sphingobacteriales
Planctomycetes_03_317	20	Bacteria;Planctomycetes;Planctomycetacia;Planctomycetales;Planctomycetaceae
Verrucomicrobia_03_335	20	Bacteria;Verrucomicrobia;Opitutae;Opitutales;Opitutaceae;Opitutus
Verrucomicrobia_03_358	20	Bacteria;Verrucomicrobia;Opitutae;Opitutales;Opitutaceae;Opitutus
Bacteroidetes_03_86	20	Bacteria;Bacteroidetes;Sphingobacteria;Sphingobacteriales;Chitinophagaceae;Sediminibacterium
Archaea_03_451	20	Archaea;Euryarchaeota;Thermoplasmata;Thermoplasmatales;Marine_Group_II
Euk_16491	20	Eukaryota;SAR;Stramenopiles;Chrysophyceae;Ochromonadales;Paraphysomonas
Eukarya_06_605	20	Eukaryota;SAR;Alveolata;Ciliophora;Intramacronucleata;Conthreep;Prostomatea;Cryptocaryon
Bacteroidetes_03_592	20	Bacteria;Bacteroidetes;Sphingobacteria;Sphingobacteriales;Sphingobacteriaceae;Sphingobacteriaceae;Pedobacter
Betaproteobacteria_03_29	20	Bacteria;Proteobacteria;Betaproteobacteria;Burkholderiales;Alcaligenaceae
Eukarya_06_850	20	Eukaryota;SAR;Alveolata;Ciliophora;Intramacronucleata;Litostomatea;Haptoria;Lacrymaria

Betaproteobacteria_03_134	20	Bacteria;Proteobacteria;Betaproteobacteria;Burkholderiales;Comamonadaceae
Bacteroidetes_03_774	20	Bacteria;Bacteroidetes;Sphingobacteria;Sphingobacteriales
Betaproteobacteria_03_199	20	Bacteria;Proteobacteria;Betaproteobacteria;Burkholderiales;Comamonadaceae
Betaproteobacteria_03_27	20	Bacteria;Proteobacteria;Betaproteobacteria;Methylophilales;Methylophilaceae;Methylotenera
Eukarya_06_1057	20	Eukaryota;SAR;Alveolata;Ciliophora;Postciliodesmatophora;Heterotrichea;Blepharisma
Verrucomicrobia_03_4	20	Bacteria;Verrucomicrobia;Verrucomicrobiae;Verrucomicrobiales;Verrucomicrobiaceae;Luteolibacter
Actinobacteria_03_23	21	Bacteria;Actinobacteria;Actinobacteria;Actinomycetales;Sporichthyaceae
Bacteroidetes_03_357	21	Bacteria;Bacteroidetes;Sphingobacteria;Sphingobacteriales;Chitinophagaceae
Alphaproteobacteria_03_15	21	Bacteria;Proteobacteria;Alphaproteobacteria;Caulobacterales;Caulobacteraceae;Brevundimonas
Actinobacteria_03_46	21	Bacteria;Actinobacteria;Actinobacteria;Actinomycetales;Sporichthyaceae
Archaea_03_23	21	Archaea;Euryarchaeota;Thermoplasmata;Thermoplasmatales;Marine_Group_II
Gammaproteobacteria_03_79	21	Bacteria;Proteobacteria;Gammaproteobacteria;Pseudomonadales;Moraxellaceae;Psychrobacter
Actinobacteria_03_55	21	Bacteria;Actinobacteria;Actinobacteria;Actinomycetales;Microbacteriaceae
Alphaproteobacteria_03_608	21	Bacteria;Proteobacteria;Alphaproteobacteria;Rhodobacterales;Rhodobacteraceae
Gammaproteobacteria_03_1505	21	Bacteria;Proteobacteria;Gammaproteobacteria;Legionellales
Bacteroidetes_03_866	21	Bacteria;Bacteroidetes;Sphingobacteria;Sphingobacteriales;Chitinophagaceae;Sediminibacterium
Alphaproteobacteria_03_431	21	Bacteria;Proteobacteria;Alphaproteobacteria;Sphingomonadales;Sphingomonadaceae;Novosphingobium
Alphaproteobacteria_03_808	21	Bacteria;Proteobacteria;Alphaproteobacteria;Rhizobiales;Methylocystaceae;Methylocystis
Archaea_03_449	21	Archaea;Euryarchaeota;Thermoplasmata;Thermoplasmatales;Terrestrial_Miscellaneous_Group
Alphaproteobacteria_03_331	21	Bacteria;Proteobacteria;Alphaproteobacteria;Rhodospirillales;Acetobacteraceae;Acidocella
Archaea_03_32	21	Archaea;Euryarchaeota;Thermoplasmata;Thermoplasmatales;Terrestrial_Miscellaneous_Group
Betaproteobacteria_03_8	21	Bacteria;Proteobacteria;Betaproteobacteria;Burkholderiales;Burkholderiaceae;Polynucleobacter
Betaproteobacteria_03_143*	21	Bacteria;Proteobacteria;Betaproteobacteria;Burkholderiales;Oxalobacteraceae;Herbaspirillum
Archaea_03_192	21	Archaea;Crenarchaeota;terrestrial_group
Verrucomicrobia_03_24	21	Bacteria;Verrucomicrobia;Verrucomicrobiae;Verrucomicrobiales;Verrucomicrobiaceae
Bacteroidetes_03_21	21	Bacteria;Bacteroidetes;Flavobacteria;Flavobacteriales;Flavobacteriaceae;Flavobacterium
Archaea_03_203	21	Archaea;Crenarchaeota;Miscellaneous_Crenarchaeotic_Group
Archaea_03_288	21	Archaea;Crenarchaeota;terrestrial_group
Eukarya_06_388	21	Eukaryota;SAR;Rhizaria;Cercozoa;Endomyxa;Novel Clade 10
Verrucomicrobia_03_224	21	Bacteria;Verrucomicrobia;Opitutae;Opitutales;Opitutaceae;Opitutus
Betaproteobacteria_03_15	21	Bacteria;Proteobacteria;Betaproteobacteria;Burkholderiales;Burkholderiaceae;Polynucleobacter
OD1_03_1	21	Bacteria;OD1
Gemmatimonadetes_03_152	21	Bacteria;Gemmatimonadetes;Gemmatimonadetes;Gemmatimonadales;Gemmatimonadaceae;Gemmatimonas
Actinobacteria_03_1	22	Bacteria;Actinobacteria;Actinobacteria;Actinomycetales;Sporichthyaceae
Bacteroidetes_03_1130	22	Bacteria;Bacteroidetes;Sphingobacteria;Sphingobacteriales;Saprospiraceae
Verrucomicrobia_03_32	22	Bacteria;Verrucomicrobia;Verrucomicrobiae;Verrucomicrobiales;Verrucomicrobiaceae;Prosthecobacter;vanneervenii
Betaproteobacteria_03_51*	22	Bacteria;Proteobacteria;Betaproteobacteria;Rhodocyclales;Rhodocyclaceae;Methyloversatilis

Alphaproteobacteria_03_42	22	Bacteria;Proteobacteria;Alphaproteobacteria;Rhodobacterales;Rhodobacteraceae;Rhodobacter
Actinobacteria_03_51	22	Bacteria;Actinobacteria;Actinobacteria;Actinomycetales;Sporichthyaceae
Actinobacteria_03_25	22	Bacteria;Actinobacteria;Actinobacteria;Actinomycetales;Microbacteriaceae
Betaproteobacteria_03_198	22	Bacteria;Proteobacteria;Betaproteobacteria;Burkholderiales;Comamonadaceae;Rhodoferax
Deltaproteobacteria_03_161	22	Bacteria;Proteobacteria;Deltaproteobacteria;Myxococcales
Actinobacteria_03_26	22	Bacteria;Actinobacteria;Actinobacteria;Actinomycetales;Sporichthyaceae;Planktophila
Actinobacteria_03_329	22	Bacteria;Actinobacteria;Actinobacteria;Solirubrobacterales;Conexibacteraceae;Conexibacter
Cyanobacteria_03_113	22	Bacteria;Cyanobacteria;Cyanobacteria;SubsectionIII;Unassigned;Leptolyngbya
Actinobacteria_03_260	22	Bacteria;Actinobacteria;Actinobacteria;Acidimicrobiales
Euk_1654	22	Eukaryota;SAR;Stramenopiles;Bicosoecida;P34.6
Euk_2679	22	Eukaryota;SAR;Rhizaria;Cercozoa;Thecofilosea;Cryomonadida;Protaspidae;Cryothecomonas
Euk_3792	22	Eukaryota;Opisthokonta;Fungi;Basidiomycota;Agaricomycotina;Agaricomycetes
Betaproteobacteria_03_4	22	Bacteria;Proteobacteria;Betaproteobacteria;Burkholderiales;Comamonadaceae;Rhodoferax
Bacteroidetes_03_563	22	Bacteria;Bacteroidetes;Sphingobacteria;Sphingobacteriales
Eukarya_06_1112	22	Eukaryota;SAR;Stramenopiles;Chrysophyceae;Ochromonadales;Paraphysomonas
Eukarya_06_1237	22	Eukaryota;Opisthokonta;Fungi;Fungi;Basal fungi;Basal fungi;Blastocladiomycota
Eukarya_06_574	22	Unknown
Eukarya_06_64	22	Eukaryota;Haptophyta;Prymnesiophyceae;Isochrysidales;Isochrysis
Euk_384	22	Eukaryota;SAR;Stramenopiles;Labyrinthulomycetes;Thraustochytriaceae;E170
Eukarya_06_136	22	Eukaryota;SAR;Stramenopiles;Incertae Sedis;Pirsonia
Eukarya_06_397	22	Eukaryota;Opisthokonta;Holozoa;Choanomonada;Craspedida;Lagenoeca
Eukarya_06_472	22	Eukaryota;SAR;Rhizaria;Cercozoa;Thecofilosea;NIF-3A7
Eukarya_06_856	22	Eukaryota;SAR;Rhizaria;Cercozoa;Thecofilosea;Cryomonadida;Protaspidae;Cryothecomonas
Gammaproteobacteria_03_32	22	Bacteria;Proteobacteria;Gammaproteobacteria
Alphaproteobacteria_03_244	22	Bacteria;Proteobacteria;Alphaproteobacteria;Sphingomonadales;Sphingomonadaceae;Sphingopyxis
Bacteroidetes_03_32	22	Bacteria;Bacteroidetes;Flavobacteria;Flavobacteriales;Flavobacteriaceae;Flavobacterium
Alphaproteobacteria_03_1505	22	Bacteria;Proteobacteria;Alphaproteobacteria;Rickettsiales;Rickettsiaceae;Rickettsia;endosymbiont
Gammaproteobacteria_03_1314	22	Bacteria;Proteobacteria;Gammaproteobacteria;Xanthomonadales;Sinobacteraceae
Bacteroidetes_03_435	22	Bacteria;Bacteroidetes;Flavobacteria;Flavobacteriales;Cryomorphaceae;Fluviicola
Bacteroidetes_03_867	22	Bacteria;Bacteroidetes;Flavobacteria;Flavobacteriales;Cryomorphaceae;Fluviicola
Betaproteobacteria_03_9	22	Bacteria;Proteobacteria;Betaproteobacteria;Burkholderiales;Comamonadaceae
Eukarya_06_769	22	Eukaryota;SAR;Stramenopiles;Synurales;Mallomonas
Bacteroidetes_03_1343	22	Bacteria;Bacteroidetes;Sphingobacteria;Sphingobacteriales
Euk_367	22	Eukaryota;Opisthokonta;Fungi;LKM11
Eukarya_06_3	22	Eukaryota;SAR;Alveolata;Dinoflagellata;Dinophyceae;SL163A10
Actinobacteria_03_2	22	Bacteria;Actinobacteria;Actinobacteria;Actinomycetales;Microbacteriaceae
Alphaproteobacteria_03_2597	22	Bacteria;Proteobacteria;Alphaproteobacteria;Rickettsiales;Rickettsiaceae;Rickettsia;endosymbiont
Alphaproteobacteria_03_136	22	Bacteria;Proteobacteria;Alphaproteobacteria;Caulobacterales;Hyphomonadaceae;Hyphomonas;Hyphomonas
Alphaproteobacteria_03_571	22	Bacteria;Proteobacteria;Alphaproteobacteria;Rickettsiales;Rickettsiaceae;Rickettsia

Actinobacteria_03_37	22	Bacteria;Actinobacteria;Actinobacteria;Acidimicrobiales;Acidimicrobiaceae
Alphaproteobacteria_03_143	22	Bacteria;Proteobacteria;Alphaproteobacteria;Rhodobacterales;Rhodobacteraceae;Rhodobacter
Betaproteobacteria_03_135	22	Bacteria;Proteobacteria;Betaproteobacteria;Methylophilales;Methylophilaceae;Methylophilus
Betaproteobacteria_03_13	22	Bacteria;Proteobacteria;Betaproteobacteria;Burkholderiales;Comamonadaceae;Rhodoferax
Eukarya_06_391	22	Eukaryota;SAR;Stramenopiles;Chrysophyceae;Chromulinales;Spumella
Gammaproteobacteria_03_20	22	Bacteria;Proteobacteria;Gammaproteobacteria;Pseudomonadales;Pseudomonadaceae;Pseudomonas
OP9_03_4	22	Bacteria;OP9
Bacteroidetes_03_652	22	Bacteria;Bacteroidetes;Sphingobacteria;Sphingobacteriales;Cytophagaceae;Dyadobacter
Eukarya_06_74	22	Eukaryota;Archaeplastida;Chloroplastida;Chlorophyta;Prasinophytae;Pyramimonas
Betaproteobacteria_03_99	22	Bacteria;Proteobacteria;Betaproteobacteria;Burkholderiales;Comamonadaceae;Hydrogenophaga
Actinobacteria_03_481	22	Bacteria;Actinobacteria;Actinobacteria
Bacteroidetes_03_960	22	Bacteria;Bacteroidetes;Flavobacteria;Flavobacteriales;Cryomorphaceae;Cryomorpha
Chlorobi_03_60	22	Bacteria;Chlorobi;Chlorobia;Chlorobiales
OD1_03_45	22	Bacteria;OD1
OD1_03_79	22	Bacteria;OD1
Alphaproteobacteria_03_3828	22	Bacteria;Proteobacteria;Alphaproteobacteria;Rhodobacterales;Rhodobacteraceae;Paracoccus
Alphaproteobacteria_03_1296	22	Bacteria;Proteobacteria;Alphaproteobacteria;Rhodobacterales;Rhodobacteraceae;Catellibacterium
Bacteroidetes_03_828	22	Bacteria;Bacteroidetes;Flavobacteria;Flavobacteriales;Cryomorphaceae;Fluviicola
Bacteroidetes_03_1652	22	Bacteria;Bacteroidetes;Flavobacteria;Flavobacteriales;Cryomorphaceae;Fluviicola
Gammaproteobacteria_03_1166	22	Bacteria;Proteobacteria;Gammaproteobacteria;Pseudomonadales;Moraxellaceae;Enhydrobacter
Deltaproteobacteria_03_283	22	Bacteria;Proteobacteria;Deltaproteobacteria;Desulfobacterales;Desulfobacteraceae;Desulfobacula
Alphaproteobacteria_03_5047	22	Bacteria;Proteobacteria;Alphaproteobacteria;Rickettsiales;Rickettsiaceae;Rickettsia;endosymbiont
Alphaproteobacteria_03_6733	22	Bacteria;Proteobacteria;Alphaproteobacteria;Rhodospirillales;Acetobacteraceae;Acidocella
Bacteroidetes_03_4962	22	Bacteria;Bacteroidetes;Flavobacteria;Flavobacteriales;Cryomorphaceae;Crocinitomix;catalasitica
Betaproteobacteria_03_11	22	Bacteria;Proteobacteria;Betaproteobacteria;Methylophilales;Methylophilaceae
TM6_03_287	22	Bacteria;TM6
Verrucomicrobia_03_27	22	Bacteria;Verrucomicrobia;Verrucomicrobiae;Verrucomicrobiales;Verrucomicrobiaceae;Roseibacillus
Bacteroidetes_03_2011	22	Bacteria;Bacteroidetes;Sphingobacteria;Sphingobacteriales;Sphingobacteriaceae;Sphingobacteriaceae
Bacteroidetes_03_1171	22	Bacteria;Bacteroidetes;Flavobacteria;Flavobacteriales;Cryomorphaceae;Cryomorpha
Archaea_03_50	22	Archaea;Euryarchaeota;Methanomicrobia;Methanomicrobiales;Unassigned;Candidatus_Methanoregula
Eukarya_06_71	22	Eukaryota;SAR;Stramenopiles;Chrysophyceae;Chromulinales;Chrysamoeba
Planctomycetes_03_30	22	Bacteria;Planctomycetes;Planctomycetacia;Planctomycetales;Planctomycetaceae
Alphaproteobacteria_03_780	22	Bacteria;Proteobacteria;Alphaproteobacteria;Rhodobacterales;Rhodobacteraceae;Pseudorhodobacter
Bacteroidetes_03_1888	22	Bacteria;Bacteroidetes;Flavobacteria;Flavobacteriales
Betaproteobacteria_03_19	22	Bacteria;Proteobacteria;Betaproteobacteria;Burkholderiales;Comamonadaceae
Archaea_03_102	22	Archaea;Euryarchaeota;Methanomicrobia;Methanomicrobiales
Archaea_03_4	22	Archaea;Euryarchaeota;Thermoplasmata;Thermoplasmatales;Marine_Group_II

Euk_22	22	Eukaryota;SAR;Rhizaria;Cercozoa;Thecofilosea
Deltaproteobacteria_03_1160	22	Bacteria;Proteobacteria;Deltaproteobacteria;Syntrophobacterales;Syntrophaceae
Archaea_03_241	22	Archaea;Crenarchaeota;terrestrial_group
Eukarya_06_933	22	Eukaryota;SAR;Alveolata;Ciliophora;Intramacronucleata;Conthreep;Oligohymenophorea;Scuticociliatia
Deltaproteobacteria_03_426	22	Bacteria;Proteobacteria;Deltaproteobacteria;Bdellovibrionales;Bacteriovoraceae;Peredibacter
Eukarya_06_140	22	Eukaryota;SAR;Alveolata;Ciliophora;Intramacronucleata;Spirotrichea;Hypotrichia;Oxytricha
Archaea_03_324	22	Archaea;Euryarchaeota;Methanomicrobia;Methanomicrobiales;Rice_Cluster_II
Euk_8710	22	Eukaryota;SAR;Rhizaria;Cercozoa;Thecofilosea;NOR26
Eukarya_06_62	22	Eukaryota;SAR;Rhizaria;Cercozoa;Thecofilosea;Cryomonadida;Protaspidae;Cryothecomonas
Euk_67	22	Eukaryota;Opisthokonta;Fungi;LKM11
Euk_1779	22	Eukaryota;Opisthokonta;Fungi;LKM11
Eukarya_06_630	22	Eukaryota;SAR;Alveolata;Ciliophora;Intramacronucleata;Litostomatea;Haptoria
Lentisphaerae_03_2116	22	Bacteria;Lentisphaerae;Lentisphaeria
OD1_03_3	22	Bacteria;OD1
Verrucomicrobia_03_26	22	Bacteria;Verrucomicrobia;Verrucomicrobiae;Verrucomicrobiales;Verrucomicrobiaceae
Eukarya_06_1718*	23	Eukaryota;SAR;Stramenopiles;Dictyochophyceae;Pedinellales;Pteridomonas
Gammaproteobacteria_03_2351	23	Bacteria;Proteobacteria;Gammaproteobacteria;Legionellales;Legionellaceae
Eukarya_06_1772*	24	Eukaryota;Archaeplastida;Chloroplastida;Chlorophyta;Chlorophyceae;Chlorogonium
Eukarya_06_1927	24	Eukaryota;Archaeplastida;Chloroplastida;Chlorophyta;Chlorophyceae;Chlamydomonas
Actinobacteria_03_1592	25	Bacteria;Actinobacteria;Actinobacteria;Acidimicrobiales;Unassigned;Microthrix
OD1_03_126	25	Bacteria;OD1
Deltaproteobacteria_03_21401	25	Bacteria;Proteobacteria;Deltaproteobacteria;Bdellovibrionales;Bacteriovoraceae;Peredibacter
Euk_6458	25	Unknown
Eukarya_06_651	25	Eukaryota;SAR;Stramenopiles;Chrysophyceae;E222
Actinobacteria_03_493	25	Bacteria;Actinobacteria;Actinobacteria;Actinomycetales;Unassigned;Fodinicola
Bacteroidetes_03_3718	25	Bacteria;Bacteroidetes;Sphingobacteria;Sphingobacteriales
Bacteroidetes_03_4936	25	Bacteria;Bacteroidetes;Sphingobacteria;Sphingobacteriales
Bacteroidetes_03_5435	25	Bacteria;Bacteroidetes;Bacteroidia;Bacteroidales;Rikenellaceae;Rikenella
Chlorobi_03_216	25	Bacteria;Chlorobi;Chlorobia;Chlorobiales
Alphaproteobacteria_03_399	25	Bacteria;Proteobacteria;Alphaproteobacteria;Rhodobacterales;Rhodobacteraceae;Pseudorhodobacter
Verrucomicrobia_03_100	25	Bacteria;Verrucomicrobia;Spartobacteria
Verrucomicrobia_03_938	25	Bacteria;Verrucomicrobia;Opitutae;Opitutales;Opitutaceae;Opitutus
Archaea_03_104	25	Archaea;Crenarchaeota;Miscellaneous_Crenarchaeotic_Group
Bacteroidetes_03_233	25	Bacteria;Bacteroidetes;Flavobacteria;Flavobacteriales;Flavobacteriaceae
Alphaproteobacteria_03_778	25	Bacteria;Proteobacteria;Alphaproteobacteria;Rhodobacterales;Rhodobacteraceae;Loktanella
Gammaproteobacteria_03_4*	25	Bacteria;Proteobacteria;Gammaproteobacteria;Pseudomonadales;Pseudomonadaceae;Pseudomonas
Gammaproteobacteria_03_72	25	Bacteria;Proteobacteria;Gammaproteobacteria;Thiotrichales;Piscirickettsiaceae;Methylophaga
TM6_03_130	25	Bacteria;TM6
Archaea_03_52	25	Archaea;Euryarchaeota;Methanomicrobia;Methanosarcinales;GOM_Arc_I

Archaea_03_167	25	Archaea;Crenarchaeota;Soil_Crenarchaeotic_Group
Archaea_03_257	25	Archaea;Crenarchaeota;Miscellaneous_Crenarchaeotic_Group
Euk_76	25	Eukaryota;SAR;Alveolata;Ciliophora;Intramacronucleata;Spirotrichea;Euplotia;Euplotes
Eukarya_06_250	25	Eukaryota;SAR;Alveolata;Ciliophora;Intramacronucleata;Conthreep;Prostomatea;Cryptocaryon
Actinobacteria_03_68	25	Bacteria;Actinobacteria;Actinobacteria;Acidimicrobiales;Acidimicrobiaceae
Actinobacteria_03_82	25	Bacteria;Actinobacteria;Actinobacteria;Actinomycetales
Alphaproteobacteria_03_684	25	Bacteria;Proteobacteria;Alphaproteobacteria;Rhodobacterales;Rhodobacteraceae
Archaea_03_159	25	Archaea;Crenarchaeota;Soil_Crenarchaeotic_Group
Bacteroidetes_03_7251	25	Bacteria;Bacteroidetes;Flavobacteria;Flavobacteriales;Cryomorphaceae;Fluviicola
Archaea_03_240	25	Archaea;Euryarchaeota;Methanomicrobia;Methanomicrobiales;Unassigned;Candidatus_Methanoregula
Archaea_03_263	25	Archaea;Euryarchaeota;Methanomicrobia;Methanomicrobiales;Methanocorpusculaceae;Methanocorpusculum
Eukarya_06_12	25	Eukaryota;SAR;Alveolata;Ciliophora;Intramacronucleata;Spirotrichea;Oligotrichia;uncultured
Eukarya_06_255	25	Eukaryota;SAR;Alveolata;Ciliophora;Intramacronucleata;Conthreep;Oligohymenophorea;Peniculia
Actinobacteria_03_49	26	Bacteria;Actinobacteria;Actinobacteria;Acidimicrobiales;Acidimicrobiaceae
Spirochaetes_03_17	26	Bacteria;Spirochaetes;Spirochaetes;Spirochaetales
Planctomycetes_03_726*	26	Bacteria;Planctomycetes;Planctomycetacia;Planctomycetales;Planctomycetaceae;Planctomyces
Actinobacteria_03_146	26	Bacteria;Actinobacteria;Actinobacteria;Acidimicrobiales;Iamiaceae;Iamia
Cyanobacteria_03_220	26	Bacteria;Cyanobacteria
Euk_2599	26	Unknown
Bacteroidetes_03_53	26	Bacteria;Bacteroidetes;Flavobacteria;Flavobacteriales;Flavobacteriaceae;Flavobacterium
Bacteroidetes_03_343	26	Bacteria;Bacteroidetes;Flavobacteria;Flavobacteriales;Cryomorphaceae;Lishizhenia
Bacteroidetes_03_505	26	Bacteria;Bacteroidetes;Sphingobacteria;Sphingobacteriales;Chitinophagaceae
Alphaproteobacteria_03_1912	26	Bacteria;Proteobacteria;Alphaproteobacteria;Rickettsiales;Rickettsiaceae
Bacteroidetes_03_544	26	Bacteria;Bacteroidetes;Flavobacteria;Flavobacteriales;Cryomorphaceae;Fluviicola
Chloroflexi_03_115	26	Bacteria;Chloroflexi;Caldilineae;Caldilineales
Actinobacteria_03_1785	26	Bacteria;Actinobacteria;Actinobacteria;Solirubrobacterales;Conexibacteraceae;Conexibacter
Actinobacteria_03_174	26	Bacteria;Actinobacteria;Actinobacteria;Acidimicrobiales;Unassigned;Microthrix
OD1_03_58	26	Bacteria;OD1
Verrucomicrobia_03_547	26	Bacteria;Verrucomicrobia;Opitutae;Puniceicoccales;Puniceicoccaceae;Coraliomargarita
Actinobacteria_03_32	26	Bacteria;Actinobacteria;Actinobacteria;Actinomycetales;Sporichthyaceae;Planktophila
Gammaproteobacteria_03_145	26	Bacteria;Proteobacteria;Gammaproteobacteria;Xanthomonadales;Xanthomonadaceae
Euk_169	26	Eukaryota;SAR;Alveolata;Ciliophora;Intramacronucleata;Spirotrichea;Euplotia;Euplotes
Bacteroidetes_03_5975	26	Bacteria;Bacteroidetes;Sphingobacteria;Sphingobacteriales;Sphingobacteriaceae;Sphingobacteriaceae;Pedobacter
OD1_03_104	26	Bacteria;OD1
Gammaproteobacteria_03_2188	26	Bacteria;Proteobacteria;Gammaproteobacteria;Legionellales;Coxiellaceae;Aquicella
Gammaproteobacteria_03_1728	26	Bacteria;Proteobacteria;Gammaproteobacteria;Thiotrichales;Piscirickettsiaceae;Methylophaga
Actinobacteria_03_722	27	Bacteria;Actinobacteria;Actinobacteria;Acidimicrobiales;Iamiaceae;Iamia
Verrucomicrobia_03_119*	27	Bacteria;Verrucomicrobia;Opitutae;Opitutales;Opitutaceae;Opitutus
Bacteroidetes_03_60	27	Bacteria;Bacteroidetes;Flavobacteria;Flavobacteriales;Flavobacteriaceae;Flavobacterium

Eukarya_06_709	27	Eukaryota;SAR;Alveolata;Ciliophora;Intramacronucleata;Conthreep;Oligohymenophorea;Apostomatia
Bacteroidetes_03_457	27	Bacteria;Bacteroidetes;Sphingobacteria;Sphingobacteriales;Cyclobacteriaceae;Algoriphagus

Table S4. Modularity Calculations for the Lake Fryxell (FRX) and West Lobe Lake Bonney (WLB) Molecular Ecological Network (MEN).

Method	*Modularity*	*Number of modules*
MCL	0.87	45
GLay	0.87	19
CCC	0.86	16
SCPS	0.82	25
ModuLand	-	27

Table S5. Major characteristics for modules with significant BC scores (>0) and those connected to the autumn proliferation of Archaea.

Module Number	*Module Betweenness Centrality Score*	*Main characteristics*
15	0.19	Photoheterotrophy; energy acquisition
17	0	Chemoautotrophy; energy acquisition
18	0.07	DOM processing
19	0.04	DOM processing
20	0.04	Phytoplankton DOM
21	0.02	Nutrient processing
22	0.04	Mixotrophy
25	0.1	Carbon/Sulfur cycling
26	0.04	Anaerobic adaptation; energy storage
27	0.005	Metazoan-associated?

CHAPTER THREE

PARTITIONING OF INORGANIC CARBON-FIXATION IN PERMANENTLY ICE-COVERED ANTARCTIC LAKES

Contribution of Authors and Co-Authors

Manuscript in Chapter 3

Author: Trista J. Vick-Majors

Contributions: Designed and conducted experiments, collected samples, analyzed and interpreted data, prepared figures and tables, wrote the manuscript.

Co-Author: John C. Priscu

Contributions: Provided funding, designed experiments, provided input to manuscript.

Manuscript Information Page

Trista J. Vick-Majors, John C. Priscu
Microbial Ecology
Status of Manuscript:
____ Prepared for submission to a peer-reviewed journal
_X_ Officially submitted to a peer-review journal
____ Accepted by a peer-reviewed journal
____ Published in a peer-reviewed journal

Springer US
Submitted November 12, 2015

PARTITIONING OF INORGANIC CARBON-FIXATION IN PERMANENTLY ICE-COVERED ANTARCTIC LAKES

The following work has been submitted to Microbial Ecology

Trista J. Vick-Majors[1] and John C. Priscu[1*]

[1]Department of Land Resources and Environmental Sciences, Montana State University, Bozeman, MT, USA
*corresponding author

Production of new carbon by phytoplankton photosynthesis forms the base of the food chain in most aquatic ecosystems. High latitude ecosystems are unique in their seasonal light-dark cycles, leading to continuous primary production during the summer months and no photoautotrophic primary production during the polar night [1]. This bimodality in photoautotrophy leads to a situation where annual respiratory consumption of organic carbon can exceed photoautotrophic organic carbon production [2]. Under these conditions chemolithoautotropic organic carbon production may contribute significantly to ecosystem processes. Lakes Fryxell and Bonney are permanently ice-covered lakes in the McMurdo Dry Valleys, the largest ice-free region of the Antarctic continent. These lakes are characterized by a paucity of metazoans and low light penetration through the ~ 4m thick permanent ice (<5% incident photosynthetically active radiation [PAR]). The water columns of both lakes are highly chemically stratified with oxygen over-saturated surface waters underlain by anoxic or suboxic saline layers [3] and water temperatures <6 ^{o}C.

Past studies have examined the occurrence and expression carbon fixation genes [4, 5], microbial community structure [6], and phytoplankton [7, 8] dynamics during the transitions to and from the polar night, when photosynthetic primary production ceases or

begins. These studies found evidence for diverse carbon fixation strategies in Lake Fryxell and Lake Bonney, including chemolithoautotrophy, which may supplement a portion of the heterotrophic carbon demand that continues year-round [2, 9, 10]. Other researchers have detected chemolithoautotrophic carbon fixation genes [11] and ammonia-oxidizing bacteria in Lakes Fryxell and Bonney [12], estimated rates of ammonia oxidation [13], and isolated sulfur-oxidizing chemolithoautotrophic bacteria from Lake Fryxell [14]. The rates of inorganic carbon fixation by these chemolithoautotrophic populations remain unknown. Here, we present rates of dissolved inorganic carbon-fixation (DIC-fixation) from the water columns of Lake Fryxell (FRX) and the East Lobe of Lake Bonney (ELB) during two austral summers (2008-2009 and 2009-2010 [FRX only]), partitioned by size fractions and functional groups.

FRX and ELB have been studied intensively since 1993 as part of the McMurdo Long Term Ecological Research program and data are publically available on the projects website (MCM LTER; mcmlter.org). We collected water samples directly below the ice covers, at the primary production maxima and at the bottom of the photic zones of each lake (ELB 6, 13, and 20 m, respectively; FRX 6, 10, and 12 m, respectively) through holes drilled in the ice covers. All depths are reported from the piezometric water level in the sampling hole.

During 2008, glass bottles filled with lake water with no headspace were amended with [^{14}C]-bicarbonate (stock concentration 133.9 uCi mL^{-1} in 2008, 144.1 uCi mL^{-1} in 2009). Final [^{14}C]-bicarbonate concentrations were based on the concentrations of dissolved inorganic carbon at each sample depth (see MCM LTER methods at

http://www.montana.edu/priscu/dataproducts.php). Vials were sealed with teflon-lined caps, and incubated in the lake at the depth of sampling for 24 hours. Following incubation, samples were size-fractionated by filtering onto 3 uCi and 0.2 uCi polycarbonate filters, acidified with 3N hydrochloric acid and dried overnight. Radioactivity retained by particulate matter on the filters was measured with a calibrated scintillation counter and converted to rates of DIC-fixation according to the MCM LTER methods. Rates of dark DIC-fixation (chemolithoautotrophy + anapleurotic reactions) were determined from incubations conducted in opaque bottles, minus controls killed with trichloroacetic acid (final concentration ~5%). Photoautotrophic DIC-fixation was determined by subtracting opaque bottle activity from that in the light bottles.

Incubations from 2009 were conducted in 33 ml test tubes in an environmental chamber (temperature = 2 ^{o}C; PAR ~ 90 umol m^{-2} s^{-1}) because logistical constraints prevented us from incubating samples in the lake. In addition to the light, dark and killed treatments, the potential contribution of ammonia-oxidizing organisms to dark DIC-fixation was determined via addition of nitrapyrin (5 mg L^{-1} final concentration) to dark bottles. Nitrapyrin is known to inhibit the activity of ammonia-oxidizing archaea and bacteria (e.g. [15]). The entire volume was filter concentrated onto 0.2 um polycarbonate filters and inorganic ^{14}C incorporation was determined by standard liquid scintillation spectrometry as described above.

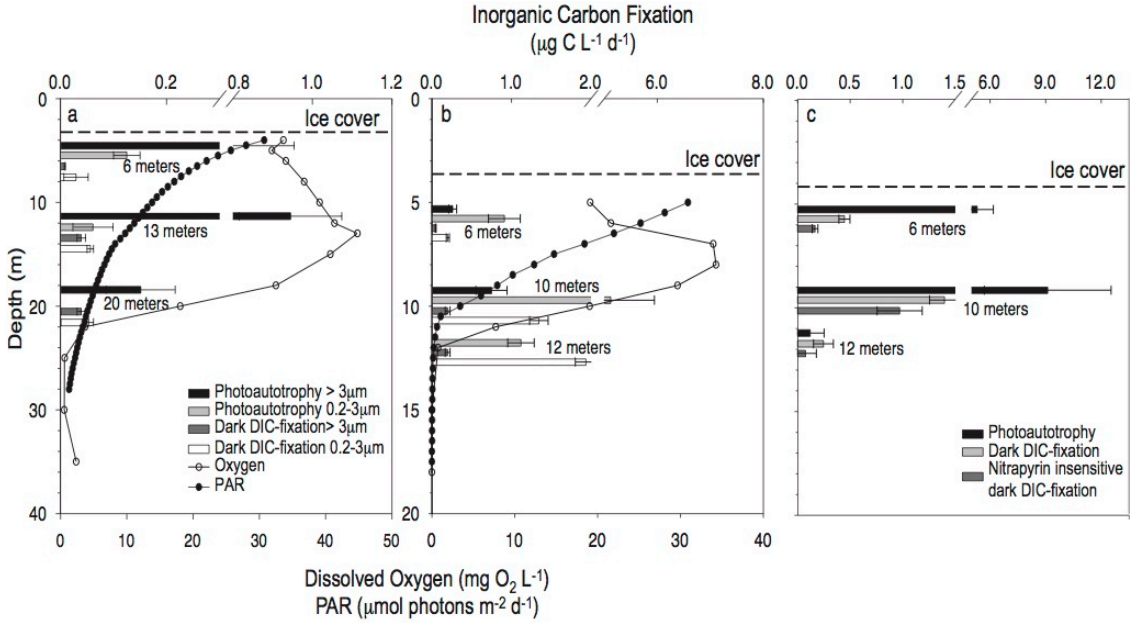

Figure 1. Rates of DIC-fixation measured in (a) East Lobe Lake Bonney during December 2008, (b) Lake Fryxell during December 2008, and (c) Lake Fryxell during December 2009. Groups of bars are centered on the depth of sample collection, which is indicated to the right of each group. Representative profiles of photosynthetically active radiation (PAR) and dissolved oxygen are given for December in panels "a" and "b". The difference between "dark DIC-fixation" and "nitrapyrin insensitive" can be attributed to DIC-fixation by ammonia- oxidizing bacteria. Error bars show the propagated standard error. The Lake Bonney ice cover was 3.5 m thick and the Lake Fryxell ice cover was 3.9 m thick (2008) and 4.1 m thick (2009) at the time of sampling.

Photoautotrophy was the dominant pathway for DIC-fixation at surface and mid-depths in both lakes (6 m and 10 m FRX and 6 m and 12 m ELB), with the highest rates occurring in the 10 m FRX sample (Fig. 1).

The majority of photoautotrophic DIC-fixation in FRX occurred in the small (0.2 – 3.0 um) size fraction dominated by small prokaryotes and pico-eukaryotes, whereas the majority of DIC-fixation in ELB occurred in the > 3 um size fraction. Higher rates of photoautotrophic DIC-fixation in 2009 may be the result of the higher PAR levels used in the incubator compared to the *in situ* PAR in 2008 (Table 1, Fig. 1; [16].

LAKE	DEPTH (m)	TOTAL DIC-FIXATION	DARK DIC-FIXATION	DARK % TOTAL	% NITRA
ELB (2008)	6	0.98	0.04	3.8	-
	13	1.1	0.10	8.3	-
	20	0.30	0.09	30	-
FRX (2008)	6	1.5	0.27	17	-
	10	7.6	1.5	20	-
	12	3.3	2.1	62	-
FRX (2009)	6	4.8	0.45	9.1	63
	10	12	1.4	11	30
	12	1.9	0.25	13	N.S

Table 1. Dark DIC-fixation (μg C L^{-1} d^{-1}) as a percentage of total DIC-fixation (photoautotrophy + chemolithoautotrophy; μg C L^{-1} d^{-1}). Size fractionated samples (2008) were summed to report total and dark DIC-fixation. Nitrapyrin sensitive dark DIC-fixation (% NITRA) is the potential contribution of ammonia-oxidizing bacteria/archaea. "-" = not measured. N.S. = No significant change versus unamended dark DIC-fixation (t-test, $p < 0.05$). See text for experimental details.

The small size fraction dominated dark DIC-fixation in both lakes and accounted for 9% to 62% of total (sum of light and dark) primary production in FRX, and from 4% to 30% in ELB (Table 1). The highest rates of dark DIC-fixation were associated with the oxyclines (and chemoclines) of both lakes (13 m in ELB and 10 m in FRX), accounting for up to 20% of light DIC-fixation at these depths. Maximum photoautotrophic inorganic DIC-fixation and heterotrophic activity [9] was also associated with the oxycline. Photoautotrophic and chemolithoautotrophic metabolism in this zone of the lakes have been shown to be supported by the upward diffusion of inorganic S, N and P [14, 17].

Previous work indicated that FRX and ELB contain active populations of ammonia-oxidizing bacteria [12, 13, 18]. We treated samples with nitrapyrin, which

inhibits the conversion of ammonia to hydroxylamine, the initial step of ammonia-oxidation [19], to determine the relative contribution of ammonia-oxidizers to DIC-fixation in FRX in 2009. A majority of dark C-fixation (63%) at 6 m was sensitive to nitrapyrin (Table 1). The proportion was lower at 10 m (30%), and the effect of nitrapyrin was insignificant at 12 m. This decrease with depth likely represents the diminishing dissolved oxygen levels through this zone; oxygen is required for the aerobic oxidation of ammonium.

LAKE	DEMAND	SOURCE		BALANCE
	Heterotrophy (kg C y^{-1})	Photoautotrophy (kg C y^{-1})	Chemolithoautotrophy (kg C y^{-1})	kg C y^{-1}
Fryxell	2200	1800	6000	5600
East Lobe Bonney	1400	1400	1100	1100

Table 2. Carbon balance for Lake Fryxell and East Lobe Lake Bonney. Annual heterotrophic carbon demand (bacterial production+bacterial respiration; heterotrophy), extracellular release by phytoplankton based on modeled photosynthetic primary production (photoautotrophy), and chemolithoautotrophy (dark DIC-fixation). The balance represents the difference between the sum of photoautotrophic and chemolithoautotrophic fixation sources minus heterotrophic carbon demand. See supplemental methods for calculations and data sources.

The extended periods of darkness in these high latitude lakes produce water column photosynthesis:respiration ratios < 1 [2], yielding organic carbon deficits of thousands of kilograms of carbon per year [20]. We compared annual heterotrophic carbon demand to new organic carbon production from chemolithoautotrophy (dark DIC-fixation) and photoautotrophy (see supplemental methods) in FRX and ELB to determine the degree to which sources of organic carbon production balance organic carbon

demand. Carbon production via phoautotrophic activity is equal to the demand from heterotrophic sinks in ELB, but not FRX (Table 2). However, the contribution of chemolithoautotrophic inorganic C-fixation brings the ratio of total inorganic carbon fixation to heterotrophic carbon demand to >1 (1.7) in ELB and in FRX (3.5), balancing the carbon budget for these lakes. In FRX, we can attribute 29% of the new production to inorganic carbon fixation by ammonia-oxidation. Much like has been suggested for Antarctic marine waters (e.g. [21, 22]), new carbon production via chemolithoautotrophy may supply an important source of new carbon to these ice-covered low light environments.

Acknowledgements

We thank the 2008-2009 and 2009-2010 McMurdo LTER limnology teams for assistance with sample collection and processing and Alexander Michaud and Pamela Santibañez for comments on the manuscript. This work was funded by NSF grants OPP-1115254, OPP-1340292, and OPP-7460252 to JCP. TJV received support from an American Association of University Women Dissertation Fellowship and a Montana Space Grant Consortium Graduate Fellowship.

Supplemental Methods

The carbon balance was determined by subtraction of heterotrophic carbon demand from total DIC-fixation by photoautotrophs and chemolithoautotrophs in the trophogenic zone of each lake (5 – 12 m for Lake Fryxell, and 4.5 – 20 m for East Lobe Lake Bonney).

Heterotrophic (bacterial and archaeal) production measurements (BP), determined via the incorporation of ^{3}H-thymidine into biomass and converted to units of carbon, were compiled for spring (September and October 1995; [9]) and summer and autumn (November 2007 – April 2008; [10]). Where multiple measurements were made in a single month (February, March, and April 2008), monthly averages were used. Winter-time values, which have never been measured, were estimated by averaging late autumn (April 2008) and early spring (September 1995) values. Rates (mgC m^{-3} d^{-1}) were determined either experimentally or by interpolating every half meter between experimentally measured values and multiplied by the volume (m^3) of each half meter layer. The mg C d^{-1} for each layer were summed to determine a total for the trophogenic zone. Total monthly masses of carbon from bacterial production (January – December) were summed to determine the annual total.

Heterotrophic (bacterial and archaeal) respiration (BR) was determined according the relationship used for Lake Fryxell and Lake Bonney [9], originally derived by [23]:

$$BR = 3.7 \text{ X } BP^{0.41}$$

Total heterotrophic carbon demand was determined as the sum of BR and BP.

Dark inorganic carbon-fixation (chemolithoautotrophy) was assumed to be unaffected by the annual light cycle and remain consistent throughout the year. Dark DIC-fixation also includes cellular anaplerotic replenishment reactions. Values measured from dark bottle incubations (minus killed controls) were integrated over depth and converted to total mass within the trophogenic zone as described for BP.

Annual photosynthetic primary production (kg C) was obtained by fitting a hyperbolic tangent model to depth and volume integrated water column productivity rates and 10 m PAR measured at 20 minute intervals throughout the year [2]. The values reported are averages of nine years between 1995 and 2007 for FRX and seven years for ELB. Extracellular release was calculated as 25% of photosynthetic primary production [20].

References

1. Priscu JC, Priscu LR, Howard-Williams C, Vincent WF (1988) Diel patterns of photosynthate biosynthesis by phytoplankton in permanently ice-covered Antarctic lakes under continuous sunlight. J Plankton Res 10:333–340. doi: 10.1093/plankt/10.3.333

2. Priscu JC, Wolf CF, Takacs CD (1999) Carbon transformations in a perennially ice-covered Antarctic lake. BioScience 49:997. doi: 10.2307/1313733

3. Spigel RH, Priscu JC (1998) Physical Limnology of the Mcmurdo Dry Valleys Lakes. Antarctic Research Series 153–187. doi: 10.1029/ar072p0153

4. Kong W, Ream DC, Priscu JC, Morgan-Kiss RM (2012) Diversity and expression of RubisCO genes in a perennially ice-covered Antarctic lake during the polar night transition. Applied and Environmental Microbiology 78:4358–4366. doi: 10.1128/AEM.00029-12

5. Kong W, Dolhi JM, Chiuchiolo A, et al. (2012) Evidence of form II RubisCO (cbbM) in a perennially ice-covered Antarctic lake. FEMS Microbiology Ecology 82:491–500. doi: 10.1111/j.1574-6941.2012.01431.x

6. Vick-Majors TJ, Priscu JC, Amaral-Zettler LA (2014) Modular community structure suggests metabolic plasticity during the transition to polar night in ice-covered Antarctic lakes. ISME J 8:778–789. doi: 10.1038/ismej.2013.190

7. Lizotte MP, Sharp TR, Priscu JC (1996) Phytoplankton dynamics in the stratified water column of Lake Bonney, Antarctica. Polar Biology 16:155–162. doi: 10.1007/bf02329203

8. Morgan-Kiss RM, Lizotte MP, Kong W, Priscu JC (2015) Photoadaptation to the polar night by phytoplankton in a permanently ice-covered Antarctic lake. Limnol Oceangr n/a–n/a. doi: 10.1002/lno.10107

9. Takacs C, Priscu J (1998) Bacterioplankton Dynamics in the McMurdo Dry Valley Lakes, Antarctica: Production and Biomass Loss over Four Seasons. Microbial Ecology 36:239–250.

10. Vick TJ, Priscu JC (2012) Bacterioplankton productivity in lakes of the Taylor Valley, Antarctica, during the polar night transition. Aquat Microb Ecol 68:77–90. doi: 10.3354/ame01604

11. Dolhi JM, Teufel AG, Kong W, Morgan-Kiss RM (2015) Diversity and spatial distribution of autotrophic communities within and between ice-covered Antarctic lakes (McMurdo Dry Valleys). Limnol Oceangr 60:977–991. doi: 10.1002/lno.10071

12. Voytek MA, Ward BB, Priscu JC (1998) The Abundance of Ammonium-Oxidizing Bacteria in Lake Bonney, Antarctica Determined by Immunofluorescence, Pcr and In Situ Hybridization. Antarctic Research Series 217–228. doi: 10.1029/ar072p0217

13. Priscu JC, Downes MT, McKay CP (1996) Extreme supersaturation of nitrous oxide in a poorly ventilated Antarctic lake. Limnol Oceangr 41:1544–1551.

14. Sattley WM, Sattley WM, Madigan MT, Madigan MT (2006) Isolation, Characterization, and Ecology of Cold-Active, Chemolithotrophic, Sulfur-Oxidizing Bacteria from Perennially Ice-Covered Lake Fryxell, Antarctica. Applied and Environmental Microbiology 72:5562–5568. doi: 10.1128/AEM.00702-06

15. Jäntti H, Jokinen S, Hietanen S, et al. (2013) Effect of nitrification inhibitors on the Baltic Sea ammonia-oxidizing community and precision of the denitrifier method. Aquat Microb Ecol 70:181–186. doi: 10.3354/ame01653

16. Priscu JC, Priscu LR, Vincent WF, Howard-Williams C (1987) Photosynthate distribution by microplankton in permanently ice-covered Antarctic desert lakes. Limnol Oceangr 32:260–270. doi: 10.4319/lo.1987.32.1.0260

17. Priscu JC (1995) Phytoplankton nutrient deficiency in lakes of the McMurdo Dry Valleys, Antarctica. Freshwater Biol 34:215–227. doi: 10.1111/j.1365-2427.1995.tb00882.x

18. Priscu JC, Christner BC, Dore JE, et al. (2008) Supersaturated N2O in a perennially ice-covered Antarctic lake: Molecular and stable isotopic evidence for a biogeochemical relict. Limnol Oceangr 53:2439–2450. doi: 10.4319/lo.2008.53.6.2439

19. Campbell NE, Aleem MI (1965) The effect of 2-chloro, 6-(trichlormethyl) pyridine on the chemoautrotrophic metabolism of nitrfying bacteria. Antonie Van Leeuwenhoek 31:124–136.

20. Takacs CD, Priscu JC, McKnight DM (2001) Bacterial dissolved organic carbon demand in McMurdo Dry Valley lakes, Antarctica. Limnol Oceangr 46:1189–1194.

21. Priscu JC (1990) Dynamics of ammonium oxidizer activity and nitrous oxide within and beneath Antarctic sea ice. 62:37–46.

22. Williams TJ, Long E, Evans F, et al. (2012) A metaproteomic assessment of winter and summer bacterioplankton from Antarctic Peninsula coastal surface waters. ISME J 6:1883–1900. doi: 10.1038/ismej.2012.28.

23. del Giorgio PA, Cole JJ (1998) Bacterial growth efficiency in natural aquatic systems. Annual Review of Ecology and Systematics 29:503–541. doi: 10.1146/annurev.ecolsys.29.1.503

CHAPTER FOUR

A MICROBIOLOGICALLY CLEAN ACCESS STRATEGY FOR ACCESS TO THE WHILLANS ICE STREAM SUBGLACIAL ENVIRONMENT

Contribution of Authors and Co-Authors

Manuscript in Chapter 4

Author: John C. Priscu

Contributions: Conceived the study, oversaw the study, obtained funding, and wrote the manuscript.

Co-Author: Amanda M. Achberger

Contributions: Conducted tests, performed lakewater pasteurization experiments, contributed to manuscript.

Co-Author: Joel Cahoon

Contributions: Analyzed data to determine system flow.

Co-Author: Brent Christner

Contributions: Conceived the study, oversaw the study, obtained funding, contributed to manuscript.

Co-Author: Robert Edwards

Contributions: Oversaw the study, managed the project, assisted with experimental design, assisted with sample collection, assisted with data analysis and manuscript preparation.

Co-Author: Warren L. Jones

Contributions: Analyzed data to determine system flow.

Co-Author: Alexander B. Michaud

Contribution of Authors and Co-Authors-Continued

Contributions: Conducted tests, collected samples, analyzed data, designed surface based cleaning experiments, cultivated bacteria for bacterial viability experiment, determined ATP concentrations, contributed to manuscript.

Co-Author: Matthew R. Siegfried

Contributions: Contributed hydrological information and map of Subglacial Lake Whillans to the manuscript.

Co-Author: Mark L. Skidmore

Contributions: Conducted tests, collected samples, analyzed data, contributed to manuscript.

Co-Author: Robert H. Spigel

Contributions: Performed data analysis for dye test.

Co-Author: Gregg W. Switzer

Contributions: Assembled filtration system and contributed operational information to manuscript.

Co-Author: Slawek Tulaczyk

Contributions: Obtained funding, contributed to the manuscript.

Co-Author: Trista J. Vick-Majors

Contributions: Conducted tests, collected samples, analyzed data, designed surface based cleaning experiments, performed microscopy for bacterial removal and bead removal experiments, calculated statistics for bead removal experiment, contributed to manuscript.

Manuscript Information Page

John C. Priscu, Amanda M. Achberger, Joel E. Cahoon, Brent C. Christner, Robert L. Edwards, Warren L. Jones, Alexander B. Michaud, Matthew R. Siegfried. Mark L. Skidmore, Robert H. Spigel, Gregg W. Switzer, Slawek Tulaczyk, Trista J. Vick-Majors
Antarctic Science
Status of Manuscript:
____ Prepared for submission to a peer-reviewed journal
____ Officially submitted to a peer-review journal
____ Accepted by a peer-reviewed journal
_X__ Published in a peer-reviewed journal

Antarctic Science 25(5), 637–647 (2013) © Antarctic Science Ltd 2013 doi:10.1017/S0954102013000035

A microbiologically clean strategy for access to the Whillans Ice Stream subglacial environment

JOHN C. PRISCU[1], AMANDA M. ACHBERGER[2], JOEL E. CAHOON[3], BRENT C. CHRISTNER[2], ROBERT L. EDWARDS[1], WARREN L. JONES[3], ALEXANDER B. MICHAUD[1], MATTHEW R. SIEGFRIED[4], MARK L. SKIDMORE[5], ROBERT H. SPIGEL[6], GREGG W. SWITZER[1], SLAWEK TULACZYK[7] and TRISTA J. VICK-MAJORS[1]

[1]*Department of Land Resources and Environmental Science, Montana State University, Bozeman, MT 59717, USA*
[2]*Department of Biological Sciences, Louisiana State University, Baton Rouge, LA 70803, USA*
[3]*Department of Civil Engineering, Montana State University, Bozeman, MT 59717, USA*
[4]*Scripps Institution of Oceanography, University of California, San Diego, La Jolla, CA 92093, USA*
[5]*Department of Earth Science, Montana State University, Bozeman, MT 59717, USA*
[6]*National Institute of Water and Atmospheric Research Ltd, Box 8602, Christchurch, New Zealand*
[7]*Department of Earth and Planetary Sciences, University of California, Santa Cruz, Santa Cruz, CA 95064, USA*
jpriscu@montana.edu

Abstract: The Whillans Ice Stream Subglacial Access Research Drilling (WISSARD) project will test the overarching hypothesis that an active hydrological system exists beneath a West Antarctic ice stream that exerts a major control on ice dynamics, and the metabolic and phylogenetic diversity of the microbial community in subglacial water and sediment. WISSARD will explore Subglacial Lake Whillans (SLW, unofficial name) and its outflow toward the grounding line where it is thought to enter the Ross Ice Shelf seawater cavity. Introducing microbial contamination to the subglacial environment during drilling operations could compromise environmental stewardship and the science objectives of the project, consequently we developed a set of tools and procedures to directly address these issues. WISSARD hot water drilling efforts will include a custom water treatment system designed to remove micron and sub-micron sized particles (biotic and abiotic), irradiate the drilling water with germicidal ultraviolet (UV) radiation, and pasteurize the water to reduce the viability of persisting microbial contamination. Our clean access protocols also include methods to reduce microbial contamination on the surfaces of cables/hoses and down-borehole equipment using germicidal UV exposure and chemical disinfection. This paper presents experimental data showing that our protocols will meet expectations established by international agreement between participating Antarctic nations.

Received 20 August 2012, accepted 25 November 2012, first published online 28 March 2013

Key words: clean access, environmental stewardship, hot water drilling, subglacial aquatic environments

Introduction

Recent discoveries of life under the thick ice sheet covering Antarctica have radically changed our view of the interior of the Antarctic continent. Subglacial exploration presents considerable challenges to the way we conduct science in an atmosphere of increasingly stringent environmental concerns (Priscu 2002, Priscu *et al*. 2003). Priscu *et al*. (1999) and Karl *et al*. (1999) were the first to show that there was microbial life in water from Subglacial Lake Vostok that had accreted to the bottom of the ice sheet. Since these seminal reports, others have confirmed the presence of microbial life both within and beneath Antarctica's ice sheet (e.g. Christner *et al*. 2006, Priscu *et al*. 2007, Lanoil *et al*. 2009). As such, the basal zones of ice sheets are now thought to harbour active microbial ecosystems and our view of the extent of Earth's biosphere has expanded substantially (Priscu & Christner 2004, Priscu *et al*. 2008).

The pristine nature of Antarctic subglacial ecosystems has led to international concern about environmental and scientific stewardship during their exploration. Following more than ten years of deliberation by international and national committees (e.g. NRC 2007, Priscu *et al*. 2010), it has become clear that sampling of lakes and sediments beneath Antarctica's ice sheets must be done in such a way that minimizes microbial and chemical contamination to the environment and to the samples being retrieved. All those involved in this research must recognize that environmental stewardship should take precedence over scientific endeavours. We can expect subglacial lakes to be at the forefront of the Antarctic tradition of melding interdisciplinary and international science in exploring one of the last unexplored frontiers on our planet (Priscu 2002).

Largely through the efforts of scientific specialists organized by SCAR, three major subglacial drilling projects are now underway (Priscu *et al*. 2005). These include the

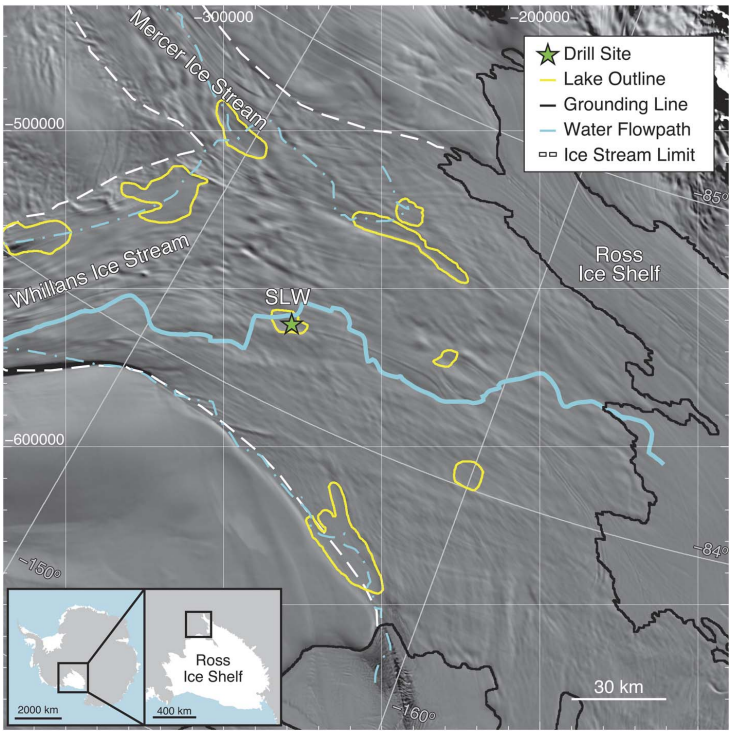

Fig. 1. Map showing the location of Subglacial Lake Whillans (green star = SLW, 84.237°S, 153.614°W) and its predicted flow path to the Ross Ice Shelf (heavy blue line). WISSARD sampling sites include the lake itself and near the end of the flow path close to the grounding line (heavy black line). The outlines of other lakes on the Whillans Ice Stream (yellow outlines) and their predicted flow paths (light blue lines) are also presented. Polar stereographic projection with true scale at -71°S; gridlines are spaced at 50 km intervals. Background imagery and grounding line are from the MODIS Mosaic of Antarctica (Scambos *et al*. 2007); lake outlines from MODIS image differencing (Fricker & Scambos 2009); ice stream boundaries were determined from InSAR velocities (Rignot *et al*. 2011); hypothesized water flow paths were determined by tracing continuous local hydropotential minima (Carter *et al*. 2011, Carter & Fricker 2012).

Lake Vostok programme funded by the Russian Antarctic Federation (Lukin & Bulat 2011), the Lake Ellsworth programme funded by the United Kingdom's Natural Environment Research Council (Ross *et al*. 2011), and the Whillans Ice Stream Subglacial Access Research Drilling (WISSARD) project, funded by the United States National Science Foundation (Fricker *et al*. 2011). All of these projects plan to access their subglacial targets within the next few years. Each project has proposed a suite of methods to ensure clean access to their respective systems, the details of which can be found on the Antarctic Treaty System's website as informational papers or comprehensive environmental evaluations (http://www.ats.aq/e/ats_keydocs.htm).

The WISSARD project proposes to sample subglacial lake Whillans (SLW) during the 2012–13 summer field season and the subglacial environment on the lower Whillans Ice Stream in a region near the grounding zone (GZ) during the 2013–14 summer season. The GZ site will be in an area where drainage from SLW is thought to enter the marine environment beneath the Ross Ice Shelf (Fig. 1). Access to the subglacial environment will be accomplished using a hot water drilling system to penetrate the ~800 m of ice overlying the basal water. To ensure that the borehole water

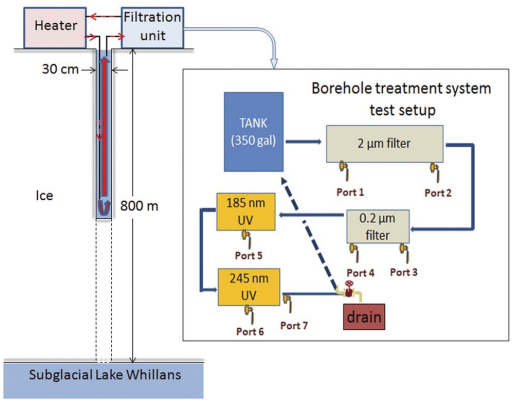

Fig. 2. Schematic (left panel, not to scale) showing the flow directions for the field operation of the Whillans Ice Stream Subglacial Access Research Drilling (WISSARD) water treatment system. The filtration and UV-treatment unit will be placed in-line between the borehole water return line and the heater modules. The enlarged inset (right panel) shows the treatment system components as set up for the laboratory tests. See text for details.

meets the cleanliness requirements promoted by a recent US National Research Council report (NRC 2007) and the scientific integrity of samples (water and sediments) is maintained, the project will include a borehole water treatment system designed to eliminate particles $>0.2\,\mu m$ in diameter, and reduce the concentration of viable microbial cells present in the borehole water (Fig. 2) and attached to deployed equipment and instrumentation.

This document presents: i) results from experiments designed to test the efficacy of the filtration system, and ii) disinfection protocols to be employed at all proposed WISSARD drilling sites where biological clean access is a requirement. These results are discussed within the context of the hydrology of SLW.

Methods

Borehole filtration and germicidal treatment system

The filtration component of the water treatment system consists of a 2 μm prefilter (pleated polypropylene cartridges, 15 cm diameter x 203 cm long, Champion Process Inc) followed by 0.2 μm filtration through a polyethersulfone membrane cartridge (7 cm diameter x 76 cm long, Champion Process Inc). After filtration, the clarified water was subsequently exposed in sequence to two separate ultraviolet (UV) irradiation modules (Glasco UV) that use 185 nm ozone-producing lamps followed by exposure to 254 nm germicidal lamps (wavelengths denote peak spectral output). Based on data supplied by the manufacturer, the tandem filtration strategy is designed to decrease the number of particles $>0.2\,\mu m$ by 99.98% (i.e. 4-log reduction). The two UV systems provide a 185 nm dosage $>40\,000\,\mu W\text{-sec cm}^{-2}$ and 254 nm germicidal dosage $>175\,000\,\mu W\text{-sec cm}^{-2}$. Doses of $40\,000\,\mu W\text{-sec cm}^{-2}$ are typically used for water disinfection, and depending on the UV transmission properties of the water and the sensitivity of the microorganisms to UV, exposures in this range have been shown to reduce the number of viable cells by 1-log to nearly 6-log (Aquafine Corp). The internal volume of the entire system (filters plus UV units) is 572 l. In a field scenario, the treated water will undergo a final pasteurization step where water temperature will progressively reach 90°C before exiting the 152 m long heating coils of the drilling unit. In summary, the WISSARD borehole water treatment system will use three complementary technologies to reduce microbial contaminants in the borehole water: i) filtration to remove particles $>0.2\,\mu m$, ii) UV irradiation (185 and 254 nm), and iii) pasteurization in the boilers of the hot water drill.

In field operations, hot water is pumped to the bottom of a 30 cm diameter borehole at high pressure (the diameter will be controlled by adjusting the water heating rate), flows upward in the hole and is pumped from the top, as shown schematically in the left-hand panel of Fig. 2. After water is pumped from the top of the borehole, it flows into a 14 000 l holding tank, then through the filtration system followed by the heater modules before again being pumped to the drilling nozzle at the bottom of the borehole. The drilling speed is expected to be $1\,m\,min^{-1}$ through most of the ice and the filtration system will be run continuously during drilling operations. The liquid water in the hole-drill-treatment system thus forms a recirculating system, with a liquid volume that increases as drilling proceeds. A 1900 l insulated melt tank will provide start-up water for the field system by melting snow using heated glycol pumped through a series of heat-radiating immersion plates that form a recirculation system. The components of the treatment system are illustrated in the right-hand panel of Fig. 2 as set up for laboratory testing.

The following laboratory tests were conducted to determine the efficacy of the system:

1) Dye study to determine the system flow characteristics.
2) Fluorescent micro-bead (1–5 μm) and microbial cell removal.
3) Silt (1.2–63 μm particle size) removal.
4) Effect of UV exposure on viability of a model bacterium (*Escherichia coli* strain K-12).
5) Lakewater test to examine the filtration efficiency and disinfecting properties of the UV lamps on populations of natural aquatic microorganisms.
6) Lakewater pasteurization test to assess the influence of the heat generated by the hot water drill on microbial viability.

Dye test

A dye test was performed to examine the hydraulic residence-time characteristics of water in the treatment system. The system was filled with water containing fluorescent Rhodamine WT (water tracing) dye at a concentration of $\sim 9\,\mu g\,l^{-1}$, and then flushed with dye-free tap water at $95\,l\,min^{-1}$ for 25 min. The flow rate of $95\,l\,min^{-1}$ is within the range of flow to be used during actual drilling operations. At this rate, the treatment system has a mean residence time (volume 572 l divided by a flow rate of $95\,l\,min^{-1}$) of 6 min. The test duration of 25 min therefore corresponds to 4.2 residence times. During the course of the test, discrete samples were collected to examine the dilution of the dye at port 7. Data from port 7 represents the integrated flow characteristics of the entire system (filter plus UV lamp canisters). All fluorescence measurements were made on a calibrated Turner Model 112 fluorometer fitted with a C5-60 excitation filter, a C56 emission filter, and F4T-4 lamp.

Bead removal experiment

Fluorescent beads (manufacturer nominal size range: 1–5 μm, mean = 2.2 μm) were added to the feed tank

containing 13251 of tap water to a final concentration of $\sim 2 \times 10^5$ beads ml^{-1} and mixed thoroughly. The bead mixture in the feed tank was then pumped through the filtration and UV canisters (the UV lamps were off for this test) at $\sim 94 l min^{-1}$ until 11131 had passed through the system (~ 12 min). The filtered water was sent to the drain (i.e. it was not recirculated through the system). Samples were then collected in clean quadruplicate vials from the source tank and from ports 1, 2, and 4 along the flow path (Fig. 2). The samples were vortexed vigorously for ~ 30 s and prepared for microscopic enumeration by filtering 10 ml of sample onto a black polycarbonate 0.2 μm filter. A Nikon 80i microscope with a Nikon B2-A filter cube was used to enumerate all samples. Percent efficacy of bead removal from each port was calculated as:

((Geometric mean bead count in the tank
- Geometric mean bead count at a selected port)/
Geometric meanbead count in the tank) * 100,

where the geometric mean = the Nth root of the product of N replicates.

Silt removal experiment

Local mineral soil was mixed with $\sim 13 l$ of tap water and sieved through 63 μm mesh to form a silt/clay slurry. The slurry was added to 4401 of water in the holding tank to a final concentration of $0.395 g l^{-1}$ and pumped through the 2 μm filtration unit at $95 l min^{-1}$. The 0.2 μm filter and the UV systems were bypassed in this test. Outflow water from the filtration unit was returned to the holding tank yielding a recirculating system with constant volume. Samples were collected from the tank six times over a 40 min period, with a final sample collected 15 hours after the pump was turned on. Additional samples were collected at ports 1 and 2, four times over the 15 hour experiment. All samples were filtered onto Whatman GF/C filters (effective particle retention 1.2 μm), dried for 24 hours at 100°C and weighed. Standard particle-size classifications (Vanoni 1975) typically specify a range of particle diameters of 4–62 μm for silt, and 0.24–4 μm for clay. The Stokes settling velocity for the largest silt particle (62 μm) is less than $0.2 cm s^{-1}$, and is much smaller than the upward average flow velocity in the 30 cm diameter ice borehole of $2.2 cm s^{-1}$ corresponding to a flow of $95 l min^{-1}$. Silt entering the ice hole with meltwater during field operations would therefore be maintained in suspension and carried into the filtration unit.

Bacterial culture removal and viability test

Cultures of *Escherichia coli* strain K-12 were grown in 25% nutrient broth and added to the holding tank to a final concentration of $\sim 10^6$ cells ml^{-1}. After mixing with 13301 of water in the holding tank for 30 min, triplicate samples were collected from the tank to estimate the bulk bacterial concentration in the test water before it passed through the UV treatment system. The pump was turned on and 2271 was allowed to pass through the UV system in three single pass experiments at flow rates of $19 l min^{-1}$, $76 l min^{-1}$, and $152 l min^{-1}$, with triplicate samples collected from port 7 (post UV treatment) in autoclaved 20 ml vials. Flushing the system with 2271 before sampling provided adequate time for the UV lamps to reach full output capacity, and allowed water in the UV system to be replaced five times before samples were taken. This ensured that all of the standing water in the UV canisters (total canister volume = 45 l) was replaced with amended tank water before sampling began. Colony forming units (CFU) from the initial inoculum and each sample were enumerated by standard dilution spread plating on nutrient agar followed by overnight incubation at 37°C, and again after two weeks of incubation. The two week incubation allowed assessment of the potential for the bacteria to recover from UV irradiation. The limit of quantification for this method is 300 CFU ml^{-1} for aqueous samples.

Lakewater bacterial removal and viability

Experiments were conducted on lakewater from the Montana State University campus. Lakewater (760 l) was sieved through a 125 μm mesh net to remove large debris and brought to 950 l with tap water in the holding tank. The cell count in the original pond water was 1.90×10^6 cells ml^{-1} and 1.52×10^6 cells ml^{-1} following dilution in the tank. The UV lamps were switched on for 5 min (allowing them to reach full capacity) before recirculating the water through all filters and both UV lamps at $76 l min^{-1}$. Four replicate 10 ml samples were collected from the tank over a period of 90 min at selected times following pump start-up for bacterial counts and determination of intracellular adenosine triphosphate (ATP) concentration. Bacterial samples were collected in 10 ml sterile glass vials, fixed with formalin (5% v/v final concentration), stained using the deoxyribonucleic acid (DNA) dye SYBR Gold™, and enumerated by epifluorescence microscopy (Lisle & Priscu 2004). Cellular ATP concentration, a proxy for microbial biomass and viability (Karl 1980), was determined by concentrating cells in a 10 ml water sample on a 0.2 μm acrodisk syringe filter (Pall Corp). Adenosine triphosphate was extracted with the Microbial ATP Kit HS (BioThema Inc), and luminosity was measured with a Glomax 20/20 luminometer. The limit of detection for this method was 10^{-15} mol ATP ml^{-1} based on two standard deviations above the y-intercept in the ATP standard curve.

Lakewater pasteurization test

Water collected from a lake on the Louisiana State University campus containing an original cell density of 2.5×10^5 (estimated by SYBR- Gold™ epifluorescence

microscopic counts) was serially diluted with filtered lakewater to create two identical sets of cell concentrations ranging from 2.5×10^4 to 25 total cells ml^{-1}. A set of control dilutions was incubated at ~25°C while the other was heated to 85°C for 2 min to mimic the effect of pasteurization in the boilers of the hot water drill. Following exposure to heat, cell viability was assayed by measuring the respiratory reduction of the tetrazolium dye 2, 3-bis-(2-methoxy-4-nitro-5sulphenyl)-(2 H)-tetrazolium-5-carboxanilide (XTT) to formazan (Roslev & King 1993). This tetrazolium salt is reduced by active respiratory electron transport, forming a water soluble formazan dye measureable as absorbance at 490 nm and serves as a proxy for cell viability.

Surface-based cleaning experiments

Triplicate flat stainless steel (2.5 cm x 10 cm) and transparent thermoplastic Poly(methyl methacrylate) (PMMA) (5 cm x 10 cm) coupons, representative of materials comprising the down-borehole instrumentation, were contaminated with either *E. coli* K-12 or the endospore-former *Bacillus subtilis*. The coupons were then analysed for cell viability following treatment with 3% hydrogen peroxide. Before inoculation with bacteria, all materials were rinsed with sterile Type 1 (18.2 MΩ cm^{-1}) water and autoclaved. The coupons were immersed in cell inocula (1×10^7 cell ml^{-1} *E. Coli*, 4×10^6 cell ml^{-1} *B. subtilis*) for 1 min and allowed to air dry for 5 min before being sprayed five times with 3% H_2O_2 (which completely wetted the surfaces) and allowed to react with the bacteria on the coupons for 1 min. Controls consisted of triplicate contaminated coupons not sprayed with H_2O_2.

A 10 cm^2 area of all control and H_2O_2-treated samples were swabbed in triplicate using sterile polyurethane swabs moistened with sterile phosphate-buffered saline (PBS). Swabs were immediately placed into 10 ml of sterile PBS where they were sonicated and vortexed to release cells into the buffer. The 10 ml PBS solution containing the cells was then serially diluted (five dilutions) into sterile PBS. One-hundred μL of each dilution was spread plated in triplicate onto nutrient agar. The cultures were incubated aerobically at 37°C and colonies were enumerated following 18 hours and 72 hours of incubation. The limits of detection for this method, accounting for the area swabbed and the ensuing dilution is 300 CFU cm^{-2}.

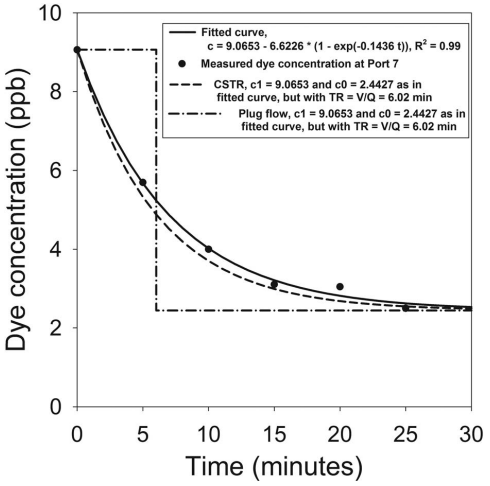

Fig. 3. Dye concentrations measured experimentally at Port 7 (filled circles); fitted exponential decay curve (solid line); the curve (dashed line) for a continuously stirred tank reactor (CSTR) with the same initial and final concentrations (C1 and C0) as for the fitted curve, but with the decay constant k computed from the mean residence time (TR = V/Q, = 6.02 min, where V = treatment system volume (572 l) and Q = flow rate (95 l min^{-1}), as k = 1/TR); and the curve (dashed-dot line) for a plug-flow reactor with the same initial and final concentrations (C1 and C0) as for the fitted curve, and residence time TR = V/Q = 6.02 min.

Results

Dye test results

A dye test was conducted for 25 min (4.1 times the mean residence time of the system) to examine the rate at which the dye decreased in the system following a clean water flush. This is the same method as that used to experimentally determine the residence time distribution for a reactor (Dankwerts 1953), except that the step-change in dye concentration here is negative. Nevertheless, the results yield the same information.

Changes in dye concentration from test 2 showed an exponential decrease of dye concentration over time (Fig. 3) and were fitted with Eq. (1):

$$C(t) = C1 - (C1 - C0) * (1 - \exp(-kt)), \quad (1)$$

where C(t) = concentration at a given time (t), C1 = initial dye concentration at t = 0, C1 - C0 = the change in concentration between time t = 0 and t = infinity (C0 represents the final, tap-water concentration), and k = exponential decay factor, which denotes 1/residence time (1/TR).

The fit to the experimental points is excellent ($r^2 = 0.99$), and as shown in Fig. 3, is very similar to the theoretical dilution curve predicted for the flushing of a continuously stirred tank reactor (CSTR). This can be expressed in non-dimensional form, in terms of the fraction of fluid in the tank that remains to be replaced or flushed out at time t, by:

$$(C(t) - C0)/(C1 - C0) = 1 - \exp(-t/TR) = 1 - \exp(-kt), \quad (2)$$

with parameters C1 and C0 equal to those of the fitted curve, but decay constant k = 1/TR = 0.166 l min^{-1}. Here TR is the mean residence time (6.0 min), computed from

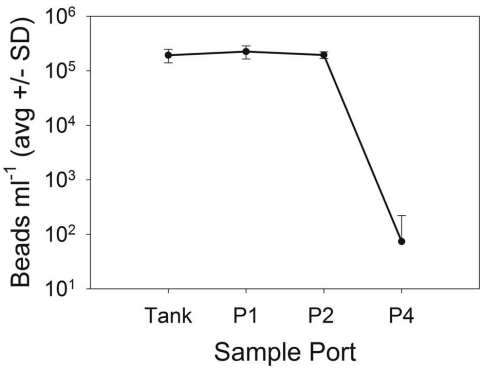

Fig. 4. Fluorescent beads counted from the tank and selected sample ports after filtering 11131 through the system. The flow rate was ~ 941 min^{-1}. Error bars = standard deviation (SD) ($n = 4$).

the treatment system volume V and the experimental flow rate Q, as TR = V/Q (Dankwerts 1953). Also shown in Fig. 3 is the theoretical flushing curve for plug-flow through the treatment system, which does not provide a good match to the treatment system's observed mixing and dilution behaviour. This is not surprising, given the complexity of internal flow paths through the various components of the treatment system.

The turnover or replacement fractions at various multiples of t/TR can be computed from Eq. (2), showing that one residence time (t/TR = 1) yields a turnover or replacement percent of 63%, and that it requires 3.0 and 4.6 residence times to replace 95% and 99%, respectively, of the fluid in the system. This equates to 95% and 99% replacement times for the fluid in the system of 21 min and 32 min, respectively for the flow of 95 l min^{-1}.

Bead removal experiment

Bead concentrations at ports 1 and 2 were not significantly different ($P > 0.05$) from those in the tank after 11131 of water had passed through the 2 μm filter (Figs 2 & 4). However, bead concentration decreased by almost four orders of magnitude at port 4 after the sample water had passed the 0.2 μm filter ($P < 0.05$). The efficacy of bead removal by the 2 μm filter was essentially zero (there was no significant difference in bead concentration between the tank and samples a ports 1 and 2) while the 0.2 μm filter had a removal efficiency of > 99%.

Silt removal experiment

The recirculation test using the 2 μm filter only showed that suspended sediment in the holding tank decreased

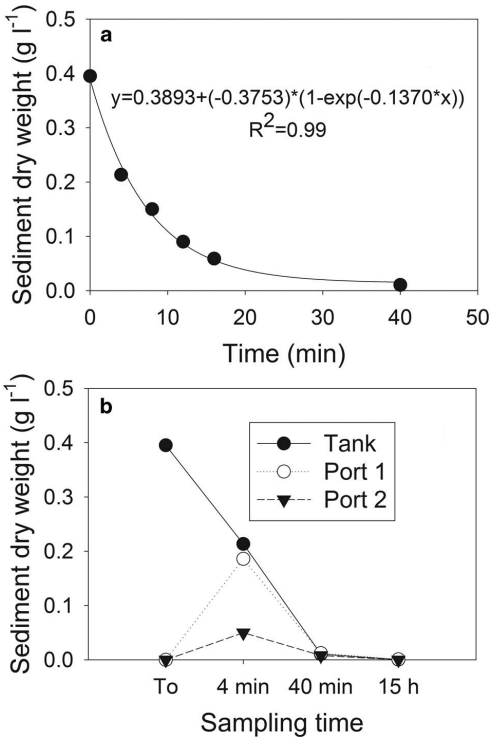

Fig. 5. a. Sediment concentration in the tank over time, and **b.** in the tank and ports 1 and 2 at specific times up to 15 hours. Water was recirculated through the tank during this experiment, passing only through the 2 μm filter, at a flow rate of 95 l min^{-1}.

exponentially from 0.4–0.01 g l^{-1} over 40 min at a flow rate of 95 l min^{-1} (Fig. 5a). The residence time of the system, calculated as 1/k from the fitted equation in Fig. 5a was 7.3 min. Both the shape of the removal curve and the value computed for the e-folding removal time closely match the flushing behaviour of the dye study. By analogy with the flushing described by Eq. (2), 95% and 99% of the sediment in the system would be removed in 22 and 34 min, respectively, under the experimental conditions.

Data from the inlet (port 1) and outlet (port 2) from the 2 μm filter system, showed that the dry weight of the sediment particles (63–1.2 μm in diameter) increased during the first 4 min interval after the pump was turned on, then dropped to background levels in the tank (Fig. 5b). These data indicate rapid mixing before filtration (port 1 data) and that a large number of particles were not retained in the initial pass through the filter. After 15 hours, no silt and clay particles were detectable (detection limit = 0.002 g l^{-1}) in samples from the tank,

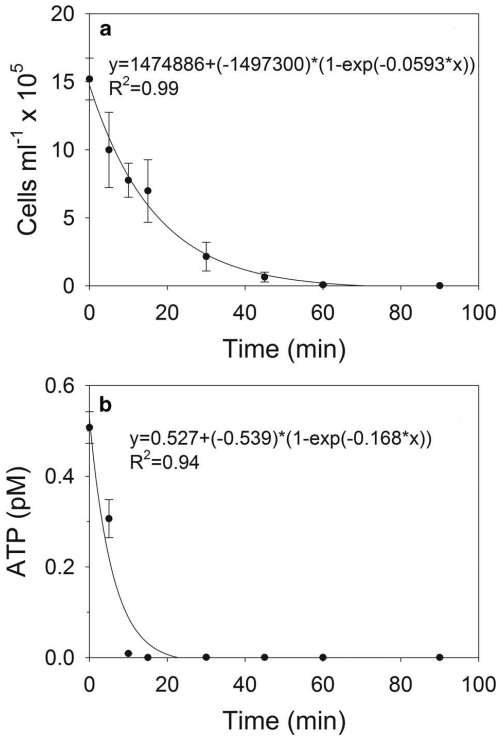

Fig. 6. a. Pond water cell, and **b.** adenosine triphosphate (ATP) concentrations in the tank at a flow rate of 76 l min^{-1} with the samples passing through both filter systems and both UV lamps. Each time point represents the mean and standard error (s.e.) ($n = 3$). Cell concentrations and ATP levels were below levels of detection after 60 min and 15 min, respectively.

port 1, or port 2 (Fig. 5b). The final sampling time at 15 hours is 75 times the theoretical hydraulic retention time of the system.

UV exposure and cell viability

Circulation of the *E. coli* suspension through the 185 nm and 254 nm UV irradiation modules reduced the number of viable *E. coli* cells in the tank (initial concentration of 7.2 x 10^6 CFU ml^{-1}) to below the methodological limit of quantification ($<$ 300 CFU ml^{-1}) on a single pass through the UV lamps at flow rates of 19, 76 and 152 l min^{-1}, which represents 2.7, 0.68 and 0.34 min of UV exposure as the sample passed through the UV system (based on a UV canister volume of 52 l). After two weeks of incubation at room temperature ($\sim$22°C), the CFUs on the plates remained below 300 CFU ml^{-1},

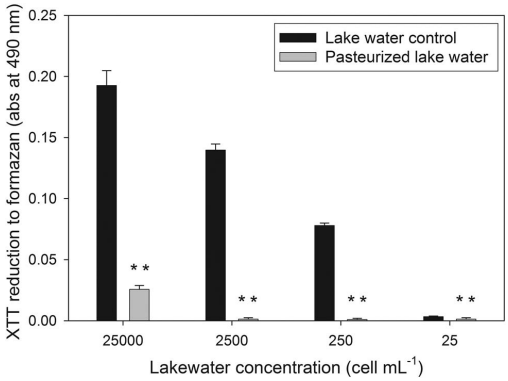

Fig. 7. Respiratory potential, detected as tetrazolium dye 2, 3-bis-(2-methoxy-4-nitro-5sulphenyl)-(2 H)-tetrazolium-5-carboxanilide (XTT) reduction to formazan dye (measured as absorption at 490 nm) of pasteurized (85°C for 2 min) lakewater samples relative to unpasteurized lakewater controls (no heat treatment) following 21 hours of incubation with XTT. The data represent a dilution series made from the original lakewater sample. Bars represent mean and 1 SD ($n = 3$). Asterisks denote that pasteurization significantly ($P < 0.001$) reduced cell viability in all dilutions.

providing evidence that the bacteria were killed by the UV treatment as opposed to incurring a level of sub-lethal damage that allowed them to remaining viable and recover.

Lakewater bacterial removal and viability

Viable lakewater bacteria within the tank were either physically removed or their DNA was irreversibly damaged by UV radiation during a 90 min experiment, reaching levels similar to that observed in procedural blanks by the end of the experiment (Fig. 6a). Based on the 76 l min^{-1} flow rate used in this experiment and the exponential curve fit shown in Fig. 6a, 99% of all bacteria were removed or killed following 78 min of run time (51 min for 95% removal).

Adenosine triphosphate measurements from the tank over the course of the experiment revealed that cellular ATP decreased by three orders of magnitude (to the limits of detection of the ATP method) following 15 min of circulation (Fig. 6b). Based on the exponential model used to fit the data, 99% of ATP-containing cells were eliminated from the system (through a combination of cell removal by the filters and decomposition by the UV lamps) in 27 min (18 min for 95% removal) at the 76 l min^{-1} flow rate used in the experiment. The almost three times greater reduction in ATP concentration relative to total cell number indicates that intracellular ATP was actually destroyed by the system, presumably by the UV lamps and

associated ozone. The reduced levels of intracellular ATP could also be the result of the synthesis of ATP-dependent enzymes used to repair UV damaged cells.

Lakewater pasteurization test

The pasteurization experiment (85°C for 2 min) conducted on lakewater showed that heating to the temperatures expected in the boiler of the hot water drill (at least 85°C) reduced respiration potential (XTT reduction to formazan dye) of the organisms significantly ($P < 0.001$) at cell densities ranging from 25–25 000 cell ml^{-1} (Fig. 7). These results indicate that the boilers in the hot water drill can produce up to a 2-log reduction in the number of viable cells.

Surface cleaning experiments

Following experimental contamination with *E. coli* and *B. subtilis*, the stainless steel coupons averaged (± SD) $8.7 \times 10^4 \pm 8.6 \times 10^4$ CFU cm^{-2} and $7.2 \times 10^4 \pm 4.0 \times 10^4$ CFU cm^{-2}, respectively. The averages (± SD) for these same organisms on the plastic coupons were $6.2 \times 10^5 \pm 1.8 \times 10^5$ CFU cm^{-2} and $4.0 \times 10^5 \pm 3.9 \times 10^5$ CFU cm^{-2}, respectively. A one-way analysis of variance (ANOVA) followed by a multi-comparison test revealed that a significantly ($P < 0.001$) greater proportion of *E. coli* and *B. subtilis* adhered to the plastic coupons per unit area than the stainless steel coupons. No significant difference ($P > 0.05$) in adherence was evident between the test organisms. Following treatment with H_2O_2, plate counts after 18 hours and 72 hours of incubation were below the limits of quantification (300 CFU cm^{-2}; i.e. no colonies formed), indicating a 2 to 3-log reduction in the concentration of viable cells.

Discussion

A flow rate of 95 l min^{-1} and a total volume for the entire treatment system (filtration plus UV components) of 572 l yields a mean retention time of 6 min, which represents the time when 63% of the water in the system is replaced for a CSTR. Timescales for the system for 95% and 99% water replacement are 21 min and 32 min, respectively, at this flow rate. Results from the dye study yielded a dilution curve for the treatment system that was very similar to that for a CSTR. Moreover, the filtration-disinfection-heater-borehole forms a recirculating system, whereby water in the borehole continually recirculates through the treatment system as the borehole volume increases during drilling operations (i.e. the borehole is deepened). The expected drilling rate of ~ 1 m min^{-1} (producing an increase in the water volume in a 0.3 m diameter borehole at a rate of 71 l min^{-1}) is slower than the upward velocity of water in the 30 cm diameter borehole (~ 1.3 m min^{-1} at a flow rate of 95 l min^{-1}). Hence, water in the borehole is being pumped through the filtration system at a faster rate than the liquid volume of the borehole is increasing.

The nature of mixing of water in the borehole itself is uncertain. Assuming an ice borehole depth and diameter of 800 m and 0.3 m, respectively (yielding a borehole volume of 57 m^3), and a system pumping rate of 95 l min^{-1}, the mean residence time for borehole water would be ten hours. This would be the actual time for complete replacement of the water in the borehole if plug-flow results from water being pumped into the bottom of a relatively smooth borehole and removed from the surface at the same rate where it enters the filtration/UV system and boilers before being returned to the bottom of the borehole. Although flow in the actual borehole will be complicated by buoyancy effects (it is likely to be turbulent; Reynolds number ~ 4500), its mixing and replacement-time characteristics will resemble plug-flow much more closely than that of a CSTR (Dankwerts 1953). Hence, it is reasonable to assume that the timescale for complete replacement of borehole water will be of the same order as the mean residence time (ten hours), rather than that given for a CSTR (i.e. 4.6 times the mean residence time for 99% replacement).

As the heated water enters the bottom of the borehole, it will mix with newly melted water. The mixed water will start to flow upward in the borehole to maintain continuity with the rate at which water is being withdrawn at the surface for treatment and reheating. The question of how much, and how often, water in the borehole is treated is difficult to answer, because of this mixing, the complicated flow in the borehole, and the fact that the borehole volume grows with time. If the filtration system is run continuously during borehole drilling, as planned, the water volume in the borehole will be much less than 57 m^3 during the early stages of drilling when the borehole depth is considerably shallower than 800 m, and borehole water originally near the surface will be passed through the water treatment system many times before the subglacial environment is entered. However, as the hole becomes very deep, a point will be reached beyond which there is not enough time for water melted at the bottom of the hole to reach the surface before the hole is melted to the base of the ice. Importantly, all of the heated water introduced into the bottom of the borehole will have passed through the treatment system at least once as the borehole reaches its maximum depth of ~ 800 m.

Based on our experimental results with sediment removal (Fig. 5b), one pass through the 2 μm filter of the filtration system alone will not eliminate all of the sediment particles in the borehole, particularly if the sinking rate of sediment particles (> 63 μm) exceeds the upward velocity of water through the borehole. However, the UV component of the system, which was shown to reduce *E. coli* by 4-log units following a single pass through the system at 95 l min^{-1} and to reduce cellular ATP levels to below the limits of detection (10^{-15} mol ATP ml^{-1})

following 15 min at 76 l min^{-1}, should significantly reduce the number of viable microbial cells. Hence, both systems working in tandem will effectively eliminate most of the relatively buoyant particles, including cells, in the system and kill a majority of the cells as melting proceeds from the surface to the bottom of the ice stream (~ 800 m).

Our pasteurization tests showed that a lake microbial assemblage exposed to 85°C for 2 min significantly ($P < 0.001$) reduced the respiratory potential of the assemblage, resulting in up to a 2-log reduction in the number of viable cells. These conditions are similar to the temperatures and retentions of the boilers on the hot water drill. As such, the heating system alone on the WISSARD drill should kill the vast majority of bacteria that pass through it, particularly if they are not heat tolerant (e.g. not endospore-forming bacteria), which we expect to be the case for most of the bacteria that exist in the ice we will melt to generate the borehole water (e.g. Christner *et al*. 2008, Priscu *et al*. 2008).

In summary, our test results indicate that one passage of a volume of water through the filtration component of the system will reduce the total number of microbes by more than 4-log units. Any cells remaining in the water after filtration will be reduced another 3.5-log units by combined effect of UV irradiance and pasteurization. To place this into context, if we assume an initial borehole cell concentration of 10^6 cell ml^{-1} (equivalent to coastal ocean waters), the system as tested would be capable of reducing the microbial burden to < 100 cells ml^{-1} in the borehole water after one borehole residence time (~ ten hours at a 95 l min^{-1} pumping rate). Because we will treat all down borehole equipment with 3% H_2O_2, which produced a 2 to 3-log reduction in our endospore and non-endospore forming test organisms, any cellular contamination introduced into the drilling and water treatment system during our operation is expected to be minimal. In addition to the safeguards discussed above, all hoses and cables on the WISSARD drilling system will pass through a clamp-on high pressure hot water cleaning system followed by a UV collar as they are deployed down the borehole. The UV collar will provide a disinfection dose of 40 000 μW-sec cm^{-2} at a maximum cable/hose deployment rate of 60 m min^{-1}.

In addition to the filtration/UV system and decontamination protocols that will be implemented during borehole drilling, the hydraulic nature of the lake itself provides a safeguard against permanent contamination by drilling procedures. Subglacial Lake Whillans belongs to the category of active subglacial lakes, which are located and defined on the basis of anomalously fast ice surface changes attributed to large water volume fluctuations in subglacial lake basins. Active subglacial lakes were discovered by InSAR (Gray *et al*. 2005) and subsequent studies using satellite altimetry have demonstrated that there are > 120 such lakes in Antarctica (Wingham *et al*. 2006, Fricker *et al*. 2007, Fricker & Scambos 2009, Smith *et al*. 2009). Active subglacial lakes are different from many previously described Antarctic subglacial lakes (e.g. review in Siegert *et al*. 2005) in a number of important ways. The defining feature of active subglacial lakes is that they actively fill and drain, undergoing volume changes large enough to cause localized, anomalously high (up to several metres) deformation of the ice surface above them that can be detected by a space borne instrument (e.g. Fricker *et al*. 2007). They also tend to occur within fast flowing parts of the Antarctic ice sheet (ice streams and outlet glaciers) as opposed to non-active lakes that are concentrated near ice divides, where ice flow is sluggish (Siegert *et al*. 2005, Smith *et al*. 2009). The active subglacial lakes discovered thus far tend to have a smaller area, and presumably volume, than their non-active counterparts. This may be largely due to observational biases because non-active lakes have been traditionally identified from airborne ice-penetrating radar surveys, which are more likely to encounter large subglacial lakes than small ones (e.g. Siegert *et al*. 2005). At the same time, active subglacial lakes have only been mapped using anomalous ice surface elevation changes occurring within the last decade, when new airborne/satellite altimetry and InSAR data provided sufficiently precise measurements of ice surface topography to reveal their existence. Hence, detection of such lakes is more likely if they have relatively small water residence time (i.e. high water throughput rates combined with low total basin volume).

Analyses of satellite data by Fricker *et al*. (2007) and Fricker & Scambos (2009) indicated that SLW has an area of 59 km^2 ± 12 km^2 and it has experienced two drain-fill cycles between 2003 and 2009. These authors estimated that each of the drain-fill cycles resulted in lake volume fluctuations of about 0.1 km^3 of water. The WISSARD surface geophysics team completed a high-density survey focused on the SLW basin in the 2010–11 field season. Improved constraints on ice geometry indicate that the subglacial water volume change during fill-drain cycles of SLW is 0.15 km^3 (unpublished data), which is 50% greater than the previous estimates of Fricker *et al*. (2007) and Fricker & Scamos (2009). Geophysical estimates of the depth of the lake at the time of the field survey, when the lake was drained, reveals that it is < 8 m (Horgan *et al*. 2012, Christianson *et al*. 2012). The relatively shallow depth of the SLW basin is consistent with its location within a region of gently undulating basal topography and low ice surface slope (e.g. Shabtaie *et al*. 1987). Given the area of the lake basin, the lake volume can be estimated to be < 0.5 km^3. Consequently, it would take fewer than three to four fill-drain cycles to exchange the total lake volume. Given that SLW has undergone two complete fill-drain cycles over a six year period, we estimate a water residence time for the lake of the order of ten years, or less.

The decadal scale flushing time for SLW is nearly 100 times faster than that predicted for Subglacial Lake Ellsworth (SLE) (750 years; Siegert *et al*. 2012) and about 1000 times faster than the water residence time estimated for Subglacial Lake Vostok (~ 10 000 years; Bell *et al*. 2002). Clearly, SLW is fundamentally different from SLE and Vostok, which contain large water volumes and do not show evidence of significant water volume changes over the period of instrumental observations. Subglacial Lake Whillans can be considered a small temporary storage basin for water draining beneath the Whillans Ice Stream and any disturbance resulting from drilling and sampling operations should have a minor and transitory impact.

Acknowledgements

We are grateful to the Department of Civil Engineering for allowing us use of the Hydraulics Laboratory at MSU. P.W. Adkins assisted with the experiments and laboratory work and R. Powell commented on the manuscript. This work was supported by NSF-OPP grants 0838933 to JCP, 0838941 to BC and 0839142 to ST as part of the Whillans Ice Stream Subglacial Access Drilling (WISSARD) Project. We appreciate the support and contributions of the WISSARD science team, and drilling and operational support contractors in accomplishing our goals. We gratefully acknowledge the constructive comments of the reviewers.

References

Bell, R.E., Studinger, M., Tikku, A.A., Clarke, G.K.C., Gutner, M.M. & Meertens, C. 2002. Origin and fate of Lake Vostok water frozen to the base of the East Antarctic ice sheet. *Nature*, **416**, 307–310.

Carter, S.P. & Fricker, H.A. 2012. The supply of subglacial meltwater to the grounding line of the Siple Coast, West Antarctica. *Annals of Glaciology*, **53**, 267–280.

Carter, S.P., Fricker, H.A., Blankenship, D.D., Young, D.A., Johnson, J.V., Price, S.F. & Lipscomb, V. 2011. Modeling five years of subglacial lake activity in the MacAyeal Ice Stream catchment through assimilation of ICESat laser altimetry. *Journal of Glaciology*, **57**, 1098–1112.

Christianson, K., Jacobel, R.W., Horgan, H.J., Anandakrishnan, S. & Alley, R.B. 2012. Subglacial lake Whillans: ice-penetrating radar and GPS observations of a shallow active reservoir beneath a West Antarctic ice stream. *Earth and Planetary Science Letters*, **331**, 237–245.

Christner, B.C., Skidmore, M.L., Priscu, J.C., Tranter, M. & Foreman, C.M. 2008. Bacteria in subglacial environments. *In* Margesin, R., Schinner, F., Marx, J.-C. & Gerday, C., *eds. Psychrophiles: from biodiversity to biotechology*. New York: Springer, 51–71.

Christner, B.C., Royston-Bishop, G., Foreman, C.M., Arnold, B.R., Tranter, M., Welch, K.A., Lyons, W.B., Tsapin, A.I. & Priscu, J.C. 2006. Limnological conditions in Subglacial Lake Vostok, Antarctica. *Limnology and Oceanography*, **51**, 2485–2501.

Dankwerts, P.V. 1953. Continuous flow systems. Distribution of residence times. *Chemical Engineering Science*, **2**, 1–13.

Fricker, H.A. & Scambos, T. 2009. Connected subglacial lake activity on lower Mercer and Whillans ice streams, West Antarctica, 2003–2008. *Journal of Glaciology*, **55**, 303–315.

Fricker, H.A., Scambos, T.A., Bindschadler, R.A. & Padman, L. 2007. An active subglacial water system in West Antarctica mapped from space. *Science*, **315**, 1544–1548.

Fricker, H.A., Powell, R., Priscu, J.C., Tulaczyk, S., Anandakrishnan, S., Christner, B., Holland, D., Horgan, H., Mikucki, J., Mitchell, A., Scherer, R. & Severinghaus, J. 2011. Siple Coast subglacial aquatic environments: the Whillans Ice Stream Subglacial Access Research Drilling (WISSARD) project. *In* Siegert, M.J., Kennicutt II, M.C., Bindschadler, R.A., *eds. Antarctic subglacial aquatic environments. American Geophysical Union Geophysical Monograph*, **192**, 199–219.

Gray, L., Joughin, I., Tulaczyk, S., Spikes, V.B., Bindschadler, R. & Jezek, K. 2005. Evidence for subglacial water transport in the West Antarctic Ice Sheet through three-dimensional satellite radar interferometry. *Geophysical Research Letters*, 10.1029/2004GL021387.

Horgan, H.J., Anandakrishnan, S., Jacobel, R.W., Christianson, K., Alley, R.B., Heeszel, D.S., Picotti, S. & Walter, J.I. 2012. Subglacial Lake Whillans: seismic observations of a shallow active reservoir beneath a West Antarctic ice stream. *Earth and Planetary Science Letters*, **331-332**, 201–209.

Karl, D.M. 1980. Cellular nucleotide measurements and applications in microbial ecology. *Microbiological Reviews*, **44**, 739–796.

Karl, D.M., Bird, D.F., Bjorkman, K., Houlihan, T., Shackelford, R. & Tupas, L. 1999. Microorganisms in the accreted ice of Lake Vostok, Antarctica. *Science*, **286**, 2144–2147.

Lanoil, B., Skidmore, M., Priscu, J.C., Han, S., Foo, W., Vogel, S.W., Tulaczyk, S. & Engelhardt, H. 2009. Bacteria beneath the West Antarctic Ice Sheet. *Environmental Microbiology*, **11**, 609–615.

Lisle, J.T. & Priscu, J.C. 2004. The occurrence of lysogenic bacteria and microbial aggregates in the lakes of the McMurdo Dry Valleys, Antarctica. *Microbial Ecology*, **47**, 427–439.

Lukin, V. & Bulat, S. 2011. Vostok Subglacial Lake: details of Russian plans/activities for drilling and sampling. *In* Siegert, M.J., Kennicutt II, M.C., Bindschadler, R.A., *eds. Antarctic subglacial aquatic environments. American Geophysical Union Geophysical Monograph*, **192**, 187–197.

NRC (National Research Council). 2007. *Exploration of Antarctic subglacial aquatic environments: environmental and scientific stewardship*. Washington, DC: National Academies Press, 166 pp.

Priscu, J.C. 2002. Commentary: subglacial lakes have changed our view of Antarctica. *Antarctic Science*, **14**, 291.

Priscu, J.C. & Christner, B. 2004. Earth's icy biosphere. *In* Bull, A.T., *ed. Microbial diversity and prospecting*. Washington, DC: ASM Press, 130–145.

Priscu, J.C., Powell, R.D. & Tulaczyk, S. 2010. Probing subglacial environments under the Whillans Ice Stream. *EOS Transactions*, **91**, 253–254.

Priscu, J.C., Christner, B.C., Foreman, C.M. & Royston-Bishop, G. 2007. Biological material in ice cores. *In* Elias, S.A., *ed. Encyclopedia of Quaternary sciences*. Vol. 2. Amsterdam: Elsevier, 1156–1166.

Priscu, J.C., Tulaczyk, S., Studinger, M., Kennicutt II, M.C., Christner, B.C. & Foreman, C.M. 2008. Antarctic subglacial water: origin, evolution and ecology. *In* Vincent, W. & Laybourn-Parry, J., *eds. Polar lakes and rivers*. Oxford: Oxford University Press, 119–135.

Priscu, J.C., Kennicutt II, M.C., Bell, R.E., Bulat, S.A., Ellis-Evans, C., Lukin, V.V., Petit, J-R., Powell, R.D., Siegert, M.J. & Tabacco, I. 2003. An international plan for Antarctic subglacial lake exploration. *Polar Geography*, **27**, 69–83.

Priscu, J.C., Kennicutt II, M.C., Bell, R.E., Bulat, S.A., Ellis-Evans, C., Lukin, V.V., Petit, J-R., Powell, R.D., Siegert, M.J. & Tabacco, I. 2005. Exploring subglacial Antarctic lake environments. *EOS Transactions*, **86**, 193–200.

Priscu, J.C., Adams, E.E., Lyons, W.B., Voytek, M.A., Mogk, D.W., Brown, R.L., McKay, C.P., Takacs, C.D., Welch, K.A., Wolf, C.F., Kirshtein, J.D. & Avci, R. 1999. Geomicrobiology of subglacial ice above Lake Vostok, Antarctica. *Science*, **286**, 2141–2144.

Rignot, E., Mouginot, J. & Scheuchl, B. 2011. Ice flow of the Antarctic Ice Sheet. *Science*, **333**, 1427–1430.

Roslev, P. & King, G.M. 1993. Application of a tetrazolium salt with a water-soluble formazan as an indicator of viability in respiring bacteria. *Applied and Environmental Microbiology*, **59**, 2891–2896.

Ross, N., Siegert, M.J., Rivera, A., Bentley, M., Blake, D., Capper, L., Clarke, R., Cockell, C., Corr, H., Harris, W., Hill, C., Hindmarsh, R., Hodgson, D., King, E., Lamb, H., Maher, B., Makinson, K., Mowlem, M., Parnell, J., Pearce, D., Priscu, J.C., Smith, A., Tait, A., Tranter, M., Wadham, J., Whalley, B. & Woodward, J. 2011. Subglacial Lake Ellsworth, West Antarctica: its history, recent field campaigns and plans for its exploration. *In* Siegert, M.J., Kennicutt II, M.C., Bindschadler, R.A., *eds. Antarctic subglacial aquatic environments. American Geophysical Union Geophysical Monograph*, **192**, 221–233.

Scambos, T., Haran, T., Fahnestock, M., Painter, T. & Bohlander, J. 2007. MODIS-based Mosaic of Antarctica (MOA) data sets: continent-wide surface morphology and snow grain size. *Remote Sensing of Environment*, **111**, 242–257.

Shabtaie, S., Whillans, I.M. & Bentley, C.R. 1987. The morphology of Ice Streams A, B, and C, West Antarctica, and their environs. *Journal of Geophysical Research*, **92**, 8865–8883.

Siegert, M.J., Carter, S., Tabacco, I., Popov, S. & Blankenship, D.D. 2005. A revised inventory of Antarctic subglacial lakes. *Antarctic Science*, **17**, 453–460.

Siegert, M.J., Clarke, R.J., Mowlem, M., Ross, N., Hill, C.S., Tait, A., Hodgson, D., Parnell, J., Tranter, M., Pearce, D., Bentley, M.J., Cockell, C., Tsaloglou, M.N., Smith, A., Woodward, J., Brito, M.P. & Waugh, E. 2012. Clean access, measurement, and sampling of Ellsworth Subglacial Lake: a method for exploring deep Antarctic subglacial lake environment. *Reviews in Geophysics*, 10.1029/2011RG000361.

Smith, B.E., Fricker, H.A., Joughin, I.R. & Tulaczyk, S. 2009. An inventory of active subglacial lakes in Antarctica detected by ICESat (2003–2008). *Journal of Glaciology*, **55**, 573–595.

Vanoni, V.A. 1975. *Sedimentation engineering.* ASCE Manual 54. Prepared by ASCE Task Committee for the preparation of the manual on sedimentation of the Sedimentation Committee of the Hydraulics Division. Reston, VA: American Society for Civil Engineering, 418 pp.

Wingham, D.J., Siegert, M.J., Shepherd, A. & Muir, A.S. 2006. Rapid discharge connects Antarctic subglacial lakes. *Nature*, **440**, 1033–1036.

CHAPTER FIVE

BIOGEOCHEMISTRY AND MICROBIAL DIVERSITY IN THE MARINE CAVITY BENEATH THE MCMURDO ICE SHELF, ANTARCTICA

Contribution of Authors and Co-Authors

Manuscript in Chapter 5

Author: Trista J. Vick-Majors

Contributions: Collected samples, oversaw sample collection, performed microbiological activity assays, performed microscopy, performed excitation-emission matrix spectroscopy, performed water mass analysis, performed particulate carbon and nitorogen measurements, assisted with dissolved nutrient analysis, analyzed data, prepared figures and tables, and wrote the manuscript.

Co-Author: Amanda M. Achberger

Contributions: Collected samples, extracted DNA and analyzed microbial community structure data, provided bar graph and diversity statistics, and assisted with manuscript preparation.

Co-Author: Pamela Santibáñez

Contributions: Conducted flow cytometry analyses, performed microscopy, analyzed flow cytometry data, and assisted with manuscript preparation.

Co-Author: John E. Dore

Contributions: Performed dissolved nutrients analyses and assisted with manuscript preparation.

Co-Author: Timothy Hodson

Contributions: Collected and analyzed current meter data, assisted with water mass analysis, commented on manuscript.

Co-Author: Alexander B. Michaud

Contributions: Collected samples, processed samples in the field, assisted with nutrients analysis, assisted with manuscript preparation.

Contribution of Authors and Co-Authors-Continued

Co-Author: Brent C. Christner

Contributions: Conceived the project, provided funding for DNA sequence sample collection and processing, oversaw DNA sequence sample collection and processing, commented on the manuscript.

Co-Author: Jill Mikucki

Contributions: Collected samples, collected CTD data, provided funding, commented on the manuscript.

Co-Author: Mark L. Skidmore

Contributions: Collected samples, provided geochemical data, oversaw analysis of DOC samples, assisted with manuscript preparation.

Co-Author: Ross Powell

Contributions: Oversaw and carried out deployment of current meter, provided current meter data, provided funding, commented on manuscript.

Co-Author: W. Peyton Adkins

Contributions: Collected and processed samples in the field, assisted with microscopy, commented on manuscript.

Co-Author: Carlo Barbante

Contributions: Provided geochemical data and commented on manuscript.

Co-Author: Andrew Mitchell

Contributions: Provided geochemical data and commented on manuscript.

Co-Author: Reed Scherer

Contributions: Collected sediment samples, performed sediment diatom analyses and assisted with manuscript preparation.

Co-Author: John C. Priscu

Contributions: Conceived the study, provided funding, assisted with manuscript preparation.

Manuscript Information Page

Trista J. Vick-Majors, Amanda Achberger, Pamela Santibáñez, John E. Dore, Timothy Hodson, Alexander B. Michaud, Brent C. Christner, Jill Mikucki, Mark L. Skidmore, Ross Powell, W. Peyton Adkins, Carlo Barbante, Andrew Mitchell, Reed Scherer, John C. Priscu
Limnology and Oceanography
Status of Manuscript:
____ Prepared for submission to a peer-reviewed journal
____ Officially submitted to a peer-review journal
_X_ Accepted by a peer-reviewed journal
___ Published in a peer-reviewed journal

John Wiley & Sons Ltd.
January, 2016
Reused with permission:
Permission is granted for you to use the material requested for your thesis/dissertation subject to the usual acknowledgements (author, title of material, title of book/journal, ourselves as publisher) and on the understanding that you will reapply for permission if you wish to distribute or publish your thesis/dissertation commercially. You must also duplicate the copyright notice that appears in the Wiley publication in your use of the Material; this can be found on the copyright page if the material is a book or within the article if it is a journal.

Permission is granted solely for use in conjunction with the thesis, and the material may not be posted online separately.

Any third party material is expressly excluded from this permission. If any of the material you wish to use appears within our work with credit to another source, authorisation from that source must be obtained.

BIOGEOCHEMISTRY AND MICROBIAL DIVERSITY IN THE MARINE CAVITY BENEATH THE MCMURDO ICE SHELF, ANTARCTICA

The following work is in press at Limnology and Oceanography.

Trista J. Vick-Majors[1], Amanda Achberger[2], Pamela Santibáñez [1], John E. Dore[1], Timothy Hodson[3], Alexander B. Michaud[1], Brent C. Christner[2], Jill Mikucki[4], Mark L. Skidmore[5], Ross Powell[3], W. Peyton Adkins[2], Carlo Barbante[6], Andrew Mitchell[7], Reed Scherer[3], John C. Priscu[1*]

[1]Department of Land Resources and Environmental Sciences, Montana State University, Bozeman, MT, USA

[2]Department of Biological Sciences, Louisiana State University, Baton Rouge, LA, USA

[3]Department of Geological and Environmental Sciences, Northern Illinois University, DeKalb, IL, USA

[4]Department of Biology, Middlebury College, Middlebury, VT, USA

[5]Department of Earth Sciences, Montana State University, Bozeman, MT, USA

[6]Institute for the Dynamics of Environmental Processes – CNR, Venice, and Department of Environmental Sciences, University of Venice, Venice, Italy

[7]Department of Geography and Earth Sciences, Aberystwyth University, Ceredigion, UK

[*]Corresponding author

Abstract

Ice shelves surround ~ 75% of Antarctica's coastline and are highly sensitive to climate change; several have recently collapsed and others are predicted to in the near future. Marine waters beneath ice shelves harbor active ecosystems, while adjacent seas can be important areas of bottom water formation. Despite their oceanographic

significance, logistical constraints have resulted in few opportunities to directly sample sub-ice shelf cavities. Here, we present the first data on microbial diversity and biogeochemistry beneath the McMurdo Ice Shelf (MIS) near Ross Island, Antarctica. Physicochemical profiles obtained via a 56 m deep borehole through the MIS revealed three vertically layered water masses (Antarctic Surface Water [AASW], Ice Shelf Water [ISW], and modified High Salinity Shelf Water [mHSSW]). Metabolically active, moderately diverse (Shannon diversity from 2.06 to 5.74) microbial communities were detected in the AASW and mHSSW. Heterotrophic bacterial production and dissolved organic matter concentrations were higher (12% to 37% and 24%, respectively) in mHSSW relative to AASW. Chemoautotrophic production was 5.3 and 6.0 nmol C L^{-1} d^{-1} in the AASW and mHSSW, respectively. Phytoplankton cells were more abundant and larger in the mHSSW sample relative to the AASW, which indicates sinking of phytoplankton produced in surface waters and, together with southerly flowing currents (0.09 to 0.16 m s^{-1}), horizontal advection of phytoplankton from McMurdo Sound. Advected phytoplankton carbon together with in situ chemoautotrophic production provide important sources of organic matter and other reduced compounds to support ecosystem processes in the dark waters in the ice shelf cavity.

Introduction

Ice shelves, which form where glaciers leave the land and float on the ocean surface, cover more than 1.5 x10^6 km^2 of coastal ocean in Antarctica (Rignot et al. 2013). Yet, only a few studies have directly measured physical or biological processes beneath

Antarctic ice shelves, in the sub-ice shelf marine waters (e.g. Azam et al. 1979; Riddle et al. 2007; Robinson et al. 2010; Carr et al. 2013). The Ross Ice Shelf (RIS) is the most extensive ice shelf on the planet, accounting for about one-third of the surface area of all Antarctic ice shelves (Fox and Cooper 1994; Depoorter et al. 2013). The RIS covers about half of the Ross Sea, an important area of Antarctic Bottom Water formation, which is vital to the global-scale thermohaline circulation (Jacobs et al. 1970; Budillon et al. 2011). The McMurdo Ice Shelf (MIS) comprises the northwestern portion of the RIS, and although they form a unified sub-ice shelf cavity and are often referred to as a single entity, the MIS originates from different source glaciers than the main body of the RIS (Robinson et al. 2010). The RIS front is typically >300 m thick and presents a significant inflow barrier to the sub-ice cavity, whereas the thinner (~20-100 m) MIS front provides an important hydrologic conduit linking the waters of the Ross Sea to the sub-RIS cavity (Robinson et al. 2010). Waters beneath the RIS are also influenced by subglacial water from continental Antarctica, making the sub-ice shelf waters an important intermediate between the open Ross Sea and subglacial outflow from the Antarctic continent (Horgan et al. 2013).

The Ross Sea is one of the most biologically productive and best-studied marine regions in Antarctica (Smith Jr. et al. 2012). Multiple studies have documented the onset of rapid phytoplankton growth during spring concurrent with the loss of winter sea-ice cover (Arrigo and McClain 1994; Smith Jr. and Gordon 1997; Arrigo and van Dijken 2004). The annual phytoplankton bloom peaks in surface waters between mid-December and early-January, with chlorophyll *a* (chl *a*) concentrations in excess of 10 μg L^{-1} (Smith

Jr. and Gordon 1997). The bloom is dominated initially by *Phaeocystis antarctica* (Smith Jr. and Gordon 1997) followed by a mixed diatom assemblage (Arrigo 1999). The summer phytoplankton blooms are sustained by high nutrient levels and shallow mixed layers initiated by melting sea-ice (Smith and Comiso 2008). Decomposition of phytoplankton biomass in this region is associated with one of the largest blooms of bacterioplankton recorded, reaching biomass levels of >10 mmol C m^{-2} (Ducklow et al. 2001). This productive sea comprises the source of the sub-MIS waters, via McMurdo Sound (Robinson et al. 2010).

In contrast to the relatively well-studied Ross Sea, sub ice-shelf cavities (marine waters beneath ice-shelves) have received far less attention, largely due to logistical constraints associated with accessing the ocean beneath thick, floating ice. The first oceanographic data from beneath the MIS was collected in 2003 and revealed net transport from McMurdo Sound to the MIS cavity, a diurnal tidal cycle, and evidence for tidally driven melting near the ice shelf front (Robinson et al. 2010). The Ross Ice Shelf Project (in 1977; Clough and Hansen 1979) was the first to make oceanographic measurements (Gilmour 1979; Jacobs et al. 1979; Williams and Robinson 1979) and detect sub-ice shelf biological communities (Azam et al. 1979; Lipps et al. 1979) beneath the RIS (420 m ice thickness) at Station J9, 450 km from the edge of the RIS. Microorganisms in the water column and seafloor sediments at Station J9 metabolized added organic substrates (Azam et al. 1979) and dark carbon dioxide (CO_2) fixation (1.5 g C m^{-2} y^{-1}) was attributed to the activity of nitrifying microorganisms (Horrigan 1981). Underwater camera observations and traps yielded fish and crustaceans (Lipps et al.

1979), suggesting the existence of an active food web under the ice shelf, although the benthic community consisted mainly of scavengers. More recently, samples from beneath the RIS and MIS near Ross Island led to the discovery of a new species of sea anemone that embeds in and inhabits the base of the ice shelf (Daly et al. 2013), and provided information on the microbial community composition of marine sediments below this region of the ice shelf (Carr et al. 2013). Underwater camera observations showed that a diverse benthic community, unlike that detected at Station J9 beneath the RIS, exists beneath the Amery Ice Shelf (Post et al. 2014). These studies suggest that sub-ice shelf biota are involved in Southern Ocean biogeochemical processes, but that we have a poor understanding of both the diversity of life and habitats beneath ice shelves.

As Antarctic ice shelves are increasingly threatened with collapse induced by changing climate (Joughin et al. 2014, Wouters et al. 2015), the need to develop an understanding of sub-ice shelf biogeochemical processes becomes progressively more important. Studies following the breakup of the Larsen A and B Ice Shelves documented changes in biological CO_2 pumping mediated by water column primary production (Bertolin and Schloss 2009) and disruption and succession of benthic communities beneath the newly open water (Domack et al. 2005; Fillinger et al., 2013). Still, a paucity of baseline data limits the context within which the ramifications of ice shelf collapse for biogeochemical processes in the Southern Ocean can be interpreted. Here, we integrate physical and chemical data with the first microbiological data obtained from the sub-MIS water column. Our results identify biogeochemical linkages between the Ross Sea via McMurdo Sound and the dark sub-ice environment beneath the MIS and RIS.

Methods

Site Description

The Ross Ice Shelf stretches ~850 km from the Antarctic coast to the open ocean, with water column depths ranging from ~50 m to ~1000 m (Greischar and Bentley 1980). The MIS comprises the thinnest area of the ice shelf, with ice thicknesses generally <100 m thick at MIS compared to up to >800 m thick near the southern extent of the RIS (most of the RIS is ~200-250 m thick; Griggs and Bamber 2011). A coastal current flows along the front of the RIS until it reaches Ross Island, where some of the water turns north along the Victoria Land coast, and some flows south, through the eastern part of McMurdo Sound and beneath the MIS (Barry, 1988).

Our drill site was located on the MIS (77.8902 S, 167.0083 E; Figure 1) near Ross Island, approximately 8 km from the edge of the transition from ice shelf to the seasonal and multi-year fast sea-ice of McMurdo Sound and ~2 km from the ANDRILL HWD-1 site described by Robinson et al. (2010) and Robinson (2004), which we use for comparison in this paper. At the time of sampling, the transition from sea-ice to the open water of McMurdo Sound was approximately 48 km to the north of the sampling site. The 56 m deep borehole (~60 cm diameter) that penetrated into the sub-ice shelf cavity was created with a clean access hot water drill (Blythe et al. 2014, Burnett et al. 2014, and Rack et al. 2014) on 18 December 2012. The sub-ice shelf cavity is defined as the ocean beneath the ice-shelf. The water column depth below the borehole was 872 m from the ice-water interface (928 m from the ice surface) to the seafloor. All depths are reported from the bottom of the ice shelf (i.e. the ice-water interface). MODIS satellite

imagery from around the time of sampling (not shown; data available from the U.S. Geological Survey EarthExplorer) indicated that we did not collect samples during the Ross Sea phytoplankton bloom.

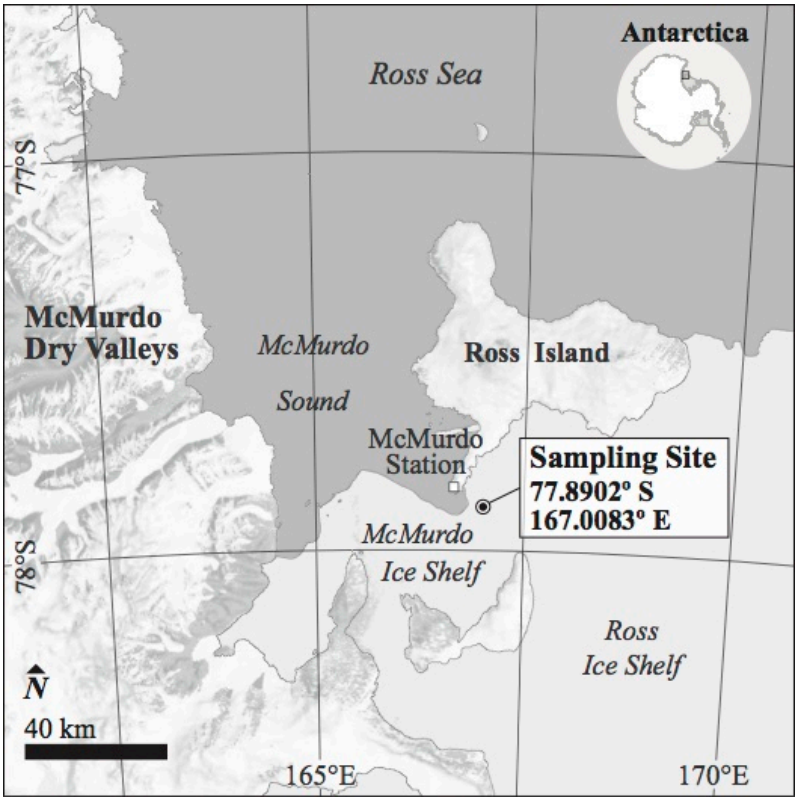

Figure 1. Sampling site location. Map by Bradley Herried, Polar Geospatial Center.

Physical and Chemical Parameters

Depth profiles of temperature and conductivity were measured with a SBE 19plusV2 SeaCAT Profiler CTD (Sea-bird Electronics, Inc.) sonde. Potential temperature relative to the surface was derived according to UNESCO equations (IOC, SCOR and IAPSO, 2010). Water masses observed in the study area were characterized according to Stover (2006) and Jacobs and Fairbanks (1985) (see also Celussi et al. 2010) as: (i)

Antarctic Surface Water (AASW) had potential temperature above the freezing point with relatively low salinity (34.2 and 34.4); (ii) Ice Shelf Water (ISW) had potential temperature below the surface freezing point and salinities between 34.5 and 34.7, and (iii) modified High Salinity Shelf Water (mHSSW) had potential temperature near the surface freezing point with salinities between 34.6 and 34.8. These water masses were graphically identified using Ocean Data View 4.5.6 (Schlitzer 2013), as shown in Figure S1. Current velocity and direction were obtained with a Contros Oceanline HS-2X series electromagnetic current meter and the appearance of the surface sediments was documented with an attached camera.

Discrete water samples were collected through the borehole with a 10 L General Oceanics Niskin bottle (AASW [30 m] sample) and a 5 L Go-Flo bottle (mHSSW [850 m] sample). Both sampling bottles were disinfected with 3% hydrogen peroxide before deployment. The water was decanted immediately through acid leached silicone tubing into appropriate vessels. Samples for dissolved oxygen and dissolved inorganic carbon (DIC) were stabilized on site with a stock solution of sodium azide (1% w/v), potassium iodide (10% w/v), sodium hydroxide (32% w/v) (dissolved oxygen) or chloroform (DIC). All water samples were stored at ~ 4 ^{o}C in the dark until return to McMurdo Station (MCM) for processing (~ 4 h).

Shallow sediment samples were collected from the top surface of a geothermal probe that penetrated the surface sediments in an operational test, and the resulting data are reported qualitatively. Diatom frustules in fine-grained sediments were processed using standard micropaleontological techniques (e.g. Scherer 1991), using 15% H_2O_2 and

mounted as strewn slides in Norland optical adhesive for light microscopy, and the results presented are qualitative.

Samples for DOC and three dimensional spectrofluorometric characterization of organic matter (excitation-emission matrix spectroscopy; EEMS) were decanted into 1% hydrochloric acid and deionized water rinsed fluorinated high density polyethylene (HDPE) carboys (Thermo Scientific, Nalgene, Waltham, MA) and filtered through acid-leached and combusted (>4 h at 450 °C) 25 mm glass fiber filters (GF/F, effective retention size 0.7 μm). The filtrate was collected in acid washed and combusted (>4 h at 450 °C) 125 ml amber borosilicate glass bottles fitted with polytetrafluoroethylene (PTFE) lined caps and stored at 4 °C until analysis. DOC concentrations were determined using a Shimadzu TOC-V Series TOC analyzer following acidification with hydrochloric acid to pH ≤ 2 to remove inorganic carbon as CO_2.

EEMS were determined with a Horiba Jobin Yvon Fluoromax-4 Spectrophotometer (Horiba, Ltd., Japan) equipped with a Xe light source using a 1 cm path length quartz cuvette. Excitation data were measured every 10 nm from 240 nm to 450 nm, and emission data every 2 nm from 300 nm to 560 nm. Measurements were corrected for background (0.2 μm filtered Milli-Q water) and Raman scattering, and for inner-filter effects using absorbance spectra collected between 190 nm and 1100 nm with a Genesys 10 Series Spectrophotometer (1 cm path length, Thermo Scientific) as described by McKnight et al. (2001). The following indices were derived to reveal the character of the DOC: (i) Fluorescence Index (the ratio of the emission at 470 nm to the emission at 520 nm at an excitation of 370 nm; McKnight et al. 2001, Cory and

McKnight 2005), (ii) Freshness Index (the emission at 380 nm divided by the maximum emission between 420 and 435 nm at an excitation 370 nm; Huguet et al. 2009), and (iii) Humification Index (the area of the peak under emission 435 to 480 nm divided by the peak area under emission 330 to 345 nm; Zsolnay et al. 1999). To compare fluorescence intensities in the two samples, standardized maximum fluorescence was calculated as follows: (value-min)/(max-min), where "value" is the maximum fluorescence in the sample, and "max" and "min" are the maximum and minimum fluorescence for the two samples combined.

Suspended matter collected on the filters from DOC and EEMS filtration was stored frozen (-20°C) in the dark until acid-fuming (to remove inorganic C) and analysis of particulate organic C (PC) and nitrogen (PN) on a CE Instruments Flash EA 112 (ThermoQuest, San Jose, CA). Dissolved oxygen and DIC were measured in MCM using the azide modification of the mini-Winkler titration and infrared gas analysis of acid sparged samples, respectively, according to the limnological methods used by the McMurdo LTER (http://www.mcmlter.org/data_methods2.htm).

Samples for dissolved inorganic nutrients (soluble reactive phosphorus [SRP], nitrate + nitrite [N+N], and ammonium [NH_4^+] were filtered through combusted GF/F filters into 1% hydrochloric acid leached and deionized water rinsed HDPE bottles and frozen at -20°C until analysis. The concentrations of these compounds were determined colorimetrically according to Strickland and Parsons (1968) and Solórzano (1969).

Biological Parameters

Chlorophyll *a* (chl *a*) concentrations were determined on 200 mL samples filtered onto 25 mm diameter GF/F filters; the filters were stored at -20°C in the dark immediately upon return to MCM. The samples were extracted in 90% acetone (v:v; acetone:water) for ~24 h in the dark at 4 ^{o}C and analyzed with a calibrated fluorometer (Turner 10-AU-10) as described by Welschmeyer (1994).

Dark carbon fixation (chemoautotrophy) was determined on quadruplicate live and trichloroacetic acid [TCA; ~ 5% final concentration] killed 40 mL samples (Christner et al. 2014). The samples were incubated in the dark in glass bottles filled to the top (no head-space) and capped with PTFE lined caps. Each sample was amended with ^{14}C-bicarbonate (stock solution = 114.41 μCi mL^{-1}) to a final radioactive concentration of 10 μCi mL^{-1} and incubated in the dark at 4 °C for 94 h. Long incubation times and high specific activity substrates were used in anticipation of low rates of biological activity in the sub-ice shelf cavity, and were similar to those used in other studies aimed at detecting chemoautotrophic carbon fixation (48 h, Horrigan 1981; 168 h, Yakimov et al. 2011). Incubations were terminated by the addition of ice-cold 100% TCA (2.5% final concentration) and size fractionated onto GF/F filters (to capture larger, aggregated and filamentous cells) and 0.2 μm polycarbonate filters (to capture smaller or non-aggregated cells). Filters were placed in 20 mL scintillation vials, acidified with 1.5 ml of 3N HCl and dried at 60 °C. Radioactivity incorporated into cellular carbon retained on the filters was counted on a calibrated scintillation counter after addition of 10 mL Cytoscint ES scintillation cocktail (MP Biomedicals).

Heterotrophic bacterial (where "bacterial" can include bacteria and archaea throughout the text) production was determined using [^{3}H]methyl-thymidine incorporation into DNA (Fuhrman and Azam 1982) and [^{3}H]L-leucine incorporation into protein (Kirchman et al. 1985). Samples (1.5 mL; 5 live and 5 TCA killed) were incubated with 20 nM radio-labeled thymidine (specific activity 20 Ci mmol^{-1}) or leucine (specific activity 84 Ci mmol^{-1}) at 4 °C in the dark for ~20 h. Incubations were terminated by the addition of 100% cold TCA (5% final). Following centrifugation, a series of extractions with cold (~4°C) 5% TCA and cold (~4°C) 80% ethanol were performed and the residual pellet was dried overnight at room temperature. One mL of Cytoscint ES scintillation cocktail was added to each vial and the samples were counted on a calibrated scintillation counter. Resulting thymidine and leucine incorporation rates (nM TdR d^{-1}or nM Leu d^{-1}, respectively) at the incubation temperature (4^o C) were converted to rates at *in situ* temperatures (-1.7 to -1.9^o C) using energy of activation of 12,600 kcal mol^{-1} determined from Antarctic lakes (Takacs and Priscu 1998). Temperature corrected rates were converted to heterotrophic bacterial production (BP TdR and BP Leu) using published conversion factors of 2.0x10^{18} cells mol^{-1} thymidine (Bell 1993) and 1.42x10^{17} cells mol^{-1} leucine (Chin-Leo and Kirchman 1988) and a cellular carbon content of 11 fg C cell^{-1} (Kepner et al. 1998). Cell specific activity (mg C cell^{-1} d^{-1}) was determined by dividing heterotrophic bacterial production by bacterioplankton cell abundance (see below) for each sample.

Heterotrophic bacterial respiration was measured in the 850 m sample by adding 60 mL of sample water to an autoclaved amber HDPE bottle (Nalgene) followed by the

addition of uniformly labeled ^{14}C-L-leucine (specific activity >300 mCi mmol^{-1}; final leucine concentration 60 nM; final activity 0.0180 μCi mL^{-1}) (del Giorgio et al. 2011). Five-milliliter aliquots of the radiolabeled sample were added to autoclaved 25 mL glass side arm flasks (6 live and 6 TCA killed controls; 250 μL of cold 100% TCA). The top of the flask was sealed with a butyl rubber septum holding a small basket containing a folded GF/C filter suspended above the aqueous phase (Christner et al. 2006); the sidearm was sealed with a butyl rubber septum. Following incubation in the dark for 39 h at 2-4 °C, the reactions in live incubations were terminated by injecting cold 100% TCA (final concentration 5%) into the sample through the sidearm which lowered the pH to ≤ 2. β-phenylethylamine (100 μL; Sigma, catalog number P2641) was added to the GF/C filter through the septum with a needle and syringe to trap respired CO_2. Killed samples were maintained at 4 ^{o}C for five days with occasional gentle swirling to liberate and trap all respired CO_2 from the aqueous phase. Cellular ^{14}C incorporation was determined on the liquid fraction following filtration onto 0.2 μm polycarbonate filters. The GF/C and polycarbonate filters were placed in 20 mL scintillation vials followed by the addition of 10 mL of Cytoscint-ES and the ^{14}C activity was determined using a calibrated scintillation counter. Bacterial growth efficiency was calculated using the leucine respiration data (described above) as ((BP Leu)/(BP Leu + Leu respiration)) x100. Leu:TdR ratios are based on molar incorporation rates.

Samples for phytoplankton (autofluorescent cells) and bacterioplankton (non-autofluorescent bacteria and archaea) enumeration were preserved with sodium borate buffered formalin (5% v/v) and stored at 4 °C in the dark. Samples were filtered through

30 μm mesh using a sterile BD Falcon 12 x 75 mm tube with cell strainer cap to eliminate large particles. Cell density was determined with a PhytoCyt flow cytometer (Turner Designs) at a flow rate of 50μL min^{-1} and core size of 12 μm. Unstained seawater samples were used for the detection of phytoplankton. Bacterioplankton were enumerated using seawater samples stained with SYBR® Green I (SGI; Molecular Probes; supplied at 10,000X) at a final concentration of 1X original (Marie et al. 2001).

Bacterioplankton cells were identified as a distinct population on a density plot of SGI emission-height (excitation 488 nm, emission 515-545 nm) versus forward light scatter-area (FSC-A: 0˚±15˚). High nucleic acid (HNA) and low nucleic acid (LNA) bacterioplankton were identified according to the intensity of their SGI emission (Gasol and del Giorgio 2000; Lebaron et al. 2001; Bouvier et al. 2007). Because FSC-A and SGI emission from small phytoplankton cells may overlap with those of stained bacterioplankton, we also examined small phytoplankton (<2 μm chl-*a* autofluorescing cells) in stained samples by plotting FSC-A vs. orange fluorescence (excitation 488 nm, emission 565-605 nm), blue laser-dependent red fluorescence (excitation 488 nm, emission >670 nm; chl *a*) and red fluorescence (excitation 640 nm; emission 650-700). Small phytoplankton cells determined using these criteria were subtracted from the total counts in this region to obtain bacterioplankton cell counts. Bacterioplankton cell counts were verified on selected samples by epifluorescence microscopy of SYBR® Gold-stained cells using the protocol of Lisle and Priscu (2004).

Larger phytoplankton cells (>2 μm) were enumerated on a density plot of FSC-A versus chl *a* using 2 mL of unstained sample. The larger phytoplankton population was

divided into subpopulations (*a*, *b*, and *c*) based on density plots of FSC versus chl *a*. The presence of each distinct population was verified by measuring the mean emission ratios of red fluorescence/chl *a* and orange fluorescence/red fluorescence. To determine cell sizes, the larger phytoplankton were also examined with an epifluorescence microscope (Nikon Eclipse 80i) equipped with a Retiga-2000R Fast 1394 camera under blue excitation cube filter (excitation 450-490 nm; emission >515 nm) following the method of Hillebrand et al. (1999). Samples were prepared for microscopy by filtering 1.6 ml (30 m sample) and 2.2 ml (850 m sample) through 0.2 μm 13 mm hydrophilic PTFE membrane filters (Millipore, catalog number JHWP013000) and mounting the filters on glass slides with 1:1 (v:v) glycerol/water. Sixty photographs were taken of random fields at 1000x magnification and the diameter of ~200 cells were measured in each sample (standard error <2% of the mean) using ImageJ software (Schneider et al. 2012).

Gating strategies for the different classes of planktonic cells are available in the MIFlowCyt-Compliant Items (Lee et al. 2008; supplemental information) and archived with the data at http://www.flowrepository.org under the ID number FR-FCM-ZZK3.

A discrete water sample for nucleic acid extraction was collected in situ at 850 m with a Large Volume Water Transfer System (WTS-LV; McLane Research Laboratories, East Falmouth, MA). This system was fitted with a stacked 143 mm diameter filter housing that allowed the sample to be size fractionated into 10μm, 3 μm, and 0.2 μm classes (Supor Membrane filters were used; Pall Inc.). This system allowed us to concentrate 295 L of seawater on 142 mm filters during a four hour in situ deployment. An additional discrete water sample (300 mL) from 30 m was obtained for nucleic acid

extraction from a 10 L Niskin bottle sample that was filtered through a 47 mm 0.2 μm Supor membrane filter (Pall Inc.). Filters from the WTS-LV were preserved as described previously (Christner et al. 2014) while the entire 47 mm filter from the 30 m sample was placed in a 7 mL cryovial and preserved with 7 mL of a solution of 40 mM EDTA pH 8.0, 50 mM Tris pH 8.3, and 0.73 M Sucrose to prevent cell lysis during during storage.

Nucleic acids were extracted from the 10 μm, 3 μm, and 0.2 μm filters from 850 m and the 0.2 μm filter from 30 m using a MO BIO PowerWater DNA Isolation Kit according to the manufactures instructions. The V4 hypervariable region of the small subunit (SSU) rRNA gene was amplified using the primers 515F and 806R (Caporaso et al. 2012) and sequenced on an Illumina MiSeq as described by Chirstner et al. (2014). Sequence reads were assembled and quality filtered using the Mothur (v1.33.2; Schloss et al. 2009) phylogenetic pipeline following the recommended MiSeq standard operating procedure. Sequences were clustered into operational taxonomic units (OTUs; cluster.split command) based on a pairwise distance matrix (dist,seq) calculated using default settings. OTUs were defined based on 97% sequence similarity cutoff. Preliminary classification of resulting SSU rRNA gene sequences was accomplished using the SILVA database as implemented within the SILVA Incremental Aligner (SINA). Poorly classified sequences were further examined using NCBI Blastn. Statistics were calculated using Mothur (v1.33.2; Schloss et al. 2009) according to Chao (1984), Good (1953) and Magurran (1988). Estimates of diversity and richness include singletons; singletons were removed from other analyses. SSU sequences obtained from chloroplasts were removed from the analyses. Sequences were uploaded to SRA under

accession number PRJNA278982. We note that recent efforts have shown that the primers used in our study underestimate the abundance and diversity of the ubiquitous SAR11 clade of bacteria. A comprehensive discussion of the primers can be found in Appril et al. (2015).

Results

Water Column Structure

The upper ~95 m of the water column (relative to the bottom of the ice shelf) was characterized by relatively warm, less saline water (-1.70 ºC to -1.89 ºC, Salinity 34.45 to 34.61) (Figure 2A). A colder layer (-1.90 ºC to -1.93 ºC) of intermediate salinity (34.60 to 34.70) was present from ~95 m to 315 m.

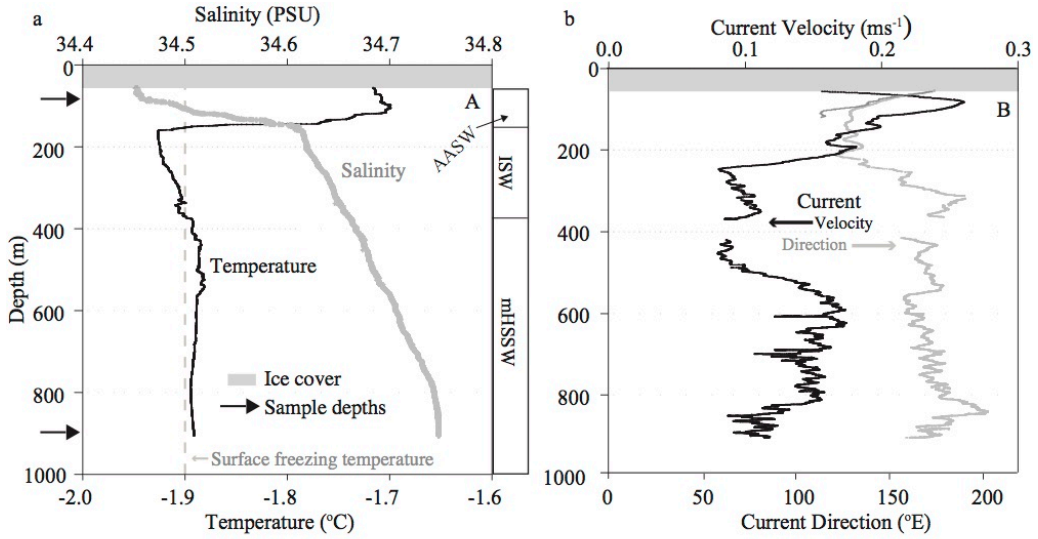

Figure 2. Profiles of salinity (practical salinity units; PSU) and temperature (A), current velocity and direction relative to true north (B). Sidebar in panel (A) designates three water layers: Antarctic Surface Water (AASW), Ice Shelf Water (ISW), and modified High Salinity Shelf Water (mHSSW).

Water below ~315 m had temperatures ranging from -1.88 ^{o}C to -1.90 ^{o}C and was relatively higher in salinity (34.66 to 34.75). These water masses were similar to those described previously in this area (Jacobs and Fairbanks 1985; Stover 2006; Celussi et al. 2010): AASW, ISW and mHSSW (Figure S1). Current flow was generally to the south-southeast with true headings (declination corrected) of 140^{o}, 161^{o} and 162^{o} for the AASW, ISW and mHSSW layers, respectively (Figure 2B). Current velocities for these respective layers averaged 0.21, 0.11 and 0.14 m s^{-1}. Current velocity in the mHSSW layer showed a clear demarcation at 500 m with average velocity in the upper part of this water layer averaging 0.09 m s^{-1} while that below 500 m averaged 0.14 m s^{-1}.

Inorganic Chemistry

Concentrations of NH_4^+, N+N, and SRP were 40%, 9% and 7%, respectively, higher in the AASW (30 m sample) relative to the mHSSW (850 m sample). Dissolved oxygen concentrations were 330 μmol L^{-1} and 370 μmol L^{-1}, representing 92% and 97% of air saturation, respectively (Table 1). The concentration of DIC was 2.2 mmol L^{-1} in both samples. The molar ratio of dissolved inorganic N (N+N + NH_4^+) to SRP was 16.1 in the AASW and 15.7 mHSSW water layers.

Sample	*DIC* mmol L^{-1}	*NH_4^+* μmol L^{-1}	*N+N* μmol L^{-1}	*SRP* μmol L^{-1}	*DO* μmol L^{-1}
AASW	2.2	0.7	25.1	1.6	333
mHSSW	2.2	0.5	23.0	1.5	367

Table 1. Water column inorganic chemistry from the AASW (30 m) and mHSSW (850 m) water masses sampled. DIC=dissolved inorganic carbon; SRP=soluble reactive phosphorus; DO=dissolved oxygen N+N=nitrate+nitrite.

Microbiological Characteristics

Bacterioplankton cell densities were 1.2 x 10^8 cells L^{-1} in the AASW and 1.1 x 10^8 cells L^{-1} in the mHSSW water layers (Table 2), and similar counts were determined via epifluorescent microscope (data not shown). High-nucleic acid and low-nucleic acid (HNA and LNA) bacterioplankton cells comprised ~35% and ~64% of total bacterioplankton cells in the AASW and mHSSW, respectively.

Sample	*Bacterio-plankton ($x10^8$)*	*LNA ($x10^7$)*	*HNA ($x10^7$)*	*Phyto < 2 um ($x10^6$)*	*Phyto >2 um ($x10^6$)*	*Phyto a ($x10^6$)*	*Phyto b ($x10^6$)*	*Phyto c ($x10^6$)*	*Total Phyto ($x10^6$)*
AASW	1.2	7.5	4.1	1.5	4.5	0.92	2.5	0.59	6.0
mHSSW	1.1	7.2	3.9	0.0010	6.7	0.41	2.9	2.7	6.7

Table 2. Bacterioplankton and phytoplankton cell counts (cells L^{-1}). Counts determined by flow cytometry for samples collected in the AASW (30 m sample) and mHSSW (850 m sample). Bacterioplankton cell counts are the sum of low nucleic acid (LNA) and high nucleic acid (HNA) cells. Phytoplankton include autofluorescent cells of <2μm and >2μm diameter. Mean intensity is fluorescence intensity (relative units) per cell excited with the blue laser and read at emission of >670 nm (chl *a*). Phytoplankton >2 um were divided into three populations: Phyto a, Phyto b, and Phyto c based on size (FSC-A). Total phytoplankton are the sum of all autofluorescing organisms.

Small (<2 μm) phytoplankton were more abundant in the surface water layer than the deep layer (1.5 x 10^6 cells L^{-1} in AASW, 1.0 x 10^4 cells L^{-1} in mHSSW), while the densities of larger (>2 μm) phytoplankton were 33% higher at depth (Table 2). Microscopic enumeration showed that 83% to 85% of phytoplankton cells in both samples were *Phaeocystis antarctica*; the remainder consisted of diatoms. Total phytoplankton (large plus small) were 10% higher in the mHSSW relative to densities in the AASW.

Large phytoplankton populations *a*, *b*, and *c* had distinctly different FSC-A intensities, where greater intensity is related to greater cell size. The mean FSC-A per cell in population *b* was approximately twice that of population *a*. The mean FSC-A per cell for population *c* was approximately twice that of *b* (Figure 3). The AASW water sample was dominated by population *b* (56% of total phytoplankton), while the mHSSW was dominated by populations *b* and *c* (43% and 40%, respectively; Table 2, Figure 3).

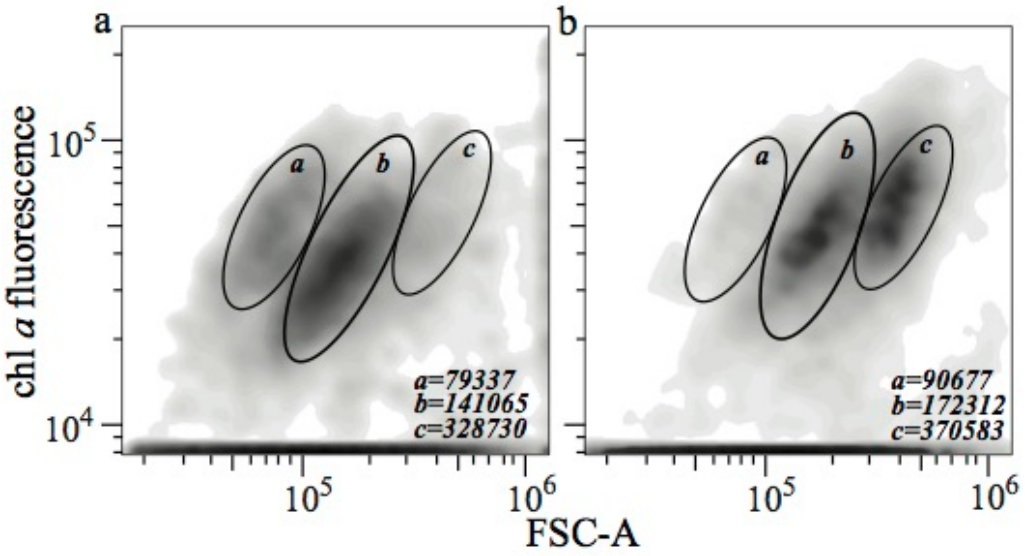

Figure 3. Density plots of chl *a* fluorescence (relative intensity units) versus forward scatter-area (FSC-A; relative intensity units) in the AASW water (30 m) (A) and mHSSW water (850 m) (B). Both samples show three distinct populations (*a*, *b*, and *c*) based on differences in FSC-A mean emission intensity for each population. Mean emission intensity for each group is given in the lower right corner of each plot.

The increase in population *c* relative abundance indicates an increase in cell size (FSC-A) at depth. Microscopic examination of the AASW and mHSSW >2 μm phytoplankton showed that the between water mass size difference was small (mean =3.27 and 3.44 μm for AASW and mHSSW, respectively) but significant (t = -4.06, n =

410, P<0.001), supporting the increase in size indicated by the shift towards population *c* dominated phytoplankton at depth. The mean emission ratios of red fluorescence/chl *a* fluorescence and orange fluorescence/chl *a* fluorescence remained constant within populations indicating a similar phytopigment composition was present at each depth and only the phytoplankton abundances and sizes changed.

Rates of both Leu and TdR incorporation were higher in the deep mHSSW waters but the difference was proportionally greater for TdR, leading to a lower Leu:TdR molar ratio in the deep waters (14 in the AASW, 9 in the mHSSW; Table 3). In terms of bacterial carbon production, BP-TdR and BP-Leu ranged from 34.5 nmol C L^{-1} d^{-1} (AASW Leu) to 63.6 nmol C L^{-1} d^{-1} (mHSSW TdR). Cell specific activity was also higher at depth (3.5 x 10^{-12} mg C $cell^{-1}$ d^{-1} (Leu) and 4.0 x 10^{-12} mg C $cell^{-1}$ d^{-1} (TdR) in the AASW versus 4.8 x 10^{-12} mg C $cell^{-1}$ d^{-1} (Leu) and 6.9 x 10^{-12} mg C $cell^{-1}$ d^{-1} (TdR) in the mHSSW. Increased activity at depth was also associated with relatively high bacterial growth efficiency (70%). Dark ^{14}C-bicarbonate incorporation ranged from 1.6 nmol C L^{-1} d^{-1} (AASW >3 μm size fraction) to 3.1 nmol C L^{-1} d^{-1} (mHSSW 0.2 – 3μm size fraction) and was higher in the 0.2 – 3 μm than the >3 μm size fraction (12% greater in AASW and 6% greater in mHSSW). The summed size fractionated dark ^{14}C-bicarbonate incorporation was greater in the mHSSW (11% difference) and ranged from 9% (mHSSW BP-TdR) to 15% (AASW BP-Leu) of heterotrophic bacterial production.

Sample	PC μM	PN μM	C:N	DOC μM	chl a μg L^{-1}	BGE	Leu		TdR		Leu:TdR	^{14}C-bicarb nM C d^{-1}		
							nM d^{-1}	nM d^{-1}	nM d^{-1}	nM C d^{-1}		0.2-3μm	>3 μm	sum
AASW	28.4	2.2	11.3	42.1	2.4	ND	0.27 (0.02)	35.1 (2.8)	0.022 (0.003)	39.5 (6.0)	12	2.8 (0.2)	2.5 (0.5)	5.3 (0.5)
mHSSW	26.1	1.9	12.0	31.8	2.9	0.7	0.36 (0.08)	47.0 (10.0)	0.035 (0.0003)	63.6 (9.0)	10	3.1 (0.6)	2.9 (1.0)	6.0 (1.0)

Table 3. Water column organic chemical composition and microbial activity (± propagated standard error) for samples collected in the AASW (30 m) and mHSSW (850 m) water masses. Particulate organic carbon and nitrogen (PC and PN), the molar PC to PN ratio (C:N), dissolved organic carbon (DOC), chlorophyll *a* (chl *a*), bacterial growth efficiency (BGE) rates of ^{3}H-leucine (Leu) and ^{3}H-thymidine (TdR) incorporation and bacterial production (nmol C L^{-1} d^{-1}) the molar ratio of Leu:TdR (nmol Leu L^{-1} d^{-1}: nmol TdR L^{-1} d^{-1}), rate of ^{14}C-bicarbonate incorporation in the dark (0.2 – 3μm and >3μm size fractions and the sum of the two size fractions). ND = Not determined.

The molar ratio of particulate organic C:N was slightly higher in the mHSSW (10.5 vs. 10.0), while DOC concentrations were higher in the AASW (42.1 μmol L^{-1} vs. 31.8 μmol L^{-1}). Chl *a* was 2.4 μg L^{-1} in the shallow water and 2.9 μg L^{-1} in the deep water (Table 4), and PC:chl *a* (μg C L^{-1}: μg chl *a* L^{-1}) was 109 in the AASW and 91 in the mHSSW.

The Fluorescence and Freshness Indices for DOM were 2% and 21% higher, respectively, in the mHSSW sample than the AASW sample while the Humification Index was 55% higher in the AASW sample (Table 4). The maximum excitation/emission of fluorescent DOM (Ex_{max}/Em_{max}) occurred in the range of tryptophan-like fluorescence (240/322-324 in the AASW and 240/334-352 in the mHSSW), and standardized maximum fluorescence revealed 1.7 times greater tryptophan-like fluorescence in the mHSSW sample compared to the AASW (Table 4)

Sample	*Fluorescence Index*	*Humification Index*	*Freshness Index*	*Max Fluor*
AASW	1.65	0.31	1.35	0.56
mHSSW	1.70	0.14	1.72	0.97

Table 4. Fluorescence characteristics of dissolved organic matter (DOM) in the two water masses sampled. A higher Fluorescence Index indicates DOM of more microbial character, a higher Humification Index indicates a higher degree of humification, and a higher Freshness Index indicates a higher proportion of recently produced DOM. Standardized maximum fluorescence (Max Fluor) occurred in the region of tryptophan-like fluorescence for both samples (excitation 240 nm and emission 334-352 (30 m) and 322-334 (850 m)).

The seafloor at the sample site was characterized by a rocky lag deposit, indicative of continuous or episodic strong bottom currents. Fine-grained sediment, including diatom frustules, was present interstitially between rocks and pebbles. The diatom assemblage recovered from near surficial sediments was characterized by Southern Ocean and Ross Sea pelagic species including *Eucampia antarctica, Thalassiosira oliverana, Thalassiosira tumida, Stelarima microtrias, Thalassiosira lentiginosa, Thlassiosira gracilis, Actinocyclus actinochilus* and *Fragilariopsis obliquicostata*. Taxa characteristic of the northern polar frontal zone and lower latitudes, including *Thalassionema nitzschioides, Thalassiosira oestrupii* and *Actinocyclus octinarius*, were also represented. *Fragilariopsis curta* accounted for less than 1% of the diatom flora in the MIS sediment.

Bacterial and Archaeal Diversity and Community Structure

Microbial diversity, as indicated by the Shannon diversity index (H') and the inverse Simpsons diversity index ($1/\lambda$), was greatest in the >10 μm size fraction of the

mHSSW sample (Table 5). Good's coverage, a non-parametric coverage estimator, indicated that the majority of the OTUs in the samples were identified through sequencing, (>99%; Table 5) with projected between 140 and 500 (calculated as 1/(1-Good's coverage)) more sequencing reads required to detect an additional OTU from each sample (Figure 4).

Sample	*# of reads*	*# of OTUs*	*Good's Coverage*	*Chao1*	*H'*	*1/λ*
AASW	238448	1475	99.8%	2140	2.06	3.79
mHSSW 0.2 to 3 μm	193331	1805	99.6%	2995	4.26	23.37
mHSSW 3 to 10 μm	101768	2208	99.3%	2960	5.27	75.10
mHSSW >10 μm	391658	3442	99.7%	4880	5.74	117.10

Table 5. Prokaryotic diversity estimates for the different water masses sampled. OTUs were calculated based on 97% similarity. H' = Shannon diversity index, 1/λ = inverse Simpsons diversity index. Good's coverage is a non-parametric coverage indicator. Chao1 gives the expected number of OTUs.

The total numbers of OTUs observed in the SSU sequence libraries represented between 60% (mHSSW 0.2 to 3 μm size fraction) and 75% (mHSSW 3 to10 μm size fraction) of the expected number of OTUs predicted by the Chao1 richness estimator (Table 5).

The three size fractions of mHSSW were dominated by phylotypes that classify within the Gammaproteobacteria and Bacteroidetes, with greater proportions of Bacteroidetes (predominantly Flavobacteria) occurring in the >10 μm and 3 to 10 μm fractions relative to the 0.2 to 3 μm fraction (Figure 4). Together, the Gammaproteobacteria and Bacteroidetes accounted for ~53% of the OTUs in the

mHSSW sample (size fractions pooled), with the Gammaproteobacteria alone accounting for nearly 75% of the OTUs observed at the sampling depth in the AASW. The most abundant operational taxonomic unit (OTU; 3.7% of sequence reads) in the mHSSW sample was most closely related (96% identity) to *Candidatus Vesicomyosocius okutanii*, a sulfide-oxidizing symbiont of a deep-sea clam. An OTU most closely related (98% sequence similarity) to the ammonia oxidizer *Nitrosopumilus maritimus,* was the third most common in the mHSSW sample, comprising 3.5% of total sequencing reads. Members of the Thuamarchaeota comprised a total of 4.1% of the mHSSW community (10.9%, 2.6% and 1.3% of reads from the 0.2 to 3 μm, 3 to 10 μm and >10 μm size fractions, respectively). The majority of sequences in the AASW were related to *Oceanospirillales sp.* (most abundant OTU, 42.4% of reads) and members of the SAR92 clade (second most abundant OTU, 28.9% of reads). OTUs most closely related to the SAR11 clade were rare, comprising 0.13% of the total library in the AASW and 1.2% in the mHSSW. A total of ~9.0% of the sequence reads from the AASW were closely related to *Polaribacter sp.,* a marine genus reported to possess gas vacuoles.

Approximately 10% of the OTUs identified in all samples were present in both the AASW and the mHSSW (Figure 4). Eighteen of these OTUs were present at relative abundances >0.1% in both water masses. In general, OTUs that were common in one water mass (≥1%) were rare in the other water mass. Exceptions to this were in OTUs related to the Oceanospirillaceae, which comprised 42.4% and 4.1% of the AASW and mHSSW populations, respectively, an OTU related to the SAR92 cluster (28.9% and

2.3% in the AASW and mHSSW, respectively), and Flavobacteriaceae (2.6% and 1.0% in the AASW and mHSSW, respectively).

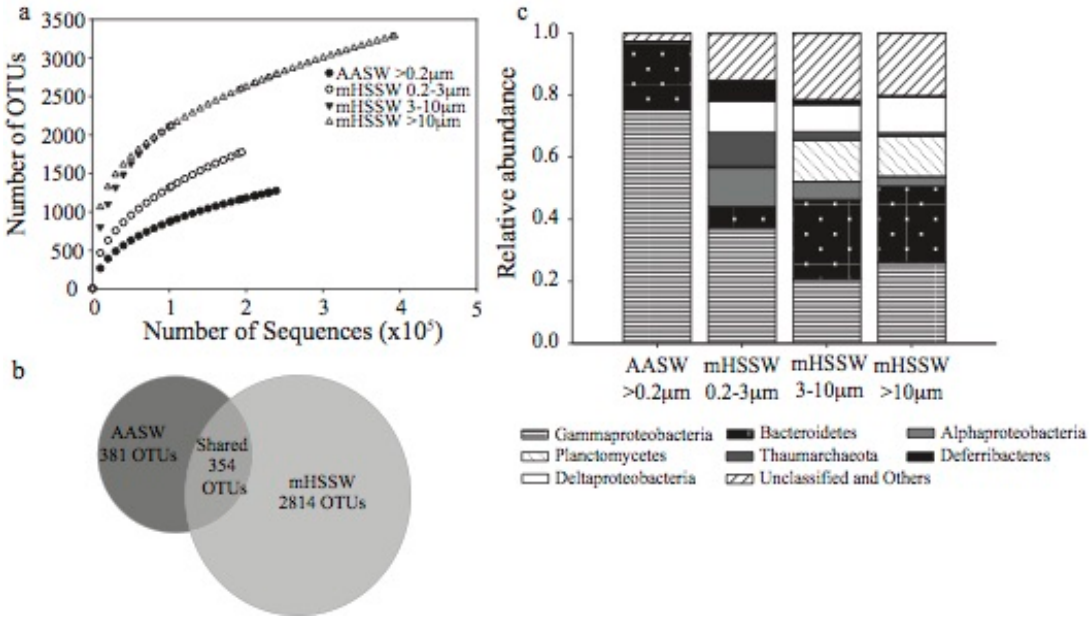

Figure 4. (a) Rarefaction curves for OTU richness of samples from AASW (30 m) and mHSSW (850 m); (b) comparison of microbial communities from the AASW water mass and mHSSW water mass samples showing a 10% overlap in community composition at the OTU level (97% SSU sequence identity); (c) and relative abundance data for AASW and mHSSW.

Discussion

Sub-ice shelf habitats are among the least-studied ecosystems in the world's oceans. Our results show an active microbial ecosystem under the MIS, supported in part via chemoautotrophic activity and in part via advection of nutrients and biomass from eastern McMurdo Sound. Thick ice prevents the penetration of sunlight, leaving sub-ice shelf waters devoid of the primary production typical of open ocean photic zones, therefore horizontal advection from adjacent open waters should play a proportionally

greater role in sub-ice shelf biogeochemistry. Sub-ice shelf habitats can be oligotrophic, such as the J9 site beneath the RIS, (Lipps et al. 1979) where chemoautotrophically produced new carbon may be an important food source (Horrigan, 1981). Conversely, the diverse assemblage that comprised the benthic community beneath the Amery Ice Shelf indicated a nutrient rich environment likely sustained by advection of phytoplankton produced organic matter (Riddle et al. 2007, Post et al. 2014). The J9 and Amery sites differ in their distance to open water (~400 km for J9 and ~100 km for Amery). These results, along with those of our study, indicate that biogeochemical processes beneath an ice shelf are controlled by the proximity to open water, the trophic state of the source waters and new (chemoautotrophic) carbon production beneath the ice shelf.

Source of Sub-MIS Waters

The currents observed at our sampling site (Fig. 2B) are in agreement with previous observations of a strong southward flow component from the Ross Sea to the MIS via the eastern side of McMurdo Sound (Robinson et al. 2010). Our biological and physicochemical measurements support an eastern McMurdo Sound source for the sub-MIS waters at our sample site. Bacterioplankton abundances in eastern McMurdo Sound were similar to those at our site (Table 2; ~10^8 cells L^{-1}, Hodson et al. 1981 and Rivkin 1991). In contrast, the oligotrophic western side, which is a mixture of sub-MIS outflow and water circulating from the Ross Sea, contained an order of magnitude fewer cells (Hodson et al. 1981). Nutrient concentrations (SRP and DIN; Table 1) were within a few μmol L^{-1} of those measured during December in eastern McMurdo Sound (Rivkin 1991). These data imply that the transport time from the open waters of McMurdo Sound to our

sample site (~ 2 days; Robinson 2004) did not result in major changes to the concentrations of inorganic nutrients or microbial cells. Given the similarity between the biological and physicochemical character of our samples and eastern McMurdo Sound waters, the prevailing current direction we conclude that nutrient and biomass-rich water advected from eastern McMurdo Sound likely plays an important role in sub-MIS biogeochemical processes.

Sedimentary diatoms can also provide tracers of water column advection, however, strong bottom currents (Fig. 2B) at our sample site suggest that little deposition occurs there at present. The most common diatoms we observed (multiple species of *Thalassiosira*, *A. actinochilus*, and *F. obliquicostata*) are also found in sediments from the eastern side of McMurdo Sound (Leventer and Dunbar 1988), however the near absence of *F. curta*, which is commonly observed in McMurdo Sound, is striking. No viable diatoms were recovered in our surface sediment samples, suggesting that the diatoms we observed may represent earlier deposition, or that they are the result of advection from pelagic sources. Together, these data indicate that diatom deposition may not be an accurate tracer of modern water sources at this site.

Organic Carbon Sources

Sub-ice shelf systems are unique from open ocean environments in their dependence on horizontal advection of food sources or in situ chemoautotrophic production, rather than on vertical fluxes of phytoplankton-derived food sources (Gutt et al. 2011). To determine whether intact phytoplankton cells are advected beneath the MIS, and consider their potential importance as a food source, we examined chl *a*

concentrations and phytoplankton abundances in the AASW and mHSSW. Chlorophyll *a* concentrations in both samples were similar to values measured in McMurdo Sound during mid-December (Rivkin 1991), suggesting that phytoplankton loss rates (i.e. due to sedimentation, cell lysis, grazing) were low by the time water from McMurdo Sound reached our sampling site. Our CTD data revealed the presence of three distinct water masses beneath the MIS, rather than a well-mixed water column that would result in even distribution of chl *a*, so the simplest explanation for the similar concentrations of chl *a* we measured in the AASW and mHSSW (2.4 and 2.9 μg L^{-1}, respectively) is settling of chl *a* containing cells into the aphotic mHSSW during the ~2 day transport time to our sample site.

Indeed, our flow cytometry and microscopy data showed that chl *a* containing phytoplankton cells were present in both water masses. Phytoplankton cells were larger in the mHSSW than in the AASW and had higher chl *a* emission per cell, suggesting that intact cells or colonies were transported to depth, a phenomenon that has been previously reported for *P. antarctica* (DiTullio et al. 2000). The PC:chl *a* (ug L^{-1}: ug L^{-1}) measured in our samples (109 in the AASW and 91 in the mHSSW) was similar to that measured in active populations from the Ross Sea (92; Ditullio and Smith, 1996), supporting our contention that cells transported to depth were intact. Intact phytoplankton cells can be advected great distances under ice from open water (Holm-Hansen et al. 1978), where they may later be decomposed as a source of nutrition for heterotrophic growth of sub-ice shelf microorganisms.

To our knowledge, no measurements of *P. antarctica* decomposition rates have been made for the MIS/RIS cavity, although DiTullio et al. (2000) tracked *P. antarctica* export in the Ross Sea and showed that intact cells are rapidly exported to depth. Based on a phytoplankton decomposition rate of 0.032% d^{-1} for a cold saline Antarctic lake near McMurdo Sound (Priscu 1992), 100% of the phytoplankton particulate carbon we observed would be decomposed after 10 years. This potential decadal scale decomposition suggests that sinking and advected phytoplankton are important sources of organic matter beneath the ice shelf, and may continue to be as they are advected farther from the ice shelf front.

Bulk DOC concentrations in our samples were relatively low, similar to Ross Sea wintertime background concentrations (e.g. Ducklow 2003). Based on our determinations of bacterial growth efficiency and bacterial carbon production, the heterotrophic bacterial carbon demand (bacterial carbon production + bacterial carbon respiration) in our samples was ~ 50 to 90 nmol C L^{-1} d^{-1}. Assuming that the entire DOC pool is bioavailable and the system in steady-state, these rates would be expected to deplete the standing stock of DOC within 1 – 2 years. The total DOC pool is likely an overestimate of the bioavailable fraction, as the labile pool is consumed quickly, concurrent with the phytoplankton bloom (Ducklow 2003). Residence times in the MIS/RIS cavity may vary between water masses and are not well constrained, but estimates range from ~ 2 to 8 years (Smethie Jr. and Jacobs 2005, Reddy et al. 2010). Based on this, our data imply that another organic carbon source would be required to maintain heterotrophic potential beneath the ice shelf during the water residence time.

The production of organic matter via fixation of CO_2 into biomass (chemoautotrophy) may also be important under the ice. Our microbial diversity, in concert with results from other studies (e.g., Gryzmski et al. 2012; Williams et al. 2012; Christner et al. 2014) show that aerobic ammonia-oxidizing microorganisms are widespread in Antarctic aquatic environments, and may be key sources of new organic carbon to ecosystems shielded from sunlight. Isolated representatives of the proposed phylum Thaumarchaeota, a major group identified in our mHSSW sample, are aerobic ammonia oxidizers that fix CO_2 (Könneke et al. 2014). We measured dark CO_2 fixation of ~3 nmol C L^{-1} d^{-1} in the 0.2 – 3 μm size fraction in both the shallow AASW and deep mHSSW samples. We attribute this CO_2 fixation to bacteria and/or archaea, rather than phytoplankton-mediated anapleurotic reactions because our flow cytometry data showed that the 0.2 – 3 μm size fraction was chiefly comprised of bacterioplankton. Still, dark CO_2 fixation was an order of magnitude less than heterotrophic bacterial carbon production at our study site, implying that heterotrophic demand in this region of the MIS must also rely on some combination of the previously discussed carbon sources (advected organic matter and biomass or the DOC pool).

Dissolved Organic Matter Quality and Microbial Growth

Dissolved organic carbon concentrations, while higher in the surface waters (42.1 μmol L^{-1}) than at depth (31.8 μM) were similar to Ross Sea wintertime background values (40-42 μmol L^{-1}; Ducklow 2003). With terrestrial sources limited by a paucity of land plants, autochthonous production dominates the DOM pool in Antarctic waters (e.g

McKnight et al. 2001). Fluorescence indices derived from our EEMS datasets were consistent with those of microbially produced organic matter, where a high index (~ 1.8) corresponds to DOM of microbial origin, and a low index (~ 1.2) corresponds to DOM of terrestrial origin (McKnight et al. 2001, Cory and McKnight 2005). Humification indices increase with the presence of more humified and/or older DOM (up to >10 for fulvic acids; Zsolnay et al. 1999), while a Freshness index >1 corresponds to recently produced microbial DOM (Huguet et al. 2009). Both the Humification and Freshness indices calculated for our samples are consistent with DOM of recent microbial origin. The 55% higher Humification and 22% lower Freshness Indices in the AASW water mass relative to the deeper mHSSW water mass reveal that the near-surface DOM was more degraded, perhaps due to high rates of heterotrophic activity associated with phytoplankton production in the photic zone of McMurdo Sound before being advected into the sub-ice cavity.

Ducklow (2003) showed that labile DOC produced during the summer Ross Sea phytoplankton bloom is quickly consumed, leaving a mainly recalcitrant pool available for consumption during the winter. This is consistent with our findings of more degraded near-surface DOM. All three indices of biological activity (^{3}H-TdR, ^{3}H-Leu, and ^{14}C-bicarbonate uptake) revealed increased metabolic rates in the deeper mHSSW water mass. Increased biological activity may explain the stronger signal for freshly produced DOM, including the elevated maximum tryptophan-like fluorescence in the mHSSW relative to the AASW.

Although the ability to take up leucine and thymidine can differ among bacterial groups (Pérez et al. 2010), the ratio of Leu (protein production or biomass maintenance) to TdR (DNA synthesis or cell division) incorporation rates can be used as a metric for understanding changes in rates of biomass maintenance relative to reproduction (Chin-Leo and Kirchman, 1988; Shiah and Ducklow, 1997; Vick and Priscu, 2012). The lower Leu:TdR we detected in the mHSSW sample may indicate faster heterotrophic bacterioplankton growth rates at depth relative to the surface, possibly a product of the availability of higher quality DOM.

Conclusions

The sub-McMurdo Ice Shelf cavity provides an important conduit for organisms and nutrients between the Ross Sea and the sub-Ross Ice Shelf cavity. Our results show that the decomposition of phytoplankton coupled with chemoautotrophic production of new carbon may be important in supporting ecosystems beneath the MIS. While inputs from phytoplankton blooms are available only during the austral summer, chemoautotrophic production is available year-round. Our sequence-based community analysis corroborates our contention and those of previous reports suggesting that new carbon produced by chemoautotrophic ammonia-oxidizing organisms can supply organic carbon to partially sustain ecosystem processes beneath Antarctic ice shelves such as the MIS and RIS. Other abundant phylotypes in our deep-water sample are related to a chemoautotrophic sulfide oxidizer, suggesting that reduced sulfur compounds may also be an important energy source to fuel chemoauotrophic production beneath the MIS.

Given that many of the ice shelves surrounding Antarctica's coastline are thinning at increasing rates (Paolo et al. 2015) and are susceptible to collapse (Joughin et al. 2014), their losses should lead to significant changes in the biogeochemistry of Antarctic coastal systems supported by sub-ice shelf processes. Changes in Southern Ocean ice cover can impact carbon biogeochemistry at local as well as global (see review by Sigman et al. 2010) scales. In the case of the RIS/MIS, the relative biogeochemical importance of chemoautotrophic production and material advected beneath the ice from the Ross Sea would decrease if photosynthetic primary production began to occur in newly open water. Assuming that the rates we measured are relatively constant over the year, the sum of heterotrophic and autotrophic C production under the MIS is currently <1% of the photosynthetic C production in the open water of the Ross Sea (per km^2 per year in the top 100 m of water column; Ross Sea estimates in Arrigo et al., 2008). Considering such disparity in productivity between ice shelf covered and open water, the loss of ice shelves can be expected to have cascading effects on elemental cycling in the region via shifts in dominant biological processes. In a less dramatic scenario than massive ice-shelf loss, climate change induced changes to winds and temperatures that modulate incursions of Circumpolar Deep Water onto the continental shelf could severely disrupt the Ross Sea food web (Smith Jr. et al 2014), leading to major effects on sub-MIS biogeochemistry. Baseline data from existing sub ice shelf environments, such as the MIS, inform the prediction of the biogeochemical impacts of ice shelf collapse and climate change in the Southern Ocean.

Acknowledgements

The Whillans Ice Stream Subglacial Access Research Drilling (WISSARD) project was funded by National Science Foundation grants (0838933, 0838896, 0838941, 0839142, 0839059, 0838885, 0838855, 0838763, 0839107, 0838947, 0838854, 0838764 and 1142123) from the Office of Polar Programs. Partial support was also provided by funds from NSF award 1023233 (B.C.C.), NSF award 1115245 (J.C.P.), the American Association of University Women Dissertation Fellowship (T.J.V.), the NSF's Graduate Research Fellowship Program (1247192; A.M.A.), the Chilean Fulbright-CONICYT Scholarship (P.S), the Italian National Antarctic Program (C.B.), and fellowships from the NSF's IGERT Program (0654336) and the Montana Space Grant Consortium (A.B.M.). The authors would like to thank two anonymous reviewers for helpful comments, Robert Edwards for project management, Andrew T. Fisher and Kenneth D. Mankoff for providing sediment samples, the WISSARD Science Team, the individuals working as part of the Antarctic Support Contractor managed by Lockheed-Martin, for logistical support, as well as K. Welch and A. Chiuchiolo for analytical and laboratory assistance and I. Alekhina for field support. The drilling was directed by F.Rack and implemented by D.Blythe, J.Burnett, C.Carpenter, D.Duling (chief driller), D.Gibson, J. Lemery, A. Melby and G. Roberts.

Supplemental Information

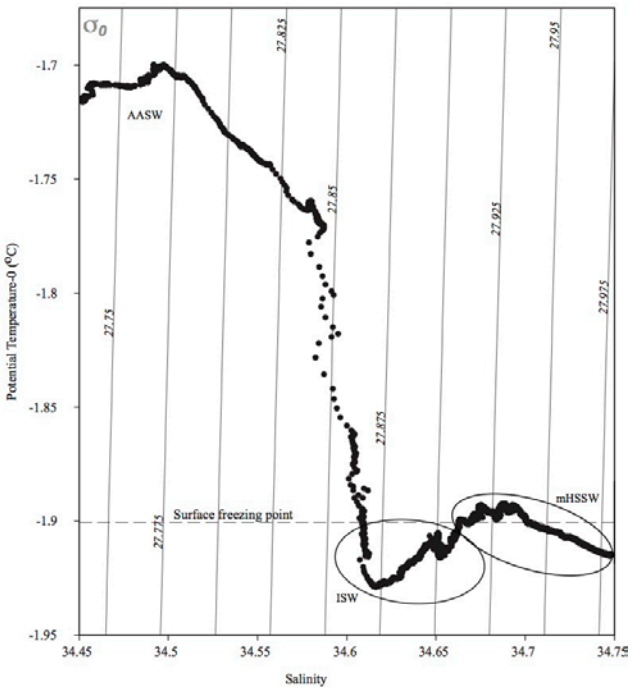

Figure S1. Potential temperature (°C, relative to the surface) plotted over salinity (PSU) showing the presence of three distinct water layers at our sampling site: Antarctic Surface Water (AASW), Ice Shelf Water (ISW), and modified High Salinity Shelf Water (mHSSW). Vertical lines denote isopycnals for the potential density anomaly, σ_0 (kg m^{-3}: potential density referenced to the surface) over the salinity and temperature range at our sampling site. Plotted with Ocean Data View (Schlitzer 2013).

References

Apprill, A., McNally, S., Parsons, R., Weber, L. 2015. Minor revision to V4 region SSU rRNA 806R gene primer greatly increases detection of SAR11 bacterioplankton. Aquat. Microb. Ecol. 75:129-137.

Arrigo, K.R. 1999. Phytoplankton Community Structure and the Drawdown of Nutrients and CO_2 in the Southern Ocean. Science. 283: 365–367.

Arrigo, K.R. and van Dijken, G.L. 2004. Annual changes in sea-ice, chlorophyll a, and primary production in the Ross Sea, Antarctica. Deep Sea Res. Part II Top. Stud. Oceanogr. 51: 117–138.

Arrigo, K.R. and McClain C.R. 1994. Spring phytoplankton production in the Western Ross Sea. Science. 266: 261–263.

Arrigo, K.R., van Dijken, G.L., and Bushinsky, S. 2008. Primary production in the Southern Ocean, 1997-2006. J. Geophys. Res. 113:C08004.

Azam F., Beers J.R., Campbell L., Carlucci A.F., Holm-Hansen O., Reid F.M., Karl D.M. 1979. Occurrence and metabolic activity of organisms under the Ross Ice Shelf, Antarctica, at Station J9. Science. 203: 451–453.

Barry, J.P. 1988. Hydrographic patterns in McMurdo Sound, Antarctica and their relationship to local benthic communities. Polar Biol. 8: 377-391.

Bell, R.T. 1993. Estimating production of heterotrophic bacterioplankton via incorporation of tritiated thymidine. In: Kemp PF, Sherr BF, Sherr EB, Cole JJ (eds) Handbook of methods in aquatic microbial ecology. Lewis Publishers.

Bertolin, M. and Schloss, I. 2009. Phytoplankton production after the collapse of the Larsen A Ice Shelf, Antarctica. Polar Biol. 32:1435-1446.

Blythe, D., Duling, D.V., and Gibson, D.E. 2014. Developing a hot-water drill system for the WISSARD project: 2. In situ water production. Ann. Glaciol. 55: 298-302

Bouvier, T., Del Giorgio P.A., and Gasol J.M. 2007. A comparative study of the cytometric characteristics of high and low nucleic-acid bacterioplankton cells from different aquatic ecosystems. Environ. Microbiol. 9: 2050–2066.

Budillon G., Castagno P., Aliani S., Spezie G., and Padman L. 2011. Thermohaline variability and Antarctic bottom water formation at the Ross Sea shelf break. Deep Sea Res. Part I Oceanogr. Res. Pap. 58: 1002–1018.

Burnett, J., Rack, F.R., Blythe, D., and others. 2014. Developing a hot-water drill system for the WISSARD project: 3. Instrumentation and control systems. Ann. Glaciol. 55: 303-310.

Caporaso, J.G., Lauber, C.L., Walters, W.A., and others. 2012. Ultra-high-throughput microbial community analysis on the Illumina HiSeq and MiSeq platforms. ISME J. 6: 1621-1624.

Carr, S.A., Vogel, S., Dunbar, R.B., and others. 2013. Bacterial abundance and composition in marine sediments beneath the Ross Ice Shelf, Antarctica. Geobiology. 11: 377-395.

Celussi, M., Bergamasco, A., Cataletto, B., Umani, S.F., and Del Negro, P. 2010. Water masses' bacterial community structure and microbial activities in the Ross Sea, Antarctica. Antarct. Sci. 22: 361–370.

Chao, A. 1984. Non-parametric estimation of the number of classes in a population. Scandinavian Journal of Statistics. 11:265-270.

Chin-Leo, G. and Kirchman, D. 1988. Estimating bacterial production in marine waters from the simultaneous incorporation of thymidine and leucine. Appl. Environ. Microbiol. 8:1934-1939.

Christner, B.C., Royston-Bishop, G., Foreman, C.M. and others. 2006. Limnological conditions in Subglacial Lake Vostok, Antarctica. Limnol. Oceanogr. 6: 2485-2501.

Christner, B.C., Priscu, J.C., Achberger, A.M., and others. 2014. A microbial ecosystem beneath the West Antarctic ice sheet. Nature 512: 310–313.

Clough, J.W. and Hansen, B.L. 1979. The Ross Ice Shelf Project. Science. 203: 433–434.

Cory, R.M. and McKnight, D.M. 2005. Fluorescence spectroscopy reveals ubiquitous presence of oxidized and reduced quinones in dissolved organic matter. Environ. Sci. Technol. 39: 8142–8149.

Daly M., Rack F., Zook, R. 2013. *Edwardsiella andrillae*, a New Species of Sea Anemone from Antarctic Ice. PLoS One 8: e83476.

del Giorgio, P.A., Condon, R., Bouvier, T., Longnecker, K., Bouvier, C., Sherr, E., and Gasol, J.M. 2011. Coherent patterns in bacterial growth, growth efficiency, and leucine metabolism along a northeastern Pacific inshore-offshore transect. Limnol. Oceanogr. 1:1-16.

Depoorter, M.A., Bamber, J.L., Griggs, J.A., Lenaerts, J.T.M., Ligtenberg, S.R.M., van den Broeke, M.R., and Moholdt, G. 2013. Calving fluxes and basal melt rates of Antarctic ice shelves. Nature. 502: 89–92.

DiTullio, G.R., Grebmeier, J.M., Arrigo, K.R., and others. 2000. Rapid and early export of *Phaeocystis antarctica* blooms in the Ross Sea, Antarctica. Nature 404: 595–598.

DiTullio, G.R. and Smith, W.O. 1996. Spatial patterns in phytoplankton biomass and pigment distributions in the Ross Sea. J. Geophys. Res. 101: 18467.

Domack, E., Leventer, A., Sylva, S., Wilmott, V., and Huber, B. 2005. A chemotrophic ecosystem found beneath Antarctic ice shelf. Trans. Am. Geophys. Union. 86: 269-276.

Ducklow, H., Carlson, C., Church, M., Kirchman, D., Smith, D., and Steward, G. 2001. The seasonal development of the bacterioplankton bloom in the Ross Sea, Antarctica, 1994-1997. Deep. Res. II 48: 4199–4221.

Ducklow, H.W. 2003. Seasonal production and bacterial utilization of DOC in the Ross Sea, Antarctica. In G.R. Ditullio and R.B. Dunbar [eds] Biogeochemistry of the Ross Sea. American Geophysical Union.

Fillinger, D., Janussen, D., Lundälv, T., and Richter, C. 2013. Rapid glass sponge expansion after climate-induced Antarctic ice shelf collapse. Curr. Biol. 23: 1330-1334.

Fox, A.J. and Cooper, A.P.R. 1994. Measured properties of the Antarctic ice sheet derived from the SCAR Antarctic digital database. Polar Record 30: 201–206.

Fuhrman, J. and Azam, F. 1982. Thymidine incorporation as a measure of heterotrophic bacterioplankton production in marine surface waters: evaluation and field results. Mar. Biol. 66: 109–120.

Gasol, J.M. and del Giorgio, P.A. 2000 Using flow cytometry for counting natural planktonic bacteria and understanding the structure of planktonic bacterial communities. Sci. Mar. 64: 197–224.

Gilmour, A. 1979. Ross Ice Shelf Sea Temperatures. Science 203: 438–439.

Good, I.J. 1953. The population frequencies of species and the estimation of population parameters. Biometrika. 40: 237-264.

Greischar, L.L. and Bently, C.R. 1980. Isostatic equilibrium grounding line between the West Antarctic inland ice sheet and the Ross Ice Shelf. Nature. 283: 651–654.

Griggs, J. and Bamber, J. 2011. Antarctic ice-shelf thickness from satellite radar altimetry. J. Glaciol. 57: 485-498.

Gryzmski, J.J., Riesenfeld, C.S., Williams, T.J., Dussaq, A.M., Ducklow, H.W., Erickson, M., Cavicchioloi, R., and Murray, A.E. 2012. A metagenomic assessment of winter and summer bacterioplankton from Antarctica Peninsula coastal surface waters. ISME J. 2: 1-15.

Gutt, J., Barratt, I., Domack, E. and others (2011) Biodiversity change after climate-induced ice-shelf collapse in the Antarctic. Deep Sea Res., Part II. 58: 74-83.

Hillebrand, H., Dürselen, C.D., Kirschtel, D., Pollingher, U. and Zohary, T. 1999 Biovolume calculation for pelagic and benthic microalgae. J. Phycol. 424: 403–424.

Hodson, R., Azam, F., Carlucci, A.F., Fuhrman, J.A., Karl, D.M., and Holm-Hansen, O. 1981. Microbial uptake of dissolved organic matter in McMurdo Sound, Antarctica. Mar. Biol. 61: 89-94.

Holm-Hansen, O., Azam, F., Campbell, L., Carlucci, A.F., and Karl, D.M. 1978. Microbial life beneath the Ross Ice Shelf. Antarctic Journal of the United States. 4: 129-130.

Horgan, H.J., Alley, R.B., Christianson, K., Jacobel, R.W., Anandakrishnan, S., Muto, A., Beem, L.H., and Siegfried, M.R. 2013. Estuaries beneath ice sheets. Geology. 11: 1159-1162.

Horrigan, S.G. 1981. Primary production under the Ross Ice Shelf, Antarctica. Limnol. Oceanogr. 26: 378–382.

Huguet, A., Vacher, L., Relexans, S., Saubusse, S., Froidefond, J.M., and Parlanti, E. 2009. Properties of fluorescent dissolved organic matter in the Gironde Estuary. Org. Geochem. 40: 706–719.

IOC, SCOR, and IAPSO. 2010. The international thermodynamic equation of seawater - 2010: Calculation and use of thermodynamic properties. Intergovernmental Oceanographic Commission, Manuals and Guides. UNESCO.

Jacobs, S.S., Amos, A.F., and Bruchhausen, P.M. 1970. Ross Sea oceanography and Antarctic Bottom Water formation. Deep-Sea Res. Oceanogr. Abstr. 17: 935–962.

Jacobs, S.S. and Fairbanks, R.G. 1985. Origin and evolution of water masses near the Antarctic continental margin: Evidence from $H_2{}^{18}O/H_2{}^{16}O$ ratios in seawater. Antarct. Res. Ser. 43: 59-85.

Jacobs, S.S., Gordon, A.L., and Ardai, Jr. J.L. 1979. Circulation and Melting Beneath the Ross Ice Shelf. Science 203: 439–443.

Joughin, I., Smith, B., and Medley, B. 2014. Marine ice sheet collapse potentially underway for the Thwaites Glacier Basin, West Antarctica. Science. 344: 735-738.

Kepner, R., Wharton, R., and Suttle, C. 1988. Viruses in Antarctic Lakes. Limnol. Oceanogr. 7: 1754-1761.

Kirchman, D., K'nees, E., and Hodson, R. 1985. Leucine incorporation and its potential as a measure of protein synthesis by bacteria in natural aquatic systems. Appl. Environ. Microbiol. 49: 599–607.

Lebaron, P., Servais, P., Agogué, H., Joux, F., Agogue, H., and Courties, C. 2001. Does the High Nucleic Acid Content of Individual Bacterial Cells Allow Us To Discriminate between Active Cells and Inactive Cells in Aquatic Systems? Appl. Environ. Microbiol. 67: 1775–1782.

Leventer, A. and Dunbar, R. 1988. Recent diatom record of McMurdo Sound, Antarctica: Implications for history of sea ice extent. Paleoceanography. 3:259-274.

Lipps, J.H.H., Ronan, T.E., Delaca, T.E.E, and Ronan Jr., T.E. 1979. Life Below the Ross Ice Shelf, Antarctica. Science. 203: 447–449.

Lisle, J.T. and Priscu, J.C. 2004. The occurreence of lysogenic bacteria and microbial aggregates in the lakes of the McMurdo Dry Valleys, Antarctica. Microb. Ecol. 47: 427-439.

Magurran, A. 1988. Ecological diversity and its measurement. Princeton University Press, Princeton NJ.

Marie, D., Partensky, F., Vaulot, D., and Brussaard, C. 2001. Enumeration of phytoplankton, bacteria, and viruses in marine samples. Current protocols in cytometry. 10:11.11:11.11.1–11.11.15.

Mcknight, D.M., Boyer, E.W., Westerhoff, P.K. and others. 2001. Spectrofluorometric Characterization of Dissolved Organic Matter for Indication of Precursor Organic Material and Aromaticity. Limnol. Oceanogr. 46: 38–48.

Montagnes, D.J.S., Berges, J.A., Harrison, P.J., and Taylor, F.J.R. 1994. Estimating carbon, nitrogen, protein, and chlorophyll a from volume in marine phytoplankton. Limnol. Oceanogr. 39: 1044–60.

Paolo, F.S., Fricker, H.A., and Padman, L. 2015. Volume loss from Antarctic ice shelves is accelerating. Science. 348: 327-331.

Pérez, M., Hörtnagl, P., and Sommaruga, R. 2010. Contrasting ability to take up leucine and thymidine among freshwater bacterial groups: implications for bacterial production measurements. Environ. Microbiol. 12:74-82.

Post, A.L., Galton-Fenzi, B.K., Riddle, M.J. and others. 2014. Modern sedimentation, circulation and life beneath the Amery Ice Shelf, East Antarctica. Cont. Shelf Res. 74: 77-87.

Priscu, J.C. 1992. Particulate organic matter decomposition in the water column of Lake Bonney, Taylor Valley. Antarct. J. United States 27: 260.

Rack, F.R., Duling, D., Blythe, D. and others. 2014. Developing a hot-water drill system for the WISSARD project: 1. Basic drill system components and design. Ann. Glaciol. 55: 285-297

Reddy, T.E., Holland, D.M., and Arrigo, K.R. 2010. Ross ice shelf cavity, circulation, residence time, and melting: Results from a model of oceanic chlorofluorocarbons. Cont. Shelf Res. 7: 733-742.

Riddle, M.J., Craven, M., Goldsworthy, P.M., and Carsey, F. 2007 A diverse benthic assemblage 100 km from open water under the Amery Ice Shelf, Antarctica. Paleoceanography. 22: PA1204.

Rignot, E., Jacobs, S., Mouginot, J., and Scheuchl, B. 2013. Ice-shelf melting around Antarctica. Science. 341: 266-269.

Rivkin, R.B. 1991. Seasonal Patterns of Planktonic Production in McMurdo Sound, Antarctica. Am. Zool. 16: 5–16.

Robinson, N.J. 2004. An oceaonographic study of the cavity beneath the McMurdo Ice Shelf, Antarctica. M.S. Thesis, Victoria University of Wellington, New Zealand.

Robinson, N.J., Williams, M.J.M., Barrett, P.J., Pyne, A.R. 2010. Observations of flow and ice-ocean interaction beneath the McMurdo Ice Shelf, Antarctica. J. Geophys. Res. 115: C03025.

Scherer, R.P. 1991. Quaternary and Tertiary microfossils from beneath Ice Stream B: Evidence for a dynamic West Antarctic Ice Sheet history. Palaeogeogr. Palaeocl. 90: 395-412.

Schlitzer, R. 2013. Ocean Data View. http://odv.awi.de.

Schloss, P.D., Westcott, S.L., Ryabin, T., and others. 2009. Introducing mothur: Open-source, platform-independent, community-supported software for describing and comparing microbial communities. Appl. Environ. Microbiol. 75: 7537-7541.

Schneider, C.A., Rasband, W.S., and Eliceiri, K.W. 2012. NIH Image to ImageJ: 25 years of image analysis. Nature Methods. 7: 671-675.

Shiah, F.K. and Ducklow, H.W. 1997. Bacterioplankton growth responses to temperature and chlorophyll variations in estuaries measured by thymidine:leucine incorporation ratio. Aquat. Microb. Ecol. 13: 151–159.

Sigman, D., Hain, M., and Haug, G. 2010. The polar ocean and glacial cycles in atmospheric CO2 concentration. Nature. 466: 47-55.

Smethie Jr. W., and Jacobs, S. 2005. Circulation and melting under the Ross Ice Shelf: estimates from evoloving CFC, salinity and temperature fields in the Ross Sea. Deep Sea Res., Part I. 6: 959-978.

Smith, W., and Comiso, J. 2008. Influence of sea ice on primary production in the Southern Ocean: A satellite perspective. J. Geophys. Res.: Oceans. C5:C05S93.

Smith Jr., W.O. and Gordon, L.I. 1997. Hyperproductivity of the Ross Sea (Antarctica) polynya during austral spring. Geophys. Res. Lett. 24: 233–236.

Smith Jr., W.O., Sedwick, P.N., Arrigo, K.R., Ainley, D.G., and Orsi, A.H. 2012. The Ross Sea in a sea of change. Oceanography 25: 90–103.

Smith Jr., W.O., Dinniman, M.S., Hofmann, E.E., and Klinck, J.M. 2014. The effects of changing winds and temperatures on the oceanography of the Ross Sea into the 21st century. Geophys. Res. Lett. 41: 1624-1631.

Solórzano, L. 1969. Determination of ammonia in natural waters by the phenolhypochlorite method. Limnol. Oceanogr. 5: 799-801.

Stover, C. 2006. A new account of Ross Sea water: characteristics, volumetrics, and variability. Thesis. Texas A&M University.

Strickland, J. and Parsons, T. 1968. A practical handbook of seawater analysis. Fisheries Research Board of Canada. Ottowa.

Takacs, C. and Priscu, J. 1998. Bacterioplankton dynamics in the McMurdo Dry Valley lakes, Antarctica: Production and biomass loss over four seasons. Microb. Ecol. 3: 239-250.

Vick, T.J. and Priscu, J.C. 2012. Bacterioplankton productivity in lakes of the Taylor Valley, Antarctica, during the polar night transition. Aquat. Micro. Ecol. 68: 77-90.

Welschmeyer, N. 1994. Fluorometric analysis of chlorophyll a in the presence of chlorophyll b and pheopigments. Limnol. Oceanogr. 8: 1985-1992.

Williams, T.J., Long, E., Evans, F. and others. 2012. A metaproteomic assessment of winter and summer bacterioplankton from Antarctic Peninsula coastal surface waters. ISME J. 6: 1883-1900.

Williams, R. and Robinson, E. 1979. Ocean Tide and Waves Beneath the Ross Ice Shelf, Antarctica. Science. 203: 443–445.

Wouters, B., Martin-Español, A., Helm, V., Flament, T., van Wessem, J. M., Ligtenberg, S. R. M., van den Broeke, M. R., and Bamber, J. L. 2015. Dynamic thinning of glaciers on the Southern Antarctic Peninsula. Science. 348: 899-903.

Yakimov, M.M., la Cono, V., Smedile, F., and others. 2011. Contribution of crenarchaeal autotrophic ammonia oxidizers to the dark primary production in Tyrrhenian deep waters (Central Mediterranean Sea). ISME J. 5: 945–961.

Zsolnay, A., Baigar, E., Jimenez, M., Steinwg, B., Saccomandi, F. 1999. Differentiating with fluorescence spectroscopy the sources of dissolved organic matter in soils subjected to drying. Chemosphere 38: 45–50.

CHAPTER SIX

A MICROBIAL ECOSYSTEM BENEATH THE WEST ANTARCTIC ICE SHEET

Contribution of Authors and Co-Authors

Manuscript in Chapter 6

Author: Brent C. Christner

Contributions: Oversaw sample collection and sequence data analyses, provided funding, prepared figures and tables, wrote the manuscript.

Co-Author: John C. Priscu

Contributions: Oversaw sample collection and data analyses, conceived the study, provided funding, analyzed DIC samples, wrote the manuscript.

Co-Author: Amanda M. Achberger

Contributions: Collected and analyzed samples for molecular data, contributed to manuscript preparation.

Co-Author: Carlo Barbante

Contributions: Collected samples, conducted and interpreted chemical measurements.

Co-Author: Sasha P. Carter

Contributions: Provided geophysical data.

Co-Author: Knut Christianson

Contributions: Provided geophysical data.

Co-Author: Alexander B. Michaud

Contributions: Collected samples, contributed sediment biogeochemical data, ATP concentration, and dissolved oxygen concentration data.

Contribution of Authors and Co-Authors-Continued

Co-Author: Jill A. Mikucki

Contributions: Collected samples, collected and examined CTD data.

Co-Author: Andrew C. Mitchell

Contributions: Collected samples, conducted and interpreted chemical measurements.

Co-Author: Mark L. Skidmore

Contributions: Collected samples, conducted and interpreted chemical measurements.

Co-Author: Trista J. Vick-Majors

Contributions: Collected samples, conducted microbiological rate experiments, assisted with nutrient and DOC analyses, performed microscopy.

Manuscript Information Page

Brent C. Christner, John C. Priscu, Amanda M. Achberger, Carlo Barbante, Sasha P. Carter, Knut Christianson, Alexander B. Michaud, Jill A. Mikucki, Andrew C. Mitchell, Mark L. Skidmore, Trista J. Vick-Majors
Nature
Status of Manuscript:
____ Prepared for submission to a peer-reviewed journal
____ Officially submitted to a peer-review journal
_ ___ Accepted by a peer-reviewed journal
_ X_ Published in a peer-reviewed journal

Nature Publishing Group
In Volume 512, 310-313, 2014

LETTER

doi:10.1038/nature13667

A microbial ecosystem beneath the West Antarctic ice sheet

Brent C. Christner[1], John C. Priscu[2], Amanda M. Achberger[1], Carlo Barbante[3], Sasha P. Carter[4], Knut Christianson[5]†, Alexander B. Michaud[2], Jill A. Mikucki[6], Andrew C. Mitchell[7], Mark L. Skidmore[8], Trista J. Vick-Majors[2] & the WISSARD Science Team‡

Liquid water has been known to occur beneath the Antarctic ice sheet for more than 40 years[1], but only recently have these subglacial aqueous environments been recognized as microbial ecosystems that may influence biogeochemical transformations on a global scale[2–4]. Here we present the first geomicrobiological description of water and surficial sediments obtained from direct sampling of a subglacial Antarctic lake. Subglacial Lake Whillans (SLW) lies beneath approximately 800 m of ice on the lower portion of the Whillans Ice Stream (WIS) in West Antarctica and is part of an extensive and evolving subglacial drainage network[5]. The water column of SLW contained metabolically active microorganisms and was derived primarily from glacial ice melt with solute sources from lithogenic weathering and a minor seawater component. Heterotrophic and autotrophic production data together with small subunit ribosomal RNA gene sequencing and biogeochemical data indicate that SLW is a chemosynthetically driven ecosystem inhabited by a diverse assemblage of bacteria and archaea. Our results confirm that aquatic environments beneath the Antarctic ice sheet support viable microbial ecosystems, corroborating previous reports suggesting that they contain globally relevant pools of carbon and microbes[2,4] that can mobilize elements from the lithosphere[6] and influence Southern Ocean geochemical and biological systems[7].

Almost 400 subglacial lakes have been identified beneath the Antarctic ice sheet[8]. Speculation on the presence of functional microbial ecosystems within these lakes followed their discovery[1] and motivated the initial studies of samples originating from Subglacial Lake Vostok (SLV)[9,10]. However, the body of microbiological data from SLV has been a point of contention, primarily because all studies were based on analyses of frozen (that is, accreted) lake water samples recovered from a borehole containing a contaminated hydrocarbon drilling fluid[3]. Our report documents the first analysis of water and surficial sediments collected directly from a subglacial lake beneath the West Antarctic ice sheet (WAIS) using microbiologically clean drilling and sampling techniques[11].

The water residence time for SLV exceeds 10,000 years[12], while that for 'active' lakes such as SLW is on the order of years to decades[5,8]. SLW is part of a network of three major reservoirs beneath the lower ice plain of the WIS that regulate water transport to a subglacial estuary at the grounding zone, linking the hydrological system to the sub-ice-ocean cavity beneath the Ross Ice Shelf[5,13] (Fig. 1). During two separate drainage events in 2006 and 2009, SLW discharged ~0.15 km^3 of water over two six-month periods, each time lowering the lake level by about 5 m[5,14]. The drilling location to access SLW was selected using reflection seismology[13] and ice-penetrating radar[14] data, and corresponded to the region of maximum predicted water column thickness, lowest hydropotential, and largest satellite-measured surface elevation changes (Fig. 1).

A hot water drilling system was used to create a ~0.6 m diameter borehole through the overlying ice sheet into SLW, allowing for physical measurements and the direct collection of water column and sediment samples. Drilling and lake entry procedures followed recommendations for environmental protection of subglacial aquatic environments[11], incorporating rigorous measures to reduce the introduction of foreign microbiota and material into SLW and the interconnected subglacial drainage

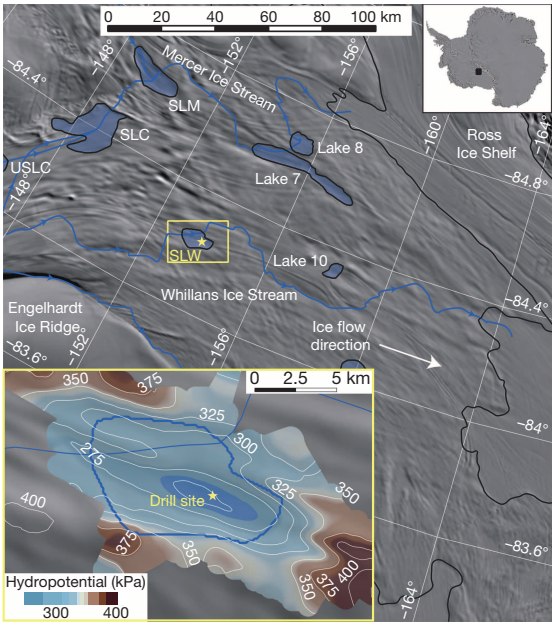

Figure 1 | Locator map of the WIS and SLW. The yellow box and star indicate the general location of the lake and the drill site; maximum extent of SLW and other lakes[28] under the ice stream are shaded in blue; predicted subglacial water flowpaths through SLW and other subglacial lakes are represented by blue lines with arrows; the black line denotes the ice-sheet grounding line at the edge of the Ross Ice Shelf[29]. Inset (expanded from area in yellow box) shows details of SLW with both maximum (solid blue line) and minimum lake extent (shaded blue area), hydropotential contours (white isolines; 25 kPa interval), and drill site (yellow star; 84.240° S 153.694° W). Background imagery is MODIS MOA[30].

[1]Department of Biological Sciences, Louisiana State University, Baton Rouge, Louisiana 70803, USA. [2]Department of Land Resources and Environmental Science, Montana State University, Bozeman, Montana 59717, USA. [3]Institute for the Dynamics of Environmental Processes – CNR, Venice, and Department of Environmental Sciences, Informatics and Statistics, Ca'Foscari University of Venice, Venice 30123, Italy. [4]Institute of Geophysics and Planetary Physics, Scripps Institution of Oceanography, University of California San Diego, La Jolla, California 92093, USA. [5]Physics Department, St Olaf College, Northfield, Minnesota 55057, USA. [6]Department of Microbiology, University of Tennessee, Knoxville, Tennessee 37996, USA. [7]Department of Geography and Earth Sciences, Aberystwyth University, Aberystwyth SY23 3DB, UK. [8]Department of Earth Science, Montana State University, Bozeman, Montana 59717, USA. †Present address: Courant Institute of Mathematical Sciences, New York University, New York, New York 10012, USA (K.C.).
‡Lists of participants and their affiliations appear at the end of the paper.

system. Video inspection of the borehole and temperature measurements revealed that the ice–water interface occurred at 801 ± 1 m below the surface (mbs) and the lake depth at the borehole site was ~2.2 m at the time of sampling. Two borehole deployments of a conductivity, temperature and depth (CTD) sonde together with data from three discrete hydrocasts showed that SLW had an average *in situ* temperature of −0.49 °C, pH of 8.1, and conductivity of 720 μS cm^{-1}; properties that were distinctly different from the borehole water (Table 1).

Water from three discrete hydrocasts in SLW had near identical geochemical compositions on the basis of major ion chemistry (Table 1) and all showed oxygen under-saturation (~16% of air-saturated water). Since there is no definitive evidence of lake water freezing to the bottom of the overlying ice sheet as in SLV[12], it is unlikely that lake water constituents in SLW are influenced significantly by freeze concentration. The $\delta^{18}O$ of H_2O for SLW (−38.0‰) was similar to glacial ice sampled approximately 10 m above the ice–water interface from the neighbouring Kamb Ice Stream[15] (KIS; −38 to −39‰), indicating that glacial melt was the dominant water source for SLW. A considerable fraction of the major anions and cations originated from mineral weathering, with a minor seawater component based on Cl^- to Br^- ratios (Extended Data Table 1). Crustally derived non-seawater solutes in SLW showed a dominance of weathering products from silicate minerals ($Na^+ + K^+$) over carbonate minerals ($Mg^{2+} + Ca^{2+}$), similar to other sub ice-sheet systems in Greenland and Antarctica[6,7] (Supplementary Discussion). The dominant non-seawater anions (SO_4^{2-} and HCO_3^-) were probably products of sulphide oxidation, carbonation reactions, and carbonate dissolution[7]. Sulphide oxidation and carbonation reactions have been demonstrated to be microbially driven in subglacial systems and linked to enhanced rates of mineral weathering[16]. Although clay minerals are a potential source of the relatively high F^- concentrations in SLW (Table 1), subglacial volcanism in the upstream catchment supplying SLW[17] may also contribute.

Table 1 | Biogeochemical data from the SLW borehole, water column, and surficial sediments

Parameter	Borehole*	Water column†	Sediments‡
Physical			
Temperature (°C)§	−0.17 (0.25)	−0.49 (0.03)	n.d.
Conductivity (μS cm^{-1} @ 25 °C)‖	5.3	720 (10)	860
pH‖	5.4	8.1 (0.1)	7.3
Redox (mV (SHE))‖	n.d.	382	n.d.
Microbiological			
Cell density (cells ml^{-1})	6.9×10^2 (51.0)	1.3×10^5 (0.4×10^5)	n.d.
Cellular ATP (pmol l^{-1})	0.04 (0.002)	3.70 (1.00)	n.d.
$^{[3]}$H]thymidine¶	n.d.	13.7 (1.3)	46.6 (5.6)
$^{[3]}$H]leucine¶	n.d.	2.9 (0.4)	0.9 (0.04)
^{14}C-bicarbonate (ng C l^{-1} d^{-1})	n.d.	32.9 (4.2)	n.d.
Carbon and nutrients			
Dissolved oxygen (μmol l^{-1})	n.d.	71.9 (12.5)	n.d.
DIC (mmol l^{-1})	n.d.	2.11 (0.03)	n.d.
DOC (μmol l^{-1})	n.d.	221 (55)	n.d.
Acetate (μmol l^{-1})	n.d	1.3 (0.2)	n.d.
Formate (μmol l^{-1})	n.d	1.2 (0.3)	n.d.
PC#	n.d.	78.5 (7.4)	384.2 (37.0)
PN#	n.d.	1.2 (0.4)	21.5 (1.7)
PC:PN (molar)	n.d.	65.4 (0.3)	17.9 (0.4)
NH_4^+ (μmol l^{-1})	n.d.	2.4 (0.6)	n.d.
NO_2^- (μmol l^{-1})	n.d.	0.1 (0.1)	n.d.
NO_3^- (μmol l^{-1})	n.d.	0.8 (0.5)	9.1
PO_4^{3-} (μmol l^{-1})	n.d.	3.1 (0.7)	7.3
DIN:SRP (molar)	n.d.	1.1 (0.4)	n.d.
Major ions (μeq l^{-1})			
Na^+	n.d.	5,276 (18)	6,977
K^+	n.d.	186 (4.2)	293 (1.0)★
Mg^{2+}	n.d.	507 (12)	596 (101)★
Ca^{2+}	n.d	859 (29)	860 (104)★
F^-	n.d.	31.5 (0.4)	34.0
Cl^-	n.d.	3,537 (3.4)	4,943
Br^-	n.d.	6 (0.01)	7 (0.4)★
SO_4^{2-}	n.d.	1,111 (0.4)	1,230
HCO_3^-	n.d	2,111 (35)	2,238**
Stable isotopes††			
$\delta^{18}O$ of H_2O	n.d.	−38.0‰	−37.5‰
$\Delta^{17}O$ of NO_3^-	n.d.	−0.1 to 0.2‰	n.d.

* Borehole water sampled by hydrocast at 672 mbs before lake entry.
† Water column data represent averages (± s.d.) from hydrocasts collected on 28 January 2013 (cast 1), 30 January (cast 2) and 31 January (cast 3) 2013, except for $^{[3]}$H]leucine incorporation, which is an average of cast 1 and 3 only.
‡ The sediment data correspond to measurements from the upper 2 cm of surficial sediments.
§ Average (± s.d.) of *in situ* measurements made through the lake water column at ~10 cm intervals with a SBE 19*plus*V2 SeaCAT Profiler CTD on 28 January and 30 January 2013.
‖ Based on measurements from discrete water samples brought to the surface.
¶ Macromolecular incorporation rates of tritium were converted to cellular carbon and presented along with bicarbonate incorporation as average ng C l^{-1} d^{-1} (± s.d.) for water or average ng C d^{-1} gram dry weight $^{-1}$ (± s.d.) of sediment.
# Average (± s.d.) μmol l^{-1} for water and average (± s.d.) μmol g dry weight sed^{-1} for surficial sediment.
★ Surficial sediment porewater major ions are the average (± range) of two replicates.
** Calculated based on charge balance.
†† Values are per thousand and reported relative to V-SMOW. The range of 2 measurements is given for $\Delta^{17}O$ of NO_3^-.
n.d., no data available.

Ammonium accounted for 73% of the dissolved inorganic nitrogen pool within the water column of SLW (Table 1). Given that mineral sources of ammonium are minor, the majority of the ammonium is probably from microbial mineralization. Soluble reactive phosphorus levels were similar to the total inorganic nitrogen pool (dissolved N:P molar ratio of 1.1), implying a biologically nitrogen-deficient environment, relative to phosphorus. Unfortunately, sample limitations precluded measurement of dissolved organic N and P concentrations to assess their nutritional contribution. In addition to its nutritional role, ammonium is also an energy source for chemolithoautotrophic ammonium-oxidizing bacteria and archaea. Evidence for complete nitrification in the aerobic SLW water column was supported by $\Delta^{17}O$ of NO_3 values (−0.1‰ to 0.2‰) that indicated microbial processes rather than atmospheric input was the dominant source for nitrate in the lake[18]. Particulate organic C (PC) to N (PN) molar ratios in the water column exceeded that of actively growing bacteria by almost 15-fold, suggestive of elevated levels of nitrogen-poor detritus. Dissolved organic carbon (DOC) in the water column averaged 221 ± 55 μmol l^{-1}, which is about five times greater than average values for the deep ocean[19] and similar to the maximum range estimate for SLV[9,20] (86–160 μmol l^{-1}). Acetate and formate concentrations in the water column averaged 1.3 and 1.2 μmol l^{-1}, respectively, indicating that at least a portion of the DOC pool was labile. The conductivity and microbiological data (Table 1 and Fig. 2a) showed that little mixing occurred between the borehole water and lake, supporting the hypothesis that DOC in the water column originated from SLW. The lack of winnowing in sediment cores from SLW, in concert with the fact that similar DOC concentrations were obtained as the overlying ice moved ~4 m during the course of our operations, provided evidence that water column DOC did not result from sediment disturbance during drilling operations. The DOC in SLW most likely originated from upward diffusion of DOC associated with ancient marine sediments[4] (SLW sediment surface area:depth ratio ≈ 30,000), chemoautotrophic production, or from a combination of both sources.

The average cell density in the SLW water column was 1.3×10^5 cells ml^{-1} (Table 1); microscopy revealed the presence of numerous morphotypes, approximately 10% of which were filamentous (Fig. 3). Cellular ATP, a proxy for viable biomass, in SLW was 3.7 pmol ATP l^{-1} (Table 1). Cell and ATP concentrations were 188- and 93-fold higher, respectively, than those observed in the borehole water before breakthrough to SLW. Carbon biomass estimates for SLW water based on the ATP data (480 ± 100 ng C l^{-1}) were 3- to 50-fold higher than those observed beneath the Ross Ice Shelf at site J9 (ref. 21). Analysis of small subunit ribosomal RNA (SSU rRNA) sequences amplified from the water column samples showed that the community was similar among replicate lake samples, was distinct from the drilling water (Fig. 2a), and contained at least 3,931 operational taxonomic units (OTUs; Extended Data Table 2). An OTU closely related to the nitrite oxidizing betaproteobacterium '*Candidatus* Nitrotoga arctica'[22] comprised 13% of the sequence data, and many of the most abundant phylotypes were closely related to chemolithoautotrophic species that use reduced nitrogen, iron or sulphur compounds as energy sources (Fig. 2b; Supplementary Discussion). Two of

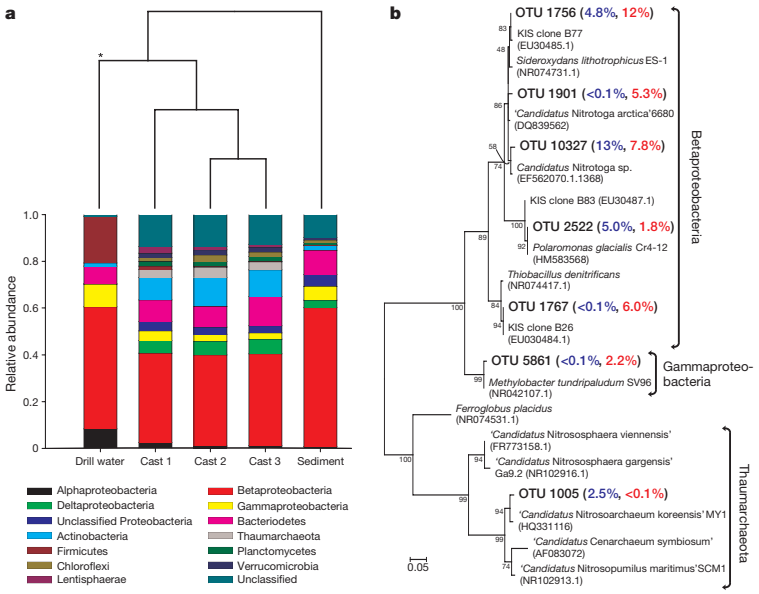

Figure 2 | Phylogenetic analysis of SSU gene sequences obtained from the SLW water column, surficial sediment (0–2 cm) and drilling water. **a**, Cluster analysis of the microbial phylogenetic structure in the samples (top) and the relative abundance of bacterial and archaeal phyla in the water and sediment samples (bottom). The Proteobacteria were split into classes for greater detail. The asterisk indicates statistical significance (analysis of molecular variance, AMOVA, P value < 0.001). **b**, Phylogenetic analysis of bacterial and archaeal OTUs abundant in the SLW water column and sediments. The accession numbers of nearest neighbours and reference taxa are listed parenthetically. Bootstrap values are shown at the nodes. SLW phylotypes are bolded and followed by the percentage each represented in the water column (blue) and sediment (red) libraries. The scale bar indicates the number of nucleotide substitutions per position.

the abundant water column OTUs had high identity (>99%) to SSU sequences previously reported from sediments sampled beneath the KIS[23] (Fig. 2b). Preliminary attempts to detect eukaryotic SSU sequences in the SLW water column were unsuccessful.

Average dark [^{14}C]bicarbonate incorporation in the water column samples (32.9 ng C l^{-1} d^{-1}; Table 1) exceeded average rates of heterotrophic production based on [^{3}H]thymidine (13.7 ng C l^{-1} d^{-1}) and [^{3}H]leucine (2.9 ng C l^{-1} d^{-1}) incorporation by 2- and 11-fold, respectively. Assuming that the thymidine and leucine values represent net incorporation, and that respiratory losses were 87% of net incorporation (which are average values for Antarctic McMurdo Dry Valley lakes[24]), the gross bacterial carbon demand (net productivity + respiration) would be 105 and 23 ng C l^{-1} d^{-1}, respectively. If dark [^{14}C]bicarbonate incorporation represents new organic carbon production via chemoautotrophy, the observed rates would meet between 31% and 143% of the heterotrophic carbon demand in the system. It should be noted that the effect of pressure (~ 8 MPa in SLW) was not tested and may influence the absolute rates of metabolism measured.

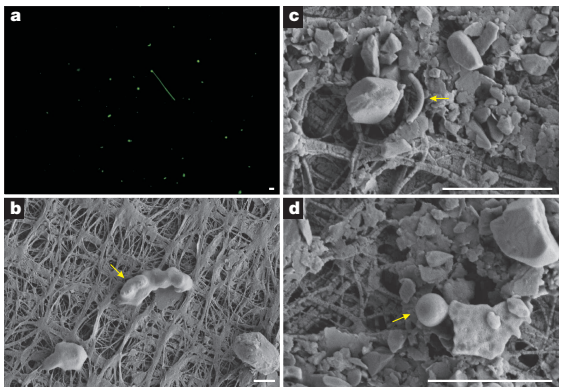

Figure 3 | Morphological diversity of microbial cells in the SLW water column. **a**, Epifluorescence micrograph showing a variety of cell morphotypes, which was confirmed by scanning electron microscopy (SEM; **b**–**d**). The yellow arrows in the SEM images indicate cells with rod (**b**), curved rod (**c**) and coccoid (**d**) morphologies. Scale bar, 2 μm.

Pore water conductivity (860 μS cm^{-1}) and pH (7.3) in SLW's surficial sediments were within 20% of the lake water values (Table 1). Upward diffusion of ions from sediment pore water is presumably the primary source of the ions in the water column. Average surficial sediment PC and PN concentrations were 384.2 and 21.5 μmol g dry weight^{-1}, respectively, and represented 0.43% and 0.03% of sediment dry weight. The molar PC:PN ratio in the surficial sediment layer (17.9) was 3.7-fold lower than that in the water column (Table 1), indicative of nitrogen-enriched sedimentary particulate organic matter, with respect to water column suspensoids. On the basis of rates of thymidine and leucine incorporation, average heterotrophic production in the surficial sediment was 46.6 and 0.9 ng C d^{-1} g dry weight^{-1}, respectively. Approximately 75% of the OTUs from the surficial sediments classified within the Proteobacteria (Fig. 2a). Although many phylotypes in the water column were also abundant in the surficial sediments (Fig. 2b), ~70% of the OTUs were unique to the sediment environment. The nearest neighbours of the most abundant phylotypes in the surface sediments were chemolithoautotrophs or species that use C1 hydrocarbons as carbon and energy sources (Fig. 2b, Supplementary Discussion).

Our data show that SLW supports a metabolically active and phylogenetically diverse ecosystem that functions in the dark at sub-zero temperatures, confirming more than a decade of circumstantial evidence regarding the presence of life beneath Antarctica's ice sheet[9,10,20,23]. Rate experiments revealed that chemoautotrophic primary production in SLW

is adequate to support heterotrophic metabolism in the subglacial ecosystem. The abundance of taxa related to nitrifiers[22,25] in concert with elevated ammonium and $\Delta^{17}O$ of NO_3 values near 0‰ in the water column (Table 1) implies that nitrification may be a fundamental chemoautotrophic pathway of new organic carbon production in SLW. Similar conclusions regarding the ecological significance of nitrification have been drawn for the water column beneath the Ross Ice Shelf[26] and in McMurdo Sound[27]. Given the prevalence of subglacial water in Antarctica[8], our data from SLW lead us to contend that aquatic microbial ecosystems are common features of the subsurface environment that exists beneath the $\sim 10^7$ km^2 Antarctic ice sheet.

Online Content Methods, along with any additional Extended Data display items and Source Data, are available in the online version of the paper; references unique to these sections appear only in the online paper

Received 2 April; accepted 9 July 2014.

1. Oswald, G. K. A. & De Robin, G. Q. Lakes beneath the Antarctic ice sheet. *Nature* **245,** 251–254 (1973).
2. Priscu, J. C. *et al.* in *Polar Lakes and Rivers* (eds Vincent, W. & Laybourn-Parry, J.) Ch.7 (Oxford Univ. Press, 2008).
3. Christner, B. C., Skidmore, M. L., Priscu, J. C., Tranter, M. & Foreman, C. M. in (eds Margesin, R., Schinner, F., Marx., J.-C. & Gerday, C.) *Psychrophiles: From Biodiversity to Biotechology* pp. 51–71 (Springer, 2008).
4. Wadham, J. L. *et al.* Potential methane reservoirs beneath Antarctica. *Nature* **488,** 633–637 (2012).
5. Fricker, H. A., Scambos, T., Bindschadler, R. & Padman, L. An active subglacial water system in West Antarctica mapped from space. *Science* **315,** 1544–1548 (2007).
6. Skidmore, M., Tranter, M., Tulaczyk, S. & Lanoil, B. Hydrochemistry of ice stream beds–evaporitic or microbial effects? *Hydrol. Processes* **24,** 517–523 (2010).
7. Wadham, J. L. *et al.* Biogeochemical weathering under ice: size matters. *Glob. Biogeochem. Cycles* **24,** GB3025 (2010).
8. Wright, A. & Siegert, M. A fourth inventory of Antarctic subglacial lakes. *Antarct. Sci.* **24,** 659–664 (2012).
9. Priscu, J. C. *et al.* Geomicrobiology of subglacial ice above Lake Vostok. *Science* **286,** 2141–2144 (1999).
10. Karl, D. M. *et al.* Microorganisms in the accreted ice of Lake Vostok. *Science* **286,** 2144–2147 (1999).
11. Priscu, J. C. *et al.* A microbiologically clean strategy for access to the Whillans Ice Stream subglacial environment. *Antarct. Sci.* **25,** 637–647 (2013).
12. Bell, R. E. *et al.* Origin and fate of Lake Vostok water frozen to the base of the East Antarctic ice sheet. *Nature* **416,** 307–310 (2002).
13. Horgan, H. J. *et al.* Estuaries beneath ice sheets. *Geology* **41,** 1159–1162 (2013).
14. Christianson, K., Jacobel, R. W., Horgan, H. J., Anandakrishnan, S. & Alley, R. B. Subglacial Lake Whillans—Ice-penetrating radar and GPS observations of a shallow active reservoir beneath a West Antarctic ice stream. *Earth Planet. Sci. Lett.* **331–332,** 237–245 (2012).
15. Vogel, S. W. *et al.* Subglacial conditions during and after stoppage of an Antarctic ice stream: is reactivation imminent? *Geophys. Res. Lett.* **32,** L14502 (2005).
16. Montross, S. N., Skidmore, M., Tranter, M., Kivimäki, A.-L. & Parkes, R. J. A microbial driver of chemical weathering in glaciated systems. *Geology* **41,** 215–218 (2013).
17. Blankenship, D. D. *et al.* Active volcanism beneath the West Antarctic ice-sheet and implications for ice-sheet stability. *Nature* **361,** 526–529 (1993).
18. Michalski, G., Bhattacharya, S. K. & Girsch, G. NO_x cycle and tropospheric ozone isotope anomaly: an experimental investigation. *Atmos. Chem. Phys. Discuss.* **13,** 9443–9483 (2013).
19. Hansell, D. A. & Carlson, C. A. Deep-ocean gradients in the concentration of dissolved organic carbon. *Nature* **395,** 263–266 (1998).
20. Christner, B. C. *et al.* Limnological conditions in Subglacial Lake Vostok, Antarctica. *Limnol. Oceanogr.* **51,** 2485–2501 (2006).
21. Azam, F. *et al.* Occurrence and metabolic activity of organisms under the Ross Ice Shelf, Antarctica, at Station J9. *Science* **203,** 451–453 (1979).
22. Alawi, M., Lipski, A., Sander, T., Pfeiffer, E.-M. & Spieck, E. Cultivation of a novel cold-adapted nitrite oxidizing betaproteobacterium from the Siberian Arctic. *ISME J.* **1,** 256–264 (2007).
23. Lanoil, B. *et al.* Bacteria beneath the West Antarctic ice sheet. *Environ. Microbiol.* **11,** 609–615 (2009).
24. Takacs, C., Priscu, J. & McKnight, D. Bacterial dissolved organic carbon demand in McMurdo Dry Valley Lakes, Antarctica. *Limnol. Oceanogr.* **46,** 1189–1194 (2001).
25. Walker, C. B. *et al. Nitrosopumilus maritimus* genome reveals unique mechanisms for nitrification and autotrophy in globally distributed marine crenarchaea. *Proc. Natl Acad. Sci. USA* **107,** 8818–8823 (2010).
26. Horrigan, S. G. Primary production under the Ross Ice Shelf, Antarctica. *Limnol. Oceanogr.* **26,** 378–382 (1981).
27. Priscu, J. C., Downes, M. T., Priscu, L. R., Palmisano, A. C. & Sullivan, C. W. Dynamics of ammonium oxidizer activity and nitrous oxide (N_2O) within and beneath Antarctic sea ice. *Mar. Ecol. Prog. Ser.* **62,** 37–46 (1990).
28. Fricker, H. A. & Scambos, T. Connected subglacial lake drainage activity on lower Mercer and Whillans Ice Streams, West Antarctica, 2003–2008. *J. Glaciol.* **55,** 303–315 (2009).
29. Depoorter, M. A. *et al.* Calving fluxes and basal melt rates of Antarctic ice shelves. *Nature* **502,** 89–92 (2013).
30. Haran, T., Bohlander, J., Scambos, T. & Fahnestock, M. MODIS mosaic of Antarctica (MOA) image map. http://dx.doi.org/10.7265/N5ZK5DM5 (National Snow and Ice Data Center, 2005).

Supplementary Information is available in the online version of the paper.

Acknowledgements The Whillans Ice Stream Subglacial Access Research Drilling (WISSARD) project was funded by National Science Foundation grants (0838933, 0838896, 0838941, 0839142, 0839059, 0838885, 0838855, 0838763, 0839107, 0838947, 0838854, 0838764 and 1142123) from the Division of Polar Programs. Partial support was also provided by funds from NSF award 1023233 (B.C.C.), NSF award 1115245 (J.C.P.), the NSF's Graduate Research Fellowship Program (1247192; A.M.A.), the Italian National Antarctic Program (C.B.), and fellowships from the NSF's IGERT Program (0654336) and the Montana Space Grant Consortium (A.B.M.). Logistics were provided by the 139th Expeditionary Airlift Squadron of the New York Air National Guard, Kenn Borek Air, and by many dedicated individuals working as part of the Antarctic Support Contractor, managed by Lockheed-Martin. The drilling was directed by F. Rack; D. Blythe, J. Burnett, C. Carpenter, D. Duling (chief driller), D. Gibson, J. Lemery, A. Melby and G. Roberts provided drill support at SLW. L. Geng, B. Vandenheuvel, A. Schauer and E. Steig provided assistance with the stable isotopic analyses. We thank J. Dore for assistance with the nutrient analysis.

Author Contributions The manuscript was written by B.C.C. and J.C.P.; A.M.A. generated and analysed the molecular data; C.B., A.C.M. and M.L.S. conducted and interpreted the chemical measurements; S.P.C. and K.C. provided geophysical data; J.A.M. obtained and examined the CTD data; A.B.M. and T.J.V. contributed and analysed physiological and biogeochemical data; M.L.S. conducted and interpreted the isotopic analyses; and T.J.V. provided the micrographs. All authors contributed to the study design and acquisition of samples and/or data.

Author Information The SSU sequence data are deposited in the NCBI SRA database under the accession number SRP041285. Reprints and permissions information is available at www.nature.com/reprints. The authors declare no competing financial interests. Readers are welcome to comment on the online version of the paper. Correspondence and requests for materials should be addressed to B.C.C. (xner@lsu.edu) or J.C.P. (jpriscu@montana.edu).

WISSARD Science Team Members

W. P. Adkins[1], S. Anandakrishnan[2], G. Barcheck[3], L. Beem[3], A. Behar[4], M. Beitch[3], R. Bolsey[3], C. Branecky[3], R. Edwards[5], A. Fisher[3], H. A. Fricker[6], N. Foley[3], B. Guthrie[7], T. Hodson[7], R. Jacobel[8], S. Kelley[5], K. D. Mankoff[3], E. McBryan[4], R. Powell[7], A. Purcell[9], D. Sampson[3], R. Scherer[7], J. Sherve[5], M. Siegfried[6] & S. Tulaczyk[3]

[1]Department of Biological Sciences, Louisiana State University, Baton Rouge, Louisiana 70803, USA. [2]Department of Geosciences, Pennsylvania State University, University Park, Pennsylvania 16802, USA. [3]Department of Earth and Planetary Sciences, University of California, Santa Cruz, Santa Cruz, California 95064, USA. [4]School of Earth and Space Exploration, Arizona State University, Tempe, Arizona 85287, USA. [5]Department of Land Resources and Environmental Science, Montana State University, Bozeman, Montana 59717, USA. [6]Institute of Geophysics and Planetary Physics, Scripps Institution of Oceanography, University of California San Diego, La Jolla, California 92093, USA. [7]Department of Geology and Environmental Geosciences, Northern Illinois University, DeKalb, Illinois 60115, USA. [8]Physics Department, St Olaf College, Northfield, Minnesota 55057, USA. [9]Department of Microbiology, University of Tennessee, Knoxville, Tennessee 37996, USA.

METHODS

Site selection and description. SLW was discovered using satellite laser altimetry and initially identified as a region ($59 \pm 12\,km^2$) of temporally varying surface elevation; it is one of 11 active subglacial lakes documented beneath the WIS[5]. SLW fills and drains every few years as part of a series of hydrologically linked subglacial lakes in the area, eventually draining to the ocean[5,28,31]. Ice-penetrating radar and active-source seismic data estimated that the maximum lake depth does not exceed 8 and 15 m at low- and high-stand, respectively[14,32]. A lake-level rise of ~5 m from the low-stand lake level plus ice-flexural effects are sufficient to initiate flow over a drainage divide and trigger lake drainage. During a drainage event, ~0.15 km^3 of water drains in a six-month timeframe at a water flux of ~10 $m^3\,s^{-1}$ (refs 5, 14). Thus, SLW is a shallow active hydrological reservoir beneath an active ice stream. The deepest point in the seismically detected water column was selected as the drill site (84.240° S 153.694° W; Fig. 1). Drilling and subglacial lake access occurred during a near low-stand state in late January 2013[33].

Hot water drilling and clean access to SLW. A hot water drilling system was used between 23–27 January 2013 to melt through the ~801 m thick ice sheet, creating an access borehole (minimum diameter ~60 cm) for direct sampling and to conduct *in situ* measurements of the SLW water column and sediments. Microbial cells in the drilling water and on exposed surfaces of the hose, cables, and deployed equipment were reduced and killed through the use of four complementary technologies: (1) filtration, (2) ultraviolet irradiation, (3) pasteurization, and (4) disinfection with 3% w/v H_2O_2 (ref. 11). The drilling water, derived from the overlying ice sheet, was continuously circulated through a water treatment system that removed micron and sub-micron sized particles (>0.2 μm), irradiated the drilling water with two germicidal wavelengths of ultraviolet radiation (185 nm ~40,000 $\mu W\,s^{-1}\,cm^{-2}$ and 254 nm ~175,000 $\mu W\,s^{-1}\,cm^{-2}$), and pasteurized the water at 90 °C to reduce the viability of persisting microbial contamination. Ports were plumbed along the system's flow path, allowing discrete water samples to be obtained before and after each stage[11]. The drill hose and instrument cables were deployed at a rate no greater than 1 $m\,s^{-1}$ through a custom borehole collar that contained 12 amalgam pellet ultraviolet lamps, providing a cumulative germicidal ultraviolet dosage of at least 40,000 $\mu W\,s^{-1}\,cm^{-2}$ (Arapahoe SciTech). All borehole sampling tools and instruments were spray-saturated with 3% w/v H_2O_2 and staged in sealed polyethylene bags until tool deployment. Single-use protective apparel (Tyvek) was worn by all personnel during borehole science operations. The efficacy of the clean access technology and procedures were tested thoroughly before use in the field and are detailed elsewhere[11].

Drilling was conducted at a flow rate of ~135 l min^{-1} to ~700 mbs, whereupon the drill was withdrawn, the borehole was inspected with video, and a hydrocast was conducted at 672 mbs to measure the chemical and microbiological properties of the borehole water. To ensure that borehole water did not enter the lake upon breakthrough, the borehole hydrostatic pressure was reduced by ~35% (that is, the water level was lowered from 80 to 108 mbs) below the expected equilibration level for 800 m of ice[14]. Drilling subsequently proceeded at the reduced flow rate of 19 l min^{-1}, and at 08:02 on 27 January (UTC+12), the load on the hose diminished as the drill reached ~801 mbs. Two minutes later, the head above the borehole water return pump (stationed at 110 mbs) rose rapidly and remained at ~80 mbs, confirming hydrostatic equilibration between the borehole and lake water (that is, breakthrough to SLW). Importantly, the rise in borehole water confirmed that no drilling water entered the subglacial environment during breakthrough. To maintain the borehole and offset freeze back, thermal energy was added to the borehole by redeploying the drill at a flow rate of ~135 l min^{-1}. Borehole reaming was conducted after breakthrough to the lake by slowly withdrawing the drill (~1 m min^{-1}). A second 24 h reaming occurred 32 h after initial penetration of the lake to ensure successful deployment of all sampling tools. All *in situ* measurements and discrete sampling occurred over a 3-day period.

Temperature and depth. A SBE 19*plus*V2 SeaCAT Profiler CTD (Seabird Electronics, Inc.) was used to measure temperature and depth within the borehole and lake water column. The instrument was deployed in profiling mode and lowered at a rate of ~0.5 $m\,s^{-1}$. Borehole depths are referenced to the snow surface in proximity to the borehole. The water column depth in SLW (that is, the distance between the ice–water interface and underlying sediments) was estimated using CTD data to distinguish differences in water mass upon entry to the lake water column from the borehole. Lake depth was obtained from the top of the lake water mass to the depth where the sonde contacted the bottom. This depth estimate was corroborated with a calibrated cable attached to a real-time borehole video camera.

Water and sediment sampling. Following ref. 11, discrete samples of the drilling water (~20 l) were obtained at two time points during the drilling process. Samples of water from the input to the filtration module, input to the borehole, water returning from the borehole, and a hydrocast at 672 mbs before lake entry were collected and concentrated onto 142 mm 0.2 μm Supor membrane filters (Pall Corporation). The filters were processed identically to those from the SLW water column (see below).

Three discrete water samples were collected between 28 and 31 January 2013 at approximately mid-depth in the ~2.2 m SLW water column. Bulk water was collected using 10 l Niskin bottles and transferred via acid (10% HCl) leached silicon tubing to clean bottles following the limnological procedures outlined by the McMurdo Long Term Ecological Research (LTER) Program[34].

SLW water column particulate matter for nucleic acid analysis was filter concentrated *in situ* using a Large Volume Water Transfer System (WTS-LV) that was modified to fit the minimum borehole diameter of 30 cm (McLane Research Laboratories Inc.). The WTS-LV has a 3-tier 142 mm filter holder that accepts filters in series for size fractionation of particulates in the sample water. There were three separate casts of the WTS-LV in SLW and between 4.9 and 7.2 l of water was filter-concentrated during each 2 h deployment. In cast 1, the filter housing was loaded with a 10 μm nylon mesh screen together with 3 μm and 0.2 μm Supor membrane filters. The filters for cast 2 and 3 had pore sizes of 3.0 μm, 0.8 μm, and 0.2 μm. Immediately after recovery, the filter housing unit was detached from the pump and opened in a class 100 laminar flow hood. The filters were placed in sterile 142 mm Petri dishes, sliced into quarters with a clean scalpel, and transferred to a cryovial that contained 7 ml of DNA lysis solution (40 mM EDTA pH 8.0, 50 mM Tris pH 8.3, 0.73 M sucrose). The preserved samples were immediately frozen for transport to McMurdo Station and stored at −80 °C.

Surficial sediments were collected using a multicoring device (Uwitec) that had a core barrel inner diameter of 59.5 mm. Sediment pore water was obtained by inserting Rhizon samplers[35] (0.2 μm pore size) through predrilled holes in the core barrel liner and extracted under negative pressure created with a 10 ml sterile syringe. Surficial sediment (0 to 2 cm depth) from the cores was sampled inside a class 100 clean hood using a cleaned core cutter (Uwitec). The sediment samples for molecular biological analysis were placed in 60 ml sterile Nalgene bottles containing 10 ml of the DNA lysis solution and frozen.

Specific electrical conductivity (at 25 °C) and pH of the lake and sediment pore water were determined using a YSI model 3252 probe connected to a YSI model 3100 conductivity meter and a Beckman model 200 pH meter. Both probe and meter combinations were calibrated immediately before sample measurements were made.

Inorganic and organic chemistry. Particulate organic C (PC) and N (PN) samples from the water column were vacuum (~0.3 atm) filtered onto pre-combusted (450 °C for 4 h) Whatman GF/F filters and analysed on a CE Instruments Flash EA 112 (ThermoQuest, San Jose, CA). The filters and sediment samples which had been dewatered via centrifugation were fumed for 24 h over fresh 12 M HCl to remove inorganic carbon and dried for 24 h at 90 °C before analysis. Dissolved oxygen was measured using the azide modification of the mini-Winkler titration[36]. Dissolved inorganic carbon was measured by infrared gas analysis of acid sparged samples. Samples for dissolved inorganic N and P were filtered through pre-combusted and 1% v/v HCl leached GF/F filters, collected in 1% HCl leached HDPE bottles, and frozen for shipment to the US where nitrate, nitrite, ammonium, and soluble reactive P were analysed colorimetrically[34]. Major ions and organic acids from SLW water and sediment porewater were analysed on a Metrohm ion chromatograph using a C4 cation column and an aSupp5 anion column.

Stable isotope analysis. Stable isotope measurements were conducted at the Isolab (University of Washington, Seattle). Measurements of oxygen isotope ratios of lake water and pore water samples were made using a Picarro cavity ring-down laser spectrometer. Nitrate for $\Delta^{17}O$ determination in the water samples was concentrated using an anionic resin[37] followed by the bacterial reduction and thermal decomposition method[38,39]. $\Delta^{17}O$ of NO_3 was analysed with a Finnigan Delta Plus Advantage isotope ratio mass spectrometer. Isotope measurements are reported using standard δ notation in per thousand relative to Vienna Standard Mean Ocean Water (VSMOW).

pH and oxidation-reduction measurements. Sediment pH was measured with a Microelectrodes Inc. MI-407P needle pH electrode and a MI 401 $Ag/AgCl_2$ micro reference electrode, calibrated with Orion low ionic strength buffers (pH 4, 7, 10). Oxidation-reduction potential (ORP) was measured in SLW water with a glass epoxy platinum electrode and a MI 401 $Ag/AgCl_2$ micro reference electrode calibrated with Zobell's solution and corrected to the standard hydrogen electrode (SHE).

Cell and ATP concentration. Samples for cell enumeration from water and sediment were collected in combusted glass bottles and fixed in sodium borate-buffered formalin (2% v/v). Sub-samples were filtered on black 0.2 μm polycarbonate membrane filters, stained with SYBR Gold (Life Technologies), and immediately counted via epifluorescence microscopy. Sediment interference did now allow accurate determination of cell density in sediment samples. Cellular ATP was measured in triplicate as previously described[11] and viable biomass was estimated from the ATP concentration using a carbon to ATP ratio of 250 by weight[10,21].

Scanning electron microscopy. Samples for scanning electron microscopy (SEM) were fixed with either 2% (w/v) formalin or 0.5% (w/v) glutaraldehyde and filtered

onto a 13 mm diameter 0.2 μm polytetrafluoroethylene (PTFE) filters. Following ethanol dehydration and critical point drying, the filters were attached to an aluminium stub, coated with either gold or palladium, and observed on a Zeiss Supra 55VP Field Emission Scanning Electron Microscope.

Heterotrophic and chemoautotrophic production. Heterotrophic productivity was measured using [^{3}H]methyl-thymidine incorporation into DNA[40] and [^{3}H] leucine incorporation into protein[41]. Samples (1.5 ml; 10 and 5 live and 10 and 5 trichloroacetic acid (TCA)-killed controls for casts 1 and 3, respectively) were incubated with 20 nM radiolabelled thymidine (specific activity 20 Ci mmol^{-1}) or leucine (specific activity 84 Ci mmol^{-1}) at 4 °C in the dark for 175 h (average). A separate time-course experiment (data not shown) revealed that incorporation was linear over this incubation period. Incubations were terminated by the addition of 100% w/v cold TCA (5% final). Following centrifugation, a series of washes with cold 5% w/v TCA and cold 80% v/v ethanol were performed. The final pellet was dried overnight at ~25 °C. Radioactivity in the pellet was determined with a calibrated liquid scintillation counter following the addition of 1 ml of Cytoscint ES (MP Biomedicals). The rates of thymidine and leucine incorporation (nM TdR d^{-1} or nM Leu d^{-1}) obtained at the incubation temperature (4 °C) were converted to the *in situ* temperature of −0.49 °C using an energy of activation of 48,821 J mol^{-1} determined from temperature gradient experiments (data not shown). Rates of macromolecular synthesis were converted to carbon production using 2.0×10^{18} cells mol^{-1} thymidine[42] and 1.42×10^{17} cells mol^{-1} leucine[43], in concert with a cellular carbon content of 11 fg C cell^{-1} (ref 44). For the sediment assays, a slurry was created by adding 1 g wet weight of sediment to 10 ml of 0.2 μm-filtered SLW water. The processing of the sediment slurries was identical to water samples except a total of three 80% v/v ethanol rinses were performed to enhance the removal of unincorporated substrate. After drying, 200 μl of tissue solubilizer (ScintiGest; Fisher Chemical) was added to each vial. The metabolic rate data were normalized per gram dry weight of sediment.

Dark CO_2 fixation was determined in sterile 40 ml glass vials filled to the top with sample (leaving no headspace) and capped with PTFE lined caps (10 and 5 live and 10 and 5 TCA-killed for casts 1 and 3, respectively). The vials were amended with sterile [^{14}C]bicarbonate (stock concentration = 0.1144 mCi ml^{-1}) to a final experimental concentration of 1 μCi ml^{-1} and incubated in the dark at 4 °C for 281 h (average). A separate time-course experiment (data not shown) revealed that incorporation was linear over this incubation period. Incubations were terminated by the addition of cold TCA (2.5% w/v final concentration) and filtering onto 0.2 μm polycarbonate filters. The filters were placed in 20 ml scintillation vials, acidified with 0.5 ml of 3N HCl, and dried at 60 °C for 24 h. Radioactivity on the filters was determined with a calibrated liquid scintillation counter following the addition of 10 ml of Cytoscint ES (MP Biomedicals).

Molecular and phylogenetic analysis of SSU rRNA gene sequences. DNA was extracted from a portion of each filter (1/8 of a 142 mm filter) using the Power Water DNA Isolation Kit and from sediments (~0.5 g wet weight) with the Power Soil DNA isolation kit (MO BIO Laboratories, Inc.). The extraction procedures followed those recommended by the manufacturer.

The SSU rRNA gene was amplified using the oligonucleotide primers 515F and 806R, as described previously[45]. Amplification reactions (50 μl each) were performed using 5 units of AmpliTaq Gold DNA polymerase LD (Invitrogen), 1× PCR Gold Buffer (Invitrogen), 3.5 mM $MgCl_2$, 10 pmol of each primer, 200 μM dNTPs, and 0.1–3 ng of DNA template. After 9 min of heat activation at 94 °C (AmpliTaq Gold DNA polymerase is a chemical hot-start enzyme), 35 cycles of PCR were performed using the following amplification conditions: denaturation at 94 °C for 45 s, annealing for 90 s at 50 °C, and elongation at 72 °C for 90 s, with a terminal elongation at 72 °C for 10 min. The optimum number of cycles for PCR was determined by successively lowering the cycle number so that false positive amplification was prevented while amplification was possible for the lowest biomass samples analysed. The concentration of the PCR products were determined using the Quant-iT Pico Green dsDNA Assay Kit (Invitrogen). The amplicons were pooled and cleaned with the MoBio UltraClean PCR Clean-Up Kit. Sequencing was performed using the Illumina MiSeq platform (Selah Genomics, Greenville, SC).

Paired end sequence reads were assembled and quality filtered using the Mothur[46] phylogenetic analysis pipeline (v1.33.2). The sequences were aligned with the SILVA Incremental Aligner[47] (SINA v1.2.11; database release 115). The aligned reads were checked for chimaeras using the Uchime algorithm[48], as implemented within Mothur, and chimaeric sequences were removed from the data. Sequences with >97% SSU rRNA gene sequence similarity were clustered into an OTU and representative sequences for each OTU were chosen for classification using the SILVA database. Diversity and richness estimates were calculated in Mothur[46]. Singletons were excluded from further analyses, and for simplicity of presentation, phyla represented by <1% of the sequence reads were grouped into the unclassified category (Fig. 2a). Community comparisons using Yue and Clayton theta similarity coefficient analysis and Weighted Unifrac were also performed within Mothur. MEGA 5.2 software was used for phylogenetic analysis using maximum likelihood, the Jukes–Cantor nucleotide substitution model (1,000 iterations), and a 253 nucleotide alignment. Attempts to detect SSU sequences from eukaryotes were based on previously published methods[50].

31. Carter, S. P. & Fricker, H. A. The supply of subglacial meltwater to the grounding line of the Siple Coast, West Antarctica. *Ann. Glaciol.* **53,** 267–290 (2012).
32. Horgan, H. J. *et al.* Subglacial Lake Whillans—Seismic observations of a shallow active reservoir beneath a West Antarctic ice stream. *Earth Planet. Sci. Lett.* **331–332,** 201–209 (2012).
33. Siegfried, M. R., Fricker, H. A., Roberts, M., Scambos, T. A. & Tulaczyk, S. A decade of West Antarctic subglacial lake interactions from combined ICESat and CryoSat-2 altimetry. *Geophys. Res. Lett.* 2013GL058616, doi:10.1002/2013GL058616 (2014).
34. Priscu, J. C. LTER Limno Methods Manual – MCM_Limno_Methods_current.pdf. http://www.mcmlter.org/data/lakes/MCM_Limno_Methods_current.pdf (2013).
35. Seeberg-Elverfeldt, J., Schlüter, M., Feseker, T. & Kölling, M. Rhizon sampling of porewaters near the sediment-water interface of aquatic systems. *Limnol. Oceanogr. Methods* **3,** 361–371 (2005).
36. American Public Health Association. *Standard methods for the examination of water and waste water* (American Public Health Society Press, 1995).
37. Costa, A. W. *et al.* Analysis of atmospheric inputs of nitrate to a temperate forest ecosystem from Δ^{17}O isotope ratio measurements. *Geophys. Res. Lett.* **38,** L15805 (2011).
38. Casciotti. K. L. Sigman, D. M., Galanter Hastings, M., Bohlke, J. K. & Hilkert, A. Measurement of the oxygen isotopic composition of nitrate in seawater and freshwater using the denitrifier method. *Anal. Chem.* **74,** 4905–4912 (2002).
39. Kaiser, J., Hastings, M. G., Houlton, B. Z., Rockmann, T. & Sigman, D. M. Triple oxygen isotope analysis of nitrate using the denitrifier method and thermal decomposition of N_2O. *Anal. Chem.* **79,** 599–607 (2007).
40. Fuhrman, J. & Azam, F. Thymidine incorporation as a measure of heterotrophic bacterioplankton production in marine surface waters: evaluation and field results. *Mar. Biol.* **66,** 109–120 (1982).
41. Kirchman, D., K'nees, E. & Hodson, R. Leucine incorporation and its potential as a measure of protein synthesis by bacteria in natural aquatic systems. *Appl. Environ. Microbiol.* **49,** 599–607 (1985).
42. Bell, R. T. Estimating production of heterotrophic bacterioplankton via incorporation of tritiated thymidine. In: Kemp, P. F., Sherr, B. F., Sherr, E. B. & Cole, J. J. (eds) *Handbook of Methods in Aquatic Ecology* (Lewis, 1993).
43. Chin-Leo, G. & Kirchman, D. Estimating bacterial production in marine waters from the simultaneous incorporation of thymidine and leucine. *Appl. Environ. Microbiol.* **54,** 1934–1939 (1988).
44. Kepner, R. L., Wharton, R., Jr & Suttle, C. A. Viruses in Antarctic Lakes. *Limnol. Oceanogr.* **43,** 1754–1761 (1998).
45. Caporaso, J. G. *et al.* Ultra-high-throughput microbial community analysis on the Illumina HiSeq and MiSeq platforms. *ISME J.* **6,** 1621–1624 (2012).
46. Schloss, P. D. *et al.* Introducing mothur: open-source, platform-independent, community-supported software for describing and comparing microbial communities. *Appl. Environ. Microbiol.* **75,** 7537–7541 (2009).
47. Pruesse, E., Peplies, J. & Glöckner, F. O. SINA: accurate high-throughput multiple sequence alignment of ribosomal RNA genes. *Bioinformatics* **28,** 1823–1829 (2012).
48. Edgar, R. C., Haas, B. J., Clemente, J. C., Quince, C. & Knight, R. UCHIME improves sensitivity and speed of chimera detection. *Bioinformatics* **27,** 2194–2200 (2011).
49. Holland, H. D. *The Chemistry of the Atmosphere and Oceans* (Wiley, 1978).
50. Amaral-Zettler, L. A., McCliment, E. A., Ducklow, H. W. & Huse, S. M. A method for studying protistan diversity using massively parallel sequencing of V9 hypervariable regions of small-subunit ribosomal RNA genes. *PLoS ONE* **4,** e6372 (2009).

Extended Data Table 1 | Crustal and seawater components to SLW waters

	μeq L^{-1}							
Sample	Na^+	K^+	Mg^{2+}	Ca^{2+}	F^-	Cl^-	SO_4^{2-}	HCO_3^-
SLW Average *	5276	186	507	859	31.5	3537	1111	2111
Sea water component †	3038	66	691	132	0.4	3537	366	16
Non-seawater, crustal weathering component ‡	2239	120	-183 §	726	31.1	0	745	2096

* Average values for hydrocasts 1, 2 and 3.
† Calculated using Cl^- concentrations and ratios of each species to Cl^- in seawater in μeq l^{-1}; Na^+ 0.859, K^+ 0.019, Mg^{2+} 0.195, Ca^{2+} 0.037, F^- 0.00013, SO_4^{2-} 0.103, and HCO_3^- 0.004 (ref. 49).
‡ Calculated by subtracting the seawater component from the average SLW solute concentration for each ion.
§ Negative values indicate the potential for ion exchange of Mg^{2+} with other cations on clay minerals present in suspended sediments of SLW.

Extended Data Table 2 | Summary of parameters for the SLW SSU gene sequence data

Site	Number of Sequences *	Number of OTUs †	Coverage ‡	Inverse Simpson Diversity Index ‡	Shannon Diversity Index ‡	Chao Richness Estimator ‡
Drill and borehole water	984,412	962	99.8%	11.0	3.4	5,370
SLW water column	2,686,526	3,931	99.5%	35.3	4.9	41,603
SLW sediments	333,600	2,424	97.3%	31.8	5.1	42,079

* Sequences remaining after quality filtering, and removal of chimaeric sequences and singletons.
† OTUs that passed quality filtering, excluding singletons.
‡ Calculated using Mothur[46].

SUPPLEMENTARY INFORMATION

doi:10.1038/nature13667

Supplementary Discussion

Solute sources for SLW waters. The Cl^- to Br^- ratios of SLW waters averaged 0.00164, which is close to that for seawater (0.00156)[49]. Thus a parsimonious assumption is that all Cl^- and Br^- in SLW was from a seawater source. The average Cl^- concentration of 3.5 mmol L^{-1} in SLW represents a dilution relative to seawater of ~154-fold, indicating that seawater was a volumetrically minor contribution to the lake water. The seawater component for other major anions and cations can then be calculated using Cl^- concentrations and ratios of each species to Cl^- in seawater in μeq L^{-1} (Extended Data Table 1). The crustally-derived component of solute to SLW was determined by subtracting the seawater values for individual ions from the average SLW composition (Extended Data Table 1). This calculation results in negative values for Mg^{2+}, indicating a deficit of Mg^{2+} relative to seawater ratios. A process that could account for the Mg^{2+} deficit is an ion exchange reaction with other cations on clay minerals present in suspended sediments of SLW. Theoretical and observational data indicate that seawater may penetrate no further than a few kilometers inland of the low-tide grounding line, making a seawater incursion to SLW (~100 km from the grounding line) extremely unlikely. Therefore, we hypothesize that the seawater source is from pre-existing marine pore waters in sediments beneath and upstream of SLW.

The inorganic nitrogen pool within the water column of SLW was dominated by ammonium relative to nitrite and nitrate (Table 1). Since mineral sources of ammonium are minor, the majority of the ammonium is presumed to originate from the microbial mineralization of nitrogen-containing organic material in the sediments, which could diffuse into the water column and also be transported to SLW from upstream portions of the subglacial hydrological network. A 1:1 relationship would be expected between NH_4^+ loss and NO_3^- gain unless N_2O or other intermediates were being produced by nitrification. Given the low oxygen concentrations, high NH_4^+, and SSU sequence data suggesting that nitrifying taxa were abundant in the SLW water column (Fig. 2b), the production of N_2O is likely[51]. Unfortunately, we do not have N_2O concentration data for SLW water. The unexpectedly low nitrate level may also result from denitrification in the sediment surface layers or in low oxygen microzones associated with suspended sediment particles. Our sequence data revealed the presence of known denitrifiers (*Thiobacillus denitrificans*) and nitrate reducers (e.g., species of *Polaromonas*), supporting this contention.

Molecular analysis of SSU gene sequences. Paired-end sequencing of the V4 region of the SSU gene generated 3,556,417 sequences from the SLW water column, 1,361,815 from the drill and borehole water, and 561,966 from the surficial sediment samples. After quality filtering and removal of chimeric sequences, 2,686,526, 984,412, and 333,600, respectively, reads were used for phylogenetic analysis (Extended Data Table 2). Calculation of sequence coverage (Extended Data Table 2) and collector curves (data not shown) indicated the depth of sequencing to be sufficient to describe the abundant members in the SLW water and sediment communities.

Analysis of molecular variance (AMOVA) in data obtained from three casts of the WTS-LV showed no statistical difference amongst the casts (pair wise p-values ≥ 0.69); therefore, all molecular data from the water column were compiled. Estimations of species diversity in the lake water revealed a community diversity comparable to many surface aquatic environments[52]. Of the 3,931 OTUs identified in the SLW water column, 3,105 (87% of the total sequence reads) and 30 (3.6% of the total sequence reads) classified within the *Bacteria* and *Archaea*, respectively, while 793 OTUs were not classified. The bacterial and archaeal OTUs were classified into 32 and 2 phyla, respectively (Fig. 2a). The majority of OTUs were taxonomically affiliated with the Proteobacteria (1,893 OTUs; 53% of all sequences) and Actinobacteria (401 OTUs; 11% of all sequences).

Within the proteobacterial OTUs from the water column, 84% of the sequences classified within the beta- and delta- classes. Phylotypes most closely related to species in the genera '*Candidatus* Nitrotoga', *Polaromonas,* and *Sideroxydans* were the 1st, 2nd, and 3rd, respectively, most abundant OTUs in the dataset. Highly abundant actinobacterial phylotypes were most closely related to SSU gene sequences reported previously from polar lake environments (e.g., ref 53). Most of the archaeal phylotypes were classified as Thaumarchaeota, with one OTU from this group representing the 5th most abundant phylotype. Phylotypes that were abundant in the water column and surficial sediment (Fig. 2b) were very rare (OTU 1756, 0.003%; OTU 10327, 0.007%; OTU 2522, 0.002%; and OTU 1767, 0.001%) or not observed (OTU 1901, OTU 5861, and OTU 1005) in data obtained from the drill water assemblage.

Nearly all the SSU gene sequences characterized from the surficial sediment were bacterial (1,935 OTUs; 94%), with only 0.3% classifying within the *Archaea*. Proteobacteria were the most abundant phylum, with the beta- and gamma- classes representing 65% of the OTUs within this group. Similar to observations for the SLW water column, phylotypes most closely related to species of *Sideroxydans* and '*Candidatus* Nitrotoga' were the most abundant OTUs (1st and 2nd, respectively). However, phylotypes that classified within the genera *Thiobacillus*, *Nitrosospira*, and *Methylobacter* were enriched in the sediments relative to the water column (<0.7% of all sequences in the water column). Cluster analysis of the water column, sediment, and drilling water community structure indicated that the SLW water and surficial sediments were not statistically different; however, the drilling water was statistically different from the water column and sediment environment (Figure 2a).

Samples of the drilling water contained no OTUs that classified as archaeal, and only 41 OTUs (<1%) were unclassifiable at the domain level. The Proteobacteria and the Firmicutes were the most abundant phyla in the dataset, representing 70% and 20% of the sequences, respectively. The most abundant phylotypes were most closely related to species of *Janthinobacterium* and *Tumebacillus*, with each representing ~19% of the dataset. Many of the other abundant OTUs in the drilling water were closely related to sequences and isolates observed previously in icy environments, including Antarctic ice cores[54].

Supplementary Discussion References

51. Goreau, R. E. *et al*. Production of NO_2^- and N_2O by nitrifying bacteria at reduced concentrations of oxygen. *Appl. Environ. Microbiol*. 40, 526–532 (1980).
52. Biers, E. J., Sun, S. & Howard, E. C. Prokaryotic genomes and diversity in surface ocean waters: interrogating the global ocean sampling metagenome. *Appl. Environ. Microbiol.* 75, 2221-2229 (2009)
53. Mosier, A. C., Murray, A. E. & Fritsen, C. H. Microbiota within the perennial ice cover of Lake Vida, Antarctica. *FEMS Microbiol. Ecol.* 59, 274-288 (2007)
54. Raymond, J. A., Christner, B.C. & Schuster, S. C. A bacterial ice-binding protein from the Vostok Ice Core. *Extremophiles* 12, 713-717 (2008)

CHAPTER SEVEN

SUBGLACIAL CARBON AND NUTRIENT FLUXES FERTILIZE THE SOUTHERN OCEAN UNDER THE ROSS ICE SHELF

Contribution of Authors and Co-Authors

Manuscript in Chapter 7

Author: Trista J. Vick-Majors

Contributions: Collected samples, oversaw sample collection, performed microbiological activity assays, performed phosphorus analyses, assisted with nitrogen analyses, performed excitation-emission matrix spectroscopy, performed statistical analyses, analyzed data, prepared figures and tables, and wrote the manuscript.

Co-Author: Alexander B. Michaud

Contributions: Performed sediment porewater extractions, assisted with nitrogen analyses, commented on manuscript.

Co-Author: John C. Priscu

Contributions: Oversaw the study and sample analyses, commented on the manuscript.

Manuscript Information Page

Trista J. Vick-Majors, Alexander B. Michaud, John C. Priscu
Nature
Status of Manuscript:
_X_ Prepared for submission to a peer-reviewed journal
____ Officially submitted to a peer-review journal
____ Accepted by a peer-reviewed journal
____ Published in a peer-reviewed journal

Nature Publishing Group

Subglacial carbon and nutrient fluxes fertilize the Southern Ocean under the Ross Ice Shelf

The following work is prepared to be submitted to Nature.

Trista J. Vick-Majors[1], Alexander B. Michaud[1], John C. Priscu[1]

[1]Department of Land Resources and Environmental Sciences, Montana State University, Bozeman, MT

Active subglacial water systems, once thought to be sealed beneath the Antarctic Ice Sheet (AIS), ultimately drain into the Southern Ocean[1] forming a conduit between subglacial and marine carbon and nutrient pools and connecting continental and oceanic biogeochemical processes. Antarctic subglacial water is estimated to contain 5.1 Pg of organic carbon[2], equivalent to the ~5.4 Pg contained in the entire Antarctic Ice Sheet[3], while relict marine sediments beneath the AIS may contain ten times the amount in northern permafrost[4]. The recent discovery of microbial ecosystems beneath the AIS in Subglacial Lake Whillans (SLW) [5] allows us to include the activities of subglacial microorganisms in estimates of subglacial-to-ocean carbon and nutrient fluxes. Here we show that subglacial organic matter can contribute substantially to the dark ocean waters beneath the Ross Ice Shelf (RIS), where the availability of organic matter may limit rates of heterotrophic carbon mineralization[6]. Our data reveal that subglacial carbon sources can explain dissolved organic carbon concentrations in the SLW water column within predicted water residence times. We demonstrate that fluxes of biologically relevant solutes from subglacial aquatic environments along the Siple Coast are sufficient to drive heterotrophic biological activity locally (at the grounded margin of the West Antarctic Ice Sheet), and perhaps regionally (in the RIS subglacial cavity). We conclude that microbial

activity in hydraulically active subglacial aquatic environments plays a key role in the fixation and mobilization of organic matter from beneath the AIS to the Southern Ocean.

Subglacial water from the Siple Coast drains to coastal embayments beneath the Ross Ice Shelf (RIS), forming subglacial estuaries[7]. Subglacial outflow accounts for a substantial portion of the variability in the RIS cavity freshwater budget and is significant in the overall freshwater budgets of the coastal embayments[8], but there is substantial uncertainty regarding the potential importance of biologically relevant solutes contained in subglacial outflow. An estimated 5.4 Pg of organic carbon is stored in Antarctic subglacial aquatic environments[2], but estimates of subglacial-to-ocean fluxes have been hindered by lack of quantitative information on actual subglacial concentrations of carbon and nutrients. Quantifying carbon and nutrient fluxes is key to understand sub-ice shelf biogeochemical processes. Life in the darkness beneath the RIS[9], where water residence times span ~1 - 8 years[10,11], depends on carbon and nutrients advected from open water (>1000 km away from the ice shelf interior), carried from the continent by the ice itself and/or subglacial water, or combinations of both sources. As Antarctic ice shelves are increasingly threatened with climate-change-induced collapse[12], understanding sub-ice-shelf biogeochemical processes and their linkages with the open ocean and the Antarctic continent become progressively more important.

Subglacial Lake Whillans (SLW), an active subglacial lake along the Siple Coast[1] is the only Antarctic subglacial lake directly sampled in a microbiologically and chemically clean manner to date[13]. SLW lies 800 m beneath the surface of the Whillans Ice Stream (WIS) and hosts an active microbial ecosystem supported by

chemoautotrophic activity[5]. The WIS is the largest contributor to subglacial groundwater along the Siple Coast, and its long sedimentary (till) pore water residence times (1000 - 10,000 years) indicate that it should be rich in solutes that can contribute both to subglacial biological activity and nutrient rich subglacial outflow. The residence time for the bulk water column in SLW is much shorter (years to decades) [1,14]. Basal ice melt (~1.8 cm y^{-1}, ref. 15) at the lake and upstream of the lake comprises the primary source of water to SLW[5], which has filled and drained three times during the past 12 years[14,16]. The sampling of SLW in early 2013 occurred when the lake was at relatively low stand during the slow fill phase.

The temporal variability of biological activity and biologically relevant solutes are not known, however, the waters and sediments of SLW were characterized by relatively high levels of organic matter, nutrients (Table 1), and biological activity at the time of sampling.

Parameter	*DOC**	*POC**	*DON*	*PN**	*DIN**	*DOP*	*PP*	*SRP**
Concentration ([-1]g l	2650	942	33.6	16.8	46.2	189	46.5	96.0
Total Pool size (x10^5 kg)	3.2	1.1	0.04	0.02	0.06	0.23	0.06	0.12

Table 1. Dissolved and particulate matter in SLW. DOC = dissolved organic carbon, POC = particulate organic carbon, DON = dissolved organic nitrogen, PN = particulate organic nitrogen, DIN = dissolved inorganic nitrogen, DOP = dissolved organic phosphorus, PP = particulate phosphorus, SRP = soluble reactive phosphorus *reported in Christner et al.

The dissolved organic carbon (DOC) concentration measured in SLW was similar to other Antarctic terrestrial aquatic systems (i.e., trophogenic zones of perennially ice covered lakes in the McMurdo Dry Valleys[17]). Concentrations were ~7 times higher than

wintertime values in the Ross Sea[18] and summer time concentrations under the northeastern edge of the McMurdo Ice Shelf [19] (~0.4 mg l^{-1}), where water enters the RIS cavity from McMurdo Sound. DOC serves as the primary source of energy and biomass for heterotrophic bacteria and archaea in the sea. Low concentrations of DOC in water advected under the RIS suggest that a DOC-rich source from subglacial outflow may be biologically important to heterotrophic bacteria and archaea in the Southern Ocean, which may be carbon-limited[6]. Subglacial dissolved organic matter (DOM) is N-poor relative to C (mass ratio of DOC:DIN = 57, DOC:DON = 79; Table 1), indicating a relatively recalcitrant nature. Recalcitrant or semi-labile DOC is biologically reactive, but remineralization usually occurs over long timescales (months to decades) [20]. Mixing with nutrient-rich water can stimulate remineralization of recalcitrant DOM; N-rich water (molar ratio of DOC:DIN ~1.7, DIN 0.35 mg l^{-1}) entering the RIS cavity from McMurdo Sound[19] may supplement C-rich subglacial outflow to support biological activity beneath the RIS.

Waters beneath the AIS are not atmospherically ventilated and, similar to other Antarctic aquatic environments, do not receive terrestrial (vegetation-derived) inputs of DOM or particulate organic matter (POM). The ultimate source of organic matter beneath the WIS is thought to be relict marine organic matter deposited during previous incursions of sea water[21], chemoautotrophic production by bacteria and/or archaea inhabiting the subglacial waters and sediments, or a combination of both. Reworking of organic matter by heterotrophic bacteria and/or archaea may be a secondary source of (often refractory) DOM[22]. Parallel factor analysis (PARAFAC) of fluorescence signatures

of DOM (FDOM; derived from excitation-emission matrix spectroscopy “EEMS”) in SLW sediment pore waters (Figure S1) showed the presence of four fluorophores (Figure S2), including two amino acid-like fluorophores (tyrosine and tryptophan, F3 and F4, respectively), which indicate microbial production of DOM. F3 (ex/em 270/300 nm) and F4 (ex/em <250,270/336 nm) accounted for 69.8% of total FDOM in the surface sediments (0-2 cm), and decreased in relative abundance with depth, down to 49.5% at the bottom of the profile (36-38 cm). While the relative abundance of F3 and F4 decreased with depth, two humic-like fluorophores, F1 (ex/em 250,300/380 nm) and F2 (ex/em 250,340/454 nm), increased at a rate of 0.5% cm^{-1}, with F1 dominating most of the depths below 18 cm (Figure 1). Humic-like fluorophores may indicate the presence of more recalcitrant DOM deeper in the sediments, however, recalcitrant DOM may still be microbially produced[23]. Indeed, F1 (ex/em 300/380) was most similar to a microbially derived component from a McMurdo Dry Valley lake[24], which also shared characteristics with the typical marine humic peak[25] and is associated with recent biological activity in the ocean[26], and with processing of organic matter by microbial communities in Antarctic mountain glaciers[27].

F2 was most similar to the mixture of humic peaks “A” and “C” identified in ref. 25, which are commonly associated with coastal environments. A similar peak was also identified in permanently ice-covered Antarctic McMurdo Dry Valley lakes, where it was associated with microbial production of DOM[24], and in the deep ocean, where it was related to microbial processing of organic matter[26]. In the water column, a single FDOM peak was present, with tyrosine-like fluorescence of ex/em 240/310 (Figure S3), as

opposed to the tyrosine-like F3 observed in the sediments (ex/em 270/300), implying different processing of DOM in the water column versus the sediments.

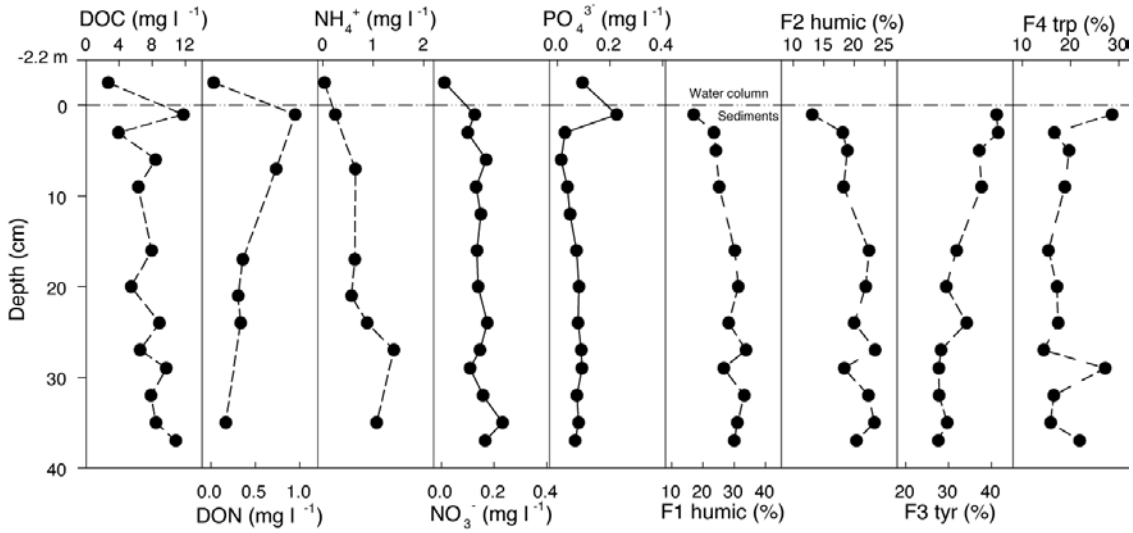

Figure 1. Profiles of organic matter and nutrients in SLW. Dissolved organic carbon (DOC), dissolved organic nitrogen (DON), ammonium, nitrate, phosphate (mg l^{-1}) and FDOM components (as % of total fluorescence) from SLW sediment porewater and water column. Water column FDOM could not be modeled with sediment porewater FDOM. The single FDOM peak present in the water column was most similar to sediment component F3. Tyr = tyrosine-like fluorescence, trip = tryptophan-like fluorescence. The dashed line indicates the sediment-water interface.

The FDOM data indicate that the ultimate source of DOM (or DOC) in SLW is microbial activity, however, the size of the observed DOC pool in SLW (3.2 x 10^5 kg C; Table 1) cannot be explained by microbial activity in the lake alone. Likely other sources of DOC to the SLW water column are surface flow during lake filling (see methods), inflow of till porewater (see methods), chemoautotrophic production by prokaryotes[5], upward flux from the sediments, and ice melt[3,15] (Table 2), which total 2.7 x 10^4 kg y^{-1} .

Chemoautotrophic activity comprises 5% of the annual DOC supply, with inflow from upstream and water flowing out of the till comprising the major sources of DOC (92%). The major sink for DOC in the lake is biological activity.

Sources $x\ 10^3\ kgC\ y^{-1}$					*Sinks* $x\ 10^3\ kgC\ y^{-1}$		*Surplus* $x\ 10^3\ kgC\ y^{-1}$	*Accumulation time (years)*
Inflow	Till water	Chemoauto-trophy	Sediment flux	Ice melt	Heterotrophic Production	Heterotrophic respiration	26.0	12.3
18.6	6.25	1.44	0.50	0.16	0.083	0.876		

Table 2. Sources and sinks of organic carbon in SLW. The accumulation time for the observed DOC pool is based on the annual surplus.

The "prokaryotic carbon demand" (PCD = 959 kg y^{-1}, where PCD is the sum of carbon respired and the carbon incorporated into biomass by heterotrophic bacteria/archaea;) in SLW is 28 times less than the DOC supplied to the lake on an annual basis, resulting in most of the DOC inputs accumulating as surplus (Table 2).

Annual DOC sources exceed the size of the PCD sink by two orders of magnitude, explaining the accumulation of the observed DOC pool in SLW in 12 years (Table 2). A 12 year accumulation time is remarkably similar to the decadal scale fill-drain cycles predicted for this region[14]. The agreement in residence and accumulation time estimates indicates that our carbon budget for the lake is reasonable; even the removal of either of the two largest and least well-characterized sources (inflow from upstream, for which the actual DOC concentration was estimated, and outflow of till porewater to the surface) increases the accumulation time to 43 or 16 years, respectively, while the removal of both increases accumulation time to 279 years. The magnitude of the biological sources and sinks of N and P in the SLW water column are unknown, but

inflow of till water containing the average SLW till porewater concentrations of N and P (Figure 1) would produce the observed N and P pools in <10 years and >100 years, respectively.

Subglacial water drainage from the Siple Coast ice streams crosses the grounding line of the West Antarctic Ice Sheet during lake discharge events and enters the ocean cavity beneath the RIS at a rate of between 0.82 and 15.8 $km^3\ y^{-1}$ (average, 1.9 $km^3\ y^{-1}$, ref. 8). Although, concentrations of biologically relevant solutes in subglacial water may vary across the Siple Coast values from SLW allow us to constrain the importance of subglacial water in fertilizing the sub-RIS cavity. Over the range of outflows reported for the Siple Coast, the input of organic carbon to the sub-RIS cavity ranges from 2.9 x 10^6 kg y^{-1} to 42 x 10^6 kg y^{-1}, with an average of 6.8 x 10^6 kg y^{-1} (74% in the dissolved fraction, 26% in the particulate fraction). Inputs of N and P are 10 fold lower than for carbon, and both are dominated by organic fractions. The mass of organic carbon supplied to the RIS from the Siple Coast is ~three orders of magnitude lower than the mass of organic carbon supplied annually to the Southern Ocean from primary production (~4400 Tg, ref. 28), however, fluxes from subglacial environments can provide important carbon, energy and nutrient sources to the biological community in the sub-RIS cavity[9]. Heterotrophic prokaryotic production under the RIS, based on the incorporation of ^{3}H-thymidine at the Ross Ice Shelf Project J9 borehole, was 0.73 ng C $l^{-1}\ d^{-1}$ (ref. 9). Assuming bacterial stoichiometry of 45:9:1, (C:N:P , ref. 29) N and P uptake can be estimated to be 0.17 ng N $l^{-1}\ d^{-1}$ and 0.04 ng P $l^{-1}\ d^{-1}$. Based on our model, subglacial outflow estimates from the Siple Coast can meet between 8% and 169% (avg 20%) of C

demand, 1% to 19% (avg 2%) of N demand, and 14% to 273% (avg 33%) of P demand under the entire RIS (Table 3).

Nutrient	*kg y^{-1} outflow ($x\ 10^6$)*			*BP demand ($ng\ l^{-1}\ d^{-1}$)*	*% of BP met by outflow*		
	Avg	Min	Max		Avg	Min	Max
Organic C	6.8	2.9	42	0.73	20.4%	8.8%	169.8%
DIN	0.09	0.04	0.73	0.17	2.4%	1.0%	19.6%
Organic N	0.10	0.04	0.80				
SRP	0.18	0.08	1.5	0.04	32.8%	14.2%	273.0%
Organic P	0.45	0.19	3.7				

Table 3. Organic matter and nutrient supply to the Ross Ice Shelf cavity. Outflow from the Siple Coast is compared to estimated carbon and nutrient demand by heterotrophic bacteria and/or archaea (BP demand). Estimated BP demand was determined from thymidine turnover times reported in ref. 9 and the bacterial C:N:P stoichiometry reported in ref. 29. DIN=dissolved inorganic nitrogen. SRP=soluble reactive phosphorus. Organic C, N, and P are the sum of dissolved and particulate fractions.

Our data show that the relatively high concentrations of organic matter and nutrients observed in SLW are microbially derived and can accumulate within a reasonable water residence time, based on known hydrology. The accumulated pools of biologically-relevant solutes can be released in subglacial outflow from the Siple Coast of West Antarctica to fertilize the sub-RIS cavity at biologically significant rates. The utilization of subglacially released DOC by heterotrophic bacteria/archaea and the degradation of POC by macrofauna[30] or microbial extracellular enzymes[31] may support life under the RIS. Microbial activity supported by subglacial outflow under the RIS should result in the further production of recalcitrant or semi-labile DOM[23,32], giving

subglacial outflow an important role in ocean biogeochemistry and carbon storage in the ocean.

Methods

Sample Collection

Subglacial Lake Whillans (SLW) water and sediment were collected through a ~0.6 m diameter borehole which was created with a microbiologically-clean, hot water drill [33-35]. Lake water samples were collected with a 10 L Niskin bottle and sediments were recovered using a gravity multicorer (Uwitec). Full details of the clean access protocol, drilling and sample recovery are described elsewhere[13,36]. Briefly, three discrete 10 L water samples were collected at mid-depth in the ~2.2 m water column using a Niskin bottle on January 28 and 30, 2013 and returned to the on-site laboratory for processing. After inverting the Niskin bottle 3 times, water was decanted into acid-washed (1% hydrochloric acid; rinsed 5X with ultra-pure water) and autoclaved opaque high density polyethylene (HDPE) bottles (biological assays), acid-washed low density polyethylene (LDPE) bottles (dissolved N and P), or either acid washed fluorinated HDPE bottles (Thermo Scientific, Nalgene, Waltham, MA) or acid washed and combusted glass bottles (particulate and dissolved organic matter).

Sediment porewater samples were extracted from a sediment core (multicore 3B) collected on 30 January 2013 for analysis of nitrate, phosphate, and dissolved organic matter using Rhizon porewater samplers (Rhizosphere) [37]. Rhizon samplers (0.1 µm filter pore size) were soaked in MilliQ water prior to installation through pre-drilled holes in

the sediment core liner. A 10 ml syringe was attached to the outlet and the plunger locked to maintain a vacuum. After 14 h of extraction, the porewater was dispensed into cleaned vials (nitrate and phosphate: 10% HCl acid washed, MilliQ rinsed (6X); dissolved organic matter: 10% HCl acid washed, MilliQ rinsed (6X), combusted for 4 hr at 450 ^{o}C). Procedural blanks using MilliQ water were handled in parallel to samples and used to determine background introduced by the Rhizon extraction. Background was subtracted out of all analyses. Nitrate and phosphate samples were stored frozen at -20 ^{o}C and DOM samples were stored at 4 ^{o}C and returned to Montana State University for analysis. The sediment core used for determination of porewater ammonium was frozen immediately after collection on January 30, 2013, and stored at -20 ^{o}C until processing at Montana State University.

Organic Matter and Nutrients

WMter column samples for DOC and three dimensional spectrofluorometric characterization of dissolved organic matter (excitation-emission matrix spectroscopy; EEMS) were filtered through acid-leached and combusted (>4 h at 450 °C) 25 mm glass fiber filters (GF/F, effective retention size 0.7 μm). The filtrate was collected in acid washed and combusted (>4 h at 450 °C) 125 ml amber borosilicate glass bottles fitted with polytetrafluoroethylene (PTFE) lined caps and stored at 4 °C until analysis. DOC and total nitrogen (TN) concentrations were determined in water column and sediment porewater samples using a Shimadzu TOC-V Series TOC analyzer following acidification with hydrochloric acid to pH $\leq$ 2 to remove inorganic carbon as CO_2.

Dissolved organic nitrogen (DON) was determined by subtracting NO_2^-, NO_3^-, and NH_4^+ (water column[5]) or NO_3^- and NH_4^+ (sediment porewater) from TN.

EEMS were determined with a Horiba Jobin Yvon Fluoromax-4 Spectrophotometer (Horiba, Ltd., Japan) equipped with a Xe light source using a 1 cm path length quartz cuvette. Excitation data were measured every 10 nm from 240 nm to 450 nm, and emission data every 2 nm from 300 nm to 560 nm. Measurements were corrected for background (0.2 µm filtered Milli-Q water), Raman scattering, and inner-filter effects using absorbance spectra collected between 190 nm and 1100 nm with a Genesys 10 Series Spectrophotometer (1 cm path length, Thermo Scientific) [38]. We used parallel factor analysis (PARAFAC) to decompose the trilinear EEMS arrays and derive a four component model describing the fluorescence characteristics of the porewater DOM using the drEEM toolbox (version 0.2.0)[39] for Matlab.

Porewater NO_3^- and PO_4^- concentrations were determined via ion chromotography (Metrohm, described in Michaud et al, 2015 submitted). Sediments for dissolved NH_4^+ were thawed at Montana State University in an ISO class 1000 cold clean room at 4°C and subsampled every 2 cm by extruding and slicing. The 2 cm sections were transferred to acid washed (10% HCl), MilliQ water-rinsed (6X), combusted (4h at 450°C) glass vials with polytetrafluoroethylene lined caps, frozen at -20°C and thawed prior to analysis. Sediments were transferred from the glass vials to acid washed and MilliQ rinsed 50 mL conical centrifuge tubes and centrifuged at 3500 x g for 20 minutes. The supernatant was transferred to acid washed and MilliQ rinsed 15 ml conical centrifuge tubes and spun for an additional 20 min at 4500 x g to pellet any remaining fine

particulates. The clean supernatant from the 15 mL centrifuge tube was transferred to an acid washed and MilliQ rinsed glass vial. The supernatant was diluted (1:10) to a final volume of 5 mL with MilliQ water for colorimetric analysis[40].

Total dissolved and particulate phosphorus (TDP and PP) were determined colorimetrically[41] on water column samples. Soluble reactive phosphorus (3.1 µm) reported previously[5] was subtracted from TDP (soluble non-reactive phosphorus) to approximate dissolved organic phosphorus (DOP).

Bacterial Carbon Demand
and Respiration of Leucine

Heterotrophic bacterial respiration was measured by adding 60 mL of sample water to an autoclaved amber HDPE bottle (Nalgene) followed by the addition of uniformly labeled ^{14}C-L-leucine (specific activity >300 mCi mmol^{-1}; final leucine concentration 60 nM; final activity 0.0180 µCi mL^{-1}) [42]. Five-milliliter aliquots of the radiolabeled sample were added to autoclaved 25 mL glass side arm flasks (6 live and 6 TCA killed controls; 250 µL of cold 100% TCA). The top of the flask was sealed with a butyl rubber septum holding a small basket containing a folded GF/C filter suspended above the aqueous phase; the sidearm was sealed with a butyl rubber septum. Following incubation in the dark for 105 h at 2-4 °C (linearity of the rate of label incorporation was determined elsewhere), the reactions in live incubations were terminated by injecting cold 100% TCA (final concentration 5%) into the sample through the sidearm which lowered the pH to ≤ 2. β-phenylethylamine (100 µl) was added to the GF/C filter through the septum with a needle and syringe to trap respired CO_2. Killed samples were maintained at ~25 °C for

24 hours with occasional gentle swirling to liberate respired CO_2 from the aqueous phase. Care was taken not to splash the aqueous phase of the incubation onto the GF/C filter or basket holding the filter. Cellular ^{14}C incorporation was determined on the liquid fraction following filtration onto 0.2 μm polycarbonate filters. The GF/C and polycarbonate filters were placed in 20 mL scintillation vials followed by the addition of 10 mL of Cytoscint-ES and the ^{14}C activity was determined using a calibrated scintillation counter. ^{14}C-leucine uptake and respiration were converted to units of carbon as described in ref. 19, and total heterotrophic prokaryotic carbon demand was calculated as the sum of respired carbon and carbon fixed into biomass.

Flux Estimates

We converted all chemical concentrations to total mass (kg) using a total SLW volume of 0.12 km^3 at the time of sampling (water column depth, 2.2 m, ref. 5; lake surface area ~60 km^2, ref. 43). The mass of carbon supplied to SLW annually was determined as follows: DOC concentration in water flowing in from upstream was assumed to be the same as that determined for SLW[5] and the volume of water entering the lake was determined for the year before sampling[14,16]; till porewater inflow concentration was assumed to be the average of sediment porewater values measured in this study, and the volume of till porewater inflow was reported previously[44] and modified to include inflow only over the surface area of SLW; the contribution from chemoautotrophic production was determined previously[5]; sediment porewater to water column fluxes were determined using Fick's first law with tortuosity and temperature corrected diffusion coefficients[45,46] assuming a well-mixed water column, from 1 cm

below the sediment surface to the surface of the sediments; DOC from ice melt was determined based on melt rate (1.728 cm y^{-1}; ref. [15]) and the published DOC concentration for the AIS (0.15 mg l^{-1}; ref. [3]). The total prokaryotic carbon demand (PCD) was subtracted from the sum of the organic carbon sources to determine the annual carbon surplus in the lake, assuming a steady state system (dDOC/dt = inflow + till water + chemoautotrophy + porewater diffusion + ice melt - PCD = 0). The surplus was then divided by the total mass of the SLW DOC pool to determine accumulation time.

To determine potential outflow to the sub-RIS cavity, we used the total mass of each carbon and nutrient pool in SLW to calculate a concentration of each solute per km^3 of water. We then used the range of annual water outflow volumes reported previously for the Siple Coast ice streams[8] to calculate the total mass of each solute carried across the grounded margin of the ice sheet into the the sub-RIS cavity annually. To determine the contribution per unit water volume under the RIS, we used a previously reported[11] sub-RIS volume estimate of 125,333 km^3.

Supplemental Information

EEMS and PARAFAC Results and Analysis

Our 4-component PARAFAC model (Figure S2) explained 99.7% of the variability in the sediment porewater EEMS dataset and had a core consistency of 58.3%. Our relatively small number of available samples (19, of which 7 water column samples were excluded from the model as outliers) may have limited our ability to validate models with more components, however, the low residuals (99.7% variability explained), along with manual analysis of the corrected EEMS profiles indicated that 4 components is reasonable. The four component model also minimized the sum of squares error (SSE=0.15) and converged after 62 iterations with random starts and non-negativity constraints. The model was successfully split-half validated using alternating splits of 6 samples per split. We were unable to include water column samples in our model, as their fluorescence characteristics made them outliers relative to the sediments (determined through visual examination of the spectra and preprocessing with the drEEM toolbox) and the small number of water column samples precluded the construction of a water column only PARAFAC model. However, manual “peak picking” (i.e. [25]) revealed the presence of a single peak, indicative of protein-like fluorescence (ex/em 240/310; Figure S3).

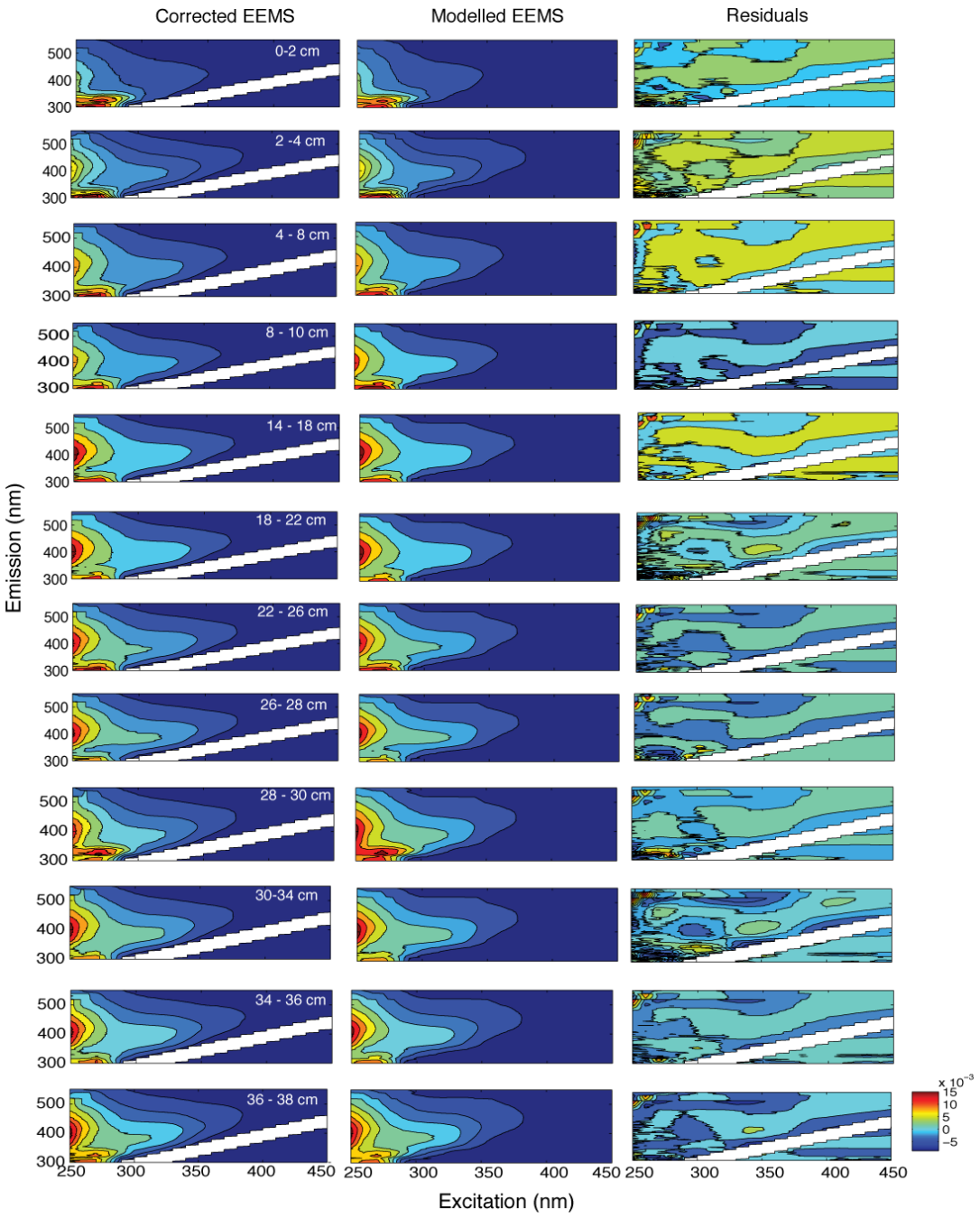

Figure S1. Fluorescence matrices for sediment porewater samples. The EEMS matrix (corrected as described in Methods), the modeled matrix (PARAFAC) and the residuals from the PARAFAC model are shown from left to right. Randomly distributed residuals in combination with a high proportion of variability explained (99.7%) indicated a good model fit. The color scale in the lower right corner indicates the intensity of relative fluorescence units. The white band results from the removal of Rayleigh scatter[39]. Samples are labeled by 2 to 4 cm increments, beginning at the sediment-water interface.

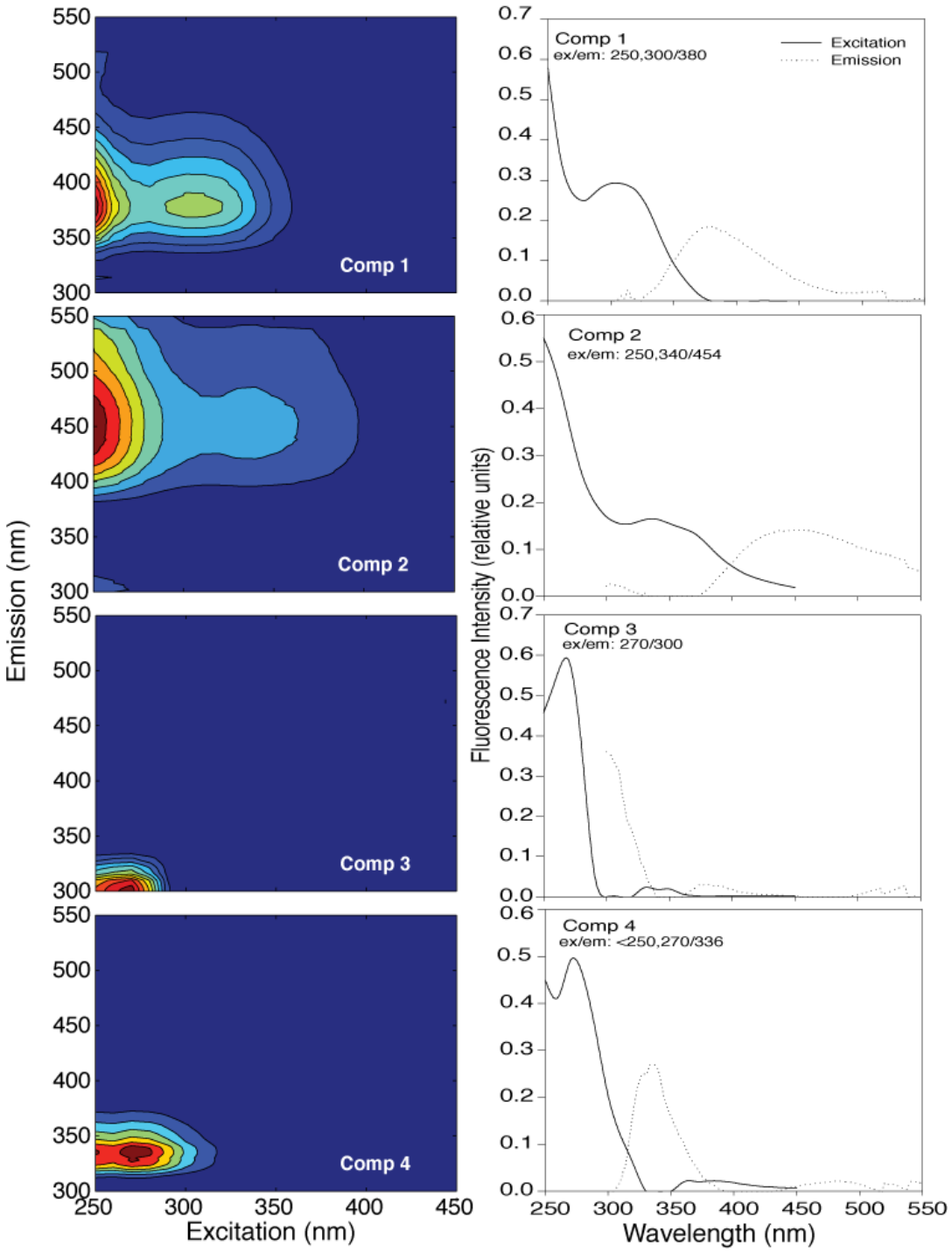

Figure S2. PARAFAC fingerprints and excitation and emission spectra. Comp 1, 2, 3, and 4 are F1, 2, 3, and 4 in the main text. Red indicates higher signal intensity of relative fluorescence units, while blue indicates lower intensity.

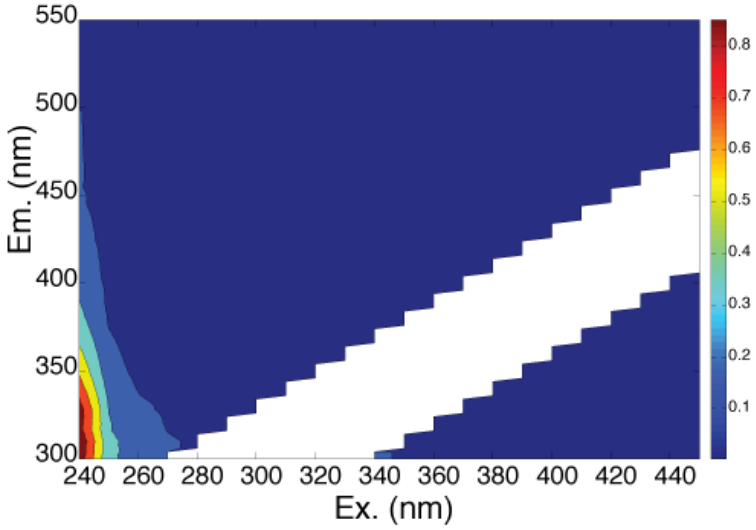

Figure S3. Representative water column EEM. The maximum ex/em is at 240/310. The color bar indicates intensity of relative fluorescence units.

References

1. Fricker, H. A., Scambos, T., Bindschadler, R. & Padman, L. An active subglacial water system in West Antarctica mapped from space. *Science* **315,** 1544–1548 (2007).

2. Priscu, J. C. *et al.* in *Polar Lakes and Rivers* (eds. Vincent, W. F. & Laybourn-Parry, J.) 119–135 (Polar Lakes and Rivers, 2008).

3. Hood, E. *et al.* Storage and release of organic carbon from glaciers and ice sheets. *Nature Geosci* **8,** 91–96 (2015).

4. Wadham, J. L. *et al.* Potential methane reservoirs beneath Antarctica. *Nature* **488,** 633–637 (2012).

5. Christner, B. C. *et al.* A microbial ecosystem beneath the West Antarctic ice sheet. *Nature* **512,** 310–313 (2014).

6. Church, M. J., Hutchins, D. A. & Ducklow, H. W. Limitation of bacterial growth by dissolved organic matter and iron in the Southern ocean. *Applied and Environmental Microbiology* **66,** 455–466 (2000).

7. Horgan, H. J. *et al.* Estuaries beneath ice sheets. *Geol* **41,** 1159–1162 (2013).

8. Carter, S. P. & Fricker, H. A. The supply of subglacial meltwater to the grounding line of the Siple Coast, West Antarctica. *Annals of Glaciology* **53,** 267–280 (2012).

9. Azam, F. *et al.* Occurrence and metabolic activity of organisms under the Ross Ice Shelf, Antarctica, at Station J9. *Science* **203,** 451–453 (1979).

10. Reddy, T. E., Holland, D. M. & Arrigo, K. R. Ross ice shelf cavity circulation, residence time, and melting Results from a model of oceanic chlorofluorocarbons. *Continental Shelf Research* **30,** 733–742 (2010).

11. Smethie, W. M., Jr., Jacobs, S. S. & Smethie, W. M., Jr. Circulation and melting under the Ross Ice Shelf: estimates from evolving CFC, salinity and temperature fields in the Ross Sea. *Deep Sea Research Part I: Oceanographic Research Papers* (2005). doi:10.1016/j.dsr.2004.11.016

12. Joughin, I., Smith, B. E. & Medley, B. Marine ice sheet collapse potentially under way for the Thwaites Glacier Basin, West Antarctica. *Science* **344,** 735–738 (2014).

13. Tulaczyk, S. *et al.* WISSARD at Subglacial Lake Whillans, West Antarctica: scientific operations and initial observations. *Annals of Glaciology* **55,** 51–58 (2014).

14. Siegfried, M. R., Fricker, H. A., Roberts, M., Scambos, T. A. & Tulaczyk, S. A decade of West Antarctic subglacial lake interactions from combined ICESat and CryoSat-2 altimetry. *Geophys. Res. Lett.* **41,** 891–898 (2014).

15. Fisher, A. T. *et al.* High geothermal heat flux measured below the West Antarctic Ice Sheet. *Science Advances* **1,** e1500093–e1500093 (2015).

16. Carter, S. P., Fricker, H. A. & Siegfried, M. R. Evidence of rapid subglacial water piracy under Whillans Ice Stream, West Antarctica. *Journal of Glaciology* **59,** 1147–1162 (2013).

17. Takacs, C. D., Priscu, J. C. & McKnight, D. M. Bacterial dissolved organic carbon demand in McMurdo Dry Valley lakes, Antarctica. *Limnol. Oceangr.* **46,** 1189–1194 (2001).

18. Ducklow, H. W. Seasonal production and bacterial utilization of DOC in the Ross Sea, Antarctica. *Biogeochemistry of the Ross Sea* **78,** 143–158 (2003).

19. Vick-Majors, T. J. *et al.* Biogeochemistry and microbial diversity in the marine cavity beneath the McMurdo Ice Shelf, Antarctica. *Limnol. Oceangr.* in press

20. Carlson, C. A. in *Biogeochemistry of Marine Dissolved Organic Matter* (eds. Carlson, C. A. & Hansell, D. A.) 91–151 (2002).

21. Scherer, R. P. *et al.* Pleistocene Collapse of the West Antarctic Ice Sheet. *Science* **281,** 82–85 (1998).

22. Yamashita, Y. & Tanoue, E. Production of bio-refractory fluorescent dissolved organic matter in the ocean interior. *Nature Geosci* **1,** 579–582 (2008).

23. Jiao, N. *et al.* Microbial production of recalcitrant dissolved organic matter: long-term carbon storage in the global ocean. *Nat Rev Micro* **8,** 593–599 (2010).

24. Cory, R. M. & McKnight, D. M. Fluorescence spectroscopy reveals ubiquitous presence of oxidized and reduced quinones in dissolved organic matter. *Environ. Sci. Technol.* **39,** 8142–8149 (2005).

25. Coble, P. G. & Coble, P. G. Characterization of marine and terrestrial DOM in seawater using excitation-emission matrix spectroscopy. *Marine Chemistry* **51,** 325–346 (1996).

26. Yamashita, Y. *et al.* Fluorescence characteristics of dissolved organic matter in the deep waters of the Okhotsk Sea and the northwestern North Pacific Ocean. *Deep Sea Research Part II: Topical Studies in Oceanography* **57,** 1478–1485 (2010).

27. Barker, J. D., Klassen, J. L., Sharp, M. J., Fitzsimons, S. J. & Turner, R. J. Detecting biogeochemical activity in basal ice using fluorescence spectroscopy. *Annals of Glaciology* **51,** 47–55 (2010).

28. Arrigo, K. R., Worthen, D., Schnell, A. & Lizotte, M. P. Primary production in Southern Ocean waters. *Journal of Geophysical Research-Oceans* **103,** 15587–15600 (1998).

29. Goldman, J. C., Caron, D. A. & Dennett, M. R. Regulation of gross growth efficiency and ammonium regeneration in bacteria by substrate C:N ratio. *Limnol. Oceangr.* **32,** 1239–1252 (1987).

30. Lipps, J. H., Ronan, T. E. & DeLaca, T. E. Life Below the Ross Ice Shelf, Antarctica. *Science* **203,** 447–449 (1979).

31. Arnosti, C. Microbial Extracellular Enzymes and the Marine Carbon Cycle. *Annu. Rev. Marine. Sci.* **3,** 401–425 (2011).

32. Osterholz, H., Niggemann, J., Giebel, H.-A., Simon, M. & Dittmar, T. Inefficient microbial production of refractory dissolved organic matter in the ocean. *Nat Comms* **6,** 7422 (2015).

33. Blythe, D. S., Blythe, D. S., Duling, D. V. & Gibson, D. E. Developing a hot-water drill system for the WISSARD project: 2. In situ water production. *Annals of Glaciology* **55,** 298–302 (2014).

34. Rack, F. R. *et al.* Developing a hot-water drill system for the WISSARD project: 1. Basic drill system components and design. *Annals of …* (2014). doi:10.3189/2014AoG68A031

35. Burnett, J. *et al.* Developing a hot-water drill system for the WISSARD project: 3. Instrumentation and control systems. *Annals of Glaciology* **55,** 303–310 (2014).

36. Priscu, J. C. *et al.* A microbiologically clean strategy for access to the Whillans Ice Stream subglacial environment. *Ant. Sci.* **25,** 637–647 (2013).

37. Seeberg-Elverfeldt, J., Schlüter, M., Feseker, T. & Kölling, M. Rhizon sampling of porewaters near the sediment- water interface of aquatic systems. *Limnol. Oceanogr. Methods* **3,** 361–371 (2005).

38. McKnight, D. M. *et al.* Spectrofluorometric characterization of dissolved organic matter for indication of precursor organic material and aromaticity. *Limnol. Oceangr.* **46,** 38–48 (2001).

39. Murphy, K. R., Stedmon, C. A., Graeber, D. & Bro, R. Fluorescence spectroscopy and multi-way techniques. PARAFAC. *Anal. Methods* **5,** 6557–11 (2013).

40. Solórzano, L. Determination of ammonia in natural waters by the phenolhypochlorite method. *Limnol. Oceangr.* **14,** 799–801 (1969).

41. Solórzano, L. & Sharp, J. H. Determination of total dissolved phosphorus and particulate phosphorus in natural waters. **25,** 754–758 (1980).

42. del Giorgio, P. A. *et al.* Coherent patterns in bacterial growth, growth efficiency, and leucine metabolism along a northeastern Pacific inshore-offshore transect. *Limnol. Oceangr.* **56,** 1–16 (2011).

43. Fricker, H. A. & Scambos, T. Connected subglacial lake activity on lower Mercer and Whillans ice streams, West Antarctica, 2003–2008. *Journal of Glaciology* **55,** 303–315 (2009).

44. Christoffersen, P., Bougamont, M., Carter, S. P., Fricker, H. A. & Tulaczyk, S. Significant groundwater contribution to Antarctic ice streams hydrologic budget. *Geophys. Res. Lett.* **41,** 2003–2010 (2014).

45. Li, Y.-H. & S, G. Diffusion of ions in sea water and in deep-sea sediments. *Geochimica et Cosmochimica Acta* **38,** 703–714 (1974).

46. Shen, L. & Chen, Z. Critical review of the impact of tortuosity on diffusion. *Chemical Engineering Science* **62,** 3748–3755 (2007).

CHAPTER EIGHT

CONCLUSIONS

Slow-growth under energy limited conditions is likely the most common physiological state of microorganisms on Earth (Lever *et al.*, 2015), yet little is known about how microbial communities persist under such conditions, or how they impact biogeochemical processes (LaRowe and Amend, 2015). Even the definition of energy-limitation is a gray area, with no consensus on the minimum amount of energy that is required to maintain a cell or for a cell to undergo cell division for population growth or maintenance (e.g. Hoehler and Jørgensen, 2013; Lever *et al.*, 2015). The "deep biosphere", which includes ecosystems and organisms living beneath the upper few meters of the Earth's surface, receives low energy fluxes and is generally considered to be energy limited and/or nutrient starved (Hoehler and Jørgensen, 2013; Jørgensen, 2011). Rates of metabolic activity in these environments are low compared to surface, or nutrient-rich, environments. Metabolic activity in Subglacial Lake Whillans (SLW) is similar to that found in the subsurface, while activity beneath the McMurdo Ice Shelf (MIS) is similar to other surface and oceanic environments and that of the McMurdo Dry Valley lakes (MCM) is intermediate (Figure 8.1). Collectively, the three environments examined by my dissertation provide a useful energetic gradient along which to study microbially-mediated processes.

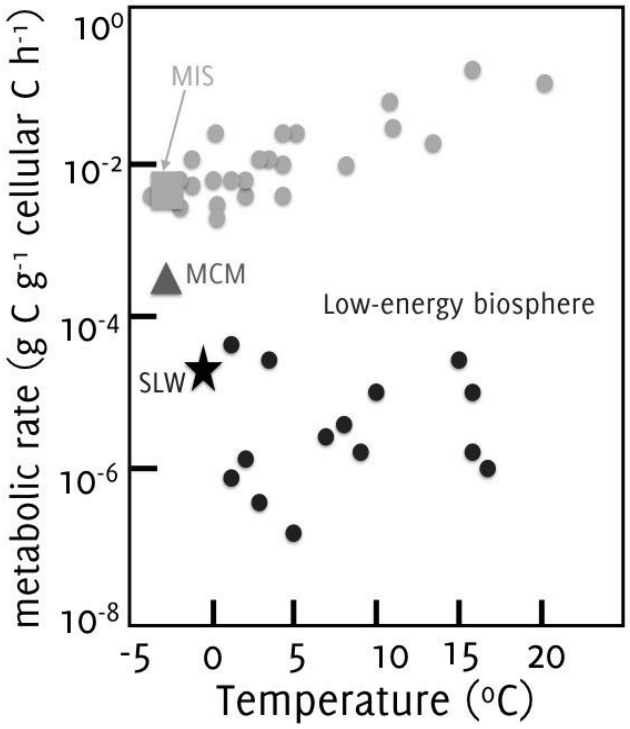

Figure 8.1. Metabolic rates of heterotrophic microbial communities in Subglacial Lake Whillans (SLW; Chapter 6), under the McMurdo Ice Shelf (MIS; Chapter 5), and the McMurdo Dry Valley Lakes during the Polar Night transition (MCM; Chapter 2 and (Vick and Priscu, 2012) compared to those of deep-biosphere (black) and surface (gray) environments. The figure is modified from (Jørgensen, 2011).

Photosynthetic microorganisms in the MCM are adapted to the low-light environment beneath the lake ice during summer (Priscu *et al.,* 1990), but the darkness of winter is a major loss of energy to the lakes. Obligate photosynthetic phytoplankton maintain downregulated photosynthetic machinery during the winter (Morgan-Kiss *et al.*, 2015), while mixotrophic protists (capable of photosynthesis and phagotrophy) increase their abundance and activity (Chapter 2, Thurman *et al.*, 2012). Bacterial and eukaryotic phylum-level community compositions differ significantly between summer and autumn within the MCM lakes, indicating a seasonal shift in community composition. Archaeal communities, on the other hand, differ between depths rather than seasons, indicating that

within-lake geochemical conditions are more important in determining community structure, although OTU-level diversity differed between seasons (Chapter 2). The proliferation of putatively chemolithotrophic OTU's and the keystone status of metabolically flexible OTU's are suggestive of the importance of shifts in community composition and flexible metabolisms in these nutrient and light limited lakes. Supporting evidence for the importance of non-photosynthetic metabolisms comes from the high rates of chemoautotrophic inorganic carbon fixation in the lakes (Chapter 3). Nutrient limitation and/or seasonal shifts in carbon sources may lead to relatively low rates of heterotrophic bacterial and archaeal activity in the MCM (Figure 8.1). Alternatively, a tradeoff in favor of metabolic flexibility could result in perceived low growth rates and the low growth efficiencies estimated for MCM bacterioplankton (Takacs *et al.*, 2001), as energy is funneled to the maintenance of enzymes that allow organisms to respond quickly to changing conditions (Teixeira de Mattos and Neijssel, 1997). Metabolic flexibility and availability of energy sources to support chemoautotrophic carbon fixation (Chapters 2 and 3) may be important in defining the lakes' intermediate position between the low-energy deep biosphere and high-energy surface environments (Figure 8.1).

The waters beneath the MIS are permanently dark, but connected via ocean circulation to the open waters of McMurdo Sound. The relatively short distance between the sample collection site and ice-free waters leads to quantitative similarities in nutrient and cell concentrations (Chapter 4). Along with dissolved organic matter and nutrients, chlorophyll *a*-containing phytoplankton cells are advected under the ice, where they may

release energy-rich organic matter similar to phytoplankton in open water, or conserve it to support their own metabolism in the dark, releasing it when they eventually lyse (Thornton, 2014). This access to phytoplankton-derived organic matter and nutrients may be key to the MIS site's energetic similarity to the open ocean and other surface environments (Figure 8.1). Chemoautotrophic carbon-fixation also occurs under the MIS, but can account for only a small proportion of the heterotrophic activity measured at the site, making it proportionally less important than in MCM.

Seasonal access to sunlight and connections with ice-free waters differentiate MCM and MIS from SLW, which is permanently dark and contains an ecosystem dependent on energy sources buried in the sediments or carried by ice-melt, the ultimate source of the lake water. SLW lies in an area of West Antarctica that may be occasionally inundated with seawater while maintaining its ice cover, however, the late-Pleistocene collapse of the West Antarctic Ice Sheet (Scherer *et al.*, 1998) presumably provided the last input of photosynthetically produced organic matter to the region ~123,000 years ago. During the intervening time, microbial activity has led to a net loss of nitrogen and net gain of organic carbon in the subglacial environment, resulting in the high C:N ratios observed in the dissolved and particulate matter pools in SLW (Chapters 6 and 7). The organic matter in SLW is microbially produced (Chapter 7), however, there may be important differences in the timescales of organic matter supply and demand, or limitations imposed by the quality of the organic matter, which lead to the energy-limited heterotrophic growth of microorganisms in SLW (Figure 8.1). Energy-limited cells are not expected to leak organic matter, a common means of energy dissipation (Carlson *et*

al., 2007), which may explain the disparity between the amount of inorganic carbon fixed by chemoautotrophy in SLW and that used to support heterotrophic production (Chapters 6 and 7). Where the availability of freshly produced organic matter is limited, heterotrophic bacteria or archaea produce polysaccharide capsules and ectoenzymes to scavenge organic molecules (Carlson *et al.*, 2007). This microbially produced organic matter can lead to the accumulation of recalcitrant organic matter, which may be bioavailable over timescales of thousands of years (Jiao *et al.*, 2010). Thus, the balance of chemoautotrophic and heterotrophic activity in SLW can explain the large pool of dissolved organic matter present in the lake and the low heterotrophic activity SLW shares with deep-biosphere environments (Figure 8.1).

Together, the five core papers of this dissertation address the overarching theme, "how does the ensemble of environmentally imposed energetic constraints impact nutrient cycling in microbially dominated systems?" My data show that, even in energy limited SLW, microbial activity shapes the geochemical environment and has the potential to impact biogeochemical processes in hydrologically connected environments. Much of the work in this dissertation was exploratory; the McMurdo Dry Valley lakes were sampled for the first time during the seasonal austral sunset, data collected from under the McMurdo Ice Shelf comprised the first biogeochemical dataset from that location, and Subglacial Lake Whillans became the first subglacial lake to be directly sampled. As such, these papers should open many avenues for future research. Our comprehension of the McMurdo Dry Valley lakes ecosystems will increase with targeted analyses of functional genes and meta-"omics" studies focused on the microbial

interactions and metabolic strategies putatively identified here. A more holistic understanding of sub-ice shelf ecosystems can be achieved through studies that also incorporate the heterotrophic eukaryotic components of the microbial communities beneath ice-shelves. Sampling under ice shelves is logistically challenging, but transects from the edge of the ice-shelf to the grounding zone would provide important information on sub-ice-shelf biogeochemistry with progressive distance from open water, as well as physical oceanographic data. The active subglacial lakes of West Antarctica are dynamic and likely comprise environments that are highly variable over time and space. The knowledge gained from studying Subglacial Lake Whillans is an important first step, allowing comparative studies to be designed and targeted hypotheses developed. Future studies aimed at determining the age and source of subglacial organic matter can be combined with information about microbial activity to inform the field of microbial physiology and energetics, and with geochemical information to further our understanding of the dynamics of the West Antarctic Ice Sheet and when previous incursions of sea water may have occurred. Similar to the need for transects across ice-shelves, sample collection from subglacial lake inflow and outflow will greatly help our understanding of these systems and the timeframes over which microbially mediated changes occur within subglacial water. Finally, ice-covered environments can serve as analogues for icy environments in the Solar System, such as the Jupiter's moon, Europa and Saturn's Enceladus, and inform the search for life in in the Universe. The microbiologically clean access strategies presented in Chapter 4 highlight the importance,

and feasibility, of collecting samples from pristine environments while minimizing forward contamination.

References

Carlson CA, del Giorgio PA, Herndl GJ. (2007). Microbes and the dissipation of energy and respiration: from cells to ecosystems. *Oceanog* **20**:89–100.

Hoehler TM, Jørgensen BB. (2013). Microbial life under extreme energy limitation. *Nat Rev Micro* **11**:83–94.

Jiao N, Herndl GJ, Hansell DA, Benner R, Kattner G, Wilhelm SW, *et al.* (2010). Microbial production of recalcitrant dissolved organic matter: long-term carbon storage in the global ocean. *Nat Rev Micro* **8**:593–599.

Jørgensen BB. (2011). Deep subseafloor microbial cells on physiological standby. *Proceedings of the National Academy of Sciences* **108**:18193–18194.

LaRowe DE, Amend JP. (2015). Catabolic rates, population sizes and doubling/replacement times of microorganisms in natural settings. **315**:167–203.

Lever MA, Rogers KL, Lloyd KG, Overmann J, Schink B, Thauer RK, *et al.* (2015). Life under extreme energy limitation: a synthesis of laboratory- and field-based investigations Giudici-Orticoni, M-T (ed). *FEMS Microbiology Reviews* **39**:688–728.

Morgan-Kiss RM, Lizotte MP, Kong W, Priscu JC. (2015). Photoadaptation to the polar night by phytoplankton in a permanently ice-covered Antarctic lake. *Limnol Oceangr* n/a–n/a.

Priscu JC, Sharp TR, Lizotte MP, Neale PJ. (1990). Photoadaptation by phytoplankton in permanently ice-covered Antarctic lakes: response to a non-turbulent environment. Antarctic Journal of the US.

Scherer RP, Aldahan A, Tulaczyk S, Possnert G, Engelhardt H, Kamb B. (1998). Pleistocene Collapse of the West Antarctic Ice Sheet. *Science* **281**:82–85.

Takacs CD, Priscu JC, McKnight DM. (2001). Bacterial dissolved organic carbon demand in McMurdo Dry Valley lakes, Antarctica. *Limnol Oceangr* **46**:1189–1194.

Teixeira de Mattos MJ, Neijssel OM. (1997). Bioenergetic consequences of microbial adaptation to low-nutrient environments. *J Biotechnol* **59**:117–126.

Thornton DCO. (2014). Dissolved organic matter (DOM) release by phytoplankton in the contemporary and future ocean. *European Journal of Phycology* **49**:20–46.

Thurman J, Parry J, Hill PJ, Priscu JC, Vick TJ, Chiuchiolo A, *et al.* (2012). Microbial dynamics and flagellate grazing during transition to winter in Lakes Hoare and Bonney, Antarctica. *FEMS Microbiology Ecology* **82**:449–458.

Vick TJ, Priscu JC. (2012). Bacterioplankton productivity in lakes of the Taylor Valley, Antarctica, during the polar night transition. *Aquat Microb Ecol* **68**:77–90.

REFERENCES CITED

Achterberg EP. (2014). Grand challenges in marine biogeochemistry. *Frontiers in Marine Science* **1**:50.

Alawi M, Lipski A, Sanders T, Eva-Maria-Pfeiffer, Spieck E. (2007). Cultivation of a novel cold-adapted nitrite oxidizing betaproteobacterium from the Siberian Arctic. *ISME J* **1**:256–264.

Alonso-Sáez L, Sánchez O, Gasol JM, Balagué V, Pedrós-Alio C. (2008). Winter-to-summer changes in the composition and single-cell activity of near-surface Arctic prokaryotes. *Environmental Microbiology* **10**:2444–2454.

Amaral-Zettler LA, McCliment EA, Ducklow HW, Huse SM. (2009). A method for studying protistan diversity using massively parallel sequencing of V9 hypervariable regions of small-subunit ribosomal RNA genes. Langsley, G (ed). *PLoS ONE* **4**:e6372.

Anderson MJ. (2001). A new method for non-parametric multivariate analysis of variance. *Austral Ecology* **26**:32–46.

Andersson AF, Riemann L, Bertilsson S. (2010). Pyrosequencing reveals contrasting seasonal dynamics of taxa within Baltic Sea bacterioplankton communities. *ISME J* **4**:171–181.

Apprill A, McNally S, Parsons R, Webe L. (2015). Minor revision to V4 region SSU rRNA 806R gene primer greatly increases detection of SAR11 bacterioplankton. *Aquat Microb Ecol* **75**:129–137.

Arnosti C. (2011). Microbial Extracellular Enzymes and the Marine Carbon Cycle. *Annu Rev Marine Sci* **3**:401–425.

Arrigo KR. (1999). Phytoplankton Community Structure and the Drawdown of Nutrients and CO2 in the Southern Ocean. *Science* **283**:365–367.

Arrigo KR, McClain CR. (1994). Spring phytoplankton production in the Western ross sea. *Science* **266**:261–263.

Arrigo KR, van Dijken GL. (2004). Annual changes in sea-ice, chlorophyll a, and primary production in the Ross Sea, Antarctica. *Deep Sea Research Part II: Topical Studies in Oceanography* **51**:117–138.

Arrigo KR, van Dijken GL, Bushinsky S. (2008). Primary production in the Southern Ocean, 1997–2006. *J Geophys Res* **113**. doi:10.1029/2007jc004551.

Arrigo KR, Worthen D, Schnell A, Lizotte MP. (1998). Primary production in Southern Ocean waters. *Journal of Geophysical Research-Oceans* **103**:15587–15600.

Atamna-Ismaeel N, Sharon I, Sharon I, Sabehi G, Witzel K-P, Labrenz M, *et al.* (2008). Widespread distribution of proteorhodopsins in freshwater and brackish ecosystems. **2**:656–662.

Azam F, Beers JR, Campbell L, Carlucci AF, Holm-Hansen O, Reid FM, *et al.* (1979). Occurrence and metabolic activity of organisms under the Ross Ice Shelf, Antarctica, at Station J9. *Science* **203**:451–453.

Barberán A, Bates ST, Casamayor EO, Fierer N. (2012). Using network analysis to explore co-occurrence patterns in soil microbial communities. *ISME J* **6**:343–351.

Bardgett RD, Richter A, Bol R, Garnett MH, Bäumler R, Xu X, *et al.* (2007). Heterotrophic microbial communities use ancient carbon following glacial retreat. *Biology Letters* **3**:487–490.

Barker JD, Klassen JL, Sharp MJ, Fitzsimons SJ, Turner RJ. (2010). Detecting biogeochemical activity in basal ice using fluorescence spectroscopy. *Annals of Glaciology* **51**:47–55.

Barry JP. (1988). Hydrographic patterns in McMurdo Sound, Antarctica and their relationship to local benthic communities. *Polar Biology* **8**:377–391.

Behrenfeld MJ, Boss E, Siegel DA, Shea DM. (2005). Carbon-based ocean productivity and phytoplankton physiology from space. *Global Biogeochem Cycles* **19**:n/a–n/a.

Bell RE, Studinger M, Tikku AA, Clarke GKC, Gutner MM, Meertens C. (2002). Origin and fate of Lake Vostok water frozen to the base of the East Antarctic ice sheet. *Nature* **416**:307–310.

Bell RT. (1993). Estimating production of heterotrophic bacterioplankton via incorporation of tritiated thymidine. Lewis Publishers.

Bertolin ML, Schloss IR. (2009). Phytoplankton production after the collapse of the Larsen A Ice Shelf, Antarctica. *Polar Biology* **32**:1435–1446.

Bielewicz S, Bell E, Kong W, Friedberg I, Priscu JC, Morgan-Kiss RM. (2011). Protist diversity in a permanently ice-covered Antarctic lake during the polar night transition. *ISME J* **5**:1559–1564.

Biers EJ, Sun S, Howard EC. (2009). Prokaryotic Genomes and Diversity in Surface Ocean Waters: Interrogating the Global Ocean Sampling Metagenome. *Applied and Environmental Microbiology* **75**:2221–2229.

Blankenship DD, Bell RE, Hodge SM, Brozena JM, BEHRENDT JC, Finn CA. (1993). Active Volcanism Beneath the West Antarctic Ice-Sheet and Implications for Ice-Sheet Stability. *Nature* **361**:526–529.

Blythe DS, Blythe DS, Duling DV, Gibson DE. (2014). Developing a hot-water drill system for the WISSARD project: 2. In situ water production. *Annals of Glaciology* **55**:298–302.

Bougamont M, Hunke EC, Tulaczyk S. (2007). Sensitivity of ocean circulation and sea-ice conditions to loss of West Antarctic ice shelves and ice sheet. *Journal of Glaciology* **53**:490–498.

Bouvier T, del Giorgio PA, Gasol JM. (2007). A comparative study of the cytometric characteristics of high and low nucleic-acid bacterioplankton cells from different aquatic ecosystems. *Environmental Microbiology* **9**:2050–2066.

Boyd ES, Hamilton TL, Havig JR, Skidmore ML, Shock EL. (2014). Chemolithotrophic primary production in a subglacial ecosystem. *Applied and Environmental Microbiology* **80**:6146–6153.

Boyd ES, Lange RK, Mitchell AC, Havig JR, Hamilton TL, Lafrenière MJ, *et al.* (2011). Diversity, abundance, and potential activity of nitrifying and nitrate-reducing microbial assemblages in a subglacial ecosystem. *Applied and Environmental Microbiology* **77**:4778–4787.

Boyd ES, Skidmore M, Mitchell AC, Bakermans C, Peters JW. (2010). Methanogenesis in subglacial sediments. *Environmental Microbiology Reports* **2**:685–692.

Budillon G, Castagno P, Castagno P, Aliani S, Aliani S, Spezie G, *et al.* (2011). Thermohaline variability and Antarctic bottom water formation at the Ross Sea shelf break. *Deep Sea Research Part I: Oceanographic Research Papers* **58**:1002–1018.

Bunge J, Woodard L, Böhning D, Foster JA, Connolly S, Allen HK. (2012). Estimating population diversity with CatchAll. *Bioinformatics* **28**:1045–1047.

Burnett J, Burnett J, Rack FR, Rack FR, Blythe D, BLYTHE D, *et al.* (2014). Developing a hot-water drill system for the WISSARD project: 3. Instrumentation and control systems. *Annals of Glaciology* **55**:303–310.

Campbell NE, Aleem MI. (1965). The effect of 2-chloro, 6-(trichlormethyl) pyridine on the chemoautrotrophic metabolism of nitrfying bacteria. *Antonie Van Leeuwenhoek* **31**:124–136.

Caporaso JG, Lauber CL, Walters WA, Berg-Lyons D, Huntley J, Fierer N, *et al.* (2012). Ultra-high-throughput microbial community analysis on the Illumina HiSeq and MiSeq platforms. *ISME J* **6**:1621–1624.

Carlson CA. (2002). Production and Removal Processes. In:*Biogeochemistry of Marine Dissolved Organic Matter*, Carlson, CA & Hansell, DA (eds), San Diego, CA, pp. 91–151.

Carlson CA, del Giorgio PA, Herndl GJ. (2007). Microbes and the dissipation of energy and respiration: from cells to ecosystems. *Oceanog* **20**:89–100.

Carr SA, Vogel SW, Dunbar RB, Brandes J, Spear JR, Levy R, *et al.* (2013). Bacterial abundance and composition in marine sediments beneath the Ross Ice Shelf, Antarctica. *Geobiology* **11**:377–395.

Carter SP, Fricker HA. (2012). The supply of subglacial meltwater to the grounding line of the Siple Coast, West Antarctica. *Annals of Glaciology* **53**:267–280.

Carter SP, Fricker HA, Siegfried MR. (2013). Evidence of rapid subglacial water piracy under Whillans Ice Stream, West Antarctica. *Journal of Glaciology* **59**:1147–1162.

Casciotti KL, Sigman DM, Hastings MG, Böhlke JK, Hilkert A. (2002). Measurement of the oxygen isotopic composition of nitrate in seawater and freshwater using the denitrifier method. *Anal Chem* **74**:4905–4912.

Cavicchioli R. (2015). Microbial ecology of Antarctic aquatic systems. *Nat Rev Micro* **13**:691–706.

Celussi M, Umani SF, Del Negro P, Cataletto B, Bergamasco A, Bergamasco A. (2010). Water masses' bacterial community structure and microbial activities in the Ross Sea, Antarctica. *Ant Sci* **22**:361–370.

Chaffron S, Rehrauer H, Pernthaler J, Mering von C. (2010). A global network of coexisting microbes from environmental and whole-genome sequence data. *Genome Research* **20**:947–959.

Chao A. (1984). Non-parametric estimation of the number of classes in a population. *Scandinavian Journal of Statistics* **11**:265–270.

Chao A, Shen TJ. Program SPADE (Species Prediction and Diversity Estimation). http://chao.stat.nthu.edu.tw/.

Charvet S, Vincent WF, Comeau A, Lovejoy C. (2012). Pyrosequencing analysis of the protist communities in a High Arctic meromictic lake: DNA preservation and change. *Front Microbio* **3**:422.

Chien MC, Morozova I, Shi SD, Sheng HT, Chen J, Gomez SM, *et al.* (2004). The genomic sequence of the accidental pathogen Legionella pneumophila. *Science* **305**:1966–1968.

Chin-Leo G, Kirchman DL. (1988). Estimating bacterial production in marine waters from the simultaneous incorporation of thymidine and leucine. *Applied and Environmental …* **54**:1934–1939.

Chown SL, Clarke A, Fraser CI, Cary SC, Moon KL, McGeoch MA. (2015). The changing form of Antarctic biodiversity. *Nature* **522**:431–438.

Christianson K, Jacobel RW, Horgan HJ, Anandakrishnan S, Alley RB. (2012). Subglacial Lake Whillans — Ice-penetrating radar and GPS observations of a shallow active reservoir beneath a West Antarctic ice stream. *Earth and Planetary Science Letters* **331-332**:237–245.

Christner BC, Priscu JC, Achberger AM, Barbante C, Carter SP, Christianson K, *et al.* (2014). A microbial ecosystem beneath the West Antarctic ice sheet. *Nature* **512**:310–313.

Christner BC, Royston-Bishop G, Foreman CM, Arnold BR, Tranter M, Welch KA, *et al.* (2006). Limnological conditions in Subglacial Lake Vostok, Antarctica. *Limnol Oceangr* **51**:2485–2501.

Christner BC, Skidmore ML, Priscu JC, Tranter M, Foreman CM. (2008). Bacteria in Subglacial Environments. Springer Berlin Heidelberg: Berlin, Heidelberg.

Christoffersen P, Bougamont M, Carter SP, Fricker HA, Tulaczyk S. (2014). Significant groundwater contribution to Antarctic ice streams hydrologic budget. *Geophys Res Lett* **41**:2003–2010.

Church MJ, Hutchins DA, Ducklow HW. (2000). Limitation of bacterial growth by dissolved organic matter and iron in the Southern ocean. *Applied and Environmental Microbiology* **66**:455–466.

Clough JW, Hansen BL. The Ross Ice Shelf Project. http://www.sciencemag.org/content/203/4379/433.short.

Coble PG, Coble PG. (1996). Characterization of marine and terrestrial DOM in seawater using excitation-emission matrix spectroscopy. *Marine Chemistry* **51**:325–346.

Comeau AM, Harding T, Galand PE, Vincent WF, Lovejoy C. (2012). Vertical distribution of microbial communities in a perennially stratified Arctic lake with saline, anoxic bottom waters. *Sci Rep* **2**:604.

Convey P, Chown SL, Clarke A, Barnes DKA, Bokhorst S, Cummings V, *et al.* (2014). The spatial structure of Antarctic biodiversity. *Ecological Monographs* **84**:203–244.

Cory RM, McKnight DM. (2005). Fluorescence spectroscopy reveals ubiquitous presence of oxidized and reduced quinones in dissolved organic matter. *Environ Sci Technol* **39**:8142–8149.

Costa AW, Michalski G, Schauer AJ, Alexander B, Steig EJ, Shepson PB. (2011). Analysis of atmospheric inputs of nitrate to a temperate forest ecosystem from Δ 17O isotope ratio measurements. *Geophys Res Lett* **38**:L15805.

Crump BC, Amaral-Zettler LA, Kling GW. (2012). Microbial diversity in arctic freshwaters is structured by inoculation of microbes from soils. *ISME J* **6**:1629–1639.

Crump BC, Kling GW, Bahr M. (2003). Bacterioplankton community shifts in an arctic lake correlate with seasonal changes in organic matter source. *Applied and Environmental Microbiology* **69**:2253–2268.

Daly M, Rack F, Zook R, Rack F, Zook R. (2013). Edwardsiella andrillae, a New Species of Sea Anemone from Antarctic Ice Thuesen, EV (ed). *PLoS ONE* **8**:e83476.

Damm E, Helmke E, Thoms S, Schauer U, Nöthig E, Bakker K, *et al.* (2010). Methane production in aerobic oligotrophic surface water in the central Arctic Ocean. *Biogeosciences* **7**:1099–1108.

Danckwerts PV. (1953). Continuous flow systems. Distribution of residence times. *Chemical Engineering Science* **2**:1–13.

del Giorgio PA, Cole JJ. (1998). Bacterial growth efficiency in natural aquatic systems. *Annual Review of Ecology and Systematics* **29**:503–541.

del Giorgio PA, Condon R, Bouvier T, Longnecker K, Bouvier C, Sherr E, *et al.* (2011). Coherent patterns in bacterial growth, growth efficiency, and leucine metabolism along a northeastern Pacific inshore-offshore transect. *Limnol Oceangr* **56**:1–16.

DeLong EF, Beja O. (2010). The light-driven proton pump proteorhodopsin enhances bacterial survival during tough times. *PLoS Biol* **8**:e1000359.

Depoorter MA, Bamber JL, Lenaerts JTM, Griggs JA, van den Broeke MR, Moholdt G, *et al.* (2013). Calving fluxes and basal melt rates of Antarctic ice shelves. *Nature* **502**:89–92.

Dieser M, Sletten R, Hagedorn B, Christner BC, Junge K, Choquette K, *et al.* (2014). Molecular and biogeochemical evidence for methane cycling beneath the western margin of the Greenland Ice Sheet. *ISME J* **8**:2305–2316.

DiTullio GR, Grebmeier JM, Arrigo KR, Lizotte MP, Robinson DH, Leventer A, *et al.* (2000). Rapid and early export of Phaeocystis antarctica blooms in the Ross Sea, Antarctica. *Nature* **404**:595–598.

DiTullio GR, Smith WO. (1996). Spatial patterns in phytoplankton biomass and pigment distributions in the Ross Sea. *J Geophys Res* **101**:18467.

Dolhi JM, Teufel AG, Kong W, Morgan-Kiss RM. (2015). Diversity and spatial distribution of autotrophic communities within and between ice-covered Antarctic lakes (McMurdo Dry Valleys). *Limnol Oceangr* **60**:977–991.

Domack E, Ishman S, Leventer A. (2005). A chemotrophic ecosystem found beneath Antarctic ice shelf. *Eos Trans AGU* **86**:269.

Dore JE, Priscu JC. (2001). Phytoplankton phosphorus deficiency and alkaline phosphatase activity in the McMurdo Dry Valley lakes, Antarctica. **46**:1331–1346.

Ducklow H, Carlson C, Church M, Kirchman D. (2001). The seasonal development of the bacterioplankton bloom in the Ross Sea, Antarctica, 1994–1997. *Deep Sea Research Part II: Topical Studies in Oceanography* **48**:4199–4221.

Ducklow HW. (2003). Seasonal production and bacterial utilization of DOC in the Ross Sea , Antarctica. *Biogeochemistry of the Ross Sea* **78**:143–158.

Edgar RC, Haas BJ, Clemente JC, Quince C, Knight R. (2011). UCHIME improves sensitivity and speed of chimera detection. *Bioinformatics* **27**:2194–2200.

Enright AJ, Van Dongen S, Ouzounis CA. (2002). An efficient algorithm for large-scale detection of protein families. *Nucleic Acids Res* **30**:1575–1584.

Erdös P, Rényi A. (1959). On random graphs. I. *Publicationes Mathematicae (Debrecen)* **6**:290–297.

Falkowski PG, Fenchel T, DeLong EF. (2008). The microbial engines that drive Earth's biogeochemical cycles. *Science* **320**:1034–1039.

Fillinger L, Janussen D, Lundälv T, Richter C. (2013). Rapid glass sponge expansion after climate-induced Antarctic ice shelf collapse. *Curr Biol* **23**:1330–1334.

Fisher AT, Mankoff KD, Tulaczyk SM, Tyler SW, Foley N, WISSARD Science Team. (2015). High geothermal heat flux measured below the West Antarctic Ice Sheet. *Science Advances* **1**:e1500093–e1500093.

Foreman CM, Sattler B, Mikucki JA, Porazinska DL, Priscu JC. (2007). Metabolic activity and diversity of cryoconites in the Taylor Valley, Antarctica. *J Geophys Res* **112**:G04S32–11.

Foreman CM, Wolf CF, Priscu JC. (2004). Impact of Episodic Warming Events on the Physical, Chemical, and Biological Relationships of Lakes in the McMurdo Dry Valleys, Antarctica. *Aquat Geochem* **10**:239–368.

Fortunato S. (2010). Community detection in graphs. *Physics Reports* **486**:75–174.

Fox AJ, Cooper APR. (1994). Measured properties of the Antarctic ice sheet derived from the SCAR Antarctic digital database. *Polar Record* **30**:201–206.

Fretwell P, Pritchard HD, Vaughan DG, Bamber JL, Barrand NE, Bell R, *et al.* (2013). Bedmap2: improved ice bed, surface and thickness datasets for Antarctica. *The Cryosphere* **7**:375–393.

Fricker HA, Powell R, Priscu J, Tulaczyk S. (2011). Siple coast subglacial aquatic environments: The whillans ice stream subglacial access research drilling project. *Geophys Monogr* ….

Fricker HA, Scambos T. (2009). Connected subglacial lake activity on lower Mercer and Whillans ice streams, West Antarctica, 2003–2008. *Journal of Glaciology* **55**:303–315.

Fricker HA, Scambos T, Bindschadler R, Padman L. (2007). An active subglacial water system in West Antarctica mapped from space. *Science* **315**:1544–1548.

Fricker HA, Smith BE, Tulaczyk S, Joughin IR, Smith BE, Joughin IR. (2009). An inventory of active subglacial lakes in Antarctica detected by ICESat (2003–2008). *Journal of Glaciology* **55**:573–595.

Frigaard N-U, Mincer TJ, DeLong EF, Martinez A. (2006). Proteorhodopsin lateral gene transfer between marine planktonic Bacteria and Archaea. *Nature* **439**:847–850.

Fuhrman JA, Azam F. (1982). Thymidine incorporation as a measure of heterotrophic bacterioplankton production in marine surface waters: evaluation and field results. *Mar Biol* **66**:109–120.

Fuhrman JA, Steele JA, Fuhrman J, Steele J. (2008). Community structure of marine bacterioplankton: patterns, networks, and relationships to function. *Aquat Microb Ecol* **53**:69–81.

Gaidos E, Marteinsson V, Thorsteinsson T, Jóhannesson T, Rúnarsson ÁR, Stefánsson A, *et al.* (2009). An oligarchic microbial assemblage in the anoxic bottom waters of a volcanic subglacial lake. *ISME J* **3**:486–497.

Galand PE, Lovejoy C, Pouliot J. (2008). Microbial community diversity and heterotrophic production in a coastal Arctic ecosystem: A stamukhi lake and its source waters. *Limnol Oceangr* **53**:813–823.

Garcia SL, McMahon KD, Martinez-Garcia M, Srivastava A, Sczyrba A, Stepanauskas R, *et al.* (2012). Metabolic potential of a single cell belonging to one of the most abundant lineages in freshwater bacterioplankton. *ISME J* **7**:137–147.

Gasol JM, del Giorgio PA. (2000). Using flow cytometry for counting natural planktonic bacteria and understanding the structure of planktonic bacterial communities *. *Scientia Marina* **64**:197–224.

Ghiglione JF, Murray AE. (2012). Pronounced summer to winter differences and higher wintertime richness in coastal Antarctic marine bacterioplankton. *Environmental Microbiology* **14**:617–629.

Gilmour AE. (1979). Ross ice shelf sea temperatures. *Science* **203**:438–439.

Giovannoni SJ, Tripp HJ, Bibbs L, Cho J-C, Stapels MD, Desiderio R, *et al.* (2005). Proteorhodopsin in the ubiquitous marine bacterium SAR11. *Nature* **438**:82–85.

Glatz RE, Lepp PW, Ward BB, Francis CA. (2006). Planktonic microbial community composition across steep physical/chemical gradients in permanently ice-covered Lake Bonney, Antarctica. *Geobiology* **4**:53–67.

Goldman JC, Caron DA, Dennett MR. (1987). Regulation of gross growth efficiency and ammonium regeneration in bacteria by substrate C:N ratio. *Limnol Oceangr* **32**:1239–1252.

González M, Martín González AM, Dalsgaard AM, Dalsgaard B, Olesen JM, Olesen JMB. (2010). Centrality measures and the importance of generalist species in pollination networks. *Ecological Complexity* **7**:36–43.

Good IJ. (1953). The population frequencies of species and the estimation of population parameters. *Biometrika* **40**:237–264.

Gordon DA, Priscu J, Giovannoni S. (2000). Origin and Phylogeny of Microbes Living in Permanent Antarctic Lake Ice. *Microbial Ecology* **39**:197–202.

Goreau TJ, Kaplan WA, Wofsy SC, McElroy MB, Valois FW, Watson SW. (1980). Production of NO2- and N2O by Nitrifying Bacteria at Reduced Concentrations of Oxygen. *Applied and Environmental Microbiology* **40**:526–532.

Gotelli NJ, McCabe DJ, McCabe DJ. (2002). Species co-occurrence: a meta-analysis of JM Diamond's assembly rules model. *Ecology*. doi:10.1890/0012-9658(2002)083[2091:SCOAMA]2.0.CO;2.

Gray L, Joughin I, Tulaczyk S, Spikes VB. (2005). Evidence for subglacial water transport in the West Antarctic Ice Sheet through three-dimensional satellite radar interferometry. *Geophysical ….*

Greenbaum JS, Blankenship DD, Young DA, Richter TG, Roberts JL, Aitken ARA, *et al.* (2015). Ocean access to a cavity beneath Totten Glacier in East Antarctica. *Nature Geosci* **8**:294–298.

Greischar LL, Bentley CR. (1980). Isostatic equilibrium grounding line between the West Antarctic inland ice sheet and the Ross Ice Shelf. *Nature* **283**:651–654.

Griggs JA, Bamber JL. (2011). Antarctic ice-shelf thickness from satellite radar altimetry. *Journal of Glaciology* **57**:485–498.

Grossart H-P, Frindte K, Dziallas C, Eckert W, Tang KW. (2011). Microbial methane production in oxygenated water column of an oligotrophic lake. *Proc Natl Acad Sci USA* **108**:19657–19661.

Grzymski JJ, Riesenfeld CS, Williams TJ, Dussaq AM, Ducklow H, Erickson M, *et al.* (2012). A metagenomic assessment of winter and summer bacterioplankton from Antarctica Peninsula coastal surface waters. *ISME J* **6**:1901–1915.

Gutt J, Barratt I, Domack E, Domack E, d'Acoz CU, Dimmler W, *et al.* (2011). Biodiversity change after climate-induced ice-shelf collapse in the Antarctic. *Deep Sea Research Part II: Topical Studies in Oceanography* **58**:74–83.

Hansell DA, Carlson CA. (1998). Deep-ocean gradients in the concentration of dissolved organic carbon. *Nature* **395**:263–266.

Hillebrand H, Dürselen CD, Kirschtel D. (1999). Biovolume calculation for pelagic and benthic microalgae. *Journal of Phycology* **35**:403–424.

Hodson RE, Azam F, Carlucci AF, Fuhrman JA, Karl DM, Holm-Hansen O. (1981). Microbial Uptake of Dissolved Organic-Matter in Mcmurdo-Sound, Antarctica. *Mar Biol* **61**:89–94.

Hoehler TM, Jørgensen BB. (2013). Microbial life under extreme energy limitation. *Nat Rev Micro* **11**:83–94.

Holland HD. (1978). The Chemistry of the Atmosphere and Oceans. Wiley.

Holm-Hansen O, Azam F, Campbell L, Carlucci AF, Karl DM. (1978). Microbial life beneath the Ross Ice Shelf. *Antarctic Journal of the United States* **4**:129–130.

Hood E, Spencer RGM, Battin TJ, Fellman J, Fellman J, O'Neel S, *et al.* (2015). Storage and release of organic carbon from glaciers and ice sheets. *Nature Geosci* **8**:91–96.

Horgan HJ, Alley RB, Christianson K, Anandakrishnan S, Horgan HJ, Alley RB, *et al.* (2013). Estuaries beneath ice sheets. *Geol* **41**:1159–1162.

Horgan HJ, Anandakrishnan S, Jacobel RW, Christianson K, Alley RB, Heeszel DS, *et al.* (2012). Subglacial Lake Whillans — Seismic observations of a shallow active reservoir beneath a West Antarctic ice stream. *Earth and Planetary Science Letters* **331-332**:201–209.

Horner-Devine MC, Silver JM, Leibold MA, Bohannan BJM, Colwell RK, Fuhrman JA, *et al.* (2007). A comparison of taxon co-occurrence patterns for macro- and microorganisms. *Ecology* **88**:1345–1353.

Horrigan SG. (1981). Primary production under the Ross Ice Shelf, Antarctica. *Limnol Oceangr* **26**:378–382.

Huber JA, Mark Welch DB, Morrison HG, Huse SM, Neal PR, Butterfield DA, *et al.* (2007). Microbial population structures in the deep marine biosphere. *Science* **318**:97–100.

Huggett MJ, Rappé MS. (2012). Genome sequence of strain HIMB30, a novel member of the marine Gammaproteobacteria. *Journal of Bacteriology* **194**:732–733.

Huguet A, Vacher L, Relexans S, Saubusse S, Froidefond JM, Parlanti E. (2009). Properties of fluorescent dissolved organic matter in the Gironde Estuary. *Organic Geochemistry* **40**:706–719.

Huse SM, Dethlefsen L, Huber JA, Mark Welch D, Welch DM, Relman DA, *et al.* (2008). Exploring microbial diversity and taxonomy using SSU rRNA hypervariable tag sequencing. Eisen, JA (ed). *PLoS Genet* **4**:e1000255.

Huse SM, Huber JA, Morrison HG, Sogin ML, Welch DM. (2007). Accuracy and quality of massively parallel DNA pyrosequencing. *Genome Biol* **8**:R143.

Huse SM, Welch DM, Morrison HG, Sogin ML. (2010). Ironing out the wrinkles in the rare biosphere through improved OTU clustering. *Environmental Microbiology* **12**:1889–1898.

Iverson V, Morris RM, Frazar CD, Berthiaume CT, Morales RL, Armbrust EV. (2012). Untangling genomes from metagenomes: revealing an uncultured class of marine Euryarchaeota. *Science* **335**:587–590.

Jacobs SS, Amos AF, Bruchhausen PM. (1970). Ross Sea oceanography and Antarctic bottom water formation. *Deep Sea Research and Oceanographic Abstracts* **17**:935–962.

Jacobs SS, Fairbanks RG. (1985). Origin and evolution of water masses near the Antarctic continental margin: Evidence from H218O/H216O ratios in seawater. *Antarctic Research Series* **43**:59–85.

Jacobs SS, Gordon AL, Ardai JL. (1979). Circulation and melting beneath the ross ice shelf. *Science* **203**:439–443.

Jäntti H, Jokinen S, Hietanen S, Jokinen S, Hietanen S. (2013). Effect of nitrification inhibitors on the Baltic Sea ammonia-oxidizing community and precision of the denitrifier method. *Aquat Microb Ecol* **70**:181–186.

Jepsen SM, Priscu JC, Grimm RE, Bullock MA. (2007). The potential for lithoautotrophic life on Mars: Application to shallow interfacial water environments. **7**:342–354.

Jiao N, Herndl GJ, Hansell DA, Benner R, Kattner G, Wilhelm SW, *et al.* (2010). Microbial production of recalcitrant dissolved organic matter: long-term carbon storage in the global ocean. *Nat Rev Micro* **8**:593–599.

Joughin I, Smith BE, Medley B. (2014). Marine ice sheet collapse potentially under way for the Thwaites Glacier Basin, West Antarctica. *Science* **344**:735–738.

Judd KE, Crump BC, Kling GW. (2006). Variation in dissolved organic matter controls bacterial production and community composition. *Ecology* **87**:2068–2079.

Jørgensen BB. (2011). Deep subseafloor microbial cells on physiological standby. *Proceedings of the National Academy of Sciences* **108**:18193–18194.

Kaiser J, Hastings MG, Houlton BZ, Roeckmann T, Sigman DM. (2007). Triple oxygen isotope analysis of nitrate using the denitrifier method and thermal decomposition of N2O. *Anal Chem* **79**:599–607.

Karl DM. (1980). Cellular nucleotide measurements and applications in microbial ecology. *Microbiol Rev* **44**:739–796.

Karl DM, Beversdorf L, Björkman KM, Church MJ, Martinez A, DeLong EF. (2008). Aerobic production of methane in the sea. *Nature Geosci* **1**:473–478.

Karr EA, Ng JM, Belchik SM, Sattley WM. (2006). Biodiversity of methanogenic and other Archaea in the permanently frozen Lake Fryxell, Antarctica. *Applied and Environmental Microbiolgy* **72**:1663–1666.

Kepner RL, Wharton RA, Suttle CA. (1998). Viruses in Antarctic Lakes. **43**:1754–1761.

Kiene RP. (1996). Production of methanethiol from dimethylsulfoniopropionate in marine surface waters. *Marine Chemistry* **54**:69–83.

Kirchman D, K'nees E, Hodson R. (1985). Leucine incorporation and its potential as a measure of protein synthesis by bacteria in natural aquatic systems. **49**:599–607.

Kong W, Dolhi JM, Chiuchiolo A, Priscu J, Morgan-Kiss RM. (2012). Evidence of form II RubisCO (cbbM) in a perennially ice-covered Antarctic lake. *FEMS Microbiology Ecology* **82**:491–500.

Kong W, Ream DC, Priscu JC, Morgan-Kiss RM. (2012). Diversity and expression of RubisCO genes in a perennially ice-covered Antarctic lake during the polar night transition. *Applied and Environmental Microbiology* **78**:4358–4366.

Kovács IA, Palotai R, Szalay MS, Csermely P. (2010). Community landscapes: an integrative approach to determine overlapping network module hierarchy, identify key nodes and predict network dynamics. Sporns, O (ed). *PLoS ONE* **5**:e12528.

Könneke M, Schubert DM, Brown PC, Hügler M, Standfest S, Schwander T, *et al.* (2014). Ammonia-oxidizing archaea use the most energy-efficient aerobic pathway for CO2 fixation. *Proc Natl Acad Sci USA* **111**:8239–8244.

Lanoil B, Skidmore M, Priscu JC, Han S, Foo W, Vogel SW, *et al.* (2009). Bacteria beneath the West Antarctic Ice Sheet. *Environmental Microbiology* **11**:609–615.

LaRowe DE, Amend JP. (2015). Catabolic rates, population sizes and doubling/replacement times of microorganisms in natural settings. **315**:167–203.

Laybourn-Parry J. (2002). Survival mechanisms in Antarctic lakes. *Philosophical Transactions of the Royal Society B: Biological Sciences* **357**:863–869.

Lebaron P, Servais P, Agogué H, Agogué H, Courties C, Joux F. (2001). Does the high nucleic acid content of individual bacterial cells allow us to discriminate between active cells and inactive cells in aquatic systems? *Applied and Environmental Microbiolgy* **67**:1775–1782.

Lee JA, Spidlen J, Boyce K, Cai J, Crosbie N, Dalphin M, *et al.* (2008). MIFlowCyt: The Minimum Information about a Flow Cytometry Experiment. *Cytometry A* **73**:926–930.

Lee PA, Priscu JC, DiTullio GR, Riseman SF, Tursich N, De Mora SJ. (2004). Elevated levels of dimethylated-sulfur compounds in Lake Bonney, a poorly ventilated Antarctic lake. *Limnol Oceangr* **49**:1044–1055.

Leventer A, Dunbar RB. (1988). Recent diatom record of McMurdo Sound, Antarctica: Implications for history of sea ice extent. *Paleoceanography* **3**:259–274.

Lever MA, Rogers KL, Lloyd KG, Overmann J, Schink B, Thauer RK, *et al.* (2015). Life under extreme energy limitation: a synthesis of laboratory- and field-based investigations Giudici-Orticoni, M-T (ed). *FEMS Microbiology Reviews* **39**:688–728.

Li Y-H, S G. (1974). Diffusion of ions in sea water and in deep-sea sediments. *Geochimica et Cosmochimica Acta* **38**:703–714.

Lipps JH, Ronan TE, DeLaca TE. (1979). Life Below the Ross Ice Shelf, Antarctica. *Science* **203**:447–449.

Lisle JT, Priscu JC. (2004). The Occurrence of Lysogenic Bacteria and Microbial Aggregates in the Lakes of the McMurdo Dry Valleys, Antarctica. *Microbial Ecology* **47**:1–13.

Lizotte MP, Priscu JC. (1994). Natural fluorescence and quantum yields in vertically stationary phytoplankton from perennially ice-covered lakes. *Limnol Oceangr* **39**:1399–1410.

Lizotte MP, Priscu JC. (1992). Spectral irradiance and bio-optical properties in perennially ice-covered lakes of the dry valleys (McMurdo Sound, Antarctica). American Geophysical Union: Washington, D. C.

Lizotte MP, Sharp TR, Priscu JC. (1996). Phytoplankton dynamics in the stratified water column of Lake Bonney, Antarctica. *Polar Biology* **16**:155–162.

Lukin V, Bulat S. (2011). Vostok Subglacial Lake: Details of Russian plans/activities for drilling and sampling. *Antarctic subglacial aquatic environments*.

Macfadyen S, Gibson R, Symondson WOC, Memmott J. (2011). Landscape structure influences modularity patterns in farm food webs: consequences for pest control. *Ecological Applications* **21**:516–524.

Magurran AE. (1988). Ecological Diversity and its Measurement.

Marie D, Partensky F, Vaulot D, Brussaard C. (2001). Enumeration of phytoplankton, bacteria, and viruses in marine samples. *Current protocols in cytometry* **Chapter 11**.

McCliment EA, Nelson CE, Carlson CA, Alldredge AL, Witting J, Amaral-Zettler LA. (2011). An all-taxon microbial inventory of the Moorea coral reef ecosystem. *ISME J* **6**:309–319.

McIlroy SJ, Kristiansen R, Albertsen M, Karst SM, Rossetti S, Nielsen JL, *et al.* (2013). Metabolic model for the filamentous ‘Candidatus Microthrix parvicella’ based on genomic and metagenomic analyses. *ISME J* **7**:1161–1172.

McKnight DM, Boyer EW, Westerhoff PK, Doran PT, Kulbe T, Andersen DT. (2001). Spectrofluorometric characterization of dissolved organic matter for indication of precursor organic material and aromaticity. *Limnol Oceangr* **46**:38–48.

Michalski G, Bhattacharya SK, Girsch G. (2014). NOx cycle and the tropospheric ozone isotope anomaly: an experimental investigation. *Atmos Chem Phys* **14**:4935–4953.

Miklós I, Podani J. (2004). Randomization of presence-absence matrices: comments and new algorithms. *Ecology* **85**:86–92.

Mikucki JA, Lee PA, Ghosh D, Purcell AM, Mitchell AC, Mankoff KD, *et al.* (2015). Subglacial Lake Whillans microbial biogeochemistry: a synthesis of current knowledge.

Mikucki JA, Priscu JC, Mikucki JA. (2007). Bacterial Diversity Associated with Blood Falls, a Subglacial Outflow from the Taylor Glacier, Antarctica. *Applied and Environmental Microbiology* **73**:4029–4039.

Mikucki JA, Schrag DP, Mikucki JA, Priscu JC, Pearson A, Johnston DT, *et al.* (2009). A Contemporary Microbially Maintained Subglacial Ferrous 'Ocean'. *Science* **324**:397–400.

Montross SN, Skidmore M, Tranter M, Kivimaki AL, Parkes RJ. (2013). A microbial driver of chemical weathering in glaciated systems. *Geol* **41**:215–218.

Montross SN, Skidmore M, Tranter M, Kivimäki A-L, Parkes RJ. (2013). A microbial driver of chemical weathering in glaciated systems. *Geol* **41**:215–218.

Moran MA, Reisch CR, Kiene RP, Whitman WB. (2012). Genomic insights into bacterial DMSP transformations. *Annu Rev Marine Sci* **4**:523–542.

Moran XAG, Moran XAG, Massana R, Massana R, Gasol JM, Gasol JM. (2001). Light Conditions Affect the Measurement of Oceanic Bacterial Production via Leucine Uptake. *Applied and Environmental Microbiology* **67**:3795–3801.

Morgan-Kiss RM, Lizotte MP, Kong W, Priscu JC. (2015). Photoadaptation to the polar night by phytoplankton in a permanently ice-covered Antarctic lake. *Limnol Oceangr* n/a–n/a.

Morita RY. (1997). Bacteria in oligotrophic environments: starvation-survival lifestyle. Chapman & Hall: New York.

Morris JH, Apeltsin L, Newman AM, Baumbach J, Wittkop T, Su G, *et al.* (2011). clusterMaker: a multi-algorithm clustering plugin for Cytoscape. *BMC Bioinformatics* **12**:436.

Mosier AC, Murray AE, Fritsen CH. (2007). Microbiota within the perennial ice cover of Lake Vida, Antarctica. *FEMS Microbiology Ecology* **59**:274–288.

Murphy KR, Stedmon CA, Graeber D, Bro R. (2013). Fluorescence spectroscopy and multi-way techniques. PARAFAC. *Anal Methods* **5**:6557–11.

National Research Council, Hobbie JE, Baker A, Clarke GKC, Doran PT, Karl D, *et al.* Exploration of Antarctic Subglacial Aquatic Environments: Environmental and Scientific Stewardship | The National Academies Press. In: Washington D.C., p. 166.

Nepusz T, Sasidharan R, Paccanaro A. (2010). SCPS: a fast implementation of a spectral method for detecting protein families on a genome-wide scale. *BMC Bioinformatics* **11**:120.

Newton RJ, Jones SE, Eiler A, McMahon KD, Bertilsson S. (2011). A guide to the natural history of freshwater lake bacteria. *Microbiol Mol Biol Rev* **75**:14–49.

Nicholls KW, Makinson K, Robinson AV. (1991). Ocean circulation beneath the Ronne ice shelf. *Nature* **354**:221–223.

Oh H-M, Kang I, Lee K, Jang Y, Lim S-I, Cho J-C. (2011). Complete genome sequence of strain IMCC9063, belonging to SAR11 subgroup 3, isolated from the Arctic Ocean. *Journal of Bacteriology* **193**:3379–3380.

Oksanen J, Kindt R, Legendre P, O'Hara B. (2009). Vegan: community ecology package. R package version 1.17-3. 2010.

Olesen JM, Bascompte J, Dupont YL, Jordano P. (2007). The modularity of pollination networks. *Proceedings of the National Academy of Sciences* **104**:19891–19896.

Orcutt BN, Sylvan JB, Knab NJ, Edwards KJ. (2011). Microbial Ecology of the Dark Ocean above, at, and below the Seafloor. *Microbiology and Molecular Biology Reviews* **75**:361–422.

Orphan VJ, Hinrichs KU, Ussler W, Paull CK, Taylor LT, Sylva SP, *et al.* (2001). Comparative analysis of methane-oxidizing archaea and sulfate-reducing bacteria in anoxic marine sediments. *Applied and Environmental Microbiology* **67**:1922–1934.

Osterholz H, Niggemann J, Giebel H-A, Simon M, Dittmar T. (2015). Inefficient microbial production of refractory dissolved organic matter in the ocean. *Nat Comms* **6**:7422.

Oswald G, Robin GQ. (1973). Lakes beneath the Antarctic ice sheet. *Nature* **245**:251–254.

Paerl H, Priscu J. (1998). Microbial Phototrophic, Heterotrophic, and Diazotrophic Activities Associated with Aggregates in the Permanent Ice Cover of Lake Bonney, Antarctica. *Microbial Ecology* **36**:221–230.

Paolo FS, Fricker HA, Padman L. (2015). Volume loss from Antarctic ice shelves is accelerating. *Science*.

Pernthaler J, Pernthaler A, Preston CM, DeLong EF, Amann R, DeLong EF, *et al.* (2002). Comparison of Fluorescently Labeled Oligonucleotide and Polynucleotide Probes for the

Detection of Pelagic Marine Bacteria and Archaea. *Applied and Environmental Microbiology* **68**:661–667.

Peura S, Eiler A, Bertilsson S, Nykänen H, Tiirola M, Jones RI. (2012). Distinct and diverse anaerobic bacterial communities in boreal lakes dominated by candidate division OD1. *ISME J* **6**:1640–1652.

Pérez MT, Sommaruga R, Hörtnagl P. (2010). Contrasting ability to take up leucine and thymidine among freshwater bacterial groups: implications for bacterial production measurements. *Environmental Microbiology* **12**:74–82.

Post AL, Galton-Fenzi BK, Riddle MJ, Herraiz-Borreguero L, O'Brien PE, Hemer MA, *et al.* (2014). Modern sedimentation, circulation and life beneath the Amery Ice Shelf, East Antarctica. *Continental Shelf Research* **74**:77–87.

Priscu JC. (2002). Commentary: Subglacial lakes have changed our view of Anatarctica. *Ant Sci* **14**:291.

Priscu JC. (2013). LTER Limno Methods Manual.

Priscu JC. (1992). Particulate organic matter decomposition in the water column of Lake Bonney, Taylor Valley... **27**:260.

Priscu JC. (1995). Phytoplankton nutrient deficiency in lakes of the McMurdo Dry Valleys, Antarctica. *Freshwater Biol* **34**:215–227.

Priscu JC, Achberger AM, Cahoon JE, Christner BC, Edwards RL, Jones WL, *et al.* (2013). A microbiologically clean strategy for access to the Whillans Ice Stream subglacial environment. *Ant Sci* **25**:637–647.

Priscu JC, Adams EE, Fritsen CH. (1998). Perennial Antarctic lake ice: an oasis for life in a polar desert. **280**:2095–2098.

Priscu JC, Adams EE, Lyons WB, Voytek MA, Mogk DW, Brown RL, *et al.* (1999). Geomicrobiology of subglacial ice above Lake Vostok, Antarctica. *Science* **286**:2141–2144.

Priscu JC, Bell RE, Bulat SA, Ellis-Evans CJ. (2003). An international plan for Antarctic subglacial lake exploration. *Polar Geography* **27**:69–83.

Priscu JC, Christner BC. (2004). Earth's icy biosphere. *Microbial Diversity and Prospecting* 130–145.

Priscu JC, Christner BC, Dore JE, Westley MB, Popp BN, Casciotti KL, *et al.* (2008). Supersaturated N2O in a perennially ice-covered Antarctic lake: Molecular and stable isotopic evidence for a biogeochemical relict. *Limnol Oceangr* **53**:2439–2450.

Priscu JC, Downes MT, McKay CP. (1996). Extreme supersaturation of nitrous oxide in a poorly ventilated Antarctic lake. *Limnol Oceangr* **41**:1544–1551.

Priscu JC, Downes MT, Priscu LR, Palmisano AC, Sullivan CW. (1990). Dynamics of Ammonium Oxidizer Activity and Nitrous-Oxide (N2o) Within and Beneath Antarctic Sea Ice. *Mar Ecol Prog Ser* **62**:37–46.

Priscu JC, Kennicutt MC II, Bell RE, Bulat SA, Ellis-Evans JC, Lukin VV, *et al.* (2005). Exploring subglacial Antarctic lake environments. *Eos Trans AGU* **86**:193.

Priscu JC, Powell RD, Tulaczyk S. (2011). Probing Subglacial Environments Under the Whillans Ice Stream. *Eos Trans AGU* **91**:253–254.

Priscu JC, Priscu LR, Howard-Williams C, Vincent WF. (1988). Diel patterns of photosynthate biosynthesis by phytoplankton in permanently ice-covered Antarctic lakes under continuous sunlight. *J Plankton Res* **10**:333–340.

Priscu JC, Priscu LR, Vincent WF, Howard-Williams C. (1987). Photosynthate distribution by microplankton in permanently ice-covered Antarctic desert lakes. *Limnol Oceangr* **32**:260–270.

Priscu JC, Sharp TR, Lizotte MP, Neale PJ. (1990). Photoadaptation by phytoplankton in permanently ice-covered Antarctic lakes: response to a non-turbulent environment. Antarctic Journal of the US.

Priscu JC, Tulaczyk S, Studinger M, Kennictt MC II, Christner BC, Foreman CM. (2008). Antarctic Subglacial Water: Origin, Evolution, and Ecology. In:*Polar Lakes and Rivers*, Vincent, WF & Laybourn-Parry, J (eds), Polar Lakes and Rivers, pp. 119–135.

Priscu JC, Wolf CF, Takacs CD. (1999). Carbon transformations in a perennially ice-covered Antarctic lake. *BioScience* **49**:997.

Pruesse E, Peplies J, Glöckner FO. (2012). SINA: accurate high-throughput multiple sequence alignment of ribosomal RNA genes. *Bioinformatics* **28**:1823–1829.

Pruesse E, Quast C, Knittel K, Fuchs BM, Ludwig W, Peplies J, *et al.* (2007). SILVA: a comprehensive online resource for quality checked and aligned ribosomal RNA sequence data compatible with ARB. *Nucleic Acids Res* **35**:7188–7196.

Purcell AM, Mikucki JA, Achberger AM, Alekhina IA, Barbante C, Christner BC, *et al.* (2014). Microbial sulfur transformations in sediments from Subglacial Lake Whillans. *Front Microbio* **5**:594.

Quince C, Turnbaugh PJ, Lanzen A, Davenport RJ. (2011). Removing noise from pyrosequenced amplicons. *BMC Bioinformatics* **12**:38.

Rack FR, DULING D, Duling D, Blythe D, BLYTHE D, Burnett J, *et al.* (2014). Developing a hot-water drill system for the WISSARD project: 1. Basic drill system components and design. *Annals of* …. doi:10.3189/2014AoG68A031.

Raymond JA, Christner BC, Schuster SC. (2008). A bacterial ice-binding protein from the Vostok ice core. *Extremophiles* **12**:713–717.

Reddy TE, Holland DM, Arrigo KR. (2010). Ross ice shelf cavity circulation, residence time, and melting Results from a model of oceanic chlorofluorocarbons. *Continental Shelf Research* **30**:733–742.

Riddle MJ, Craven M, Goldsworthy PM, Carsey F. (2007). A diverse benthic assemblage 100 km from open water under the Amery Ice Shelf, Antarctica. *Paleoceanography* **22**:n/a–n/a.

Rignot E, Jacobs S, Mouginot J, Scheuchl B. (2013). Ice-shelf melting around Antarctica. *Science* **341**:266–270.

Rivkin RB. (1991). Seasonal patterns of planktonic production in McMurdo Sound, Antarctica. *American Zoologist* **31**:5–16.

Roberts D. Labdsv: Ordination and Multivariate Analysis for Ecology Package.

Robinson NJ. (2004). An oceanographic study of the cavity beneath the McMurdo Ice Shelf, Antarctica. 156.

Robinson NJ, Pyne AR, Barrett PJ, Williams MJM, Robinson NJ, Williams MJM. (2010). Observations of flow and ice-ocean interaction beneath the McMurdo Ice Shelf, Antarctica. *J Geophys Res* **115**:C03025.

Roslev P, King GM. (1993). Application of a tetrazolium salt with a water-soluble formazan as an indicator of viability in respiring bacteria. *Applied and Environmental Microbiology* **59**:2891–2896.

Ross N, Siegert MJ, Rivera A. (2011). Ellsworth Subglacial Lake, West Antarctica: A review of its history and recent field campaigns. *Antarctic Subglacial* ….

Rousk J, Bengtson P. (2014). Microbial regulation of global biogeochemical cycles. *Front Microbio* **5**:103.

Røy H, Kallmeyer J, Adhikari RR, Pockalny R, Jørgensen BB, D'Hondt S. (2012). Aerobic microbial respiration in 86-million-year-old deep-sea red clay. *Science* **336**:922–925.

Sangwan P, Chen XL, Hugenholtz P, Janssen PH. (2004). Chthoniobacter flavus gen. nov., sp nov., the first pure-culture representative of subdivision two, Spartobacteria classis nov., of the phylum Verrucomicrobia. *Applied and Environmental Microbiology* **70**:5875–5881.

Sattley WM, Sattley WM, Madigan MT, Madigan MT. (2006). Isolation, Characterization, and Ecology of Cold-Active, Chemolithotrophic, Sulfur-Oxidizing Bacteria from Perennially Ice-Covered Lake Fryxell, Antarctica. *Applied and Environmental Microbiology* **72**:5562–5568.

Scherer RP. (1991). Quaternary and tertiary microfossils from beneath ice stream B: evidence for a dynamic West Antarctic ice sheet history. *Global and Planetary Change* **4**:395–412.

Scherer RP, Aldahan A, Tulaczyk S, Possnert G, Engelhardt H, Kamb B. (1998). Pleistocene Collapse of the West Antarctic Ice Sheet. *Science* **281**:82–85.

Schlitzer R. Ocean Data View. http://odv.awi.de.

Schloss PD, Westcott SL, Ryabin T, Hall JR, Hartmann M, Hollister EB, *et al.* (2009). Introducing mothur: open-source, platform-independent, community-supported software for describing and comparing microbial communities. *Applied and Environmental Microbiology* **75**:7537–7541.

Schneider CA, Rasband WS, Eliceiri KW. (2012). NIH Image to ImageJ: 25 years of image analysis. *Nat Meth* **9**:671–675.

Seeberg-Elverfeldt J, Schlüter M, Feseker T, Kölling M. (2005). Rhizon sampling of porewaters near the sediment-water interface of aquatic systems. *Limnol Oceanogr Methods* **3**:361–371.

Shabtaie S, Whillans IM. (1987). The morphology of Ice Streams A, B, and C, West Antarctica, and their environs. *J Geophys Res* **92**:8865.

Shannon P, Markiel A, Ozier O, Baliga NS, Wang JT, Ramage D, *et al.* (2003). Cytoscape: a software environment for integrated models of biomolecular interaction networks. *Genome Research* **13**:2498–2504.

Sharp M, Parkes J, Cragg B, Fairchild IJ, Lamb H. (1999). Widespread bacterial populations at glacier beds and their relationship to rock weathering and carbon cycling. *Geol* **27**:107.

Shen L, Chen Z. (2007). Critical review of the impact of tortuosity on diffusion. *Chemical Engineering Science* **62**:3748–3755.

Siegert MJ, CARTER S, TABACCO I, POPOV S, BLANKENSHIP DD. (2005). A revised inventory of Antarctic subglacial lakes. *Ant Sci* **17**:453.

Siegert MJ, Clarke RJ, Mowlem M, Ross N. (2012). Clean access, measurement, and sampling of Ellsworth Subglacial Lake: a method for exploring deep Antarctic subglacial lake environments. *Rev Geophys* **50**:RG1003.

Siegfried MR, Fricker HA, Roberts M, Scambos TA, Tulaczyk S. (2014). A decade of West Antarctic subglacial lake interactions from combined ICESat and CryoSat-2 altimetry. *Geophys Res Lett* **41**:891–898.

Sigman DM, Hain MP, Haug GH. (2010). The polar ocean and glacial cycles in atmospheric CO2 concentration. *Nature* **466**:47–55.

Skidmore M, Tranter M, Tulaczyk S, Lanoil B. (2010). Hydrochemistry of ice stream beds - evaporitic or microbial effects? *Hydrol Process* **24**:517–523.

Skidmore ML, Foght JM, Sharp MJ. (2000). Microbial life beneath a high Arctic glacier. *Applied and Environmental Microbiology* **66**:3214–3220.

Smethie WM Jr., Jacobs SS, Smethie WM Jr. (2005). Circulation and melting under the Ross Ice Shelf: estimates from evolving CFC, salinity and temperature fields in the Ross Sea. *Deep Sea Research Part I: Oceanographic Research Papers*. doi:10.1016/j.dsr.2004.11.016.

Smith BE, Fricker HA, Joughin IR. (2009). An inventory of active subglacial lakes in Antarctica detected by ICESat (2003–2008). *Journal of Glaciology* **55**:573–595.

Smith WO Jr, Orsi AH, Arrigo KR, Sedwick PN, Orsi AH, Sedwick PN, *et al.* (2012). The Ross Sea in a sea of change. **25**:90–103.

Smith WO Jr, Smith WO, Comiso JC, Comiso JC. (2008). Influence of sea ice on primary production in the Southern Ocean: A satellite perspective. *J Geophys Res* **113**:C05S93.

Smith WO, Dinniman MS, Hofmann EE, Klinck JM. (2014). The effects of changing winds and temperatures on the oceanography of the Ross Sea in the 21st century. *Geophys Res Lett* **41**:1624–1631.

Smith WO, Gordon LI. (1997). Hyperproductivity of the Ross Sea (Antarctica) polynya during austral spring. *Geophys Res Lett* **24**:233–236.

Solórzano L. (1969). Determination of ammonia in natural waters by the phenolhypochlorite method. *Limnol Oceangr* **14**:799–801.

Solórzano L, Sharp JH. (1980). Determination of total dissolved phosphorus and particulate phosphorus in natural waters. **25**:754–758.

Spigel RH, Priscu JC. (1998). Physical Limnology of the Mcmurdo Dry Valleys Lakes. American Geophysical Union: Washington, D. C.

Squyres SW, Andersen DW, Nedell SS, Wharton RA. (1991). Lake Hoare, Antarctica: sedimentation through a thick perennial ice cover. *Sedimentology* **38**:363–379.

Steele JA, Countway PD, Xia L, Vigil PD, Beman JM, Kim DY, *et al.* (2011). Marine bacterial, archaeal and protistan association networks reveal ecological linkages. *ISME J* **5**:1414–1425.

Stibal M, Šabacká M, Žárský J. (2012). Biological processes on glacier and ice sheet surfaces. *Nature Geosci* **5**:771–774.

Stone L, Stone L, Roberts A, Roberts A. (1990). The checkerboard score and species distributions. *Oecologia* **85**:74–79.

Stover CL. (2007). A new account of Ross Sea waters: characteristics, volumetrics, and variability.

Strickland JDH, Parsons TR. (1968). A Practical Handbook of Seawater Analysis.

Su G, Kuchinsky A, Morris JH, States DJ, Meng F. (2010). GLay: community structure analysis of biological networks. *Bioinformatics* **26**:3135–3137.

Szalay-Beko M, Palotai R, Szappanos B, Kovács IA, Papp B, Csermely P. (2012). ModuLand plug-in for Cytoscape: determination of hierarchical layers of overlapping network modules and community centrality. *Bioinformatics* **28**:2202–2204.

Šabacká M, Priscu JC, Priscu JC, Basagic HJ, Fountain AG, Fountain AG, *et al.* (2012). Aeolian flux of biotic and abiotic material in Taylor Valley, Antarctica. *Geomorphology* **155-156**:102–111.

Takacs C, Priscu J. (1998). Bacterioplankton Dynamics in the McMurdo Dry Valley Lakes, Antarctica: Production and Biomass Loss over Four Seasons. *Microbial Ecology* **36**:239–250.

Takacs CD, Priscu JC, McKnight DM. (2001). Bacterial dissolved organic carbon demand in McMurdo Dry Valley lakes, Antarctica. *Limnol Oceangr* **46**:1189–1194.

Teixeira de Mattos MJ, Neijssel OM. (1997). Bioenergetic consequences of microbial adaptation to low-nutrient environments. *J Biotechnol* **59**:117–126.

Telling J, Boyd ES, Bone N, Jones EL, Tranter M, MacFarlane JW, *et al.* (2015). Rock comminution as a source of hydrogen for subglacial ecosystems. *Nature Geosci* **8**:851–855.

Thornton DCO. (2014). Dissolved organic matter (DOM) release by phytoplankton in the contemporary and future ocean. *European Journal of Phycology* **49**:20–46.

Thurman J, Parry J, Hill PJ, Priscu JC, Vick TJ, Chiuchiolo A, *et al.* (2012). Microbial dynamics and flagellate grazing during transition to winter in Lakes Hoare and Bonney, Antarctica. *FEMS Microbiology Ecology* **82**:449–458.

Tison DL, Pope DH, Cherry WB, Fliermans CB. (1980). Growth of Legionella-Pneumophila in Association with Blue-Green-Algae (Cyanobacteria). *Applied and Environmental Microbiology* **39**:456–459.

Tulaczyk S, Mikucki JA, Siegfried MR, Priscu JC, Barcheck CG, Beem LH, *et al.* (2014). WISSARD at Subglacial Lake Whillans, West Antarctica: scientific operations and initial observations. *Annals of Glaciology* **55**:51–58.

Vick TJ, Priscu JC. (2012). Bacterioplankton productivity in lakes of the Taylor Valley, Antarctica, during the polar night transition. *Aquat Microb Ecol* **68**:77–90.

Vick-Majors TJ, Achberger A, Santibanez P, Dore JE, Hodson T, Michaud AB, *et al.* Biogeochemistry and microbial diversity in the marine cavity beneath the McMurdo Ice Shelf, Antarctica. *Limnol Oceangr* in press.

Vick-Majors TJ, Priscu JC, Amaral-Zettler LA. (2014). Modular community structure suggests metabolic plasticity during the transition to polar night in ice-covered Antarctic lakes. *ISME J* **8**:778–789.

Vincent WF, Howard-Williams C. (1986). Antarctic stream ecosystems : physiological ecology of a blue-green algal epilithon. **16**:219–233.

Vogel SW, Tulaczyk S, Kamb B, Engelhardt H, Carsey FD, Behar AE, *et al.* (2005). Subglacial conditions during and after stoppage of an Antarctic Ice Stream: Is reactivation imminent? *Geophys Res Lett* **32**:L14502.

Voytek MA, Ward BB, Priscu JC. (1998). The Abundance of Ammonium-Oxidizing Bacteria in Lake Bonney, Antarctica Determined by Immunofluorescence, Pcr and In Situ Hybridization. American Geophysical Union: Washington, D. C.

Wadham JL, Arndt S, Tulaczyk S, Stibal M, Tranter M, Telling J, *et al.* (2012). Potential methane reservoirs beneath Antarctica. *Nature* **488**:633–637.

Wadham JL, Tranter M, Skidmore M, Hodson AJ, Priscu J, Lyons WB, *et al.* (2010). Biogeochemical weathering under ice: Size matters. *Global Biogeochem Cycles* **24**:n/a–n/a.

Walker CB, la Torre de JR, Klotz MG, Urakawa H, Pinel N, Arp DJ, *et al.* (2010). Nitrosopumilus maritimus genome reveals unique mechanisms for nitrification and autotrophy in globally distributed marine crenarchaea. *Proceedings of the National Academy of Sciences* **107**:8818–8823.

Wang Q, Garrity GM, Tiedje JM, Cole JR. (2007). Naive Bayesian classifier for rapid assignment of rRNA sequences into the new bacterial taxonomy. *Applied and Environmental Microbiology* **73**:5261–5267.

Watts DJ, Strogatz SH. (1998). Collective dynamics of ‘small-world’ networks. *Nature* **393**:440–442.

Welschmeyer NA. (1994). Fluorometric analysis of chlorophyll a in the presence of chlorophyll b and pheopigments. *Limnol Oceangr* **39**:1985–1992.

Whitman WB, Whitman WB, Coleman DC, Coleman DC, Wiebe WJ, Wiebe WJ. (1998). Prokaryotes: The unseen majority. *Proceedings of the National Academy of Sciences* **95**:6578–6583.

Williams RT, Robinson ES. (1979). Ocean tide and waves beneath the ross ice shelf, antarctica. *Science* **203**:443–445.

Williams TJ, Long E, Evans F, Demaere MZ, Lauro FM, Raftery MJ, *et al.* (2012). A metaproteomic assessment of winter and summer bacterioplankton from Antarctic Peninsula coastal surface waters. *ISME J* **6**:1883–1900.

Wingham DJ, Siegert MJ, Shepherd A, Muir AS. (2006). Rapid discharge connects Antarctic subglacial lakes. *Nature* **440**:1033–1036.

Wouters B, Martin-Español A, Helm V, Flament T, van Wessem JM, Ligtenberg SRM, *et al.* (2015). Dynamic thinning of glaciers on the Southern Antarctic Peninsula. *Science* **348**:899–903.

Wright A, Siegert M. (2012). A fourth inventory of Antarctic subglacial lakes. *Ant Sci* **24**:659–664.

Yakimov MM, Cono VL, Smedile F, DeLuca TH, Juárez S, Ciordia S, *et al.* (2011). Contribution of crenarchaeal autotrophic ammonia oxidizers to the dark primary production in Tyrrhenian deep waters (Central Mediterranean Sea). *ISME J* **5**:945–961.

Yamashita Y, Tanoue E. (2008). Production of bio-refractory fluorescent dissolved organic matter in the ocean interior. *Nature Geosci* **1**:579–582.

Yamashita Y, Yamashita Y, Cory RM, Cory RM, Nishioka J, Nishioka J, *et al.* (2010). Fluorescence characteristics of dissolved organic matter in the deep waters of the Okhotsk Sea and the northwestern North Pacific Ocean. *Deep Sea Research Part II: Topical Studies in Oceanography* **57**:1478–1485.

Yilmaz P, Kottmann R, Field D, Knight R, Cole JR, Amaral-Zettler L, *et al.* (2011). Minimum information about a marker gene sequence (MIMARKS) and minimum information about any (x) sequence (MIxS) specifications. *Nat Biotechnol* **29**:415–420.

Yoon K-S, Tsukada N, Sakai Y, Ishii M, Igarashi Y, Nishihara H. (2008). Isolation and characterization of a new facultatively autotrophic hydrogen-oxidizing Betaproteobacterium, Hydrogenophaga sp. AH-24. *FEMS Microbiology Letters* **278**:94–100.

Zsolnay A, Baigar E, Jimenez M, Steinweg B, Saccomandi F. (1999). Differentiating with fluorescence spectroscopy the sources of dissolved organic matter in soils subjected to drying. *Chemosphere* **38**:45–50.